

## ABSTRACT

Title of Document:  $^{13}\text{C}$  AND  $^{15}\text{N}$  METABOLIC FLUX ANALYSIS  
ON THE MARINE DIATOM  
*PHAEODACTYLUM TRICORNUTUM* TO  
INVESTIGATE EFFICIENT UNICELLULAR  
CARBON AND NITROGEN ASSIMILATION  
MECHANISMS

Yuting Zheng, Doctor of Philosophy, 2013

Directed By: Assistant Professor Ganesh Sriram, Department  
of Chemical and Biomolecular Engineering

Photosynthesis is indispensable in carbon cycling and obtaining renewable carbon. Operated by cyanobacteria, algae and plants, this process provides reduced carbon and molecular oxygen, consumes atmospheric  $\text{CO}_2$  and harnesses solar energy. Photosynthesis is also central to the production of biofuels. Diatoms, a class of marine algae, contribute 20% to 40% of global photosynthetic productivity despite surviving in  $\text{CO}_2$ -depleted and nitrogen-limited environments. This makes diatoms ideal models to study efficient photosynthetic, specifically carbon concentrating mechanisms (CCM). It has been long debated that whether the unicellular marine diatom *Phaeodactylum tricornutum* operates a CCM, and whether the CCM is biophysical or biochemical ( $\text{C}_4$ ) in nature, with existing (circumstantial) experimental

evidence divided amongst the two possibilities. Through isotope labeling experiments (ILE) and metabolic flux analysis (MFA), we provide for the first time significant, direct evidence for a biochemical CCM and the potential combined operation of a biochemical and a biophysical CCM. Additionally, we shed light on how genes regulating this complex process respond to critical environmental variables.

Furthermore, we report the use of isotope-assisted metabolic flux analysis to study organic carbon (especially glucose) assimilation in *P. tricornutum*. Our steady state ILEs reveal glucose assimilation under light and potentially which genes may be responsible for glucose metabolism. We then studied nitrogen (mainly urea) assimilation through instationary  $^{15}\text{N}$  and  $^{13}\text{C}$  labeling experiments, to find indications of an unusual pathway of urea assimilation. Gene expression trends under various environmental conditions suggest the possible participation of the urea cycle in assimilating nitrogen in *P. tricornutum*, and how this metabolically differs from nitrate and ammonium assimilation. We anticipate that this work will not only improve understanding of unicellular  $\text{C}_4$  CCMs, but provide insights to explain the ecological success of diatoms in adapting to challenging environments.

<sup>13</sup>C AND <sup>15</sup>N METABOLIC FLUX ANALYSIS ON THE MARINE DIATOM  
*PHAEODACTYLUM TRICORNUTUM* TO INVESTIGATE EFFICIENT  
UNICELLULAR CARBON AND NITROGEN ASSIMILATION MECHANISMS

By

Yuting Zheng

Dissertation submitted to the Faculty of the Graduate School of the  
University of Maryland, College Park, in partial fulfillment  
of the requirements for the degree of  
Doctor of Philosophy  
2013

Advisory Committee:

Assistant Professor Ganesh Sriram, Committee Chair

Professor Srinivasa R. Raghavan

Associate Professor Nam Sun Wang

Professor and Chair of Fischell Dept. of Bioengineering William E. Bentley

Professor Zhongchi Liu, Dept. of Cell Biology & Molecular Genetics

© Copyright by  
Yuting Zheng  
2013

(Certain chapters or sections of chapters are copyrighted by publishers,  
or their copyright may be transferred to publishers in the future.  
This is indicated on the title pages of the relevant chapters.)

## Dedication

This work is dedicated to **my parents** for their unconditional love and support.

## Acknowledgements

I would like to sincerely thank my advisor, **Dr. Ganesh Sriram**, for his support and guidance throughout my research, and for his constant encouragement, valuable suggestions, patience and freedom on my study and career development.

I would also like to thank my committee members, **Dr. Srinivasa R. Raghavan, Dr. Nam Sun Wang, Dr. William E. Bentley and Dr. Zhongchi Liu**, who have provided valuable and constructive criticism of my work.

I would also like to thank for the funding support from:

**Jan and Anneke Sengers Fellowship** for supporting my first year of PhD study; **Minta Martin Foundation, Maryland Industrial Partnerships, A. James Clark School of Engineering, Dept. of Chemical and Biomolecular Engineering, University of Maryland** and **National Science Foundation (CBET-1134115)** for the rest of the years.

Additionally, I would like to acknowledge **my colleagues** from the **Metabolic Engineering Lab**. I thank **Andrew Quinn** for the helps on algae cell maintenance and experimental data analysis; I thank these undergraduate researchers **Ali Eslami, Michael Kang** and **Dennis Tran** for their hard work on biomass extraction and steady state isotope labeling experiments.

# Table of Contents

Dedication .....	ii
Acknowledgements .....	iii
Table of Contents .....	iv
List of Tables .....	vii
List of Figures .....	viii
List of Abbreviations .....	x
1. Introduction .....	1
1.1. Problem Description and Motivation .....	1
1.2. Approach .....	6
1.2.1. Isotopes Labeling Experiments (ILEs) .....	6
1.2.2. Metabolic Flux Analysis (MFA) .....	7
1.2.3. Quantitative Real-time Polymerase Chain Reaction (qRT-PCR) .....	8
1.3. Construction of the Dissertation .....	8
2. Background: Steady State and Instationary Modeling of Proteinogenic and Free Amino Acid Isotopomers for Flux Quantification .....	10
2.1. Materials .....	15
2.1.1. Metabolic Network Databases .....	15
2.1.2. Collecting Information from Isotope Labeling Experiments .....	15
2.1.3. Computational Platforms .....	16
2.2. Methods .....	17
2.2.1. Assumptions Underlying Isotopomer Network Models .....	18
2.2.2. Mass Fragmentography and Interpretation of Mass Spectral Data .....	19
2.2.3. Retrobiosynthetic Deduction of Isotope Labeling of Central Carbon Metabolites from Labeling Measurements of Biomass Components .....	21
2.2.4. Quantification of Flux Ratios at Metabolic Branch Points via Steady State Isotope MFA .....	25
2.2.5. General Procedures for Construction of Steady State Models .....	31
2.2.6. Construction of Instationary Models .....	38
3. Isotope Labeling Experiments and Metabolic Flux Analysis Elucidate a C <sub>4</sub> Photosynthetic Pathway in the Unicellular Diatom <i>Phaeodactylum tricornutum</i> .....	40
3.1. Introduction .....	40
3.2. Materials and Methods .....	48
3.2.1. Cell Culture .....	48
3.2.2. Quantification of Mass Isotopomer Abundances and Metabolite Pool Sizes by GC-MS .....	48
3.2.3. Instationary H <sup>13</sup> CO <sub>3</sub> <sup>-</sup> ILE, Intracellular Metabolite Extraction and Derivatization .....	50
3.2.4. Evaluation of Metabolic Fluxes from Instationary Isotopomer Data .....	52
3.2.5. Gene Expression Analysis by Quantitative Real-time Polymerase Chain Reaction (qRT-PCR) .....	54
3.2.6. Mixotrophic ILEs, Cell Harvest, Protein Extraction, Hydrolysis and Derivatization .....	56
3.2.7. Evaluation of Metabolic Fluxes from Steady-state Isotopomer Data .....	58

3.3. Results.....	60
3.3.1. Instationary H <sup>13</sup> CO <sub>3</sub> <sup>-</sup> ILE Reveals the Evidence of a C <sub>4</sub> CCM.....	61
3.3.2. Instationary <sup>13</sup> C MFA Suggests that the C <sub>4</sub> CCM Contributes Substantially to Photosynthesis.....	68
3.3.3. Two <i>P. tricornutum</i> Genes Encoding HCO <sub>3</sub> <sup>-</sup> -capturing Enzymes are Induced by Light.....	72
3.3.4. Mixotrophic ILEs Employing U- <sup>13</sup> C Glucose or U- <sup>13</sup> C Acetate Reveal Substantial Capture of Inorganic Carbon into C <sub>4</sub> Metabolites.....	75
3.3.5. 4- <sup>13</sup> C Asp ILE Suggests Photosynthetic Assimilation of CO <sub>2</sub> released from OAA C-4.....	81
3.3.6. <sup>13</sup> C MFA Estimates that CO <sub>2</sub> Released from OAA C-4 Contributes a Minimum of 21% ± 3% of Photosynthetically Fixed CO <sub>2</sub> .....	84
3.4. Discussion.....	89
4. Experimental Evidence and Isotopomer Analysis of Mixotrophic Glucose Metabolism in the Marine Diatom <i>Phaeodactylum tricornutum</i> .....	97
4.1. Introduction.....	97
4.2. Materials and Methods.....	101
4.2.1. Cell Culture and Counting.....	101
4.2.2. Gene Expression Analysis by Quantitative Real-time Polymerase Chain Reaction (qRT-PCR).....	102
4.2.3. Mixotrophic ILEs, Cell Harvest, Protein Extraction, Hydrolysis and Derivatization.....	104
4.2.4. Quantification of Mass Isotopomer Abundances by GC-MS.....	106
4.2.5. Evaluation of Metabolic Fluxes from Steady-State Isotopomer Data.....	107
4.3. Results.....	108
4.3.1. Carbon from U- <sup>13</sup> C Glucose Appears in Proteinogenic Amino Acids of <i>P. tricornutum</i> .....	109
4.3.2. <i>Fba3</i> is Upregulated Significantly under Light while Glucose Transporters are Less Sensitive to Light and Carbon Substrates.....	112
4.4. Discussion.....	114
5. <sup>13</sup> C and <sup>15</sup> N Isotopes Labeling Experiments Reveal Nitrogen Assimilation Mechanism in <i>Phaeodactylum tricornutum</i> .....	117
5.1. Introduction.....	117
5.2. Materials and Methods.....	119
5.2.1. Instationary Parallel ILE, Intracellular Metabolite Extraction and Derivatization.....	119
5.2.2. Gene Expression Analysis by Quantitative Real-time Polymerase Chain Reaction (qRT-PCR).....	121
5.2.3. Instationary Labeled Urea ILE, Intracellular Metabolite Extraction and Derivatization.....	122
5.3. Results.....	124
5.3.1. Nitrogen Source Parallel Experiments reveal Pattern of Urea Assimilation.....	124
5.3.2. Gene Expression Results Suggest Potential Participation of Urea Cycle in Urea Assimilation.....	126



5.4. Discussion.....	128
6. Conclusions and Future Work.....	129
6.1. Conclusions.....	129
6.2. Future Work.....	131
6.2.1. C <sub>4</sub> CCM Enzyme Identification.....	131
6.2.2. Identification of the Role of Urea Cycle in Urea Assimilation in <i>P. tricornutum</i> .....	131
Appendices:.....	133
A.1. Table A.1 Mass Isotopomers from H <sup>13</sup> CO <sub>3</sub> <sup>-</sup> Instationary ILE. ....	133
A.2. Table A.2 Mass Isotopomers from 100% U- <sup>13</sup> C Glc ILE. ....	134
A.3. Table A.3 Mass Isotopomers from 100% U- <sup>13</sup> C Ace ILE.....	135
A.4. Table A.4 Mass Isotopomers from 100% 1- <sup>13</sup> C Ace ILE. ....	136
A.5. Table A.5 Mass Isotopomers from 100% 4- <sup>13</sup> C Asp ILE. ....	137
A.6. Table A.6 Mass Isotopomers from 50% U- <sup>13</sup> C Glc ILE. ....	138
A.7. Table A.7 Mass Isotopomers from 100% 1- <sup>13</sup> C Glc ILE. ....	139
A.8. Table A.8 Parallel experiment: Mass Isotopomers from <sup>15</sup> N urea instationary ILE.....	140
A.9. Table A.9 Parallel experiment: Mass Isotopomers from <sup>15</sup> N NH <sub>4</sub> Cl instationary ILE.....	141
A.10. Table A.10 Parallel experiment: Mass Isotopomers from <sup>15</sup> N NaNO <sub>3</sub> instationary ILE.....	142
References.....	143

## List of Tables

Table 2.1 Retrobiosynthetic calculation of the isotopomer distribution of an intracellular metabolite (Pyr) from the MIDs of biomass components (amino acids Ala and Val) known to be synthesized from it. ....	23
Table 2.2 Isotopomer abundances in the glycolysis-PPP network resulting from feeding 1- <sup>13</sup> C or 6- <sup>13</sup> C glucose, expressed in terms of the flux $v_2$ .....	27
Table 2.3 Correspondence between the carbon atoms of the amino acids shown in Figure 2.3 and the carbon atoms of their central carbon metabolic precursors. ....	30
Table 3.1 H <sub>13</sub> CO <sub>3</sub> <sup>-</sup> instationary ILE: metabolic model and evaluated fluxes. ....	52
Table 3.2 Primers used for qRT-PCR.....	56
Table 3.3 4- <sup>13</sup> C Asp ILE: C <sub>4</sub> scenario metabolic model and evaluated fluxes. ....	59
Table 3.4 4- <sup>13</sup> C Asp ILE: alternative scenario metabolic model.....	60
Table 3.5 Flux and pool size (metabolite concentration) parameters estimated during instationary <sup>13</sup> C MFA. ....	71
Table 3.6 Summary of metabolic scenarios used to model the 4- <sup>13</sup> C Asp ILE. ....	87
Table 4.1 Primers used for qRT-PCR.....	103
Table 5.1 Primers used for qRT-PCR.....	123

## List of Figures

Figure 1.1 The morphology of C <sub>4</sub> photosynthesis in many land plants.....	2
Figure 2.1 A simple network with two parallel pathways differing in carbon atom rearrangement. ....	12
Figure 2.2 Relationships between precursor metabolites and amino acids. ....	22
Figure 2.3 A simplified metabolic network. ....	25
Figure 2.4 The predicted MIDs of Ala[23] and Leu[23455] fragments under different flux scenarios. ....	31
Figure 2.5 Iterative methodology for evaluating fluxes from isotopomer data. ....	37
Figure 3.1 pH-dependence of (a) equilibrium aqueous concentrations and (b) relative aqueous abundances of three forms of CO <sub>2</sub> : H <sub>2</sub> CO <sub>3</sub> (= CO <sub>2</sub> + H <sub>2</sub> O), HCO <sub>3</sub> <sup>-</sup> and CO <sub>3</sub> <sup>2-</sup> . ....	42
Figure 3.2 Hypothesized CCMs in diatoms. ....	43
Figure 3.3 Instationary H <sup>13</sup> CO <sub>3</sub> <sup>-</sup> ILE evidences CO <sub>2</sub> incorporation via a C <sub>4</sub> CCM over a 6 d period.....	63
Figure 3.4 Proposed carbon rearrangements in the C <sub>4</sub> CCM, with <sup>13</sup> C enrichments from the H <sup>13</sup> CO <sub>3</sub> <sup>-</sup> ILE at 20 min.....	64
Figure 3.5 <sup>13</sup> C enrichments of fragments of metabolites in the C <sub>4</sub> CCM measured from the H <sup>13</sup> CO <sub>3</sub> <sup>-</sup> ILE (points), and simulated by an instationary isotopomer model (lines). ....	65
Figure 3.6 <sup>13</sup> C enrichments and simulation of intracellular TCA cycle metabolites. .	66
Figure 3.7 Metabolic flux model of the C <sub>4</sub> CCM as deduced from instationary <sup>13</sup> C MFA.....	70
Figure 3.8 Genes encoding putative HCO <sub>3</sub> <sup>-</sup> -capturing enzymes in the C <sub>4</sub> CCM are induced by light.....	74
Figure 3.9 Hypothesized <sup>13</sup> C enrichment patterns of metabolites in a mixotrophic ILE feeding 100% U- <sup>13</sup> C glucose and naturally abundant CO <sub>2</sub> . ....	77
Figure 3.10 Mixotrophic ILEs feeding (a, U- <sup>13</sup> C glucose and unlabeled CO <sub>2</sub> ) as well as (b, U- <sup>13</sup> C acetate and unlabeled CO <sub>2</sub> ) evidence substantial HCO <sub>3</sub> <sup>-</sup> capture via a C <sub>4</sub> CCM. ....	80
Figure 3.11 MIDs and <sup>13</sup> C enrichments for mixotrophic ILE feeding 1- <sup>13</sup> C acetate (added to medium) and naturally abundant CO <sub>2</sub> (from headspace).....	82
Figure 3.12 Mixotrophic ILE feeding 4- <sup>13</sup> C Asp and unlabeled CO <sub>2</sub> evidences photosynthetic recapture of CO <sub>2</sub> released from a C <sub>4</sub> CCM. ....	84
Figure 3.13 The “C <sub>4</sub> scenario” and “alternative scenario” steady-state models for the 4- <sup>13</sup> C Asp ILE. ....	86
Figure 4.1 Evidence for isotopic steady state from 20-22 d .....	105
Figure 4.2 Cell counts evidence that Pt grows on glucose under light but not under dark. ....	109
Figure 4.3 <sup>13</sup> C enrichments of amino acid fragments synthesized from 100% and 50% U- <sup>13</sup> C glucose evidence significant glucose uptake.....	110
Figure 4.4 Expression levels of key glucose-related and glycolytic genes under different environmental conditions.....	113

Figure 5.1 Amino acid fragment $^{15}\text{N}$ enrichment in nitrogen source instationary parallel experiments. ....	125
Figure 5.2 Genes examined in gene expression experiments. ....	126
Figure 5.3 Gene expression of those regulate urea cycle and related pathway. ....	127

## List of Abbreviations

3PG, 3-phosphoglycerate  
ACA, acetyl-CoA  
Ace, acetate (used in figures)  
CA, carbonic anhydrase  
CCM, carbon-concentrating mechanism  
E4P, erythrose-4-phosphate  
F6P, fructose-6-phosphate  
Fum, fumarate  
Glc, glucose (used in figures and appendix tables)  
ILE, isotope labeling experiment  
Lac, lactate  
ME, malic enzyme  
MFA, metabolic flux analysis  
MID, mass isotopomer distribution  
MS, mass spectrometry/mass spectrometric/mass spectrum (depending on context);  
Mal, malate  
NA, naturally abundant (used in figures)  
OAA, oxaloacetate  
P5P, ribose-5-phosphate or pentose-5-phosphate (consolidation of ribose-, ribulose- and xylulose-5-phosphates)  
PEP, phosphoenolpyruvate  
PYC, pyruvate carboxylase  
Pyr, pyruvate  
qRT-PCR, quantitative real-time polymerase chain reaction  
RuBisCO, ribulose biphosphate carboxylase/oxygenase  
S7P, sedoheptulose-7-phosphate  
SD, standard deviation  
SSR, sum of squared residuals or  $\chi^2$  metric  
SVD, singular value decomposition  
Succ, succinate  
 $\alpha$ KG,  $\alpha$ -ketoglutarate.

All amino acids are referred to by their standard three-letter abbreviations, e.g. Ala, alanine; Ile: isoleucine; Leu: leucine; Val: valine.

**Notation.** Carbon atoms in metabolite fragments are indicated thus:  $\alpha$ KG[1] or  $\alpha$ KG[2345]. Carbon atom positions are indicated thus: C-2 or Pyr C-2. “C<sub>3</sub>” denotes a compound with three carbon atoms; “C<sub>4</sub>” denotes a compound with four carbon atoms or the type of CCM in which such compounds play a critical role.

# 1. Introduction

## 1.1. Problem Description and Motivation

Photosynthesis is indispensable in carbon cycling and obtaining renewable carbon. It provides reduced carbon and molecular oxygen, consumes atmospheric CO<sub>2</sub> and harnesses solar energy (Caemmerer and Farquhar, 1981; Govindjee, 2012; Kirk, 1994). Although this fundamentally important biochemical process has evolved for millions of years, it is a slow process. In most plants ribulose biphosphate carboxylase/oxygenase (RuBisCO), the first enzyme that reduces CO<sub>2</sub> to the three-carbon metabolite (C<sub>3</sub> acid) 3-phosphoglycerate (3PG) in photosynthesis, is limited by the concentration of dissolved, uncharged CO<sub>2</sub> in its vicinity (Bowes, 1991; Spreitzer and Salvucci, 2002). In these so-called “C<sub>3</sub>” plants, a controlled increase of CO<sub>2</sub> concentration around the leaves may slightly accelerate the rate of this enzyme. However, the atmospheric CO<sub>2</sub> concentration (~400 ppm) and the solubility of CO<sub>2</sub> in water (1.45 g L<sup>-1</sup> at ambient conditions) limit the CO<sub>2</sub> concentration in the vicinity of RuBisCO to ~15 μM, which is significantly lesser than the Michaelis constant  $K_M$  for CO<sub>2</sub> (~30 μM). This need to concentrate sufficient CO<sub>2</sub> around RuBisCO is overcome by a small group of plants known as “C<sub>4</sub>” plants. C<sub>4</sub> plants and the C<sub>4</sub> carbon concentrating mechanism (CCM) were first discovered in the 1960’s in land plants (Slack and Hatch, 1967). Studies have shown that in C<sub>4</sub> plants, CO<sub>2</sub> that diffuses into cells first appears on C-4 carbon atom of oxaloacetic acid (or oxaloacetate, OAA) or malic acid (or malate, Mal) instead of in 3PG, the direct product of RuBisCO. The C<sub>4</sub> acid OAA is then transported between specialized cell types called the mesophyll

cells to the CO<sub>2</sub>-impermeable bundle sheath cells, where the carbon assimilated into OAA or Mal is released by decarboxylation (Dai et al., 1993). The CO<sub>2</sub> thus released in the bundle sheath cells can accumulate around RuBisCO to concentrations significantly higher than  $K_M$ , thereby enabling C<sub>4</sub> plants to exhibit enhanced photosynthetic rates than C<sub>3</sub> plants (**Figure 1.1**).

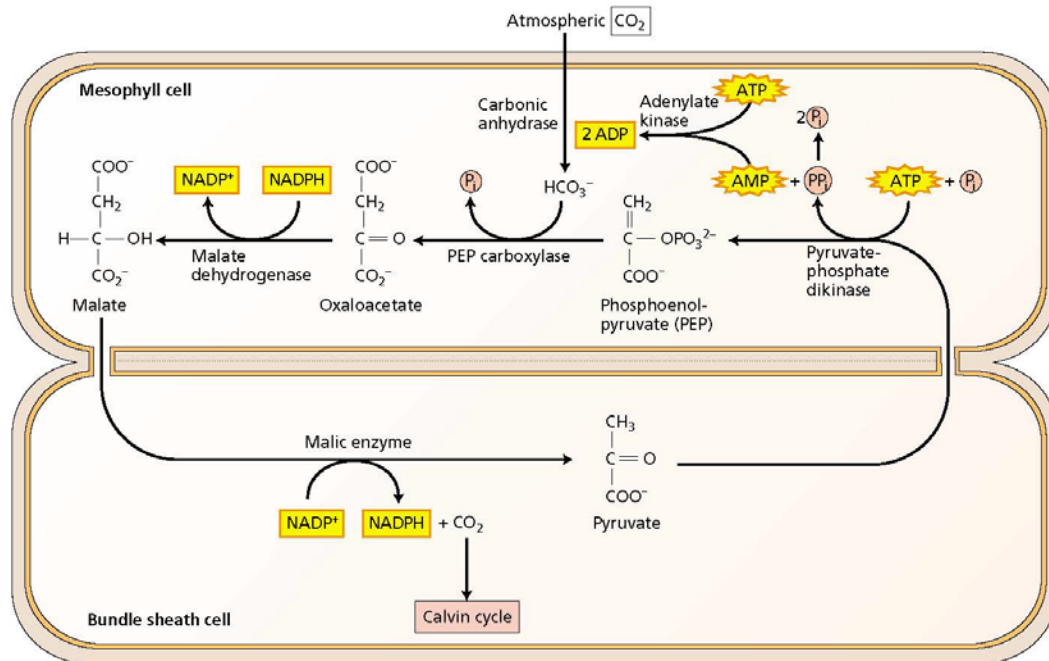


**Figure 1.1** The morphology of C<sub>4</sub> photosynthesis in many land plants.

(From Taiz and Zeiger, 2006, **Chapter 8**).

Compared to C<sub>3</sub> plants, C<sub>4</sub> plants show less sensitivity to environmental CO<sub>2</sub> concentration change, which indicates C<sub>4</sub> plants' higher adaptability to CO<sub>2</sub>-depleted environments (Kramer, 1981; Ward et al., 1999). Also, their more efficient photosynthesis can potentially lead to higher biomass production under the same ambient CO<sub>2</sub> concentration. Inspired by C<sub>4</sub> plants' high efficient photosynthesis, scientists have attempted to engineer C<sub>4</sub> CCMs into C<sub>3</sub> plants such as rice, to promote

improved growth rate and biomass production and ultimately to alleviate global food and energy shortages. However, simply transplanting known key genes from C<sub>4</sub> plants led to little or no success (Caemmerer et al., 2012; Sheehy et al., 2007; Zhu et al., 2010b). These obstacles revealed that simple enzyme overexpression may not be adequate to mimic the metabolic mechanisms underlying a C<sub>4</sub> CCM, and points to an urgent need to mechanistically investigate C<sub>4</sub> CCMs. In this regard, single-cell C<sub>4</sub> CCMs are of particular interest not only because of their fascinating biology, but also from a metabolic engineering standpoint as it should be easier to engineer single-cell C<sub>4</sub> CCMs than multicellular ones which require specialized cell types.

Unicellular or single-cell C<sub>4</sub> photosynthesis was initially found in a diatom *Thalassiosira weissflogii* about ten years ago, through a short-term radioactive <sup>14</sup>CO<sub>2</sub> assimilation experiment (Reinfelder et al., 2000). Diatoms are reported to contribute 20% to 40% to global CO<sub>2</sub> fixation (Bowler et al., 2008; De Riso et al., 2009; Falkowski et al., 1998; Kroth et al., 2008; Smetacek, 1999; Tesson et al., 2009). This, combined with their widespread habitat and thriving in low-CO<sub>2</sub> environments (Burkhardt et al., 2001), suggests that they may operate CCMs. However, it has been extensively debated whether specific diatoms operate either a biophysical (Hopkinson et al., 2011) or a biochemical (C<sub>4</sub>) CCM (Kroth et al., 2008; Reinfelder et al., 2004).

The marine diatom *Phaeodactylum tricornutum* has a fully sequenced genome (Bowler et al., 2008), which makes it a model organism to explore diatom CCMs in photosynthesis. *P. tricornutum* is hypothesized to operate a CCM; however, there is controversy about whether this is underlying a biophysical or a C<sub>4</sub> CCM. Gene expression studies suggest that it may operate both a biophysical and a C<sub>4</sub> CCM



(Kroth et al., 2008), while circumstantial and direct evidence for a solely biophysical CCM (reviewed in Reinfelder, 2011) as well as circumstantial evidence for an independent C<sub>4</sub> CCM have been reported (Chauton et al., 2013; Maheswari et al., 2010; Nymark et al., 2009). In contrast, evidence against a C<sub>4</sub> CCM has also been reported by Haimovich-Dayana et al. (2013), who found that suppressing a seemingly crucial C<sub>4</sub> enzyme pyruvate (Pyr) orthophosphate dikinase (PPDK) would not reduce the overall photosynthetic  $K_{1/2}$  for CO<sub>2</sub>. In this work we report the first and direct metabolic evidences for a C<sub>4</sub> CCM in *P. tricornutum*, and we also address or discuss (i) the metabolic flux patterns accompanying the CCMs, (ii) the carbon-concentrating efficiency of the CCMs, (iii) the identities of the molecules, enzymes and genes that participate in the mechanism, and (iv) whether C<sub>4</sub> and biophysical CCMs can operate concomitantly in the same organism.

Furthermore, during this study, we further clarified a long time debate on whether wild type *P. tricornutum* assimilates glucose under light. This debate arose in the 1950's, when multiple research groups reported that *P. tricornutum* cannot grow heterotrophically on glucose in the dark, and cellular growth rates did not increase when they were cultured under mixotrophic condition with glucose (Hayward, 1968; Lewin, 1958; Ukeles and Rose, 1976). More recently, one group (Zaslavskaja et al., 2001) who engineered *P. tricornutum* to express the human *GLUT1* glucose transporter protein showed that transformants grew on glucose in both light and dark, whereas wild type cells neither grew in the dark nor consumed glucose. Conversely, other researchers (Liu et al., 2009) have reported that *P. tricornutum* may consume and metabolize glucose. Given this conflicting evidence, the question of glucose

metabolism by *P. tricornutum* needs to be addressed by convincing molecular evidence. Through carefully designed isotope labeling experiment (ILE) and MFA, we have not only provided direct metabolic evidences indicating *P. tricornutum* assimilates glucose under light, but also identified the Entner-Doudoroff (ED) pathway in addition to the conventional Embden-Meyerhof-Parnas (EMP) pathway (Fabris et al., 2012) underlying glucose assimilation in this diatom.

Besides carbon assimilation, researchers have pointed out that in general higher photosynthesis rate leads to more biomass production, including proteins. Increased biomass in C<sub>4</sub> species when compared to C<sub>3</sub> species under the same condition, suggests higher efficiency of C<sub>4</sub> species such as *P. tricornutum* in using nitrogen sources (Brown, 1978). More interestingly, recent studies have found that this diatom may be operating the urea cycle in a biosynthetic role (Andrew E. Allen et al., 2011). Unlike the conventionally known nitrogen-eliminating role of urea cycle, this cycle in *P. tricornutum* putatively *assimilates* nitrogen under nitrogen-depleted conditions. Previous studies have suggested (i) the operation of an incomplete ornithine-urea cycle in this diatom, and (ii) a role for amino acids such as aspartic acid and glutamic acid in nitrogen assimilation, perhaps in conjunction with the tricarboxylic acid (TCA) cycle.

Diatoms are already known to be photosynthetically efficient. This, combined with an unusual role for the urea cycle, may explain the ecological success of diatoms in adapting to challenging environments. In this work we report several series of isotope labeling experiments (ILEs) that conducted for tracking nitrogen source consumption and metabolism, as well as gene expression results during this study.

We also reveal pathways of inorganic carbon, glucose and nitrogen assimilation including fluxes through the urea cycle in *P. tricornutum* through experimental data, and discuss the interrelationship between the urea and tricarboxylic acid cycles.

## **1.2. Approach**

To investigate carbon and nitrogen incorporation mechanisms in *P. tricornutum*, we conducted ILEs at isotopic steady state as well as during the transient approach to steady state. On basis of gas chromatography-mass spectrometry (GC-MS) measurements of isotope labeling patterns in these ILEs, metabolic flux analysis (MFA) was employed to identify metabolic pathway activities and estimate intracellular metabolic fluxes. Expression levels of crucial genes whose products may be rate-limiting in certain pathways was further examined via quantitative real-time polymerase chain reaction (qRT-PCR). Altogether, the approaches employed in this work depict various metabolic perspectives of the unicellular marine diatom *P. tricornutum* including the C<sub>4</sub> CCM, glucose assimilation and nitrogen recovery through urea cycle.

### **1.2.1. Isotopes Labeling Experiments (ILEs)**

To track metabolic fluxes and to thus quantify impact of substrates onto corresponding pathways, we employed several series of ILEs. To perform ILEs, specifically designed stable isotopically labeled substrates were added to a “default”

carbon-depleted growth medium (L1 medium obtained from the Provasoli-Guillard National Center for Marine Algae and Microbiota, NCMA; East Boothbay, ME). Cell cultures were grown in 125 mL Erlenmeyer flasks containing 50 mL culture medium (NCMA), and flasks were placed at 24.5 °C under constant light in refrigerated New Brunswick Innova 44R shakers (Eppendorf Hauppauge, NY) with a 2-inch stroke and programmable temperature, light and photoperiod controls. After two to six weeks (depending on whether a steady-state or an instationary experiment was conducted), isotopically labeled *P. tricornutum* biomass was extracted, derivatized and analyzed via GC-MS. Detailed culturing, extraction, sample preparation and GC-MS settings will be discussed in the following chapters.

### **1.2.2. Metabolic Flux Analysis (MFA)**

Analytical methods such as GC-MS provide isotope labeling information on molecules and molecular fragments; however, to infer what metabolic events caused these labeling patterns requires more thorough analysis. Metabolic flux analysis (MFA) takes into account a variety of information including biomass (or metabolite) labeling information, mass balances, information on metabolic reaction (often encoded as matrices), metabolite concentration pools, etc. to quantify metabolic fluxes. Because of the complexity of biological systems, fluctuations of intracellular metabolite levels, organelle compartmentalization, flux bidirectionality and metabolic cycling, MFA requires significant, nontrivial computation. From MFA, we expect to reveal flux distributions in investigated metabolic pathways or networks as well as

acquire crucial unmeasurable information, e.g. carbon partitioning and the contributions of competing pathways or metabolites.

### **1.2.3. Quantitative Real-time Polymerase Chain Reaction (qRT-PCR)**

Although metabolic flux maps enable visualization of carbon traffic, they do not easily provide information the regulation of the underlying genes. This can be remedied by gene expression measurements, which provide significant information to enhance a metabolic flux map. Also, knowledge of genes responsible for an observed metabolic phenotype could enable researchers to develop metabolic engineering strategies for the organism. Despite development of massive gene regulation measurement techniques such as DNA microarrays or high-throughput gene sequencing (Ball et al., 2002; Brazma et al., 2001; Schena et al., 1995), results from quantitative real-time polymerase chain reaction (qRT-PCR) are still widely employed as more accurate indicators of target gene expressions. To examine gene expression levels, we RNA extracted at the desired culture stage or condition and converted it to complementary DNA (cDNA). To measure transcription levels of target genes, this cDNA was amplified by qRT-PCR.

## **1.3. Construction of the Dissertation**

To investigate the efficient unicellular carbon and nitrogen assimilation in *P. tricornutum*, we divided this work into six chapters. After this introductory chapter,

we discussed the metabolic flux analysis background in Chapter 2, followed with detailed investigation on a C<sub>4</sub> CCM of the marine diatom in Chapter 3, which revealed the efficient inorganic carbon assimilation pathways underlying *P. tricornutum* photosynthesis. In Chapter 4, we further provided direct evidence that *P. tricornutum* would assimilate glucose under light, shown variety of the diatom in assimilating carbon sources. In the last but not least experimental section Chapter 5 we revealed nitrogen assimilation in the diatom through instationary isotope labeling experiments and gene expression measurement. Finally, conclusions and future perspectives are outlined in Chapter 6.

## **2. Background: Steady State and Instationary Modeling of Proteinogenic and Free Amino Acid Isotopomers for Flux Quantification**

Adapted from a book chapter accepted for publication:

Yuting Zheng<sup>1</sup> and Ganesh Sriram<sup>1,2</sup>. Steady state and instationary modeling of proteinogenic and free amino acid isotopomers for flux quantification. In: Alonso A, Dieuaide-Noubhani M (eds), Plant Metabolic Flux Analysis. *Methods in Molecular Biology*, Vol. 1090, Humana Press, New York, NY.

Copyright of the entire chapter transferred to Humana Press.

<sup>1</sup>Department of Chemical and Biomolecular Engineering, University of Maryland

<sup>2</sup>Principal investigator and corresponding author

Metabolic flux analysis (MFA) is a methodology for quantifying carbon traffic through chemical reactions that interconvert metabolites in a cell or a biological system (Stephanopoulos, 1999). Being a powerful tool to assess the metabolic impacts of genetic and environmental perturbations, MFA provides valuable guidance toward metabolic engineering, which involves performing mass balances on metabolites, solving which by linear algebraic methods ultimately results in a metabolic flux map. For implementation on simple metabolic networks, this procedure only requires growth rates, measurements of extracellular fluxes and fluxes

toward biomass as experimental inputs. In complex biological systems such as plants, this approach may by itself not be sufficient to unambiguously determine the values of all or most fluxes. In such cases, tracing isotope labels through the metabolic network provides critical information toward completing the flux map. MFA involving tracing of isotope labels is called isotope-assisted MFA (isotope MFA). This approach is especially beneficial for parallel pathways with common, intracellular start and end points as well as for metabolic cycles (Wiechert, 2001).

The central idea of this approach is that different pathways feature different carbon atom rearrangements, so that any given pathway will likely process a mixture of carbon isotopes (e.g.  $^{13}\text{C}$  and  $^{12}\text{C}$ ) uniquely. Thus, when an appropriately designed mixture of carbon isotopes is supplied to a set of pathways, the resulting isotopic mixture will reflect the metabolic “signatures” of the pathways that contributed to it. **Figure 2.1** illustrates a simple scenario. Here, a mixture of labeled and naturally abundant (NA, 98.8% unlabeled) version of metabolite A is fed to a network that converts metabolite A to metabolite D through two available pathways. In **Figure 2.1**, pathway (b) is “straightforward” and does not involve carbon atom rearrangements, whereas pathway (a) affects a carbon atom rearrangement by splitting metabolite A into metabolites B and C that condense to form D. Because the two pathways differ in their carbon atom rearrangements and because enzymes exhibit no macroscopic preference toward  $^{12}\text{C}$  and  $^{13}\text{C}$  (a very reasonable assumption in metabolic flux analysis), each pathway synthesizes different  $^{12}\text{C}$ - $^{13}\text{C}$  patterns or isotopomers of D. For instance, pathway (a) in this figure uniquely synthesizes a  $^{12}\text{C}$ - $^{12}\text{C}$ - $^{13}\text{C}$  and a  $^{13}\text{C}$ - $^{13}\text{C}$ - $^{12}\text{C}$  isotopomer. The isotopomers synthesized by different pathways generally



differ in their masses or magnetic properties. In **Figure 2.1**, pathway (a) alone produces isotopomers of mass  $m+1$  and  $m+2$  (in addition to isotopomers of mass  $m+0$  and  $m+3$ ), where  $m$  is the molecular weight of metabolite D. Contrastingly, pathway (b) only produces isotopomers of mass  $m+0$  and  $m+3$ . The mass spectra of metabolites such as D, or of biomass components derived from them, can be measured via gas chromatography-mass spectrometry (GC-MS) to not only identify which metabolic pathways are active, but to evaluate the relative fluxes through each pathway.

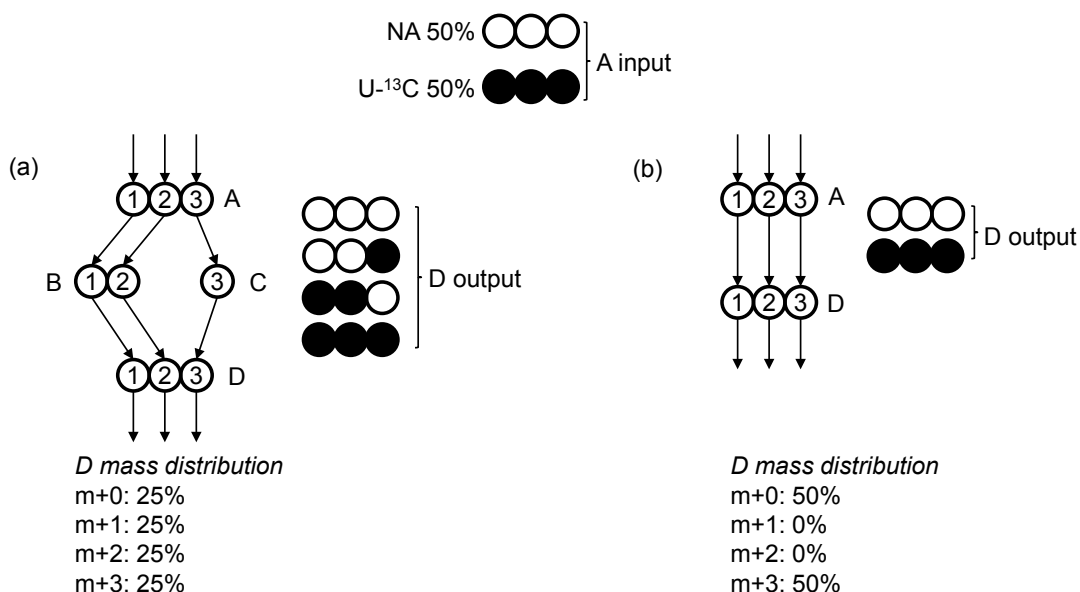


**Figure 2.1 A simple network with two parallel pathways differing in carbon atom rearrangement.**

Carbon isotopes and isotopomers are notated using empty circles for  $^{12}\text{C}$  and filled circles for  $^{13}\text{C}$ . The network has two available pathways between metabolites A and D. Feeding a mixture of 50% natural abundant (NA, nearly unlabeled) and 50% uniformly  $^{13}\text{C}$ -labeled (U- $^{13}\text{C}$ ) A to this network will result in different isotopomers of D, whose  $^{13}\text{C}$ - $^{12}\text{C}$  patterns will depend on the pathway that contributed to their synthesis. These isotopomers will generally differ in mass. Thus, each of the two pathways in this example has a signature mass distribution for D. (a) shows the theoretical isotopomer combination of D when product C and D is formed from A before D, and (b) shows the other case that the connection between A and D is straightforward.

Several experimental steps are necessary to obtain isotopomer abundance measurements from a cell or tissue after it reaches metabolic steady state. These include timely cell or tissue harvesting, extraction and processing of biomass components (proteinogenic and free amino acids, fatty acids, sugars and soluble metabolites), GC-MS or nuclear magnetic resonance (NMR) sample preparation and analysis, and post-analysis processing of data. In this work modeling of isotopomers of biomass components that are measurable by GC-MS is principally discussed.

Mathematically modeling of an isotope labeling experiment can involve significant complexity as determined by the structural sophistication of the underlying metabolic network, the amount of isotopomer abundance data available from labeling experiments and whether isotope MFA is to be performed at isotopic steady state or unsteady state. Several methods broadly based on mass balancing enable isotope label-free, stoichiometric or kinetic analysis of metabolic networks. These include flux balance analysis (FBA) (Edwards and Palsson, 2000; Kauffman et al., 2003; Lee et al., 2006), genome-scale metabolic modeling (AbuOun et al., 2009; Feist et al., 2007; Resendis-Antonio et al., 2007) and ensemble modeling (Tran et al., 2008). Genome-scale modeling involves the construction of an organism-specific stoichiometric model inferred from the organism's annotated genome or from a metabolic pathway database that is based on the genome annotation. FBA models a metabolic network as a system of linear, stoichiometric equations constrained by extracellular flux measurements and thermodynamic irreversibilities of reactions. Optimization of different objective functions (e.g. maximization of biomass production) via this model results in metabolic flux distributions or maps.

Akin to the aforementioned methods, models for isotope labeling experiments involve mass balances of metabolites and isotopomers. However, these balances can be bilinear (Wiechert et al., 1997), making solution strategies iterative and complex. Researchers have developed several model frameworks and methods to reduce this complexity. This includes the use of compartmental matrix techniques such as cumulative isotopomers (cumomers) (Wiechert et al., 1999a), bond isomers (bondomers) (Sriram and Shanks, 2004; W. A. van Winden et al., 2002), or elementary metabolite units (EMUs) (Antoniewicz et al., 2007). All these methods involve condensing a nonlinear set of isotopomer balance equations to a cascade of linear equations that can be solved by straightforward matrix computations (Wiechert et al., 1999a). Although these techniques were developed for analysis at isotopic steady state, they have now been successfully extended to isotopically instationary situations (Nöh and Wiechert, 2006; Young et al., 2008).

The mathematical methods listed above have progressively improved the efficiency and speed of isotopomer data analysis while not sacrificing the information contained in isotope labeling datasets. Despite their availability, the workload of data processing and flux evaluation can be tremendous. Currently, many computer-aided flux evaluation tools are available that significantly shorten the time between data acquisition and evaluation of fluxes and confidence intervals. These tools are especially useful in instationary flux analysis. Programming platforms used by these tools are wide-ranging, with C/C++ and MATLAB being favored.

## **2.1. Materials**

### **2.1.1. Metabolic Network Databases**

Detailed information on metabolic pathways is now available through several metabolic pathway databases including KEGG (Masoudi-Nejad et al., 2008) and MetaCyc (Zhang et al., 2005). KEGG and MetaCyc have online interfaces ([www.genome.jp/kegg/kegg2.html](http://www.genome.jp/kegg/kegg2.html) and [www.metacyc.org](http://www.metacyc.org) respectively); additionally, many of their functionalities are available offline. These databases provide detailed information on metabolites, reactions, pathways and genomic information (e.g. gene loci) across various species, often quite comprehensively. Additionally, because most information in these databases is curated from previous research, they host significantly more information on model species such as Arabidopsis. Information on relatively unexplored species is best obtained by searching the literature, especially via Google Scholar or PubMed with appropriate keywords. An alternative method is to begin with canonical pathways or pathways known to exist in related species and to iteratively improve the model on the basis of discrepancies observed while fitting the model to isotopomer measurements.

### **2.1.2. Collecting Information from Isotope Labeling Experiments**

Isotope labeling experiments also provide information toward constructing a metabolic network. Particularly, an initial metabolic network model can be iteratively refined on the basis of isotope labeling patterns that are not satisfactorily explained by it (Iyer et al., 2007; Schwender et al., 2004; e.g. Sriram et al., 2007). Additionally,

labeling data can help narrow down feasible pathways when (re)constructing a network. Appropriately designing labels of the carbon source is crucial for this to be effective (Nargund and Sriram, 2013; Wittmann and Heinzle, 2001; Yang et al., 2005).

### **2.1.3. Computational Platforms**

Isotope labeling experiments may be modeled on several computational platforms, depending on the level of sophistication of the underlying metabolic network and the number and types of labeling measurements available. For simple networks such as those in **Figure 2.1**, it is easy to manually obtain algebraic equations relating isotopomers and fluxes. Somewhat more complicated networks can be solved by using the Solver function on Microsoft Excel. More complex networks will need to be modeled on MATLAB, C, C++ or other platforms by writing ad hoc programs or by using programs specifically suited for modeling isotope labeling experiments, such as <sup>13</sup>CFlux2 (Weitzel et al., 2012), OpenFLUX (Quek et al., 2009), Metran (Antoniewicz et al., 2007), NMR2Flux+ (Sriram et al., 2004) or FiatFlux (Zamboni et al., 2005). Although we have historically used NMR2Flux+ (Sriram et al., 2008, 2004) and continue to do for routine isotope MFA (Nargund and Sriram, 2013), we use MATLAB as a demonstrative tool in the classroom or for illustration. MATLAB is an excellent platform to initially execute the modeling examples presented in this chapter, principally because of its user-friendly interface and flexibility. Furthermore, with its versatile optimization and parallel computing toolboxes, MATLAB is adequate for steady state flux analyses of many realistic

metabolic networks. However, development of more robust tools may require programming languages such as C or C++.

## **2.2. Methods**

After collecting all the necessary data from either metabolic network databases or previous iterations of isotope labeling experiments, different modeling strategies may be employed depending on the nature of the labeling experiment and the supplied carbon source. For many cases, especially if (i) multiple carbon sources or a carbon source containing covalently bonded carbon atoms are (is) supplied, and (ii) labeling data is collected at a single time point after isotope steady state is attained, then steady state modeling should be employed. In other cases, if (i) a single carbon source containing exactly one carbon atom or multiple, non-covalently bonded carbon atoms is supplied, or (ii) the labeling data is collected transiently at multiple time points, then an instationary model is indispensable. The type of model employed also determines which metabolites need to be sampled and analyzed to measure isotope labeling. The typical length of time over which steady state experiments are conducted enables the accumulation of substantial amounts of label in biomass components including proteinogenic amino acids, fatty acids, sugars and nucleic acids. Therefore, it is not surprising that steady state experiments involve quantification of isotopomer abundances in these compounds (e.g. Sriram et al., 2004; Masakapalli et al., 2010) rather than in intracellular metabolites, which are typically present in low amounts in the biomass. However, instationary experiments are conducted over time frames so short that sufficient label does not accumulate in

biomass components. Therefore, it is advisable to isolate and measuring labeling in intracellular metabolites such as those present in glycolysis, the tricarboxylic acid (TCA) cycle and other central carbon metabolic pathways. Metabolic steady state, i.e. the constancy of the fluxes to be measured, is necessary for both types of experiments and can be partially verified by examining if extracellular flux measurements are constant during the labeling experiment.

### **2.2.1. Assumptions Underlying Isotopomer Network Models**

The following assumptions are usually implicit in the construction of isotopomer network models.

- 1) Carbon participates only in the reactions included in the model. For this reason, it is essentially that the model includes all reactions known to account for more than ~1% of the total carbon flux.
- 2) The system (cell or tissue) being modeled is at metabolic steady state; therefore, (i) the metabolic flux values, directions of net fluxes and reaction reversibilities are constant and (ii) the pool sizes (concentrations) of the metabolites are constant.
- 3) Enzymes do not distinguish between  $^{12}\text{C}$  and  $^{13}\text{C}$ . Although in reality enzymes do show a slight preference for one isotope over another (e.g. RuBisCO, Ribulose-1,5-bisphosphate carboxylase oxygenase (O'Leary, 1988)), this isotopic discrimination is almost negligible in isotope MFA wherein substantial amounts of label are fed.

4) In steady-state models, the system has reached isotopic steady state and the isotope labeling patterns of metabolites do not vary with time. This assumption does not apply to instationary models. Since the objective of isotope MFA is to measure (constant) flux values, the kinetics of the underlying enzymatic reactions or the regulatory effects governing them are irrelevant to the analysis. Typically, the overall flux of a metabolic reaction varies with the activity of the catalyzing enzyme and the concentrations of the participating metabolites. However, because these quantities are constant at metabolic steady state, the overall flux is constant and its dependence on enzyme activities or metabolite concentrations can be ignored. This argument enables the decoupling of kinetics from flux analysis, so that the only unknown parameters in the flux model are the unknown fluxes and (in case of instationary models) metabolite concentrations. Furthermore, comparative isotope MFA of two environmental conditions, chemical treatments or genetic variants can be used as a tool to probe into the effects of conditions or genetic interventions on kinetics or regulatory mechanisms.

### **2.2.2. Mass Fragmentography and Interpretation of Mass Spectral Data**

Mass Spectrum (MS) can detect both entire molecules and (more often) fragments of molecules, and distinguishes isotopomers of these molecules or fragments by mass. The fragmentography of a particular analyte depends on its chemical structure, whether it is derivatized prior to analysis (often the case if GC-MS is used) and the particular derivatization chemistry used. For instance, MS detects two distinct metabolic fragments of the *t*-butyldimethylsilyl (tBDMS) derivative of



the three-carbon amino acid alanine (Ala). One fragment, corresponding to the ions with  $m/z = 158$  or  $232$ , contains carbon atoms C-2 and C-3 of Ala. We therefore notate this fragment as “Ala[23]”. Another fragment, corresponding to an ion with  $m/z = 260$ , contains all three carbon atoms of Ala and we therefore notate it as “Ala[123]”. MS, however, detects three distinct metabolic fragments of another three-carbon amino acid, serine (Ser). Using the notation above, these fragments are Ser[12] ( $m/z = 302$ ), Ser[23] ( $m/z = 288$  or  $362$ ), and Ser[123] ( $m/z = 390$ ).

A close examination of these fragments will reveal a mass isotopomer distribution (MID). For example, the Ala[123] fragment could exhibit several isotopomers of masses  $m$ ,  $m+1$ ,  $m+2$ , etc., where  $m$  is the molecular weight of the fragment. The abundances of these mass isotopomers depend on: (i) the metabolically generated labeling pattern of the three carbon atoms constituting the Ala[123] fragment (e.g. a  $^{12}\text{C}$ - $^{12}\text{C}$ - $^{12}\text{C}$  fragment will have a mass 3 amu lesser than a  $^{13}\text{C}$ - $^{13}\text{C}$ - $^{13}\text{C}$  fragment), and (ii) natural isotopic distributions of atoms other than metabolic carbon in the fragment. The effect in (ii) can easily be decoupled from the effect of interest in (i) by using algorithms described elsewhere (e.g. Sriram et al., 2008; W. A. V. Winden et al., 2002). While processing MID data of biomass components such as amino acids, two important problems need to be solved: (i) relating amino acid MIDs to the isotopomer distributions of their central carbon metabolic precursors and (ii) mathematically relating isotopomer distributions of central carbon metabolic precursors to pathway fluxes. The first problem is relevant in steady state experiments, where amino acid MIDs are usually measured as surrogates for

isotopomer distributions of central carbon metabolic precursors. The second problem is relevant in both steady state and instationary labeling experiments.

### **2.2.3. Retrobiosynthetic Deduction of Isotope Labeling of Central Carbon Metabolites from Labeling Measurements of Biomass Components**

To keep flux-isotopomer models reasonably small in size, it is convenient to restrict them to central carbon metabolism. Such models will, therefore, not simulate isotopomers of biomass components (e.g. amino acids) because the pathways leading from central carbon metabolism to biomass synthesis are not directly incorporated into the model. However, especially in steady state isotope MFA, labeling patterns of biomass components are the ones that are best measured. Therefore, it is necessary to relate the labeling patterns of biomass components to the isotopomers of central carbon metabolites. This requires information on the biosynthesis of proteinogenic amino acids from central carbon metabolic precursors, which is available from the literature (Szyperski, 1998a) as well as metabolic pathway databases such as MetaCyc. Amino acids are synthesized from one or more metabolic precursors through almost universally valid pathways. For example, Ala is synthesized from pyruvate (Pyr) with a one-to-one correspondence between its three carbon atoms and those of Pyr, whereas isoleucine (Ile) is synthesized from one molecule each of Pyr and oxaloacetate (OAA) (**Figure 2.2**). Some central carbon metabolites are precursors for the synthesis of multiple amino acids. For instance Ala, valine (Val) as well as parts of leucine (Leu) and Ile originate from Pyr (**Figure 2.2**). Pyr, being a three-carbon compound, has eight ( $= 2^3$ ) different isotopomers as shown in **Table 2.1** using

the notation 0 =  $^{12}\text{C}$ , 1 =  $^{13}\text{C}$ . Because Ala, Val, Leu and Ile are entirely or partially synthesized from Pyr, their mass isotopomer distributions should reflect the abundances of the eight Pyr isotopomers. However, the Pyr isotopomer abundances cannot be directly back-calculated from the MID of any single amino acid derived from it. For example, the two available mass fragments of Ala, Ala[23] and Ala[123], do not distinguish between labeling at C-2 and C-3 of Ala and therefore do not provide complete information on mass isotopomers of Pyr. A mass spectrum of tBDMS-derivatized Val contains the fragments Val[COOH·C $^{\alpha}$ ] (or Val[12], which corresponds to Pyr[12]) and Val[C $^{\alpha}$ ·C $^{\beta}$ ·C $^{\gamma^1}$ ·C $^{\gamma^2}$ ] (or Val[2344], which corresponds to Pyr[2233]). As with Ala, the two Val fragments do not, by themselves, provide information to back-calculate the abundances of the eight Pyr isotopomers. However, the MIDs of the two Ala fragments Ala [23] and Ala[123] and one Val fragment (Val[COOH·C $^{\alpha}$ ] or Val[12]) can be combined to provide sufficient information to infer the abundances of the eight Pyr isotopomers.

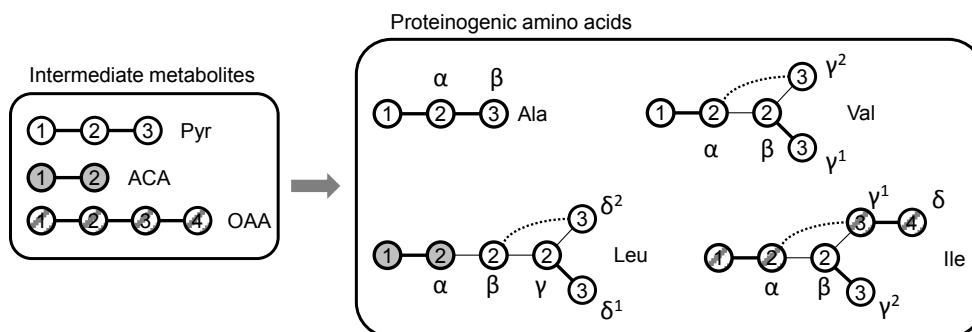


**Figure 2.2 Relationships between precursor metabolites and amino acids.**

Circles filled with different patterns denote carbon atoms of different precursors. Bold solid lines in amino acid molecules denote intact carbon-carbon bonds that were not broken during the synthesis of the amino acid from the precursor(s). Thin straight lines denote biosynthetic bonds that were formed by reassembling carbon atoms from two different precursor molecules. Dashed lines connect carbon atoms of amino acid molecules that originated from the same precursor and were covalently bonded, but are not covalently bonded in the amino acid molecule.

**Table 2.1 Retrobiosynthetic calculation of the isotopomer distribution of an intracellular metabolite (Pyr) from the MIDs of biomass components (amino acids Ala and Val) known to be synthesized from it.**

The amino acids Ala and Val are known to be synthesized from Pyr. We employ an optimization algorithm to convert the MIDs of the fragments Ala [23], Ala [123] and Val [12] to the eight isotopomers of Pyr. Toward this we minimize a statistical  $\chi^2$  criterion, whose expression is shown in this table. Abundances of Pyr isotopomers are simulated and optimized as shown in the last two columns. Isotopomers are represented using the notation 1= $^{13}\text{C}$ , 0= $^{12}\text{C}$ . SD: measurement standard deviation.

Fragment	Mass ( $m+n$ )	MI D	SD	Predicted formula	Predicted value	$\chi^2$	Pyr isotopomer	Optimized abundance
Ala[23]	0	0.69	0.04	= $[000]+[100]$	0.69	0.00	000	0.63
	1	0.30	0.04	= $[010]+[110]$ + $[001]+[101]$	0.30	0.00	100	0.06
	2	0.01	0.00	= $[011]+[111]$	0.01	0.43	010	0.09
Ala[123]	0	0.63	0.03	= $[000]$	0.63	0.01	110	0.02
	1	0.34	0.03	= $[100]+[010]$ + $[001]$	0.34	0.00	001	0.19
	2	0.03	0.00	= $[110]+[101]$ + $[011]$	0.03	0.39	101	0.00
	3	0.00	0.00	= $[111]$	0.00	0.05	011	0.01
Val[12]	0	0.81	0.01	= $[000]+[001]$	0.82	0.00	111	0.00
	1	0.16	0.01	= $[100]+[010]$ + $[101]+[011]$	0.16	0.00	$\chi^2 = \frac{(\text{Prediction} - \text{MID})^2}{\text{SD}^2}$	
	2	0.03	0.00	= $[110]+[111]$	0.02	1.05		Total $\chi^2 = 1.93$

**Table 2.1** summarizes our method for accomplishing this. Given the experimentally observed MIDs of three fragments Ala[23], Ala[123] and Val[23], the abundances of any seven Pyr isotopomers are collectively guessed (the abundance of the eighth isotopomer is automatically determined as the eighth isotopomer

abundances of Pyr should sum up to unity), and the three MIDs are predicted on the basis of the guess. Then, the guesses for the Pyr isotopomer abundances are successively refined until a set of abundances is obtained that best matches the experimental MIDs. We use the  $\chi^2$  criterion as a metric for the discrepancy between experimental and predicted MIDs:

$$\chi^2 = \sum_j \left( \frac{l_j - l_j^x}{\sigma_j} \right)^2 \quad (1)$$

where  $l_j^x$  and  $l_j$  are, respectively, the experimentally measured and predicted abundances of the  $j$ th mass isotopomer  $\sigma_j$  is the experimental standard deviation of this isotopomer. Thus, this problem can be cast as an optimization problem with the objective of minimizing  $\chi^2$ . The optimization can be readily solved using the Solver utility in Microsoft Excel or by writing a small MATLAB script. Ultimately, a robust method of determining the isotopomer distribution of a central carbon metabolite such as Pyr, is to estimate it statistically by combining information from the MIDs of all amino acids of which Pyr is a precursor. Furthermore, because many central carbon metabolites are precursors of multiple amino acids and many amino acids have multiple precursors, usually a comprehensive version of the problem illustrated in **Table 2.1** is solved. Amino acids contain redundant metabolic information, and the above method enables leveraging this redundancy toward estimating statistics (means and standard deviations) for the isotopomer distributions of the central carbon metabolite precursors. Also, compartmentalization of amino acid biosynthesis in plants should be considered while performing the analyses described above.

## 2.2.4. Quantification of Flux Ratios at Metabolic Branch Points via Steady State Isotope MFA

Modeling of flux-isotopomer relationships for a simplified, unicompartmental version of glycolysis and the pentose phosphate pathway (PPP) (**Figure 2.3**) is illustrated as an example. An important metabolic branch point in this network is at glucose-6-phosphate (G6P), where carbon traffic splits between glycolysis and the PPP. The flux partitioning at this branch point is difficult to measure on the basis of extracellular measurements alone, making isotope labeling indispensable for accurate evaluation of fluxes through this network.

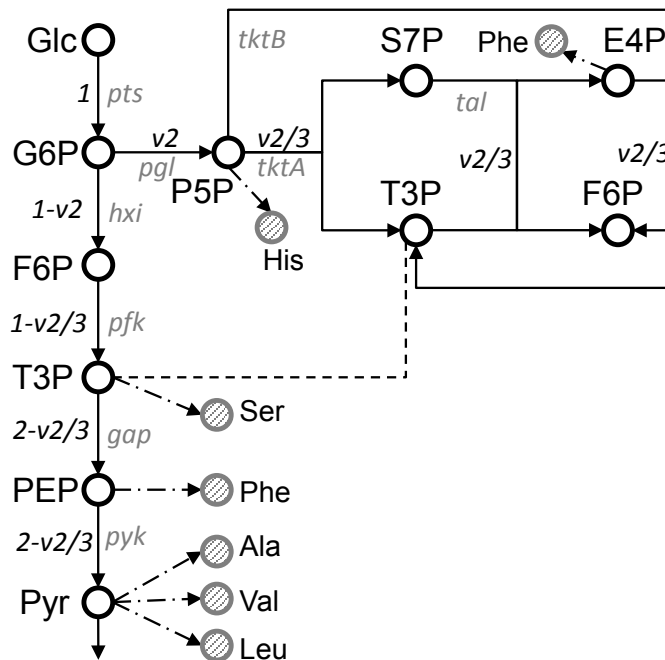


**Figure 2.3** A simplified metabolic network.

Open circles denote carbon atoms of metabolic precursors and gray hashed circles denote carbon atoms of proteinogenic amino acids derived from the precursor(s). Arrows denote net fluxes, with solid lines representing pathway fluxes and dashed-dotted lines representing fluxes toward biomass synthesis. Dashed lines connect multiple occurrences of the same metabolite. Reaction names are marked in gray italic letters. Numbers alongside pathway flux arrows denote expressions for the corresponding fluxes in terms of the *pgl* flux ( $v_2$ ), derived by performing mass balances on the metabolites.

Assumed that all reactions in this network are irreversible in the directions as indicated in **Figure 2.3**, and that natural abundance of  $^{13}\text{C}$  is negligible. However, the realistic version of this problem that relaxes these assumptions and uses appropriately compartmentalized pathways can also be solved by extending the concepts explained here to a computational algorithm. In this figure, the fluxes in the network are expressed in terms of two variables: the glucose uptake flux (arbitrarily set to 1 unit because isotope MFA can only evaluate relative and not absolute fluxes (Isermann and Wiechert, 2003) and the flux of *pgl* reaction, which we choose as a free flux and designate it as  $v_2$ . By performing mass balances on the intracellular metabolites in the network, all other fluxes in the network can be expressed in terms of  $v_2$  as shown in **Figure 2.3**. Below, we discuss how the isotopomers of metabolites in this network, specifically the consolidated triose-3-phosphates (T3P), can be expressed as functions of  $v_2$ . This enables (i) estimation of  $v_2$  given the measurements of these isotopomers, and (ii) assessment of the relative merit of one labeled carbon source over another on the basis of sensitivities of the isotopomer expressions to changes  $v_2$ .

Feeding certain labeled varieties of glucose to the network in **Figure 2.3** will result in isotopomer distributions that depend on the flux split ratio at the G6P branch point. For example, manual isotopomer delineation shows that feeding either 1- $^{13}\text{C}$  or 6- $^{13}\text{C}$  glucose will result in the isotopomers listed in **Table 2.2**.

**Table 2.2 Isotopomer abundances in the glycolysis-PPP network resulting from feeding 1-<sup>13</sup>C or 6-<sup>13</sup>C glucose, expressed in terms of the flux  $v_2$ .**

Labeled carbon atoms are underlined. Carbon atom numbering follows IUPAC rules.

Fed 1- <sup>13</sup> C glucose			Fed 6- <sup>13</sup> C glucose		
Metabolite	Isotopomer	Abundance	Metabolite	Isotopomer	Abundance
G6P	<u>1</u> 23456	100%	G6P	12345 <u>6</u>	100%
P5P	1234 <u>5</u>	100%	P5P	1234 <u>5</u>	100%
S7P	123456 <u>7</u>	100%	S7P	123456 <u>7</u>	100%
E4P	123 <u>4</u>	100%	E4P	123 <u>4</u>	100%
F6P	<u>1</u> 23456	$\frac{3 - 3v_2}{3 - v_2}$	F6P	12345 <u>6</u>	$\frac{6 - 2v_2}{6 - v_2}$
	12345 <u>6</u>	$\frac{3v_2(1 - v_2)}{(3 - v_2)(6 - v_2)}$		123456	$\frac{v_2}{6 - v_2}$
	123456	$\frac{v_2(9 + v_2)}{(3 - v_2)(6 - v_2)}$			
T3P/PEP/Pyr	1 <u>2</u> <u>3</u>	$\frac{3 - 3v_2}{6 - v_2}$	T3P/PEP/Pyr	1 <u>2</u> <u>3</u>	$\frac{3}{6 - v_2}$
	123	$\frac{2v_2 + 3}{6 - v_2}$		123	$\frac{3 - v_2}{6 - v_2}$

To derive isotopomer expressions in terms of  $v_2$ , we proceed as follows:

- 1) Comprehensively delineate the isotopomers. This will generate the isotopomer list shown in **Table 2.2**.
- 2) Perform mass balances on the individual isotopomers by accounting for all generation and consumption fluxes. For example, when 6-<sup>13</sup>C glucose is fed, the balance equation for isotopomer T3P 123 is as follows (underline denotes <sup>13</sup>C, no underline denotes <sup>12</sup>C):

$$\left(1 - \frac{v_2}{3}\right)[F6P\ 123456] + \frac{2v_2}{3}[P5P\ 12345] - \left(2 - \frac{v_2}{3}\right)[T3P\ 123] - \frac{v_2}{3}[T3P\ 123] = 0 \quad (2)$$



where square brackets represent abundance. In Equation (2), the first two terms are generation fluxes for T3P  $12\bar{3}$ : this isotopomer is generated from F6P  $12345\bar{6}$  through the *pfk* reaction whose flux is  $(1 - v_2/3)$ , as well as from P5P  $1234\bar{5}$  through the *tktA* and *tktB* reactions whose combined flux is  $2v_2/3$ . The next (last) two terms in Equation (2) are consumption fluxes for T3P  $12\bar{3}$ , which is consumed by the *gap* and *tal* reactions, whose fluxes are  $(2 - v_2/3)$  and  $v_2/3$ , respectively. Along these lines, isotopomer balance equations can be written for all the other isotopomers in **Table 2.2**. Solving these balances simultaneously will result in the final expressions for the isotopomers in terms of  $v_2$ , as displayed in this table.

After examining the sensitivities of isotopomer abundances to changes in flux values, this information will be utilized in deciding if one labeled version of a carbon source provide more flux information than another labeled variety (Crown and Antoniewicz, 2012; Libourel et al., 2007; Nargund and Sriram, 2013; Wiechert et al., 1999a). As a simple example, we can use the isotopomer expressions derived above to analyze whether an experiment using  $1\text{-}^{13}\text{C}$  glucose or one using  $6\text{-}^{13}\text{C}$  glucose provides superior information on the flux partitioning at the G6P branch point. Assuming that we can only measure the isotopomers of T3P (either directly or via amino acids or biomass components synthesized from T3P), we examine its isotopomer abundances for extreme values of the free flux  $v_2$ . For instance, when  $v_2 = 0$  (all flux through glycolysis), the isotopomer distribution of T3P is  $\{12\bar{3}: 0.5, 12\bar{3}: 0.5\}$  irrespective of whether  $1\text{-}^{13}\text{C}$  glucose or  $6\text{-}^{13}\text{C}$  glucose is fed. When  $v_2 = 1$  (all flux through the PPP), feeding  $1\text{-}^{13}\text{C}$  glucose will result in a distribution of  $\{12\bar{3}: 1.0, 12\bar{3}: 0.0\}$ , whereas feeding  $6\text{-}^{13}\text{C}$  glucose will result in a distribution of  $\{12\bar{3}: 0.40,$

123: 0.60}. Thus, if T3P is the only metabolite whose labeling state can be measured, 1-<sup>13</sup>C glucose is a superior to 6-<sup>13</sup>C glucose because it results in isotopomer distributions that are more sensitive to the flux partitioning between glycolysis and the PPP. However, this situation may change significantly if the isotopomers of both T3P and F6P are measurable, or if the isotopomers of T3P, F6P and P5P are simultaneously measurable.

As discussed above, we relate a flux split ratio at a branch point in a simple metabolic network to the isotopomer distribution of the central carbon metabolite T3P. However, as measuring labeling in amino acids and other biomass components is more practical for steady state isotope MFA, we need to establish relationships between pathway fluxes and amino acid MIDs. For this, we employ the methodology described in Section 2.2.3 and obtain information on the correspondence between the carbon atoms of their central carbon metabolic precursors and the carbon atoms of the proteinogenic amino acids of **Figure 2.3**. This relationship is nearly universal and can be obtained either from the literature (Szyperski, 1998a) or in case of rare organisms with unusual metabolic pathways, by performing targeted labeling experiments. The relationships pertaining to the network of **Figure 2.3** are illustrated in **Table 2.3**. On basis of this, **Figure 2.4** depicts, for an experiment in which 1-<sup>13</sup>C glucose is fed, the MIDs of the amino acid fragments Ala[23] and Leu[23455] for  $v_2 = 0$  (only glycolysis),  $v_2 = 1$  (only PPP) and an intermediate value of  $v_2 = 0.6$ . Because all isotopomer abundances and MIDs are dependent on one flux ( $v_2$ ) in this example, measuring the relevant amino acid MIDs will enable direct determination of  $v_2$ , the carbon partitioning at the G6P branchpoint. However, a realistic network will contain

several flux variables akin to  $v_2$  of the network just discussed, and multiple MID's will be dependent on these flux variables. To model such a circumstance, the concepts used in this simple model need to be generalized and automated, as explained below.

**Table 2.3 Correspondence between the carbon atoms of the amino acids shown in Figure 2.3 and the carbon atoms of their central carbon metabolic precursors.**

Repeated numbers in amino acid fragments indicate chemically identical carbons.

Amino acid	Amino acid fragments	Metabolite source
His	His 12345	P5P 54321
Phe	Phe 123	PEP 123
	Phe 45	PEP 23
	Phe 5667	E4P 1234
Ser	Ser 123	T3P 123
Ala	Ala 123	Pyr 123
Val	Val 124	Pyr 123
	Val 34	Pyr 23
Leu	Leu 12	Pyr 23
	Leu 35	Pyr 23
	Leu 45	Pyr 23

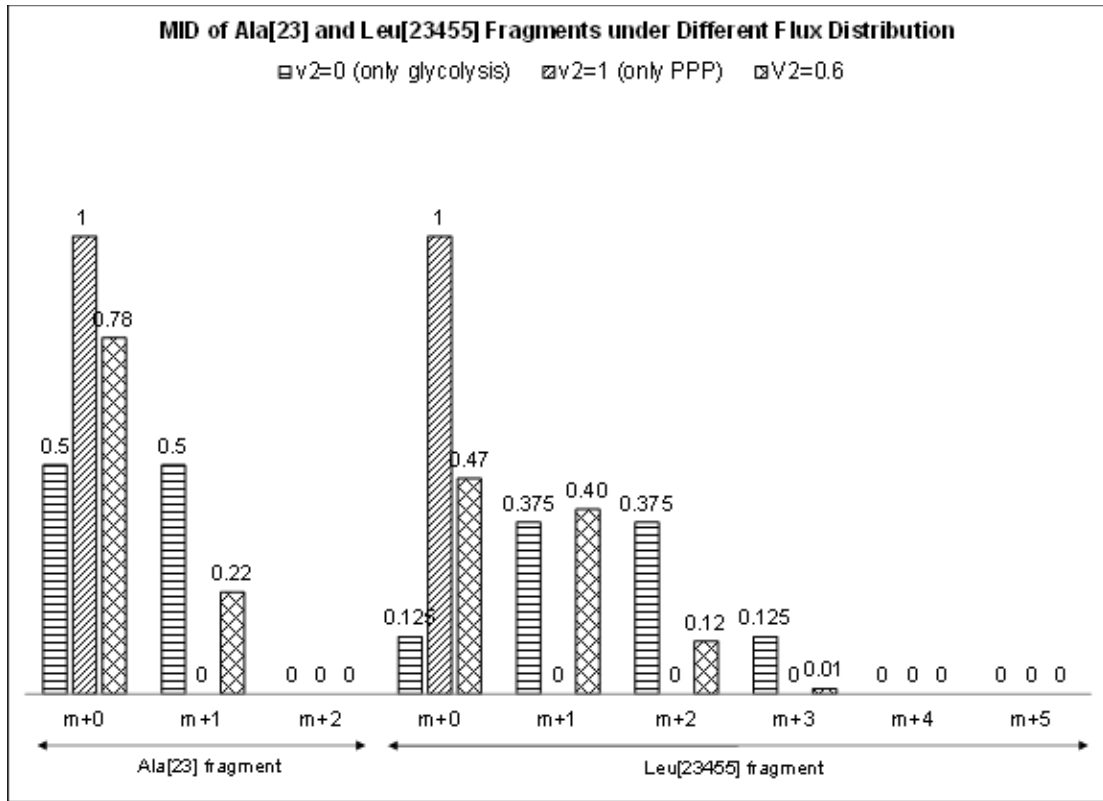


**Figure 2.4** The predicted MIDs of Ala[23] and Leu[23455] fragments under different flux scenarios.

MIDs are calculated on the basis of information provided in **Table 2.2** and **Table 2.3**.

### 2.2.5. General Procedures for Construction of Steady State Models

The steady state modeling for flux evaluation could be generalized as follows:

- 1) Determining the number of free flux variables and using mass balances to derive expressions for fluxes. The assumption of metabolic steady state implies that no metabolite accumulates or depletes in the system (cell or tissue) under consideration. Therefore, for each metabolite, we have the mass balance:

$$\frac{d[M]}{dt} = 0 = \{ \sum v_{in} + \sum v_{generation} \} - \{ \sum v_{out} + \sum v_{consumption} \} \quad (3)$$

where, at metabolic steady state,  $[M]$  is the time-invariant concentration of the metabolite being balanced,  $\Sigma v_{in}$  is the sum of all extracellular fluxes that transport M into the system across its boundary (e.g. the  $v_1$  in the network of Figure 5 transports acetyl-CoA into the system) and  $\Sigma v_{generation}$  is the sum of all fluxes that generate M through chemical reactions. Likewise,  $\Sigma v_{out}$  is the sum of all extracellular fluxes that transport M out of the system across its boundary (e.g. the flux  $v_{10}$  in the network of Figure 5 transports malate [Mal] out of the system) and  $\Sigma v_{consumption}$  is the sum of all fluxes that consume M through chemical reactions. Biomass synthesis fluxes, if significant, are conveniently modeled as extracellular fluxes.

Mass balances for all metabolites in a network can be collected into a matrix equation:

$$\mathbf{G} \cdot \mathbf{v} = 0 \quad (4)$$

where  $\mathbf{G}$  is called the stoichiometric matrix for the network. The matrix  $\mathbf{G}$  represents the mathematical interdependency of the fluxes in the network. Algebraic processing of  $\mathbf{G}$  enables the expression of a large number of “dependent” fluxes in the network in terms of a few “independent” fluxes whose values are known, measured or assumed. For example, in the glycolysis-PPP network discussed in **Figure 2.3**, we expressed all fluxes in terms of two independent fluxes: the glucose uptake flux (a measurement; 1 unit) and the flux variable  $v_2$  (a free flux). In isotope MFA, this expression permits a reduction of the problem, so that the identification of only a few independent fluxes on the basis of the labeling measurements can be followed by the algebraic steps explained below to obtain values and statistics for all fluxes.

2) To express dependent fluxes in terms of independent fluxes, it is first necessary to determine a quantity called the degrees of freedom (DOF) of the network. This quantity is defined as:

$$\begin{aligned} \text{DOF} = & \text{total number of fluxes in the network} - \text{number of intracellular metabolites} \\ & - \text{number of independent extracellular and biomass synthesis} \\ & \text{fluxes in the network} \end{aligned} \quad (5)$$

This expression is valid only if there are no linearly dependent rows (metabolite balances) in  $\mathbf{G}$ . If there are linearly dependent metabolite balances, only an independent set of balances should be counted in Equation (5). A zero DOF indicates that all unknown fluxes in the network can be calculated from the measured extracellular or biomass synthesis fluxes via Equation (4). A positive DOF indicates there are certain “free fluxes” whose values cannot be unequivocally determined from the measured fluxes. Isotope MFA guesses the values of all free fluxes that best account for a given set of isotope labeling measurements (e.g. amino acid MIDs). Once DOF has thus been determined for a network, the flux vector  $\mathbf{v}$  can be split into two vectors  $\mathbf{v}_m$  and  $\mathbf{v}_x$ , such that  $\mathbf{v}_m$  contains the independent fluxes, i.e. the (measured) extracellular and biomass synthesis fluxes as well as the free fluxes, and  $\mathbf{v}_x$  contains the other, dependent fluxes. The matrix  $\mathbf{G}$  can be correspondingly split into matrices  $\mathbf{G}_m$  and  $\mathbf{G}_x$ . Applying this partitioning, Equation (4) can be rewritten as:

$$\mathbf{G} \cdot \mathbf{v} = \mathbf{G}_m \cdot \mathbf{v}_m + \mathbf{G}_x \cdot \mathbf{v}_x = 0 \quad (6)$$

or:

$$\mathbf{v}_x = (\mathbf{G}_x)^{-1}(\mathbf{G}_m \cdot \mathbf{v}_m) \quad (7)$$

which is an expression for the dependent fluxes in terms of the measured and free fluxes. To obtain the unknown  $v_x$ , we need to make use of isotopomer abundance measurements or MIDs.

3) Simulating isotopomer abundances from guessed or given flux values.

Isotopomer balance equations can often be bilinear, which require iterative methods for direct solution. However, the bilinearity can be circumvented by expressing the labeling state in terms of transformed variables such as cumomers (Wiechert et al., 1999a), bondomers (Sriram and Shanks, 2004; W. A. van Winden et al., 2002) (when applicable) or EMUs (Antoniewicz et al., 2007). In this work we employ cumomer expression system. Whereas an isotopomer representation expresses labeling states of individual atoms as labeled (“1”) or unlabeled (“0”), a cumomer representation expresses these labeling states as labeled (“1”) and undetermined or irrelevant (“x”). For example, a three-carbon metabolite has eight isotopomers (000, 100, 010, 110, 001, 101, 011, 111) and eight cumomers (xxx, 1xx, x1x, 11x, xx1, 1x1, x11, 111). Each cumomer is the sum of a certain number of isotopomers, and the cumomer and isotopomer abundance distributions of a metabolite are easily interconvertible (Wiechert et al., 1999a).

The order of a cumomer is the number of atoms in it that are definitively labeled. For example, the cumomer xx1 is order 1, 1x1 is order 2 and 111 is order 3. The advantage of the cumomer representation is that bilinear isotopomer balance equations are transformed into cascades of linear equations. For example, the balances for the first-order cumomers in a network can be written as (8):

$$\text{diag}[X] \cdot \frac{d^1x}{dt} = 0 = {}^1A(v) \cdot {}^1x + {}^1b(v, {}^1x_{\text{inp}}) \quad (8)$$

where  $\text{diag}[X]$  is a diagonal matrix containing metabolite concentrations,  ${}^1x$  is a vector containing all first-order cumomers in the network,  ${}^1A(v)$  is a constant matrix whose entries depend on the flux vector  $v$  and  ${}^1b(v, {}^1x_{\text{inp}})$  is a constant vector whose entries depend on the first-order cumomers of the carbon source fed to the network ( ${}^1x_{\text{inp}}$ ). At isotopic steady state, Equation (8) is linear with  ${}^1x$  as the only unknown, so that it can be solved by matrix inversion or decomposition of  ${}^1A(v)$ :

$$\begin{aligned} 0 &= {}^1A(v) \times {}^1x + {}^1b(v, {}^1x_{\text{inp}}) \\ {}^1x &= -\{ {}^1A(v) \}^{-1} \times {}^1b(v, {}^1x_{\text{inp}}) \end{aligned} \quad (9)$$

Upon solution of the first-order cumomer balances, the second-order cumomer balances become linear at isotopic steady state:

$$0 = {}^2A(v) \cdot {}^2x + {}^2b(v, {}^2x_{\text{inp}}, {}^1x) \quad (10)$$

where  ${}^2x$  is a vector containing all second-order cumomers,  ${}^2A(v)$  is a constant matrix whose entries depend on the flux vector  $v$  and  ${}^2b(v, {}^2x_{\text{inp}}, {}^1x)$  is a constant vector whose entries depend on the known second-order cumomers of the carbon source fed to the network ( ${}^1x_{\text{inp}}$ ) and the already solved first-order cumomer abundances  ${}^1x$ . Again, Equation (10) is linear with  ${}^2x$  as the only unknown, and can be solved by matrix inversion of  ${}^2A(v)$ . This balance can be generalized to  $n$ th-order cumomers:

$$0 = {}^nA(v) \times {}^n x + {}^n b(v, {}^n x_{\text{inp}}, {}^1 x, {}^2 x, \dots, {}^{n-1} x) \quad (11)$$



where the only unknown is  $\mathbf{v}_x$ . As before, this balance can be solved by inverting  $\mathbf{A}(\mathbf{v})$  as above (Wiechert et al., 1999a).

The following overall modeling methodology summarizes the steps described above:

- 1) Assemble the stoichiometric matrix  $\mathbf{G}$  for the network. Determine DOF for the network and choose a valid set of free fluxes accordingly. On the basis of this choice, split the flux vector  $\mathbf{v}$  into  $\mathbf{v}_m$  and  $\mathbf{v}_x$  and correspondingly, split  $\mathbf{G}$  into  $\mathbf{G}_m$  and  $\mathbf{G}_x$ .
- 2) Write cumomer balances from order 1 to the highest order that needs to be simulated in the network.
- 3) Assume values for the free fluxes.
- 4) Using Equation (7) and the current guesses for free fluxes, calculate the values of all fluxes in the network.
- 5) Solve for the cumomer abundances corresponding to the current flux values calculated in step 4.
- 6) Convert the cumomer abundances first to isotopomer abundances and then to MIDs of biomass components, or directly to MIDs of biomass components.
- 7) Compare the predicted MIDs of step 6 with the experimentally obtained MIDs and compute a  $\chi^2$  metric:

$$\chi^2 = \sum_j \left( \frac{I_j - I_j^x}{\sigma_j} \right)^2 \quad (12)$$

where  $l_j^x$  and  $l_j$  are, respectively, the experimentally measured and predicted abundances of the  $j$ th mass isotopomer;  $\sigma_j$  is the experimental standard deviation of this isotopomer.

8) If the value of the  $\chi^2$  metric is acceptable, report the current flux values. Else, use an optimization algorithm to minimize the  $\chi^2$  metric, thereby refining the previous free flux guesses. Then return to step 4 and iterate. In our experience, optimization algorithms require  $\sim 10,000$  or more iterations to converge.

The iterative steps of this methodology are depicted in **Figure 2.5**.

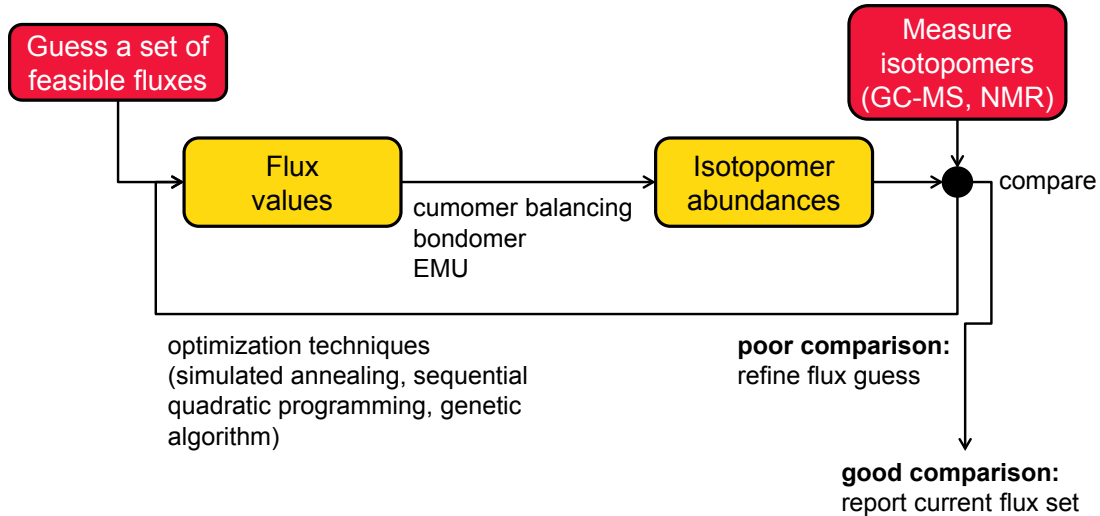


**Figure 2.5 Iterative methodology for evaluating fluxes from isotopomer data.** Adapted from (Wiechert, 2001).

Steady state isotope MFA is essentially a parameter estimation problem wherein the unknown (free) fluxes are parameters that are estimated from isotope labeling data. Therefore, global optimization algorithms are enormously beneficial in refining previous free flux guesses to efficiently arrive at a flux guess that reasonably account for the labeling data. Examples of previously used optimization algorithms include simulated annealing (Onbaşoğlu and Özdamar, 2001), which we use in our

software NMR2Flux+ (Sriram and Shanks, 2004), sequential quadratic programming (Wiechert, 2001), and genetic algorithms. Often, it is helpful to use local optimization algorithms to fine-tune the results of a global search. Programs such as 13CFLUX2 (Weitzel et al., 2012) offer several optimization libraries that users can choose from.

### 2.2.6. Construction of Instationary Models

As explained at the beginning of Section 2.2, instationary models differ from steady state ones in experimental and computational aspects. Experimentally, it is essential to obtain transient measurements of labels and if feasible, metabolite concentrations. Computationally, it is necessary to solve the isotopomer balance equations as functions of time. Thus, the steady state n-order cumomer balance now becomes an instationary balance:

$$\text{diag}[X] \cdot \frac{d^n x}{dt} = {}^n A(v) \cdot {}^n x + {}^n b(v, {}^n x_{inp}, {}^1 x, {}^2 x, \dots, {}^{n-1} x) \quad (13)$$

The cascades of algebraic equations encountered in the steady state model now become cascades of ordinary differential equations. The extensive nature of computation in instationary models makes flux evaluation a lengthy process. Despite this, flux evaluation for relatively small networks can be performed by using home-grown MATLAB or C code. While methods for detailed flux evaluation have been presented in detail (Nöh and Wiechert, 2006; Young et al., 2011a, 2008), a few points are listed from our experience:

- 1) For instationary experiments involving a single carbon source containing exactly one carbon atom (e.g.  $^{13}\text{CO}_2$ ), much of the labeling information is available in

the first- and second-order cumomers. Therefore, it is unadvisable to expend computational resources to simulate cumomer abundances beyond the second order. Often, this will save significant simulation time with minimal loss of information.

2) It is important that the matrices  $^n A(v)$  are well-conditioned, with condition numbers between 1 and 100. This prevents complex eigenvalues from occurring during matrix decomposition.

### **3. Isotope Labeling Experiments and Metabolic Flux**

#### **Analysis Elucidate a C<sub>4</sub> Photosynthetic Pathway in the Unicellular Diatom *Phaeodactylum tricornutum***

This chapter was submitted as a manuscript to *Metabolic Engineering*, and is currently under revision after peer review. If accepted for publication, copyright is likely to be transferred to Elsevier.

Yuting Zheng<sup>1</sup> and Ganesh Sriram<sup>1,2</sup>.

<sup>1</sup>Department of Chemical and Biomolecular Engineering, University of Maryland

<sup>2</sup>Principal investigator and corresponding author

#### **3.1. Introduction**

Photosynthesis is indispensable to both life and sustainable economic development because it generates molecular oxygen and reduced carbon toward respiration, food, fuel (Vega-Sánchez and Ronald, 2010; Yuan et al., 2008) and chemical industry feedstocks (Nikolau et al., 2008; Shanks, 2005; Yoon et al., 2013). A rapidly growing human population and an increasing need for renewable fuel and carbon warrant a two-fold or greater increase in photosynthetic output over the next few decades, despite scarcer land availability for agriculture (Zhu et al., 2010a). In this context, investigating the metabolism of photosynthetically efficient organisms may facilitate metabolic engineering for enhanced photosynthetic productivity.

However, most natural photosynthesis is sluggish, because physical constraints force its principal enzyme ribulose biphosphate carboxylase/oxygenase (RuBisCO) to operate at sub-maximal rates (Ellis, 2010; Yokota and Shigeoka, 2008). RuBisCO-catalyzed photosynthesis is the most efficient natural process for harvesting light energy and reducing CO<sub>2</sub> (Boyle and Morgan, 2011). RuBisCO, which catalyzes the first metabolic step of this process, can only utilize molecular CO<sub>2</sub> rather than charged alternatives such as HCO<sub>3</sub><sup>-</sup> or CO<sub>3</sub><sup>2-</sup>. A typical atmospheric CO<sub>2</sub> concentration of ~400 ppm equilibrates with an aqueous CO<sub>2</sub> concentration of ~13 μM; therefore, atmospheric CO<sub>2</sub> is sparingly soluble in water (**Figure 3.1**). This low solubility restricts CO<sub>2</sub> concentration in the vicinity of RuBisCO to ~6 μM (Evans and Loreto, 2004; Heldt and Piechulla, 2010) (**Figure 3.2a**). This is significantly lower than typical  $K_m$  values of RuBisCO for CO<sub>2</sub>, which are ~30 μM or higher (Yokota and Shigeoka, 2008), implying that RuBisCO usually operates at a small fraction of its maximal rate. Photosynthesis is also inefficient because O<sub>2</sub> is a competitive inhibitor of RuBisCO (Heldt and Piechulla, 2010), and this competition tilts significantly in favor of O<sub>2</sub> at temperatures over 30 °C, resulting in a process called photorespiration (Jamai et al., 2009) that wastes up to 25% of the carbon assimilated by photosynthesis (Ellis, 2010).

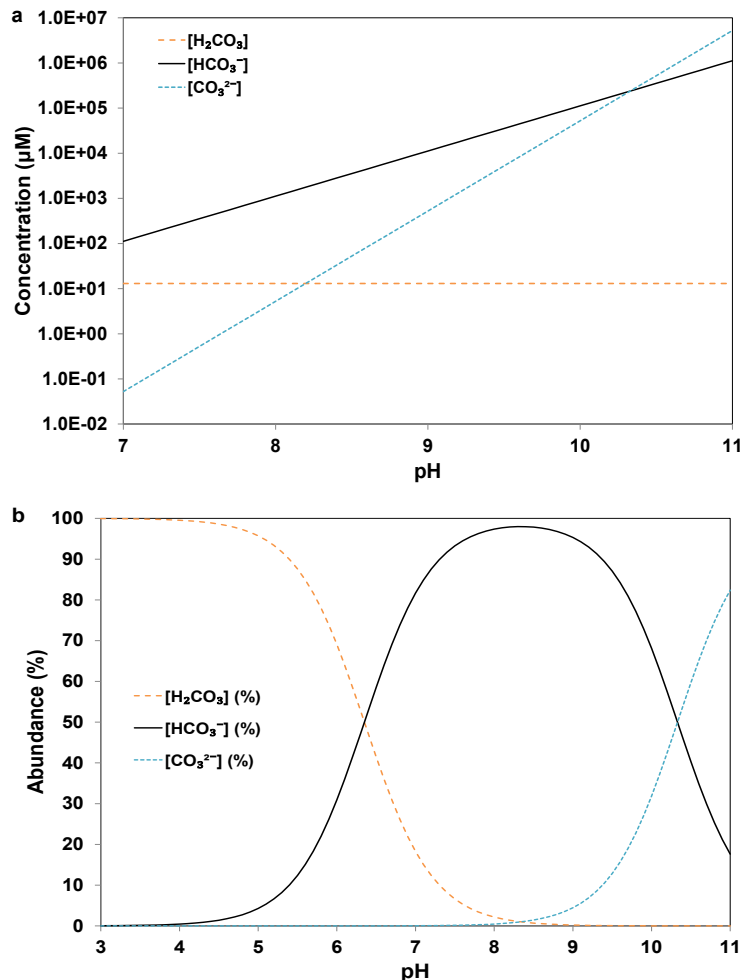


**Figure 3.1 pH-dependence of (a) equilibrium aqueous concentrations and (b) relative aqueous abundances of three forms of CO<sub>2</sub>: H<sub>2</sub>CO<sub>3</sub> (= CO<sub>2</sub> + H<sub>2</sub>O), HCO<sub>3</sub><sup>-</sup> and CO<sub>3</sub><sup>2-</sup>.**

The concentration of dissolved molecular CO<sub>2</sub> in equilibrium with atmospheric (400 pm) CO<sub>2</sub> is 13 μM and is invariant with pH. The corresponding concentration of the hydrated form H<sub>2</sub>CO<sub>3</sub> is 25 μM. H<sub>2</sub>CO<sub>3</sub> sequentially dissociates into HCO<sub>3</sub><sup>-</sup> and CO<sub>3</sub><sup>2-</sup> as per the reactions:



Therefore, the variation of HCO<sub>3</sub><sup>-</sup> and CO<sub>3</sub><sup>2-</sup> concentrations with pH can be obtained by simultaneously solving the following relationships:

$$K_1 = \frac{[H^+][HCO_3^-]}{H_2CO_3}, K_2 = \frac{[H^+][CO_3^{2-}]}{HCO_3^-}$$

We prepared these plots by using standard values of  $K_1 = 4.47 \times 10^{-7}$  M and  $K_2 = 4.68 \times 10^{-11}$  M. The overall solubility of CO<sub>2</sub> (i.e., the combined solubility of all three species) increases with pH. At the typical pH of seawater (8.0 to 8.2), HCO<sub>3</sub><sup>-</sup> is the overwhelmingly dominant species at a concentration of 1000 to 1800 μM, whereas CO<sub>2</sub> and CO<sub>3</sub><sup>2-</sup> have concentrations in the range of ~10 μM. The abundance of HCO<sub>3</sub><sup>-</sup> peaks at of 8.4, where it constitutes 98% of dissolved inorganic carbon.

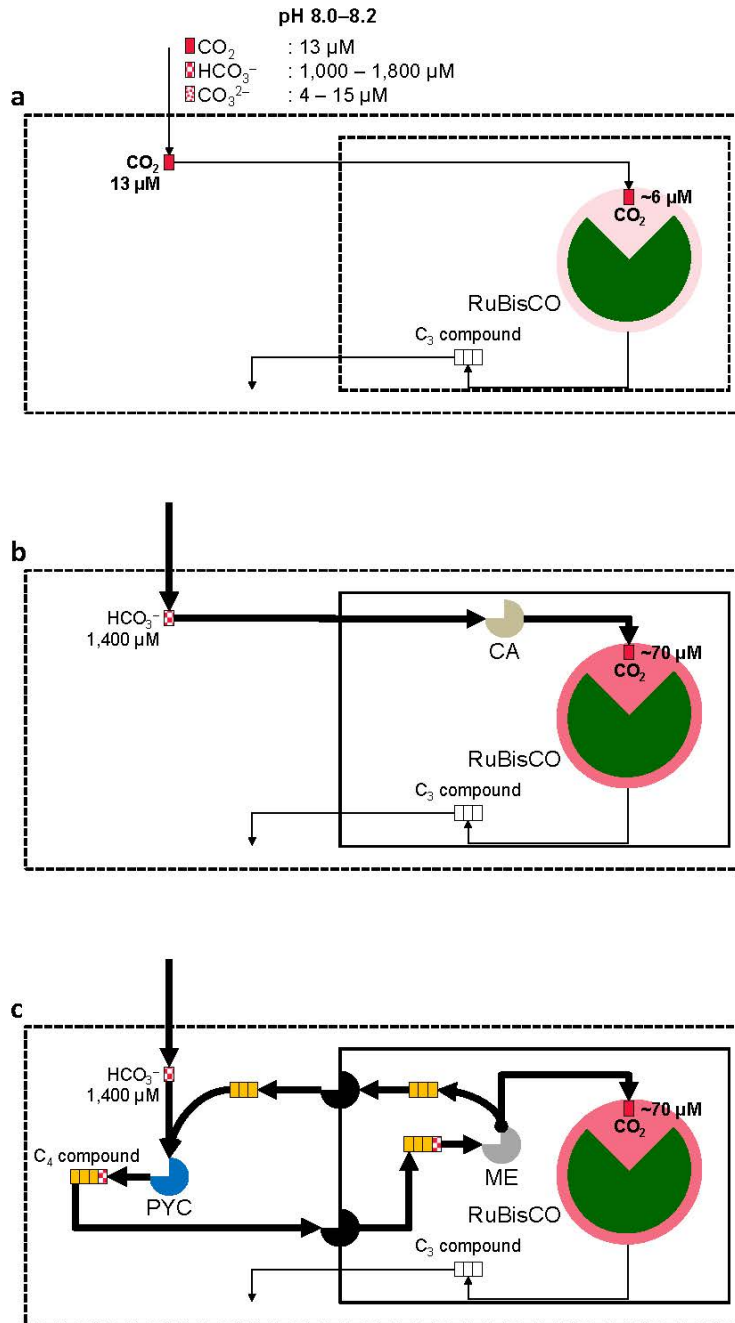


**Figure 3.2 Hypothesized CCMs in diatoms.**

Pie-shaped objects represent enzymes: green, RuBisCO; gold, CA; blue, PYC; gray, ME; black, intercompartmental transporters. The intensity of red color around RuBisCO signifies the CO<sub>2</sub> concentration in its vicinity. Rectangles denote carbon atoms, with different fill colors and patterns corresponding to different chemical structures. Arrows signify hypothesized flux distributions, with thicknesses proportional to flux values. Dashed lines denote CO<sub>2</sub>-permeable membranes; solid lines denote membranes relatively impermeable to CO<sub>2</sub>.



These two impediments to photosynthesis can be eliminated if CO<sub>2</sub> could be “pumped” to a sufficient concentration around RuBisCO. A small minority of photosynthetic organisms accomplish this via one of two carbon-concentrating mechanisms (CCMs): (i) a biophysical CCM (**Figure 3.2b**) or (ii) a biochemical “C<sub>4</sub>” CCM (**Figure 3.2c**). Both these CCMs utilize HCO<sub>3</sub><sup>-</sup>, the dominant form of dissolved inorganic carbon in water above pH 7 (**Figure 3.1**). The biophysical CCM uses carbonic anhydrase (CA) to convert HCO<sub>3</sub><sup>-</sup> to CO<sub>2</sub> in the vicinity of RuBisCO (Duanmu et al., 2009) (**Figure 3.2b**). Contrastingly, the C<sub>4</sub> CCM uses anaplerotic enzymes to condense HCO<sub>3</sub><sup>-</sup> with a C<sub>3</sub> compound such as phosphoenolpyruvate (PEP) or pyruvate (Pyr), resulting in a C<sub>4</sub> compound such as oxaloacetate (OAA) or malate (Mal). The C<sub>4</sub> compound is transported to a different cell or subcellular compartment, where it is enzymatically decarboxylated to release CO<sub>2</sub> in the vicinity of RuBisCO (Yokota and Shigeoka, 2008) (**Figure 3.2c**). By spatially separating the site of HCO<sub>3</sub><sup>-</sup> capture from the site of CO<sub>2</sub> release near RuBisCO, cells can achieve CO<sub>2</sub> concentrations from 70 μM (Heldt and Piechulla, 2010) to even 500 μM (Yokota and Shigeoka, 2008) around RuBisCO. Although the orchestration of the C<sub>4</sub> CCM usually requires multiple cell types, circumstantial evidence for single-cell C<sub>4</sub> CCMs has been found in certain plants and unicellular photosynthetic microorganisms (Voznesenskaya et al., 2001, 2002; Sage, 2002; Edwards et al., 2004; Akhani et al., 2005; Park et al., 2010; Reinfelder et al., 2000).

Despite their rarity in the plant kingdom, CCM-operating species are often ecologically successful, e.g. many grasses and weeds, and their CCMs are thought to contribute largely to this success (Long, 1999). Not surprisingly, researchers have

attempted engineering conventional, CCM-lacking plants such as rice to express putative C<sub>4</sub> enzymes. However, these attempts have met with limited success (Sheehy et al., 2007), possibly because enzyme overexpression may not be adequate to mimic the metabolic mechanisms underlying a C<sub>4</sub> CCM (Kajala et al., 2011; Furbank et al., 2009). All this points to an urgent need to mechanistically investigate C<sub>4</sub> CCMs. In this regard, single-cell C<sub>4</sub> CCMs are of particular interest not only because of their fascinating biology, but also from a metabolic engineering standpoint as it should be easier to engineer single-cell C<sub>4</sub> CCMs than multicellular ones requiring specialized cell types.

A class of unicellular, marine algae called diatoms may facilitate detailed investigations of single-cell C<sub>4</sub> CCMs. Diatoms are reported to contribute substantially to global CO<sub>2</sub> fixation, assimilating between 20% to 40% of the 100 billion metric tons of CO<sub>2</sub> fixed on the Earth annually (Bowler et al., 2008; De Riso et al., 2009; Falkowski et al., 1998; Kroth et al., 2008; Smetacek, 1999; Tesson et al., 2009). This, combined with their thriving in low-CO<sub>2</sub> environments (Burkhardt et al., 2001), suggests that they may operate CCMs. However, the exact nature of their CCMs is debated (Kroth et al., 2008; Reinfelder et al., 2004), with existing evidence pointing toward both C<sub>4</sub> (e.g. Reinfelder et al., 2000) and biophysical (Hopkinson et al., 2011) CCMs (reviewed in Reinfelder, 2011).

The diatom *Phaeodactylum tricornerutum* has a sequenced genome (Bowler et al., 2008) and available genetic toolkits (e.g. De Riso et al., 2009) that make it a model organism to dissect CCMs in photosynthesis. *P. tricornerutum* is hypothesized to operate a CCM; however, there is controversy about whether this is a biophysical or a

C<sub>4</sub> CCM. Bioinformatic analyses of *P. tricornutum*'s annotated genome initially showed that it may possess the enzymatic machinery to operate both a biophysical and a C<sub>4</sub> CCM (Kroth et al., 2008). Subsequently, circumstantial and direct evidence for a biophysical CCM as well as circumstantial evidence for a C<sub>4</sub> CCM have been reported. For example, the localization of several putative CAs in the chloroplast (reviewed in Reinfelder, 2011) and direct <sup>18</sup>O isotopic data describing the role of CA in efficiently concentrating CO<sub>2</sub> in the chloroplast (Hopkinson et al., 2011) are strong pointers to a biophysical CCM. In contrast, the expression of genes encoding putative C<sub>4</sub> enzymes in a coordinated manner (e.g. Valenzuela et al., 2012) or in response to light or high dissolved inorganic carbon concentrations (Chauton et al., 2013; Maheswari et al., 2010; Nymark et al., 2009), provides circumstantial evidence for a C<sub>4</sub> CCM. Evidence against a C<sub>4</sub> CCM has also been reported by Haimovich-Dayana et al. (2013), who suppressed a gene encoding a seemingly crucial C<sub>4</sub> enzyme Pyruvate orthophosphate dikinase (PPDK) and found that this did not reduce the overall photosynthetic  $K_{1/2}$  for CO<sub>2</sub>.

In addition to the controversy about the type of CCM operated by *P. tricornutum*, many profound questions about single-cell C<sub>4</sub> CCMs remain shrouded in mystery, such as: (i) the metabolic flux patterns accompanying the CCMs, (ii) the carbon-concentrating efficiency of the CCMs, (iii) the identities of the molecules, enzymes and genes that participate in the mechanism, and (iv) whether C<sub>4</sub> and biophysical CCMs can operate concomitantly in the same organism. To begin unraveling the answers to these questions, it is necessary to use metabolic engineering tools such as isotope-assisted metabolic flux analysis (MFA) (Ahn and Antoniewicz,

2013; Alonso et al., 2011; Feng et al., 2010b; Sriram et al., 2004; Wiechert and Nöh, in press; Young et al., 2011b).

In this work, we test the hypothesis that *P. tricornutum* operates a C<sub>4</sub> CCM. Toward this, we report the first use of isotope-assisted steady-state and instationary MFA on *P. tricornutum*. We performed isotope labeling experiments (ILEs) by feeding several <sup>13</sup>C- and <sup>12</sup>C- labeled carbon sources including atmospheric CO<sub>2</sub>, dissolved HCO<sub>3</sub><sup>-</sup>, glucose, acetate and aspartic acid (Asp), individually or in combination. Then, we used mass spectrometry (MS) to measure the incorporation of these carbon sources into soluble metabolites and biomass components at timescales ranging from a few minutes to three weeks, and analyzed selected ILEs by employing flux-isotopomer models to obtain metabolic flux maps. These experiments and analyses confirmed our hypothesis, showing that *P. tricornutum* incorporates significant HCO<sub>3</sub><sup>-</sup> via a C<sub>4</sub> CCM. This article presents the results of our ILEs and discusses how our isotope labeling data and its analysis led to this conclusion. We anticipate that the knowledge obtained from this investigation will have important implications toward metabolic engineering of diatoms and other organisms for improved CO<sub>2</sub> fixation, and ultimately toward engineering synthetic CO<sub>2</sub>-sequestering devices.

## **3.2. Materials and Methods**

### **3.2.1. Cell Culture**

The marine diatom *P. tricornutum* (strain CCMP 632) was obtained from the Provasoli-Guillard National Center for Marine Algae and Microbiota (NCMA) (East Boothbay, ME), and was maintained aseptically by subculturing every two weeks. This culture was grown in 125 mL Erlenmeyer flasks containing 50 mL L1 culture medium (NCMA). The flasks were placed at 24.5 °C under constant light in refrigerated New Brunswick Innova 44R shakers (Eppendorf Hauppauge, NY) with a 2-inch stroke and programmable temperature, light and photoperiod controls. The photosynthetic photon flux density inside the shaker is  $20 \pm 2 \mu\text{mol m}^{-2} \text{s}^{-1}$  during the period of experiments, measured by Apogee MQ-100 Quantum Meter (Apogee Instruments, UT).

### **3.2.2. Quantification of Mass Isotopomer Abundances and Metabolite Pool Sizes by GC-MS**

All GC-MS analyses were performed on a Varian 300MS quadrupole GC-MS unit (Bruker Corporation, Fremont, CA), equipped with an autoinjector and a VF5-ms column of dimensions 0.25 mm  $\times$  30 m  $\times$  0.25  $\mu\text{m}$ . Typically, 1  $\mu\text{L}$  of derivatized amino acids or soluble metabolites, in 1 to 4 technical replicates, was automatically injected at a split ratio of 1:15, with helium as the carrier gas at a constant flow rate of 1.0 mL  $\text{min}^{-1}$ . For analysis of proteinogenic amino acids, the oven temperature was initially held at 150°C for 2 min, then increased at 3°C  $\text{min}^{-1}$  to 250°C and then at

10°C min<sup>-1</sup> to 275°C, where it was held constant up to a run time of 43 min. For soluble metabolite analysis, the oven temperature initially held at 150°C for 2 min, then increased at 2°C min<sup>-1</sup> to 175°C where it was held for 2 min, and then increased at 3°C min<sup>-1</sup> to 240°C for a total run time of 38 min. The MS ran in electron ionization mode with a collection delay for 3 min. Mass spectra were recorded in the selected ion monitoring (SIM) mode. All mass spectral data were analyzed and quantified with the manufacturer's Varian MS Workstation software (Bruker, Billerica, MA). Raw mass spectral data were processed to filter out natural abundances of elements other than metabolic carbon, using a previously developed in-house MATLAB program (see Supplementary Material of Sriram et al., 2008), whose accuracy has been verified by us by processing a variety of amino acid isotopomer mixtures of known isotopomeric compositions (data not shown). The resulting mass isotopomer distribution (MID) data were converted to <sup>13</sup>C enrichments of individual amino acid fragments by using singular value decomposition (SVD). Briefly, a "measurement matrix" (Möllney et al., 1999) was used to map all the cumomers of each relevant metabolite to its measurable MIDs. The forward problem of calculating the MIDs from the cumomer abundances is always solvable; however, there may not be sufficient information to solve the inverse problem of calculating the cumomer abundances from the MIDs. In such a case, SVD of the measurement matrix (Press et al., 2007) provides information on which cumomer abundances or sums of cumomer abundances can be evaluated from the MIDs. Using this information and the pseudoinverse of the measurement matrix as reconstructed from SVD, we obtained the <sup>13</sup>C enrichments of only those atoms or fragments that were

calculable from the data. The accuracy of the SVD method for obtaining  $^{13}\text{C}$  enrichments was verified by processing a synthetic set of amino acid MIDs and ensuring that this method yielded the expected enrichment values (G Sriram, unpublished calculations). Selected MIDs and  $^{13}\text{C}$  enrichments are shown and discussed in Results.

### **3.2.3. Instationary $\text{H}^{13}\text{CO}_3^-$ ILE, Intracellular Metabolite Extraction and Derivatization**

Cells were cultured in L1 medium for six weeks to obtain sufficient biomass. After this period, cell suspensions were first centrifuged at  $8873 \times g$  for 5 min. Most of the supernatant medium was removed, leaving the cells suspended in  $\sim 1$  mL of medium. The cells were slightly mixed by shaking and transferred to 2 mL microcentrifuge tubes, after which the supernatant was removed by centrifugation at  $6039 \times g$ . To set up the instationary ILE, 0.5 mL of L1 medium containing  $35 \text{ g L}^{-1}$   $\text{NaH}^{13}\text{CO}_3$  was added to each microcentrifuge tube, and the cells were resuspended by shaking quickly with the photosynthetic photon flux density measured  $18 \pm 1 \mu\text{mol m}^{-2} \text{ s}^{-1}$  during the period of experiments. Enough tubes were set up so that six time points (1 min, 2 min, 5 min, 8 min, 12 min and 20 min) could each be represented by three biological replicates. The time points were staggered so that the three replicates for each time point could be simultaneously and precisely quenched and harvested. At the appropriate time points, tubes were immediately dropped into liquid nitrogen to quench metabolism. Another longer instationary ILE that lasted 480 min (8 h) was performed in triplicate in shake flasks, followed by cell harvesting, centrifugation and

quenching as described above. To quantify metabolite pool sizes (concentrations), during the period the ILE was conducted, cells were separately grown for six weeks in three replicate flasks containing L1 medium, followed by quenching, metabolite extraction and quantification.

To isolate intracellular metabolites after quenching, 0.7 mL boiling methanol and 25  $\mu$ L deionized H<sub>2</sub>O were added to the tubes, which were then incubated in a water bath at 30 °C to 35 °C for 30 min. When the liquid in the tubes turned green (due to secretion of chlorophyll from the ruptured cells) and white flocculent precipitates appeared, 0.7 mL deionized H<sub>2</sub>O and 0.37 mL chloroform were added. After vortexing, the tubes were centrifuged at 17,000 x g at 4 °C for 10 min. The upper methanol/H<sub>2</sub>O layer was collected and evaporated overnight in a RapidVap at room temperature and 65 m bar. The dried sample was dissolved in 80  $\mu$ L deionized H<sub>2</sub>O, transferred to a 300  $\mu$ L GC vial and lyophilized overnight. The lyophilized residue was reconstituted in 50  $\mu$ L of a freshly made solution of 20 mg mL<sup>-1</sup> methoxyamine hydrochloride in pyridine, in a GC vial at 30 °C for 90 min. This sample was then derivatized with 50  $\mu$ L MTBSTFA + 1% TBDMCS at 70 °C for 30 min. The derivatized sample was injected into a GC-MS, using DMF as solvent. Furthermore, one more instationary ILE lasting 6 d (144 h) was performed in triplicate in shake flasks. Since a significant amount of biomass can be expected to accumulate in such a long ILE, we measured isotopomer abundances of proteinogenic amino acids as described in **Sec. 3.2.3**. MIDs obtained from the instationary ILE are listed in appendix **Table A.1**.



### 3.2.4. Evaluation of Metabolic Fluxes from Instationary Isotopomer Data

For flux evaluation from the instationary  $\text{H}^{13}\text{CO}_3^-$  ILE, we used the model listed in **Table 3.1**.

**Table 3.1**  $\text{H}^{13}\text{CO}_3^-$  instationary ILE: metabolic model and evaluated fluxes.

Flux		Reaction	Net flux	Flux SD	Reversibility
v <sub>1</sub>	<i>co2in</i>	→ $\text{HCO}_3^-$	0.06	0.01	
v <sub>2</sub>	<i>pppin</i>	→ P5P	0.07	0.01	
v <sub>3</sub>	<i>oaain</i>	→ OAA	0.11	0.02	
v <sub>4</sub>	<i>pepcf</i>	PEP (123) + $\text{HCO}_3^-$ (4) → OAA (1234)	0.03	0.00	
v <sub>5</sub>	<i>otranf</i>	OAA (1234) → Asp (1234)	0.05	0.01	
v <sub>6</sub>	<i>otranb</i> p	Asp (1234) → OAAp (1234)	0.05	0.01	
v <sub>7</sub>	<i>pepcbp</i>	OAAp (1234) → CO <sub>2</sub> (4) + PEP (123)	0.05	0.01	
v <sub>8</sub>	<i>c4refix</i>	CO <sub>2</sub> (1) + P5P (23456) → 3PG (132) + 3PG (456)	0.05	0.01	
v <sub>9</sub>	<i>c3fix</i>	$\text{HCO}_3^-$ (1) + P5P (23456) → 3PG (132) + 3PG (456)	0.02	0.00	
v <sub>10</sub>	<i>lacdh</i>	PEP (123) → Lac (123)	0.02	0.01	
v <sub>11</sub>	<i>maldh</i> b	OAA (1234) ↔ Mal (1234)	0.09	0.02	0.91
*v <sub>1</sub> 2	<i>fumab</i>	Mal (1234) ↔ Fum (1234)	0.09	0.02	0.92
*v <sub>1</sub> 3	<i>fumabs</i>	Mal (1234) ↔ Fum (4321)	0.09	0.02	0.92
*v <sub>1</sub> 4	<i>sucdhb</i>	Fum (1234) ↔ Succ (1234)	0.09	0.02	0.78
*v <sub>1</sub> 5	<i>sucdhs</i>	Fum (1234) ↔ Succ (4321)	0.09	0.02	0.78
v <sub>16</sub>	<i>3pgout</i>	3PG →	0.07	0.01	
v <sub>17</sub>	<i>lacout</i>	Lac →	0.02	0.01	
*v <sub>1</sub> 8	<i>sucout</i>	Succ →	0.09	0.02	

Fluxes with \* were included in modeling, but simulation result of metabolites involved (Mal, Fum and Succ) is not optimized with measurements in this model.

We assumed that metabolic steady state was maintained under constant light during the 30 min to 8 h time frame of the instationary ILE. Therefore, flux values

and metabolite pool sizes were constant in our model. All ILE simulations were performed in MATLAB (The Mathworks, Natick, MA). Using the metabolic network described in Results, we assembled a stoichiometric matrix  $\mathbf{S}$  and flux vector  $\mathbf{v}$ . To determine a set of fluxes that accounted for the instationary isotopomer measurements, we proceeded as follows. Assuming the fluxes  $CO2in$ ,  $pepcf$ ,  $pppin$  and  $oaain$  to be the free fluxes, we calculated the remaining fluxes in the network using the equation  $\mathbf{v}_x = -\mathbf{S}_x^{-1} \cdot (\mathbf{S}_m \cdot \mathbf{v}_m)$ , where  $\mathbf{v} = [\mathbf{v}_m \mid \mathbf{v}_x]$  is a partitioning of  $\mathbf{v}$  into independent (measured and free;  $\mathbf{v}_m$ ) and dependent ( $\mathbf{v}_x$ ) fluxes, and  $\mathbf{S} = [\mathbf{S}_m \mid \mathbf{S}_x]$  is a corresponding partitioning of  $\mathbf{S}$ . Then, we used these fluxes  $\mathbf{v}$  to solve cumomer balances (Möllney et al., 1999) of the form:

$$\mathbf{P} \cdot \frac{d(\boxed{{}^1\mathbf{x}})}{dt} = {}^1\mathbf{A}(\mathbf{v}) \cdot \boxed{{}^1\mathbf{x}} + {}^1\mathbf{b}(\mathbf{v}, {}^1\mathbf{x}_{inp}) \quad (14)$$

$$\mathbf{P} \cdot \frac{d(\boxed{{}^2\mathbf{x}})}{dt} = {}^2\mathbf{A}(\mathbf{v}) \cdot \boxed{{}^2\mathbf{x}} + {}^2\mathbf{b}(\mathbf{v}, {}^1\mathbf{x}, {}^2\mathbf{x}_{inp}) \quad (15)$$

where  ${}^1\mathbf{x}$  and  ${}^2\mathbf{x}$  are first- and second-order cumomer vectors,  ${}^1\mathbf{x}_{inp}$  and  ${}^2\mathbf{x}_{inp}$  are first and second-order vectors consisting of cumomers input to the system through the carbon source ( $NaH^{13}CO_3$ ),  ${}^1\mathbf{A}(\mathbf{v})$  and  ${}^2\mathbf{A}(\mathbf{v})$  are stoichiometric balance matrices,  ${}^1\mathbf{b}$  and  ${}^2\mathbf{b}$  are vectors whose elements are functions of the known quantities indicated in parentheses, and  $\mathbf{P}$  is a diagonal matrix containing metabolite pool sizes (Wiechert and Wurzel, 2001). The unknown quantities in Eqs. (14) and (15) are enclosed in boxes. Because of their linearity, Eqs. (14) and (15) could be solved sequentially by matrix inversion. We did not simulate cumomers higher than second-order, as these would have very small abundances in our model. To determine metabolite pool sizes and free fluxes that accounted for our instationary isotopomer measurements, we

guessed values of these parameters and iteratively refined these guesses, using an in-house simulated annealing global optimization routine until convergence was obtained.

During each iteration of this optimization routine, we evaluated the  $^{13}\text{C}$  enrichment of each metabolite or metabolite fragment on the basis of its (i) experimentally measured MIDs and (ii) simulated cumomer abundances. We then evaluated a  $\chi^2$  metric that represented the goodness of fit between the simulated ( $e_{sim}$ ) and experimental ( $e_{exp}$ ) enrichments:

$$\chi^2 = \frac{(e_{sim} - e_{exp})^2}{\sigma^2} \quad (16)$$

where  $\sigma$  is the measurement error of the enrichment. The global optimization was allowed to run until it converged to a  $\chi^2$  minimum, at which point the corresponding parameter set was recorded. Metabolic fluxes and confidence intervals were then calculated based upon parameter sets obtained from repeated runs of the global optimization from different starting points.

### **3.2.5. Gene Expression Analysis by Quantitative Real-time Polymerase Chain Reaction (qRT-PCR)**

Cells were aseptically grown in 125 mL Erlenmeyer flasks containing 50 mL L1 culture medium for 9 d to obtain sufficient biomass. On day 9, the flasks were apportioned into four groups to assess the effects of six conditions on gene expression: (i) light/L1, (ii) dark/L1, (iii) light/ $\text{HCO}_3^-$ , (iv) dark/ $\text{HCO}_3^-$ , (v) light/Glc and (vi) dark/Glc, with each condition being represented by three biological replicates. Flasks

in the first two groups (L1) continued to be incubated in (50 mL of) L1 medium, whereas those in the remaining four groups ( $\text{HCO}_3^-$  and Glc) were incubated in (50 mL of) L1 medium supplemented aseptically with 0.5 mL of 33 g  $\text{L}^{-1}$   $\text{NaHCO}_3$  solution and 0.5 mL of 200 g  $\text{L}^{-1}$  glucose solution, respectively. After incubation for 14 h under constant light, flasks from the dark/L1, dark/ $\text{HCO}_3^-$  and dark/Glc groups were incubated in complete darkness for 90 min. Following this, the cell suspension from each flask was centrifuged at 8873 x g for 5 min. Wet cell pellets suspended in less than 0.5 mL medium were transferred to separate 2 mL sterilized micro-centrifuge tubes and quenched immediately by liquid nitrogen. RNA was extracted with RNeasy Plant Mini Kits and RNase-Free DNase Set (QIAGEN, Valencia, CA). RNA concentrations in the extracts were measured by a NanoDrop 2000 UV-Vis spectrophotometer (Thermo Scientific). cDNA was synthesized from RNA using a High Capacity RNA-to-cDNA Kit (Life Technologies, Grand Island, NY) and random primers. qRT-PCR analyses were conducted with Power SYBR Green PCR Master Mix (Life Technologies) on a 7500 Real-Time PCR System (Life Technologies). The genes encoding 18S rRNA (*18S*), histone 4 (*HIS4*) and elongation factor 1 $\alpha$  (*EF1 $\alpha$* ) were used as housekeeping genes (Siaut et al., 2007). The gene-specific primers used for amplification are listed in **Table 3.2**. The three biological replicates for each condition were each analyzed three times. For each of the four conditions tested, gene expression fold changes relative to the dark/L1, dark/ $\text{HCO}_3^-$  and dark/Glc conditions were obtained by using the  $2^{-\Delta\Delta C_t}$  method (Livak and Schmittgen, 2001), and statistical significance was determined by using a Student's *t*-test.

**Table 3.2 Primers used for qRT-PCR**

Gene group	Gene name	Primer sequence	
Housekeeping genes	<i>18s</i>	Forward	5'-GATCCATTGGAGGGCAAGTC-3'
		Reverse	5'-ACAGCAACGGCCAACTAAGG-3'
	<i>HIS4</i>	Forward	5'-AGGTCCTTCGCGACAATATC-3'
		Reverse	5'-ACGGAATCACGAATGACGTT-3'
	<i>EF1<math>\alpha</math></i>	Forward	5'-GCGGTCCTCGTCATTGACTC-3'
		Reverse	5'-TTCGGCGTACTTGACGGTCT-3'
Target genes	<i>PYC1</i>	Forward	5'-GGAGCTAGGGATTTTCGACCG-3'
		Reverse	5'-GTGGGTCAGGAGTGTGCAAT-3'
	<i>PYC2</i>	Forward	5'-ATGAATACGCCGTCCGACTC-3'
		Reverse	5'-TCACTTCTTCCGTGACGGTG-3'
	<i>SLC4A 1</i>	Forward	5'-TGGATATGGTGTGCGCACT-3'
		Reverse	5'-GGCGTACCTTCTCATCTCCG-3'
	<i>PEPC1</i>	Forward	5'-ACGTCCAAAGGAATGAGCGT-3'
		Reverse	5'-AAGAGTGCCTCGGGTATTGC-3'
	<i>PEPC2</i>	Forward	5'-AACCCATCCGTCTATCGTGC-3'
		Reverse	5'-TACGCCAGCCGTGTAATGT-3'
	<i>PEPCK</i>	Forward	5'-AAGAGCGTCCTTGTGGATGG-3'
		Reverse	5'-AAGGTGGCTGCTACGCTAAG-3'

### 3.2.6. Mixotrophic ILEs, Cell Harvest, Protein Extraction, Hydrolysis and Derivatization

Steady-state, mixotrophic ILEs were performed by supplementing L1 medium with the  $^{13}\text{C}$ -labeled organic carbon sources U- $^{13}\text{C}$  glucose (amounting to  $2.0 \text{ g L}^{-1}$  in L1 medium), U- $^{13}\text{C}$  acetate (amounting to  $0.9 \text{ g L}^{-1}$  in L1 medium), 1- $^{13}\text{C}$  acetate (amounting to  $0.9 \text{ g L}^{-1}$  in L1 medium) or 4- $^{13}\text{C}$  Asp (amounting to  $0.75 \text{ g L}^{-1}$  in L1 medium). Only one isotopically labeled form of a single carbon source was added in each experiment. The addition was performed aseptically before subculturing so as to result in the final concentrations listed above. After addition of organic carbon sources (especially acids), the pH of the growth medium was adjusted to the range

8.0–8.2 by using NaOH pellets. Each mixotrophic ILE was represented by 3 to 4 biological replicates. Cells from the mixotrophic ILEs were harvested at 21 d of culture. The cell suspensions were first centrifuged at 8873 x g for 10 min, and the supernatant was removed. The cell pellet was briefly resuspended in 50 mL deionized water to rinse out salts and then centrifuged again, after which the supernatant was removed. Cellular metabolism was quenched by immersing tubes containing the pellets in liquid nitrogen. The quenched cells were lyophilized overnight at  $-40\text{ }^{\circ}\text{C}$  and 133  $\mu\text{bar}$ . To obtain proteinogenic amino acids, this lyophilized pellet was hydrolyzed by adding 3 mL 6 N HCl and incubating at  $155\text{ }^{\circ}\text{C}$  for 4 h. Before hydrolysis, the hydrolysis tube was evacuated, then flushed with nitrogen to remove residual oxygen, and then re-evacuated, followed by two more repetitions of these steps. The resulting hydrolysate was cooled to room temperature, filtered by glass wool and dried overnight in a RapidVap evaporator (Labconco, Kansas City, MO) at  $55\text{ }^{\circ}\text{C}$  and 80 mbar, mixed with deionized water and lyophilized again. After lyophilization, this mixture was reconstituted in 200  $\mu\text{L}$  dimethylformamide (DMF) and derivatized with 80  $\mu\text{L}$  N-(tert-butyldimethylsilyl)-N-methyltrifluoroacetamide MTBSTFA + 1% tert-butyldimethylchlorosilane (TBDMCS) (Thermo Scientific, Rockford, IL) at  $70\text{ }^{\circ}\text{C}$  for 1.5 h. The derivatized sample was injected into a gas chromatograph (GC)- MS, using DMF as solvent. MIDs obtained from steady-state ILEs are listed in appendix **Table A.2** to **Table A.5**.

### 3.2.7. Evaluation of Metabolic Fluxes from Steady-state Isotopomer Data

For steady-state flux evaluation from the 4-<sup>13</sup>C Asp ILEs, we used our computer program NMR2Flux+ (Nargund and Sriram, 2013; Sriram et al., 2004, 2008). This program employs cumomer balancing (Wiechert and Wurzel, 2001; Wiechert et al., 1999b) to simulate ILEs, a simulated annealing-based global optimization algorithm to evaluate fluxes from MS- and NMR-derived isotopomer abundances and a bootstrap Monte Carlo algorithm (Press et al., 2007) to evaluate standard deviations or confidence intervals of fluxes. The two metabolic models used for flux evaluation from the 4-<sup>13</sup>C Asp ILEs are listed in **Table 3.3** and **Table 3.4**.

**Table 3.3 4-<sup>13</sup>C Asp ILE: C<sub>4</sub> scenario metabolic model and evaluated fluxes.**

Flux	Reaction	Net flux	Flux SD	Reversibility
v <sub>1</sub>	→ HCO <sub>3</sub> <sup>-</sup>	5.63	1.58	
v <sub>2</sub>	→ OA Ain	0.20	0.00	
v <sub>3</sub>	OA Ain (1234) ↔ OAA (1234)	0.20	0.00	0.94
v <sub>4</sub>	ACA (12) + OAA (3456) → αKG (65421) + CO <sub>2</sub> (3)	0.27	0.15	
v <sub>5</sub>	αKG (12345) → Succ (2345) + CO <sub>2</sub> (1)	0.14	0.13	
v <sub>6</sub>	Succ (1234) ↔ Mal (1234)	0.14	0.13	0.69
v <sub>7</sub>	Succ (1234) ↔ Mal (4321)	0.14	0.13	0.55
v <sub>8</sub>	Mal (1234) ↔ OAA (1234)	0.14	0.13	0.61
v <sub>9</sub>	Pyr (123) + HCO <sub>3</sub> <sup>-</sup> (4) ↔ OAA (1234)	0.07	0.07	0.95
v <sub>10</sub>	HCO <sub>3</sub> <sup>-</sup> (1) + P5Pp (23456) → 3PGp (132) + 3PGp (456)	3.11	0.70	
v <sub>11</sub>	3PGp (123) + 3PGp (456) ↔ F6Pp (321456)	1.04	0.23	0.51
v <sub>12</sub>	F6Pp (123456) + 3PGp (789) ↔ P5Pp (12789) + E4Pp (3456)	1.04	0.23	0.54
v <sub>13</sub>	3PGp (123) + E4Pp (4567) → S7Pp (3214567)	1.04	0.23	
v <sub>14</sub>	S7Pp (1234567) + 3PGp (890) ↔ P5Pp (12890) + P5Pp (34567)	1.04	0.23	0.58
v <sub>15</sub>	Pyrp (123) → ACA (23) + CO <sub>2</sub> (1)	0.27	0.15	
v <sub>16</sub>	3PGp (123) ↔ 3PG (123)	0.07	0.07	0.20
v <sub>17</sub>	Pyrp (123) ↔ Pyr (123)	0.09	0.09	0.40
v <sub>18</sub>	3PG (123) ↔ Pyr (123)	0.07	0.07	0.95
v <sub>19</sub>	3PGp (123) ↔ Pyr (123)	0.96	0.25	0.24
v <sub>20</sub>	HCO <sub>3</sub> <sup>-</sup> → CO <sub>2</sub>	2.45	1.67	
v <sub>21</sub>	Pyr →	0.09	0.09	
v <sub>22</sub>	Pyrp →	0.60	0.32	
v <sub>23</sub>	OAA →	0.14	0.13	
v <sub>24</sub>	αKG →	0.14	0.11	
v <sub>25</sub>	CO <sub>2</sub> →	3.12	1.65	



**Table 3.4 4-<sup>13</sup>C Asp ILE: alternative scenario metabolic model**

Flux	Reaction	Net flux	Flux SD	Reversibility
v <sub>1</sub>	→ HCO <sub>3</sub> <sup>-</sup>	1.16	0.53	
v <sub>2</sub>	→ OA Ain	0.20	0.00	
v <sub>3</sub>	OA Ain (1234) ↔ OAA (1234)	0.20	0.00	0.95
v <sub>4</sub>	ACA (12) + OAA (3456) → αKG (65421) + CO <sub>2</sub> (3)	0.40	0.10	
v <sub>5</sub>	αKG (12345) → Succ (2345) + CO <sub>2</sub> (1)	0.36	0.11	
v <sub>6</sub>	Succ (1234) ↔ Mal (1234)	0.36	0.11	0.90
v <sub>7</sub>	Succ (1234) ↔ Mal (4321)	0.36	0.11	0.50
v <sub>8</sub>	Mal (1234) ↔ OAA (1234)	0.36	0.11	0.89
v <sub>9</sub>	Pyr (123) + CO <sub>2</sub> (4) ↔ OAA (1234)	-0.16	0.06	0.99
v <sub>10</sub>	HCO <sub>3</sub> <sup>-</sup> (1) + P5P (23456) → 3PG (132) + 3PG (456)	1.16	0.53	
v <sub>11</sub>	3PG (123) + 3PG (456) ↔ F6P (321456)	0.39	0.18	0.46
v <sub>12</sub>	F6P (123456) + 3PG (789) ↔ P5P (12789) + E4P (3456)	0.39	0.18	0.47
v <sub>13</sub>	3PG (123) + E4P (4567) → S7P (3214567)	0.39	0.18	
v <sub>14</sub>	S7P(1234567) + 3PG (890) ↔ P5P (12890) + P5P (34567)	0.39	0.18	0.53
v <sub>15</sub>	3PG (123) ↔ Pyr (123)	0.39	0.18	0.97
v <sub>16</sub>	Pyr (123) → ACA (23) + CO <sub>2</sub> (1)	0.40	0.10	
v <sub>17</sub>	Pyr →	0.14	0.10	
v <sub>18</sub>	CO <sub>2</sub> →	1.33	0.31	
v <sub>19</sub>	αKG →	0.04	0.02	

### 3.3. Results

To investigate if *P. tricornutum* operates a C<sub>4</sub> CCM, we performed instationary and steady-state ILEs, and assayed the expression levels of genes encoding selected C<sub>4</sub> enzymes. To replicate the natural environment of *P. tricornutum* where organic carbon sources are rarely present, we performed instationary ILEs by supplying H<sup>13</sup>CO<sub>3</sub><sup>-</sup> and measuring isotope labeling over periods ranging from a few minutes to 6 d. In the steady-state ILEs, we grew *P. tricornutum* for three weeks on

pure ( $\approx 100\%$ )  $^{13}\text{C}$ -labeled organic carbon sources, viz.  $\text{U-}^{13}\text{C}$  glucose,  $\text{U-}^{13}\text{C}$  acetate,  $1\text{-}^{13}\text{C}$  acetate and  $4\text{-}^{13}\text{C}$  Asp. Intracellular metabolites and biomass components synthesized during these ILEs would have derived carbon from these partially or fully  $^{13}\text{C}$ -labeled organic carbon sources, and from the naturally abundant ( $\approx 99\%$   $^{12}\text{C}$ )  $\text{CO}_2$  in the flask headspace. Thus, these ILEs afforded dissection of various steps in the  $\text{C}_4$  CCM. For example, the  $\text{U-}^{13}\text{C}$  glucose and  $\text{U-}^{13}\text{C}$  acetate ILEs explicitly revealed the major path(s) taken by  $\text{CO}_2$  through the metabolic network and identified the  $\text{HCO}_3^-$ -capture step of the CCM. Oppositely, the  $4\text{-}^{13}\text{C}$  Asp ILE revealed an isotopic signature of the  $\text{CO}_2$ -release step and the photosynthetic  $\text{CO}_2$  re-assimilation step of the  $\text{C}_4$  CCM. These ILEs detected the  $\text{HCO}_3^-$  capture,  $\text{CO}_2$  release and photosynthetic  $\text{CO}_2$  re-assimilation steps of the  $\text{C}_4$  CCM and enabled estimation of the timescale and efficiency of the CCM.

### **3.3.1. Instationary $\text{H}^{13}\text{CO}_3^-$ ILE Reveals the Evidence of a $\text{C}_4$ CCM**

To examine carbon assimilation by *P. tricornutum* in its natural environment, it is necessary to perform ILEs in which labeled  $\text{HCO}_3^-$  is unaccompanied by organic carbon sources. Therefore, we conducted short-term and long-term instationary ILEs by supplementing the organic carbon-free L1 medium with  $\text{H}^{13}\text{CO}_3^-$ . For the short-term ILEs, we added  $\text{NaH}^{13}\text{CO}_3$  to cells suspended in L1 medium in small tubes, followed by quenching and harvesting of the cells at different time points ranging from 1 to 20 min. We also performed an 8 h-version of this ILE in shake flasks. From the quenched cells, we isolated and quantified mass isotopomer abundances of soluble intracellular metabolites. Finally, we performed a long-term ILE for 6 d in

shake flasks. Together, these experiments provided strong evidence for the operation of a C<sub>4</sub> CCM.

In the short-term ILEs, the supplied <sup>13</sup>C was detected earliest in Asp as opposed to the photosynthetic product 3PG or its downstream glycolytic metabolites (**Fig. 2**). The Asp[1234] fragment was <sup>13</sup>C-enriched to 4.0% ± 0.3% within 1 min (*m*+1 abundance: 11.0% ± 1.0%, *m*+2 abundance: 2.0% ± 1.0%), and to 8.0% ± 0.3% by 20 min (*m*+1 abundance: 22.0% ± 1.0%, *m*+2 abundance: 5.0% ± 1.0%). The fragments Asp[234] and Asp[12] were also labeled rapidly. The enrichment of Asp[234] increased from 3.0% ± 0.5% at 1 min to 6.5% ± 0.6% at 20 min, with its *m*+1 abundance increasing from 9.0% ± 0.5% to 19.0% ± 2.0% during this 20 min period. The enrichment of Asp[12] rose from 3.4% ± 0.3% (*m*+1 abundance: 4.5% ± 1.0%) to 8.3% ± 0.4% (*m*+1 abundance: 13.0% ± 1.5%) from 1 to 20 min. (**Figure 3.3** and appendix **Table A.1**).

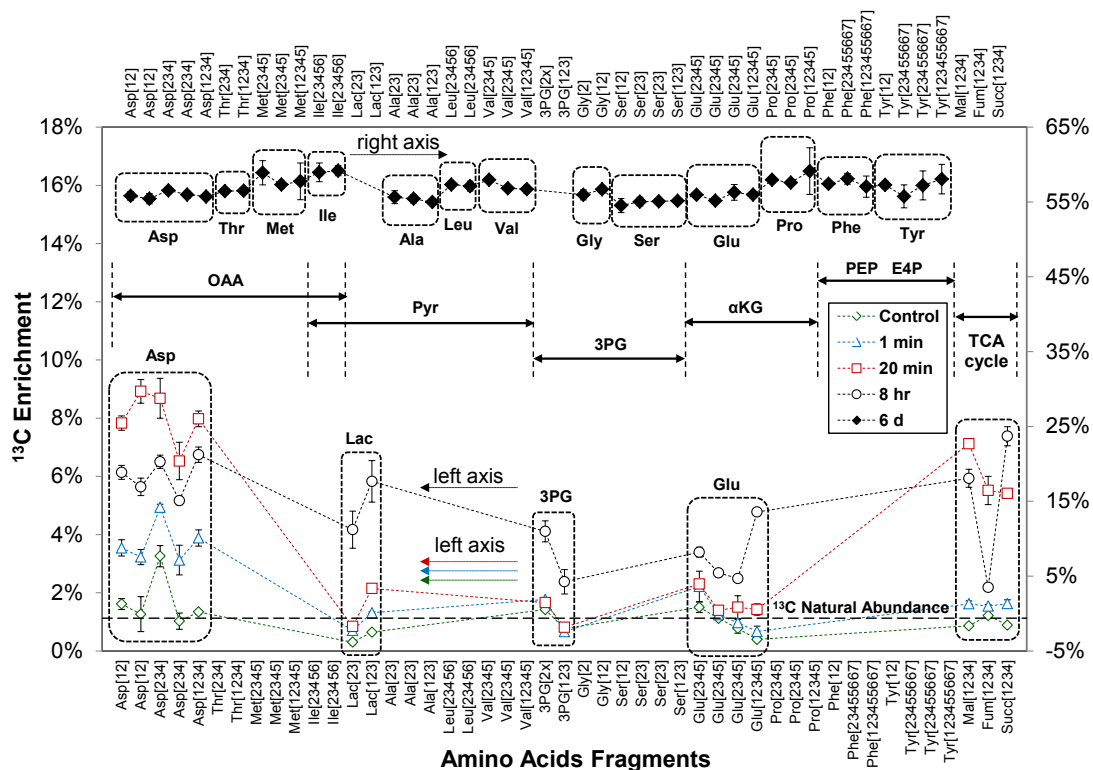


**Figure 3.3** Instationary  $\text{H}^{13}\text{CO}_3^-$  ILE evidences  $\text{CO}_2$  incorporation via a  $\text{C}_4$  CCM over a 6 d period.

*P. tricornutum* cultures were supplied with  $\text{H}^{13}\text{CO}_3^-$ , followed by measurement of intracellular metabolite MIDs at various time points and calculation of  $^{13}\text{C}$  enrichments from these MIDs (see text). The  $^{13}\text{C}$  enrichments of fragments of soluble intracellular metabolite fragments at 1 min, 20 min and 8 h following  $\text{H}^{13}\text{CO}_3^-$  addition, as well as of proteinogenic amino acid fragments at time 6 d following  $\text{H}^{13}\text{CO}_3^-$  addition, are depicted here. Amino acids are grouped according to their metabolic precursors. Asp responded very quickly to  $\text{H}^{13}\text{CO}_3^-$  addition (evidencing  $\text{HCO}_3^-$  capture), followed first by metabolites such as Lac (evidencing  $\text{CO}_2$  release) and then by 3PG (evidencing photosynthetic assimilation of the released  $\text{CO}_2$ ). At 6 d, all proteinogenic amino acids showed approximately the same  $^{13}\text{C}$  enrichment of ~57%. This ILE was very reproducible; MIDs were measured from 3 to 4 biological replicates with standard derivations ~1%.

These trends are consistent with a model in which the  $\text{C}_4$  CCM captures  $\text{HCO}_3^-$  into OAA (**Figure 3.4**). The enrichments of the Asp fragments plateaued around 20 min, as evident from the 8 h enrichments of Asp[1234] ( $6.7\% \pm 0.3\%$ ), Asp[234] ( $5.2\% \pm 0.1\%$ ) and Asp[12] ( $5.8\% \pm 0.3\%$ ) in shake flask experiments (**Figure 3.3** and **Figure 3.5 a-d**). However, this apparent saturation may not be

because the  $\text{HCO}_3^-$  capture slows down, but because carbon is transferred from OAA C-4 to other metabolic destinations including  $\alpha\text{KG}$  C-1, and is complemented from C-4 to other metabolic destinations including  $\alpha\text{KG}$  C-1, and is complemented from initially unlabeled biomass. Attesting to this, Glu[12345] was significantly more enriched ( $4.8\% \pm 0.1\%$ ;  $m+1$  abundance:  $16.0\% \pm 0.1\%$ ) than Glu[2345] ( $2.9\% \pm 0.2\%$ ;  $m+1$  abundance:  $7.0\% \pm 0.1\%$ ) at 8 h (Figure 3.3).

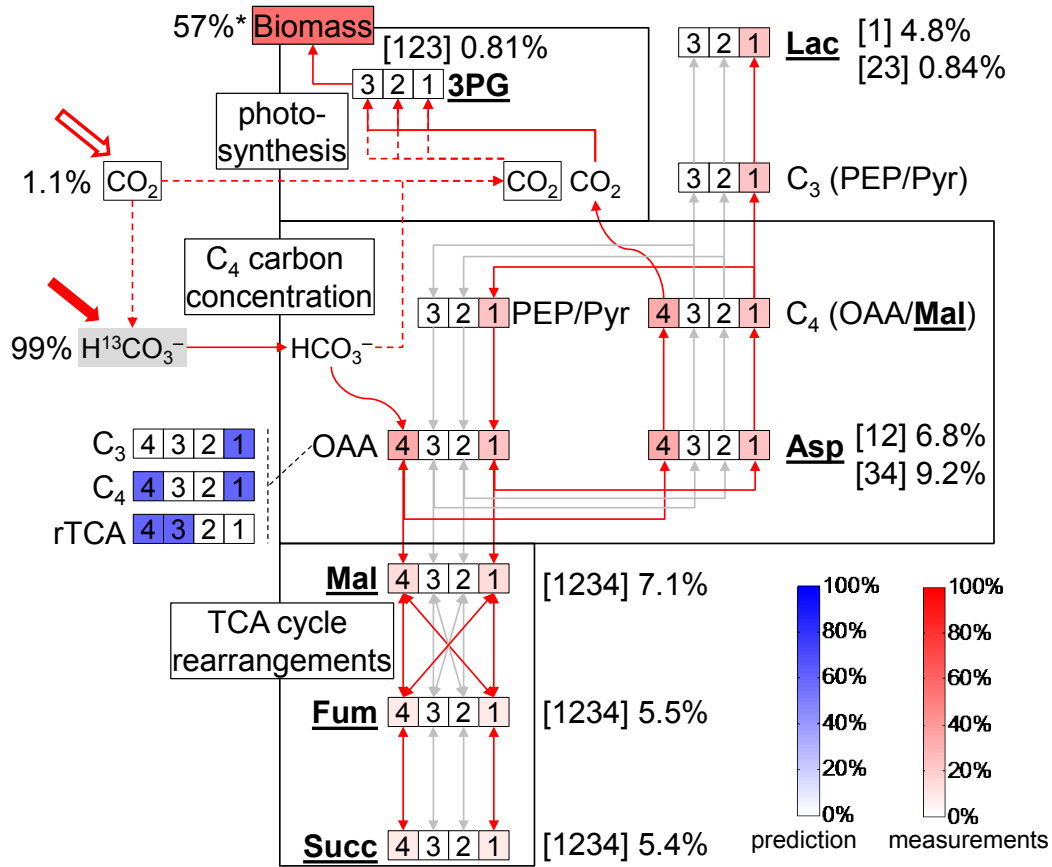


**Figure 3.4 Proposed carbon rearrangements in the C<sub>4</sub> CCM, with <sup>13</sup>C enrichments from the H<sup>13</sup>CO<sub>3</sub><sup>-</sup> ILE at 20 min.**

Small rectangles represent carbon atoms, with the intensity of red color in them proportional to their <sup>13</sup>C enrichment. <sup>13</sup>C enrichments of key metabolite fragments from the instationary H<sup>13</sup>CO<sub>3</sub><sup>-</sup> ILE at 20 min and for the overall biomass (marked with an asterisk “\*”) from the 6 d instationary ILE are shown numerically. Arrows represent fluxes; red arrows correspond to the hypothesized C<sub>4</sub> CCM. Red dashed lines depict two alternative mechanisms of communicating extracellular CO<sub>2</sub> to RuBisCO: pure diffusion or a biophysical CCM. The “99%” figure adjacent to H<sup>13</sup>CO<sub>3</sub><sup>-</sup> refers to the <sup>13</sup>C enrichment of the supplied HCO<sub>3</sub><sup>-</sup>; the <sup>13</sup>C enrichment of HCO<sub>3</sub><sup>-</sup> in the medium would be lower because the supplied H<sup>13</sup>CO<sub>3</sub><sup>-</sup> would have mixed with H<sup>12</sup>CO<sub>3</sub><sup>-</sup> generated by dissociation of atmospheric <sup>12</sup>CO<sub>2</sub>.

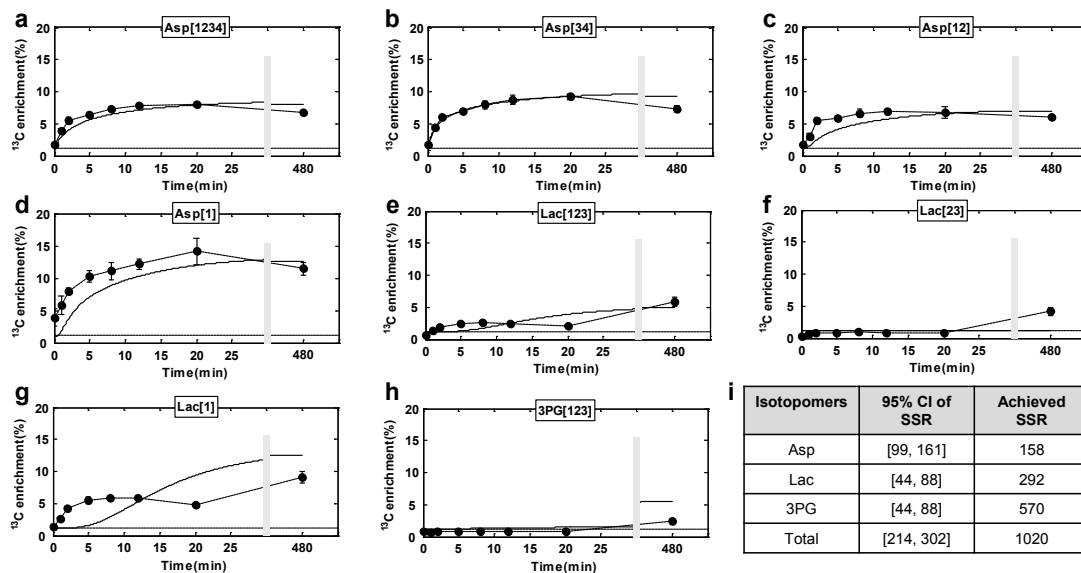


**Figure 3.5**  $^{13}\text{C}$  enrichments of fragments of metabolites in the  $\text{C}_4$  CCM measured from the  $\text{H}^{13}\text{CO}_3^-$  ILE (points), and simulated by an instationary isotopomer model (lines).

$^{13}\text{C}$  enrichments of intracellular metabolite fragments were measured by GC-MS at  $t = 1$  min, 2 min, 5 min, 8 min, 12 min, 20 min and 8 h after adding  $\text{H}^{13}\text{CO}_3^-$ . An experiment in which cells were incubated with naturally abundant  $\text{HCO}_3^-$  was used as a control representing  $t = 0$  min. These  $^{13}\text{C}$  enrichments are shown as solid circle with error bars representing standard deviations across three biological replicates.  $^{13}\text{C}$  enrichments of Asp fragments [1] and [34] were calculated by SVD from the MIDs of Asp fragments [12], [234] and [1234], whereas the enrichment of Lac [1] was calculated from the MIDs of Lac [23] and Lac [123].  $^{13}\text{C}$  enrichments simulated by an instationary isotopomer model are depicted as solid lines. The dashed line near the bottom of each panel indicates the  $^{13}\text{C}$  natural abundance of 1.1%.

Furthermore, the Asp isotopomer data revealed carbon exchange between OAA C-4 and C-1 through the reversible steps of the TCA cycle:  $\text{OAA} \leftrightarrow \text{Mal} \leftrightarrow \text{Fum} \leftrightarrow \text{Succ}$  (**Figure 3.4**), where the symmetry of Fum and Succ effects carbon exchange between C-4 and C-1. The exchange of OAA C-4 and C-1 is evident from the appearance of  $^{13}\text{C}$  on the Asp[1] fragment (**Figure 3.5 d**) as well as in Mal, Fum and Succ (**Figure 3.6**). For example, the enrichment of Succ[1234] increased from  $1.7\% \pm 0.1\%$  ( $m+1$  abundance:  $5.0\% \pm 0.2\%$ ) at 1 min to  $5.4\% \pm 0.0\%$  ( $m+1$

abundance:  $16.0\% \pm 0.6\%$ ) at 20 min. However, this exchange was insufficient to fully equilibrate OAA C-1 with C-4, as is clear from the observation that the enrichment of Asp[34] (**Figure 3.5 b**) was always higher than that of Asp[12] (**Figure 3.5c**).

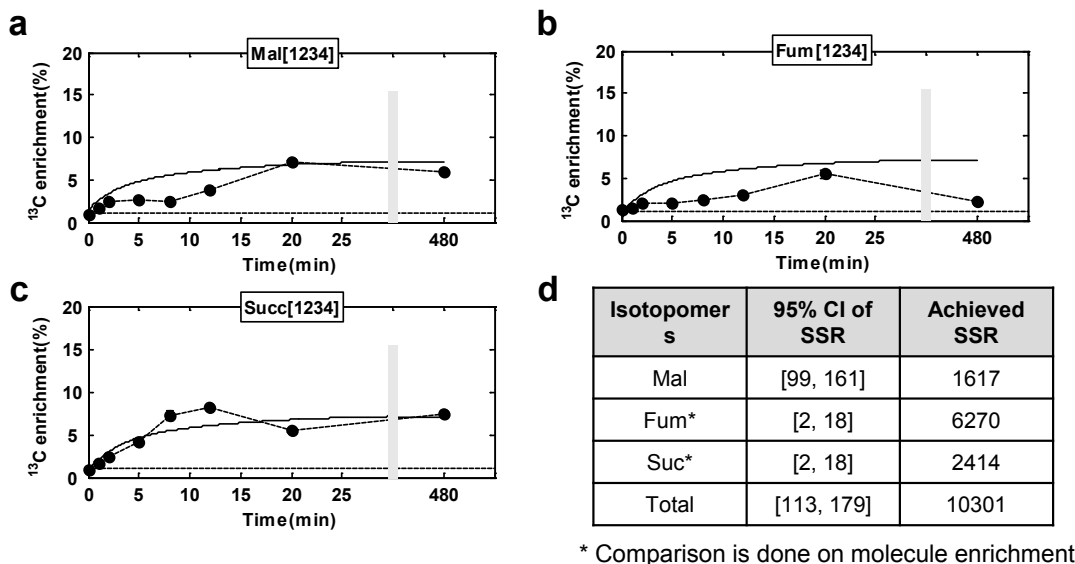


**Figure 3.6** <sup>13</sup>C enrichments and simulation of intracellular TCA cycle metabolites.

<sup>13</sup>C enrichments and simulations, following the scheme of **Figure 3.5**.

CO<sub>2</sub> release from the C<sub>4</sub> CCM (OAA/Mal ↔ PEP/Pyr in **Figure 3.4**) is inferable from the isotope labeling data, particularly from the MIDs and calculated enrichments of lactate (Lac) (**Figure 3.5 e-g**). CO<sub>2</sub> release from OAA labeled at C-1 (see previous paragraph) would generate Pyr labeled at C-1. As Lac is fermentatively derived from Pyr, its isotopomer abundances reflect those of Pyr. We observed that the <sup>13</sup>C enrichment of Lac[123] (**Figure 3.5 e**) was consistently higher than that of Lac[23] (**Figure 3.5 f**), revealing that Lac was almost exclusively enriched at C-1

(**Figure 3.5 g**). Moreover, the enrichment of Lac[1] continued to increase after that of Asp had slowed down, as is clear from **Figure 3.3**. Specifically, the  $m+1$  abundance of Lac[123] increased from  $6.0\% \pm 0.2\%$  at 20 min to  $11.0\% \pm 0.7\%$  at 8 h. The corresponding increase in the  $m+1$  abundance of Lac[23] was lower, from  $2.0\% \pm 0.2\%$  at 20 min to  $5.0\% \pm 0.6\%$  at 8 h during this time. This suggests that the timescale of  $\text{CO}_2$  release by the  $\text{C}_4$  CCM is longer than that of  $\text{HCO}_3^-$  capture.

The timescale of photosynthetic incorporation of  $\text{CO}_2$  released by the  $\text{C}_4$  CCM appeared to be even longer. This is evident from the  $^{13}\text{C}$  enrichment of the [123] fragment of the RuBisCO product 3PG, which increased from  $0.81\% \pm 0.1\%$  ( $m+1$  abundance:  $2.0\% \pm 0.1\%$ ) at 20 min to  $2.4\% \pm 0.4\%$  ( $m+1$  abundance:  $5.0\% \pm 0.3\%$ ) at 8 h (**Figure 3.3**, **Figure 3.5 h**). Another incompletely identified 3PG fragment [2x] ( $m/z$  231; x could be either C-1 or C-3) showed a larger increase in enrichment, from  $1.7\% \pm 0.1\%$  abundance at 20 min ( $m+1$  abundance:  $5.0\% \pm 0.3\%$ ) to  $4.1\% \pm 0.4\%$  ( $m+1$  abundance:  $4.0\% \pm 0.3\%$ ,  $m+2$  abundance:  $3.0\% \pm 0.3\%$ ) at 8 h (**Figure 3.3**). Overall, we find an undeniable trail of a  $\text{C}_4$  CCM involving rapid  $\text{HCO}_3^-$  capture, slower  $\text{CO}_2$  release and even slower photosynthetic  $\text{CO}_2$  re-assimilation (**Figure 3.4**). The difference in the timescales of photosynthetic re-assimilation step is likely due to the inefficiency of the CCM. Very likely, not all  $\text{CO}_2$  released by the CCM is available to RuBisCO.

This instationary ILE data suggest that OAA is the most likely  $\text{C}_4$  candidate into which the  $\text{C}_4$  CCM captures  $\text{HCO}_3^-$ . Although the direct measurement of OAA is analytically challenging, Asp serves as a very good surrogate. It is not metabolically possible to generate Asp directly by capturing  $\text{HCO}_3^-$  or  $\text{CO}_2$  into a  $\text{C}_3$  compound;



therefore, the rapid increase in  $^{13}\text{C}$  enrichment of Asp must reflect rapid  $\text{HCO}_3^-$  capture into OAA. Additionally, the higher enrichment of Asp[1234] (**Figure 3.5 a**) compared to Mal[1234] (**Figure 3.6 a**) for time points below 15 min rules out Mal as the first  $\text{C}_4$  metabolite to receive  $\text{HCO}_3^-$ . However, the species that is actually transported into the vicinity of RuBisCO may be OAA, Mal or even Asp. Finally, a long-term instationary ILE lasting 6 d revealed proteinogenic amino acids to be  $^{13}\text{C}$ -enriched approximately uniformly at 57%. Any enrichment differences between amino acid fragments were small in comparison to those observed for the time points from 0 to 20 min. This indicates that the metabolic precursors of these amino acids (3PG, PEP, Pyr, OAA,  $\alpha\text{KG}$ , P5P and E4P) were approaching or had approached isotopic steady state. Together with the 8 h time point, the long-term ILE suggests that the timescale of  $\text{CO}_2$  incorporation into biomass is longer than 8 h but substantially lesser than 6 d.

### **3.3.2. Instationary $^{13}\text{C}$ MFA Suggests that the $\text{C}_4$ CCM Contributes Substantially to Photosynthesis**

We evaluated metabolic fluxes from the instationary ILE by using  $^{13}\text{C}$  MFA with the metabolic network model shown in **Figure 3.4** and **Table 3.1**. This model accounts for the observations described in the preceding section and includes a complete  $\text{C}_4$  CCM and a second mode of  $\text{CO}_2$  transport to RuBisCO independent of the  $\text{C}_4$  CCM. The  $\text{C}_4$  CCM included the following steps. First,  $\text{HCO}_3^-$  is captured into OAA C-4 by carboxylation of PEP or Pyr in the cytosol. Carbon is then exchanged between C-1 and C-4 of OAA through the symmetric molecules Fum and Succ of the

TCA cycle, causing some of the label on OAA C-4 to transfer to C-1. Next, a labeled C<sub>4</sub> metabolite (OAA or Mal) is transported to the vicinity of RuBisCO, where it is decarboxylated to release CO<sub>2</sub>. The C<sub>3</sub> metabolite resulting from this decarboxylation (PEP or Pyr) is transported back to the cytosol. The CO<sub>2</sub> available from the decarboxylation is mixed with the CO<sub>2</sub> made available by a biophysical CCM and fixed by RuBisCO to generate 3PG. The model also contained auxiliary reactions including the synthesis of biomass and of C<sub>3</sub> and C<sub>4</sub> metabolites.

Fluxes evaluated by instationary <sup>13</sup>C MFA are depicted in **Figure 3.7** and listed in **Table 3.1**. Flux and pool size (metabolite concentration) parameters estimated during flux evaluation are listed in **Table 3.5**. Our flux model showed that 67% of photosynthetically fixed CO<sub>2</sub> (flux *c4refix* = 0.045 μmol s<sup>-1</sup> gdw<sup>-1</sup>) was contributed by the C<sub>4</sub> CCM, with a biophysical CCM or CO<sub>2</sub> diffusion contributing the remaining 33% (flux *c3refix* = 0.025 μmol s<sup>-1</sup> gdw<sup>-1</sup>) (**Figure 3.7**).

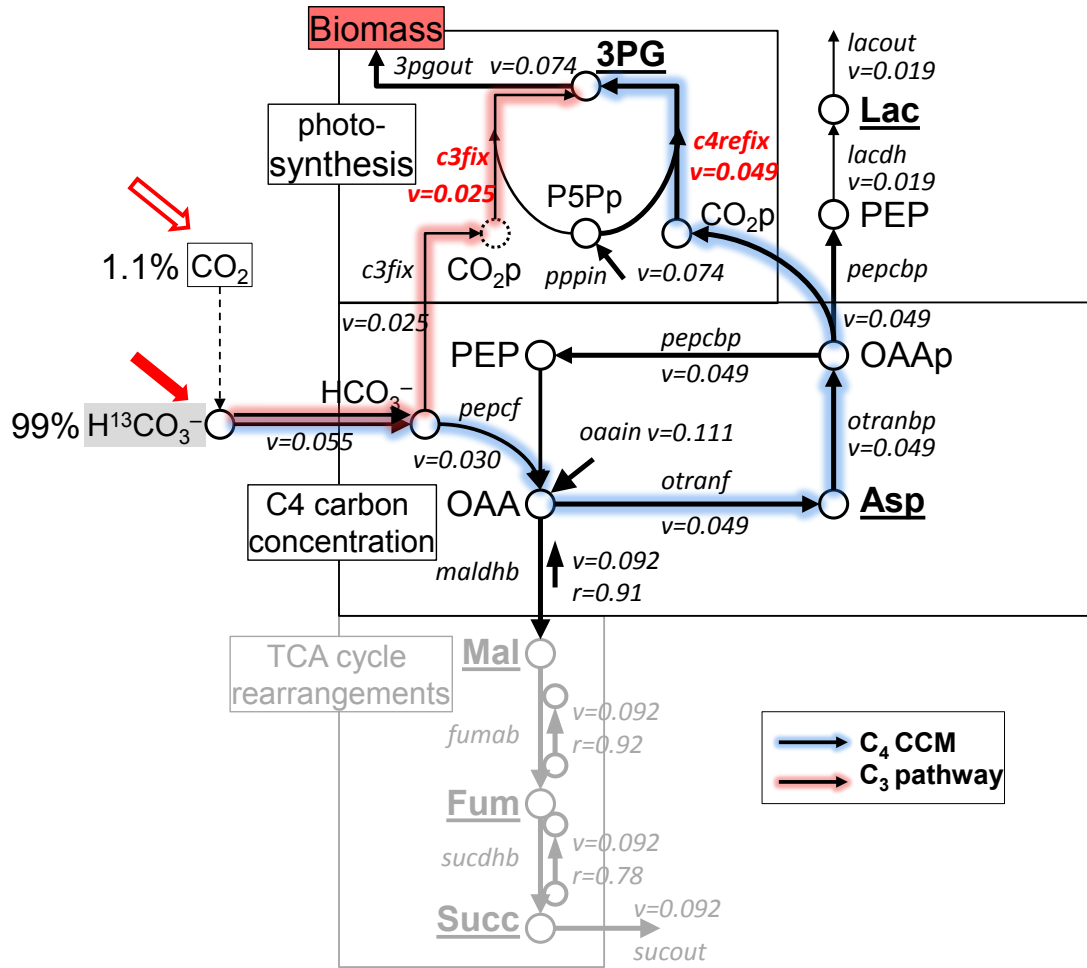


**Figure 3.7 Metabolic flux model of the C<sub>4</sub> CCM as deduced from instationary <sup>13</sup>C MFA.**

This map summarizes the results of our instationary H<sup>13</sup>CO<sub>3</sub><sup>-</sup> ILE. Circles indicate metabolites and arrows indicate net flux directions (flux names are shown in italics). Arrow widths are proportional to relative flux values indicated numerically. A substantial amount of the supplied H<sup>13</sup>CO<sub>3</sub><sup>-</sup> initially appeared on Asp C-4, indicating its capture by C<sub>4</sub> reactions. Exchange fluxes between Mal, Fum and Succ in the reversible section of the TCA cycle were also very dynamic, causing the captured <sup>13</sup>C to appear on Asp C-1. The supplied H<sup>13</sup>CO<sub>3</sub><sup>-</sup> appeared significantly on the photosynthetic product 3PG, although this was detectable only at 8 h. Our simulations show the C<sub>4</sub> CCM and a biophysical CCM may be contributing jointly to photosynthetic carbon fixation in *P. tricornutum*.

**Table 3.5 Flux and pool size (metabolite concentration) parameters estimated during instationary <sup>13</sup>C MFA.**

These quantities were free parameters in the instationary <sup>13</sup>C MFA model. The following values were estimated by the flux evaluation routine described in **Sec. 2.2.6** and correspond to the minimum SSR with respect to the labeling measurements. Pool sizes that were also measured are marked with stars (\*). Fluxes are reported in (μmol s<sup>-1</sup> gdw<sup>-1</sup>) or as a percentage of the CO<sub>2</sub> influx *CO2in*. Pool sizes are reported in μmol. SD, standard deviation.

Parameter		Measurement		Simulation		
Flux	Pool size	Mean (μmol)	SD (μmol)	Mean	SD	Unit
	Asp*	0.0080	0.0030	0.0079	0.0003	μmol
	CO <sub>2p</sub>	nd	nd	10.0117	0.1827	μmol
	Fum*	0.0270	0.0070	0.1213	0.0259	μmol
	3PG*	0.0100	0.0010	9.9785	0.2294	μmol
	Lac*	0.0170	0.0070	0.0233	0.0033	μmol
	Mal*	0.0150	0.0060	0.0232	0.0022	μmol
	OAA	nd	nd	0.0140	0.0019	μmol
	OAA <sub>p</sub>	nd	nd	0.0609	0.0047	μmol
	PEP	nd	nd	0.0712	0.0053	μmol
	Succ*	0.0100	0.0030	0.0104	0.0023	μmol
<i>CO2in</i>		NA	NA	0.0550	0.0074	μmol s <sup>-1</sup> gdw <sup>-1</sup>
<i>pepcf</i>		NA	NA	0.5613	0.0315	% of <i>CO2in</i>
<i>pppin</i>		NA	NA	1.3363	0.1220	% of <i>CO2in</i>
<i>oaain</i>		NA	NA	1.6500	0.1348	% of <i>CO2in</i>
<i>maldh</i> reversibility		NA	NA	0.9130	0.0258	NA
<i>fuma</i> reversibility		NA	NA	0.9162	0.0236	NA
<i>sucdh</i> reversibility		NA	NA	0.7847	0.0282	NA
<i>3pgout</i>		NA	NA	0.0739	0.0130	μmol s <sup>-1</sup> gdw <sup>-1</sup>
<i>c3fix</i>		NA	NA	0.0246	0.0046	μmol s <sup>-1</sup> gdw <sup>-1</sup>
<i>c4refix</i>		NA	NA	0.0493	0.0109	μmol s <sup>-1</sup> gdw <sup>-1</sup>
<i>co2in</i>		NA	NA	0.0550	0.0074	μmol s <sup>-1</sup> gdw <sup>-1</sup>
<i>fumab</i>		NA	NA	0.0920	0.0162	μmol s <sup>-1</sup> gdw <sup>-1</sup>
<i>lacdh</i>		NA	NA	0.0189	0.0083	μmol s <sup>-1</sup> gdw <sup>-1</sup>
<i>lacout</i>		NA	NA	0.0189	0.0083	μmol s <sup>-1</sup> gdw <sup>-1</sup>
<i>maldhb</i>		NA	NA	0.0920	0.0162	μmol s <sup>-1</sup> gdw <sup>-1</sup>
<i>oaain</i>		NA	NA	0.1109	0.0200	μmol s <sup>-1</sup> gdw <sup>-1</sup>
<i>otranbp</i>		NA	NA	0.0493	0.0109	μmol s <sup>-1</sup> gdw <sup>-1</sup>
<i>otranf</i>		NA	NA	0.0493	0.0109	μmol s <sup>-1</sup> gdw <sup>-1</sup>
<i>pepcbp</i>		NA	NA	0.0493	0.0109	μmol s <sup>-1</sup> gdw <sup>-1</sup>
<i>pepcf</i>		NA	NA	0.0304	0.0037	μmol s <sup>-1</sup> gdw <sup>-1</sup>
<i>pppin</i>		NA	NA	0.0739	0.0130	μmol s <sup>-1</sup> gdw <sup>-1</sup>
<i>sucdhb</i>		NA	NA	0.0920	0.0162	μmol s <sup>-1</sup> gdw <sup>-1</sup>
<i>sucout</i>		NA	NA	0.0920	0.0162	μmol s <sup>-1</sup> gdw <sup>-1</sup>

The ability of our flux model to match the measured  $^{13}\text{C}$  labeling patterns of TCA metabolites was less than satisfactory (**Figure 3.6**). Despite this, the Asp group exhibited a reasonably good fit (**Figure 3.5 a-d, Figure 3.5 i**), and the measured and simulated pool sizes for Asp were nearly identical (**Table 3.5**). The SSR achieved between the  $^{13}\text{C}$  enrichments derived from the measured MIDs and the simulated  $^{13}\text{C}$  enrichments of the fragments shown in **Figure 3.5** was 1,020. Of this value, the Asp fragments carried 15% (SSR of 158, 95% confidence interval of SSR is [99, 161]), the Lac fragments carried 29% (SSR of 292, 95% confidence interval of SSR is [44, 88]) and the 3PG fragment carried 56% (SSR of 570, 95% confidence interval of SSR is [214, 302]). Therefore, our fit is statistically acceptable for Asp fragments. Although fit of TCA cycle fragments is not satisfactory (**Figure 3.6**, SSR of 10,301, total 95% confidence interval for all the TCA cycle fragments is [113, 179]), TCA cycle metabolites contributed significantly to C1 labeling of Asp. We could have further reduced the SSR by eliminating the TCA cycle metabolites and fitting (i) only Asp or (ii) only Asp (reflecting  $\text{HCO}_3^-$  capture), Lac (reflecting  $\text{CO}_2$  release) and 3PG (reflecting photosynthetic fixation of released  $\text{CO}_2$ ), we elected to retain the current model. The possible reasons for the unsatisfactory fit are discussed in **Sec. 3.4**.

### **3.3.3. Two *P. tricornutum* Genes Encoding $\text{HCO}_3^-$ -capturing Enzymes are Induced by Light**

Our instationary  $\text{H}^{13}\text{CO}_3^-$  labeling experiment verified that a  $\text{C}_4$  CCM is underlying *P. tricornutum* photosynthesis mechanism, while participating genes were still unveiled. Previously reported gene expression patterns in *P. tricornutum* have

provided circumstantial evidence for a C<sub>4</sub> CCM. These patterns include the upregulation of genes encoding carboxylases in response to light (Chauton et al., 2013; Nymark et al., 2009), an unidentified decarboxylase in response to high dissolved CO<sub>2</sub> concentration (Maheswari et al., 2010) and coordinated expression of a suite of three genes (Pyr carboxylase [*PYCI*], Mal dehydrogenase [*MDH*] and malic enzyme [*ME*]) jointly capable of catalyzing a C<sub>4</sub> cycle during a growth phase transition (Valenzuela et al., 2012). An important gap in the previous studies is a concurrent investigation of the effect of light, increased HCO<sub>3</sub><sup>-</sup> concentration, adding of glucose as well as both light, increased HCO<sub>3</sub><sup>-</sup> concentration and adding of glucose on the expressions of candidate genes in the C<sub>4</sub> and the biophysical CCMs. To address this, we profiled genes encoding (i) putative HCO<sub>3</sub><sup>-</sup>-capturing enzymes in the C<sub>4</sub> CCM: mitochondrial Pyr carboxylase (*PYCI*), plastidic Pyr carboxylase (*PYC2*), PEP carboxylases (*PEPC1*, *PEPC2*), PEP carboxykinase (*PEPCK*) and (ii) the plastidic HCO<sub>3</sub><sup>-</sup> transporter (*SLC4A\_1*), which may play a crucial role in the biophysical CCM. We performed qRT-PCR on cells incubated under six conditions: L1 medium in light (light/L1), L1 medium in dark (dark/L1), HCO<sub>3</sub><sup>-</sup>-supplemented L1 medium in light (light/HCO<sub>3</sub><sup>-</sup>), HCO<sub>3</sub><sup>-</sup>-supplemented L1 medium in dark (dark/HCO<sub>3</sub><sup>-</sup>), glucose-supplemented L1 medium in light (light/Glc) and glucose-supplemented L1 medium in dark (dark/Glc).

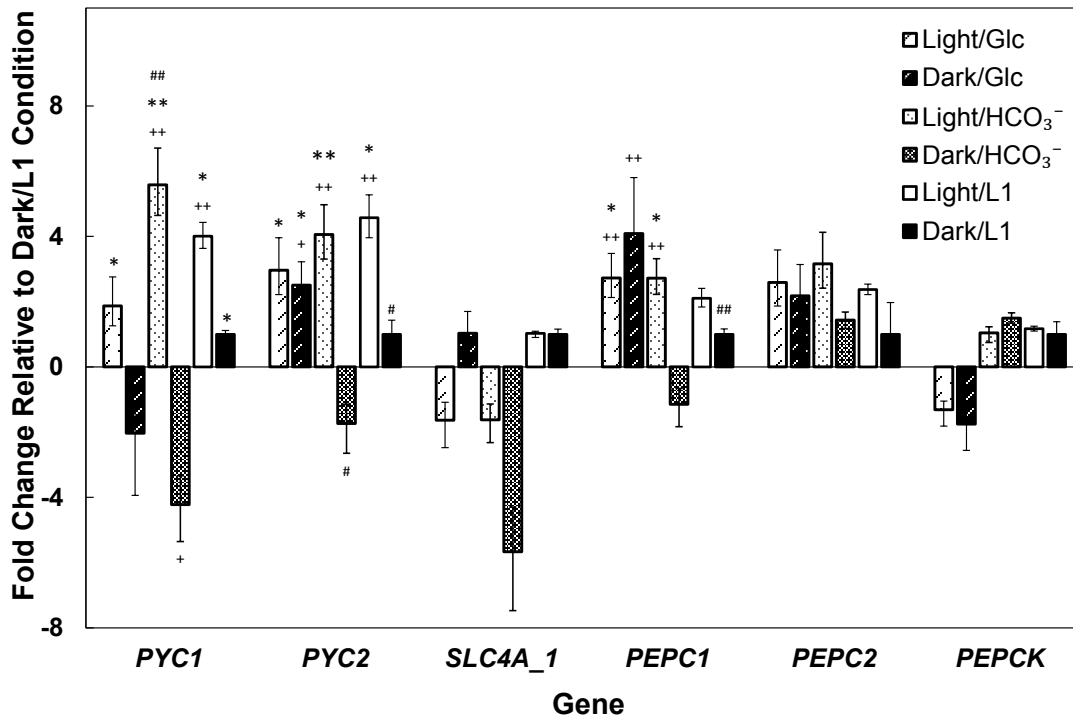


**Figure 3.8 Genes encoding putative HCO<sub>3</sub><sup>-</sup>-capturing enzymes in the C<sub>4</sub> CCM are induced by light.**

Expression levels of genes under six conditions (light/L1, dark/L1, light/HCO<sub>3</sub><sup>-</sup>, dark/HCO<sub>3</sub><sup>-</sup>; light/Glc and dark/Glc; see Materials and Methods), as compared to the dark/L1, dark/HCO<sub>3</sub><sup>-</sup> or dark/Glc conditions. Fold changes were calculated with respect to the housekeeping gene *18S* and were verified with respect to two other housekeeping genes. Results are presented as mean ± SD of three biological and three technical replicates (a total of 9 replicates per gene and condition). <sup>+</sup>: 0.01 < *p* < 0.05 when compared to the dark/L1 condition; <sup>++</sup>: *p* ≤ 0.01 when compared to the dark/L1 condition; <sup>\*</sup>: 0.01 < *p* < 0.05 when compared to the dark/HCO<sub>3</sub><sup>-</sup> condition; <sup>\*\*</sup>: *p* ≤ 0.01 when compared to the dark/HCO<sub>3</sub><sup>-</sup> condition; <sup>#</sup>: 0.01 < *p* < 0.05 when compared to the dark/Glc condition; <sup>##</sup>: *p* ≤ 0.01 when compared to the dark/Glc condition;

**Figure 3.8** depicts fold changes with respect to the housekeeping gene *18S* for all genes whose expression levels were consistent across three housekeeping genes (*18S*, *HIS4* and *EF1α*; **Table 3.2**). Clearly, Pyr carboxylase is induced by light or by a combination of light, HCO<sub>3</sub><sup>-</sup> and glucose, but not by HCO<sub>3</sub><sup>-</sup> alone. In L1 medium, exposure to light upregulated *PYC1* and *PYC2* by 4.0 ± 0.4-fold and 4.6 ± 0.7-fold,

respectively. In  $\text{HCO}_3^-$ -supplemented L1 medium, exposure to light upregulated *PYCI* and *PYC2* by  $5.6 \pm 1.0$ -fold and  $4.1 \pm 0.8$ -fold, respectively. Expression of *PYCI* and *PYC2* seemed to be depressed by adding glucose, and *PYCI* in this case was upregulated by  $2.2 \pm 0.7$ -fold when exposed to light (**Figure 3.8**). The expressions of *PEPCI* and *PEPC2* exhibited some response to light, but the corresponding fold changes were neither as high nor as significant as those for *PYCI*. *PEPCK* was not regulated to a noticeable extent by either light,  $\text{HCO}_3^-$  or glucose. In concordance with previous gene expression studies (Chauton et al., 2013; Nymark et al., 2009), our results show that light transcriptionally activates genes encoding the  $\text{HCO}_3^-$ -capturing enzymes *PYCI* and *PYC2* in *P. tricornutum*, suggesting the operation of a C<sub>4</sub> CCM in which Pyr carboxylation may play a prominent role. Conversely, the bicarbonate transporter *SLC4A\_1* showed no significant regulation by light,  $\text{HCO}_3^-$ , or glucose, suggesting that the biophysical CCM may either not be operational under the conditions we examined or may not be activated by light.

#### **3.3.4. Mixotrophic ILEs Employing U-<sup>13</sup>C Glucose or U-<sup>13</sup>C Acetate Reveal Substantial Capture of Inorganic Carbon into C<sub>4</sub> Metabolites**

Instationary labeling experiment shown that *P. tricornutum* is underlying C<sub>4</sub> CCM in its natural environment, and the light-induced transcriptional activation of  $\text{HCO}_3^-$ -capturing enzymes motivates the examination of C<sub>4</sub> CCM when organic carbon sources (such as glucose) is added. Toward this, we performed a steady-state, mixotrophic ILE by supplying *P. tricornutum* with 100% U-<sup>13</sup>C glucose (added to the medium) and atmospheric, naturally abundant CO<sub>2</sub> (from the headspace). This



experiment is feasible because *P. tricornutum* consumes glucose under light (Ceron Garcia et al., 2006; Liu et al., 2009), and putative glucose transporters in this organism have been reported in TransportDB (Ren et al., 2007) and the Joint Genome Institute genome annotation (<http://genome.jgi-psf.org>) databases. Carbon atoms of metabolites synthesized mixotrophic metabolism of U-<sup>13</sup>C glucose and <sup>12</sup>CO<sub>2</sub> would be <sup>13</sup>C-enriched at 100% if they originated solely in glucose or at natural abundance (1.1%) if they originated solely in CO<sub>2</sub>. Intermediate values of <sup>13</sup>C enrichment would reflect the relative contributions of glucose and CO<sub>2</sub> to the pertinent atom or fragment, thus providing a trail of CO<sub>2</sub> through metabolism. The 21 d-length of our experiment precluded any contributions of the initially present, naturally abundant biomass to any observed depletion in <sup>13</sup>C labeling. This is because as per our cell number measurements, the initially present biomass would have constituted only 2% of the biomass at 21 d (data not shown). In this experiment, if <sup>12</sup>CO<sub>2</sub> were made available to RuBisCO by diffusion or a biophysical CCM, then the Calvin cycle carbon atom rearrangements would cause the <sup>12</sup>C to appear most prominently at C-1 of the RuBisCO product 3-phosphoglycerate (3PG) as well as the downstream glycolytic C<sub>3</sub> metabolites PEP and Pyr. Thus, these metabolites would be depleted of <sup>13</sup>C at C-1. This dilution would also manifest at C-2 and C-3 of these metabolites, but to a smaller extent. **Figure 3.9a** depicts this prediction. Conversely, if <sup>12</sup>CO<sub>2</sub> were assimilated via a C<sub>4</sub> CCM, it would appear at the C-4 atoms of the C<sub>4</sub> metabolites OAA or Mal, so that these metabolites would exhibit significantly reduced <sup>13</sup>C enrichments at C-4. Additionally, <sup>12</sup>C would also appear at C-1, C-2 and C-3 of the

glycolytic C<sub>3</sub> metabolites due to recapture of <sup>12</sup>CO<sub>2</sub> by RuBisCO. Supplementary

Figure 3.9 b illustrates this prediction.

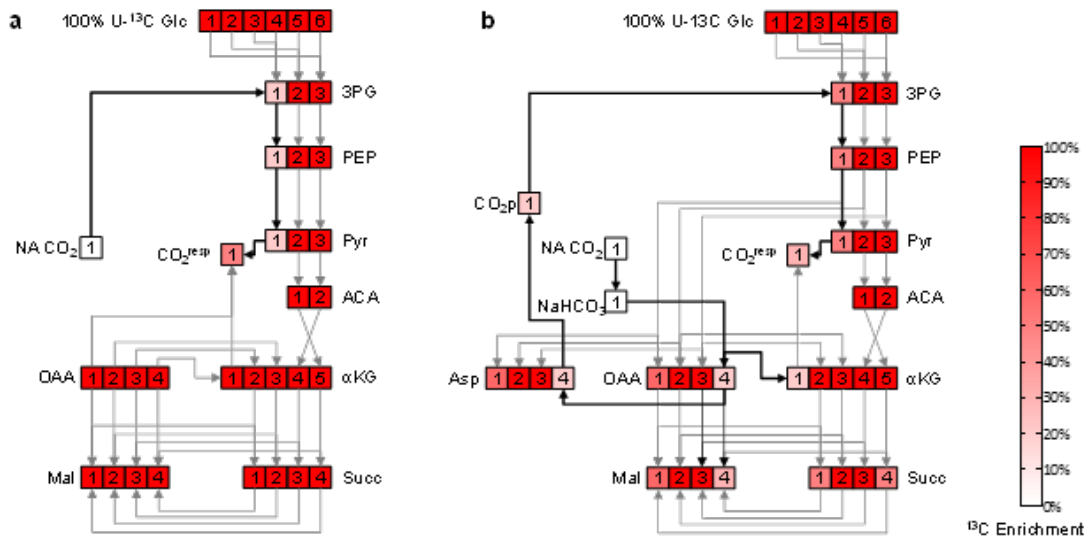


**Figure 3.9 Hypothesized <sup>13</sup>C enrichment patterns of metabolites in a mixotrophic ILE feeding 100% U-<sup>13</sup>C glucose and naturally abundant CO<sub>2</sub>.**

(a) If CO<sub>2</sub> were communicated to RuBisCO by either diffusion or a biophysical CCM, or by (b) a C<sub>4</sub> CCM. The intensity of red color in the rectangles signifies the degree of <sup>13</sup>C enrichment of atoms or fragments comprising multiple atoms, as explained in the color bar. HCO<sub>3</sub><sup>-</sup> or CO<sub>2</sub> capture by diffusion or a biophysical CCM would cause naturally abundant CO<sub>2</sub> to appear predominantly at C-1 (and to a lesser extent, at C-2 and C-3) of the three-carbon glycolytic metabolites 3PG, PEP and Pyr, thus causing these atoms to exhibit a reduced <sup>13</sup>C enrichment. Contrastingly, HCO<sub>3</sub><sup>-</sup> capture by a C<sub>4</sub> CCM would cause it to appear predominantly at C-4 of OAA and due to the TCA cycle, also at C-1 of αKG. A mixotrophic ILE feeding U-<sup>13</sup>C acetate and naturally abundant CO<sub>2</sub> (but no glucose) should also result in similar <sup>13</sup>C enrichment patterns if a C<sub>4</sub> CCM were operational (predicted enrichment patterns not shown).

We estimated the <sup>13</sup>C enrichments of fragments or individual atoms of central carbon metabolites retrobiosynthetically from the MIDs of proteinogenic amino acids derived from them (Szyperski, 1998b). Specifically, we estimated the enrichments of OAA fragments or atoms from the MIDs of Asp, α-ketoglutarate (αKG) from

glutamic acid (Glu), 3PG from serine (Ser) and glycine (Gly), PEP from phenylalanine (Phe) and tyrosine (Tyr) and Pyr from alanine (Ala) and valine (Val). These  $^{13}\text{C}$  enrichments evinced substantial incorporation of  $^{12}\text{CO}_2$  into OAA C-4 (**Figure 3.10 a**). For example, the OAA[34] fragment showed a  $^{13}\text{C}$  enrichment of  $76\% \pm 0.8\%$  (errors represent 3 to 4 biological replicates), which is significantly lower than the  $^{13}\text{C}$  enrichment of the fragments OAA[1] ( $85\% \pm 0.9\%$ ) or OAA[2] ( $89\% \pm 1.1\%$ ) (**Figure 3.10 a**). This is supported by the MIDs of Asp fragments: the Asp[1234] fragment exhibited a substantial  $m+n-1$  (i.e.  $m+3$ ) mass isotopomer ( $24\% \pm 0.5\%$ ), indicating that  $^{12}\text{C}$  was incorporated into one of its atoms. The fully labeled mass isotopomer ( $m+4$ ) of Asp[1234] ( $59\% \pm 1.5\%$ ) was significantly less abundant than that of the fully labeled mass isotopomer ( $m+2$ ) of Asp[12] ( $82\% \pm 2.0\%$ ), pointing to  $^{12}\text{CO}_2$  incorporation into C-3 or C-4 (**Figure 3.10 a** and appendix **Table A.2**).  $\text{C}_4$ -type carbon capture is further substantiated by the low enrichment of  $\alpha\text{KG}$  C-1. Because no glutamine was supplied in our experiment,  $\alpha\text{KG}$  C-1 was exclusively derived from OAA C-4 via the first few steps of the tricarboxylic acid (TCA) cycle. The  $^{13}\text{C}$  enrichment of  $\alpha\text{KG}$ [1] ( $74\% \pm 0.7\%$ ) was substantially lower than the overall enrichment of  $\alpha\text{KG}$ [2345] fragment ( $87\% \pm 0.5\%$ ), which is derived from C-2 and C-3 of oxaloacetate as well as C-1 and C-2 of acetyl-CoA. The  $^{13}\text{C}$  depletion at  $\alpha\text{KG}$  C-1 is obvious from the MIDs of Glu: the fully labeled mass isotopomer ( $m+5$ ) of Glu[12345] ( $58\% \pm 1.6\%$ ) was substantially less abundant than the fully labeled mass isotopomer ( $m+4$ ) of Glu[2345] ( $75\% \pm 2.0\%$ ). Moreover, Glu[12345] exhibited a substantial  $m+n-1$  (i.e.  $m+4$ ) abundance of  $24\% \pm 0.6\%$ , revealing that it contained substantial  $^{12}\text{C}$ . Amongst the  $\text{C}_3$  glycolytic compounds, the enrichments of 3PG C-1

(80%), C-2 (86%) and C-3 (84%) as well as Pyr C-1 (82%), C-2 (87%) and C-3 (90%) indicated photosynthetic CO<sub>2</sub> (re)capture, although to a lesser extent than HCO<sub>3</sub><sup>-</sup> capture by the C<sub>4</sub> CCM.

Similar trends were evident in another mixotrophic ILE in which we fed 100% U-<sup>13</sup>C acetate (added to medium) and atmospheric, naturally abundant CO<sub>2</sub> (from headspace) (**Figure 3.10 b**). The most obvious isotopic signature of C<sub>4</sub>-type <sup>12</sup>CO<sub>2</sub> incorporation was on αKG[1], whose <sup>13</sup>C enrichment (45.0% ± 1.5%) was substantially lesser than αKG[2345] (59.0% ± 2.0%) (**Figure 3.10 b**). Correspondingly, the fully labeled mass isotopomer (*m*+5) of Glu[12345] (40.0% ± 1.2%) was less abundant than the fully labeled mass isotopomer (*m*+4) of Glu[2345] (47.0% ± 1.7%) (appendix **Table A.3**). In this experiment, direct detection of <sup>12</sup>CO<sub>2</sub> incorporation on OAA C-4 was difficult. This is because the TCA cycle and the glyoxylate shunt carbon atom rearrangements that occur during acetate metabolism would cause OAA C-2 and C-3 to be significantly more <sup>13</sup>C-enriched than OAA C-1 and C-4. Because single quadrupole MS only permits estimation of the overall enrichment of the OAA[34] fragment and not the individual enrichments at C-3 or C-4, any dilution of OAA C-4 due to <sup>12</sup>CO<sub>2</sub> capture may not necessarily reduce the overall enrichment of the OAA[34] fragment compared to the OAA[1] and OAA[2] fragments. Nevertheless, the footprint of <sup>12</sup>CO<sub>2</sub> incorporation into OAA C-4 is obvious in αKG C-1, which is derived solely from OAA C-4.

The experiments described above revealed that under light, *P. tricornutum* captures considerable amounts of exogenous inorganic carbon into C<sub>4</sub> metabolites, likely OAA or Mal. Together with the observation that Pyr carboxylase is

transcriptionally activated by light, these experiments suggest to a C<sub>4</sub> CCM involving the Pyr carboxylase-catalyzed reaction  $\text{Pyr} \leftrightarrow \text{OAA}$  as the  $\text{HCO}_3^-$ -capture step.

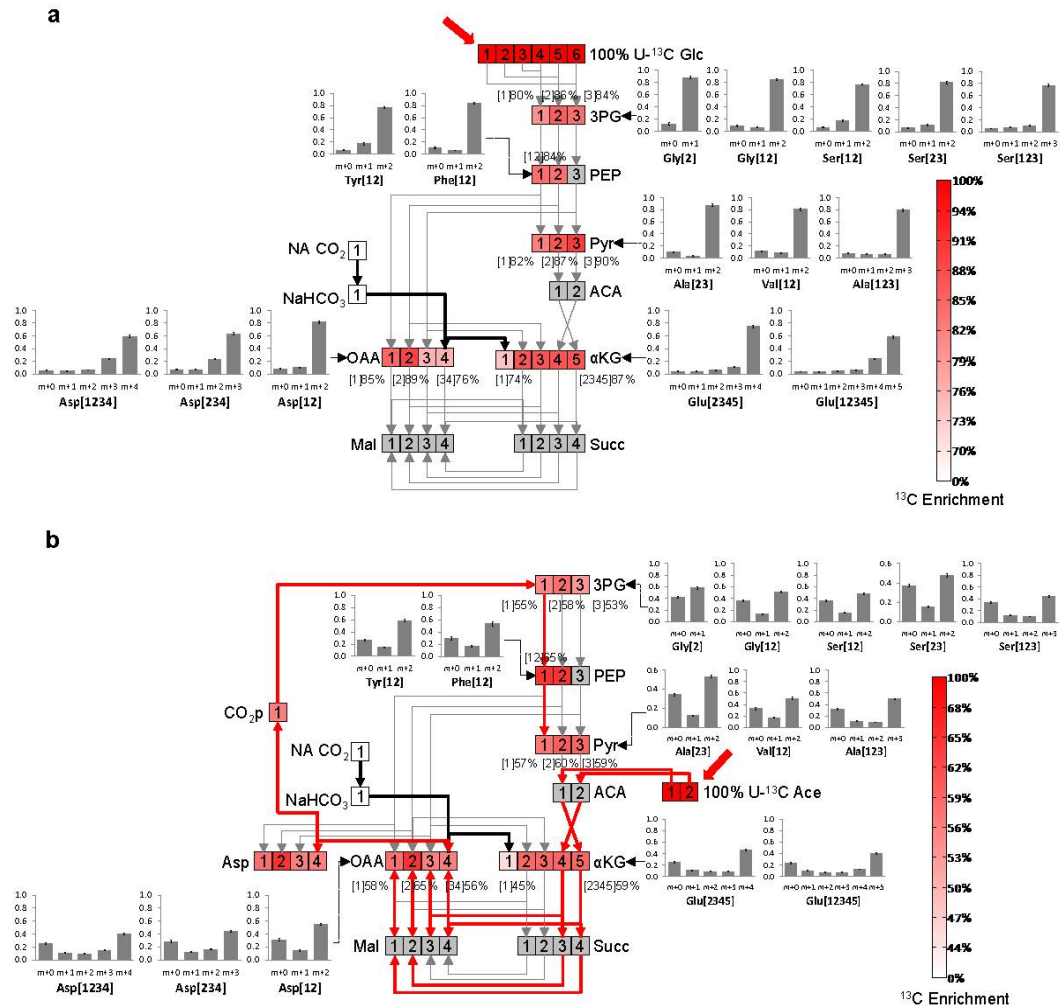


**Figure 3.10** Mixotrophic ILEs feeding (a, U-<sup>13</sup>C glucose and unlabeled CO<sub>2</sub>) as well as (b, U-<sup>13</sup>C acetate and unlabeled CO<sub>2</sub>) evidence substantial HCO<sub>3</sub><sup>-</sup> capture via a C<sub>4</sub> CCM.

Small rectangles denote carbon atoms of metabolites, numbered as per IUPAC nomenclature. The intensity of red color signifies the degree of <sup>13</sup>C enrichment of atoms or fragments comprising multiple atoms, as explained in the color bar. The <sup>13</sup>C enrichments of selected fragments are shown numerically, and the corresponding amino acid MIDs are shown alongside. The enrichments of the metabolites and fragments not measured shown in gray. Arrows indicate inferred carbon flow, with black arrows denoting naturally abundant (~1.1% <sup>13</sup>C) carbon and red arrows denoting <sup>13</sup>C carbon.

### 3.3.5. 4-<sup>13</sup>C Asp ILE Suggests Photosynthetic Assimilation of CO<sub>2</sub> released from OAA C-4

Although we have shown that *P. tricornutum* exhibits C<sub>4</sub>-type HCO<sub>3</sub><sup>-</sup> capture, the purpose of a C<sub>4</sub> CCM is accomplished only when the captured carbon is released and re-assimilated photosynthetically (**Figure 3.2 c**). We found evidence for this by tracking the fate of the OAA C-4 atom through the metabolic network. Toward this objective, we initially performed a mixotrophic ILE by feeding 100% 1-<sup>13</sup>C acetate. The <sup>13</sup>C labeling patterns in this ILE (**Figure 3.11** and appendix **Table A.4**) were consistent with the operation of a C<sub>4</sub> CCM. However, the carbon exchanges between C<sub>4</sub> and C<sub>3</sub> metabolites necessitated by acetate metabolism did not permit the elimination of alternative scenarios that could also explain the labeling data (analysis not shown). Therefore, to unequivocally detect the CO<sub>2</sub>-release step of the C<sub>4</sub> CCM, we performed another mixotrophic ILE by feeding 100% 4-<sup>13</sup>C Asp (added to medium) with atmospheric, naturally abundant CO<sub>2</sub> (from headspace). As in **Sec. 3.3.4**, we estimated <sup>13</sup>C enrichments of central carbon metabolite fragments from the MIDs of proteinogenic amino acids derived from them. In this ILE, 4-<sup>13</sup>C Asp can be expected to exchange carbon with OAA, causing OAA C-4 to become partially <sup>13</sup>C-labeled. Thus, <sup>13</sup>C enrichment of an atom or fragment significantly above natural abundance (1.1%) would imply that it partially originated in Asp or OAA C-4. Particularly, the release of CO<sub>2</sub> from OAA C-4 and its photosynthetic re-assimilation in the plastid would lead to two labeling patterns: (i) the photosynthetic product 3PG and the glycolytic C<sub>3</sub> metabolites downstream of 3PG would be <sup>13</sup>C-enriched at C-1,

and to a lesser extent, at C-2 and C-3; (ii) metabolites in the plastid would be more  $^{13}\text{C}$ -enriched than those outside the plastid.

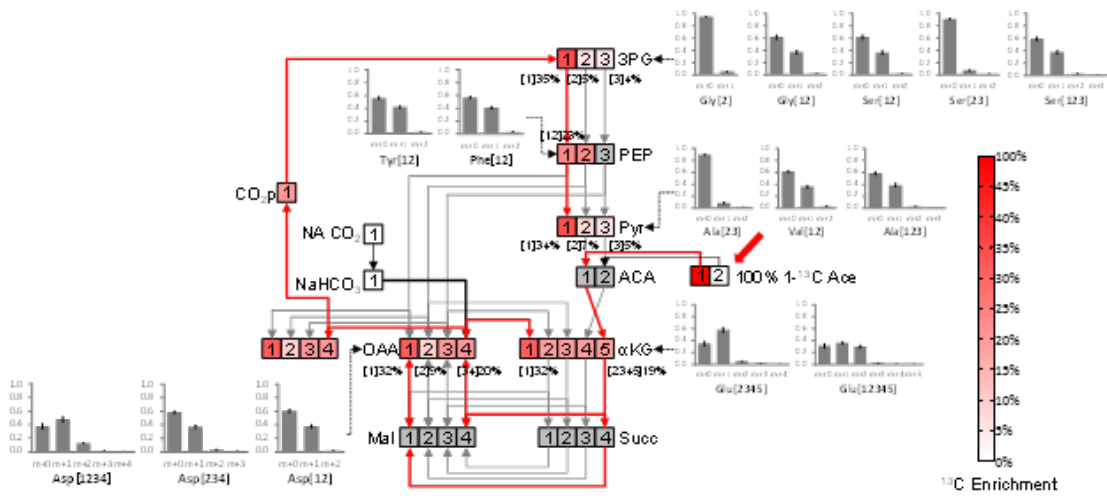


**Figure 3.11** MIDs and  $^{13}\text{C}$  enrichments for mixotrophic ILE feeding 1- $^{13}\text{C}$  acetate (added to medium) and naturally abundant  $\text{CO}_2$  (from headspace).

This figure follows the scheme of **Figure 3.10**. Briefly, MIDs of proteinogenic amino acids were measured by GC-MS and  $^{13}\text{C}$  enrichments of atoms or fragments of metabolic intermediates were retrobiosynthetically calculated from the MIDs. This ILE was very reproducible; all MIDs varied by  $\sim 1\%$  across four biological replicates. Arrows indicate inferred carbon flow, with black arrows denoting NA ( $\sim 99\%$  unlabeled) carbon and red arrows denoting  $^{13}\text{C}$  carbon. Acetate passing through the glyoxylate shunt and the TCA cycle is expected to predominantly label C-1 and C-4 of OAA. The fact that this carbon is passed on to C-1 of the glycolytic three-carbon metabolites 3PG, PEP and Pyr is consistent with  $\text{CO}_2$  release by anaplerotic reactions, but is not sufficient to show that a  $\text{C}_4$  CCM is operational.

Our results (**Figure 3.12**) agree with these expectations. Foremost, several data points confirmed that Asp is co-metabolized with  $\text{CO}_2$  and that the  $^{13}\text{C}$  atom in 4- $^{13}\text{C}$  Asp enriches OAA C-4 by 15%–20%. For instance, the  $^{13}\text{C}$  enrichment of the OAA[34] fragment ( $11.0\% \pm 1.0\%$ ) was significantly higher than that of OAA[1] ( $3.0\% \pm 0.1\%$ ) or OAA[2] ( $2.0\% \pm 0.1\%$ ), as evident from the MIDs of proteinogenic Asp fragments. The  $m+1$  abundances of the fragments Asp[234] ( $22.0\% \pm 3.0\%$ ) and

Asp[1234] ( $24.0\% \pm 3.0\%$ ) were substantially higher than the  $m+1$  abundance of Asp[12] ( $5.0\% \pm 0.3\%$ ) (appendix **Table A.5**). Derived exclusively from OAA C-4 via the TCA cycle,  $\alpha$ KG[1] also displayed a much higher  $^{13}\text{C}$  enrichment ( $15.0\% \pm 1.0\%$ ) than  $\alpha$ KG[2345] ( $3.0\% \pm 0.2\%$ ). This is clear from the difference between the  $m+1$  masses of the fragments Glu[2345] ( $8.0\% \pm 0.2\%$ ) Glu[12345] ( $21.0\% \pm 2.0\%$ ). Next, the glycolytic  $\text{C}_3$  metabolites were  $^{13}\text{C}$ -enriched to 4%–6% at C-1 and to lesser extents at C-2 and C-3, suggesting photosynthetic assimilation of  $\text{CO}_2$  released from OAA C-4 by the  $\text{C}_4$  CCM. For instance, 3PG displayed a  $^{13}\text{C}$  enrichment of  $4.0\% \pm 0.2\%$  at C-1,  $2.0\% \pm 0.2\%$  at C-2 and  $1.0\% \pm 0.1\%$  at C-3. Likewise, the  $^{13}\text{C}$  enrichments of Pyr C-1, C-2 and C-3 were  $6.0\% \pm 0.3\%$ ,  $2.0\% \pm 0.6\%$  and  $3.0\% \pm 0.7\%$ , respectively (**Figure 3.12**). Finally, the plastidic metabolite ribose-5-phosphate (P5P), which is a precursor of histidine (His) in plants (Fujimori and Ohta, 1998), exhibited significant  $^{13}\text{C}$  enrichment. The appreciable  $6.0\% \pm 0.5\%$  enrichment of P5P[1234] was evident from the  $m+1$  ( $16.6\% \pm 0.9\%$ ) and  $m+2$  ( $2.6\% \pm 0.4\%$ ) abundances of the corresponding His fragment [2345] (**Figure 3.12** and appendix **Table A.5**). The mass fragments of aromatic amino acids phenylalanine (Phe) and tyrosine (Tyr), which are synthesized from plastidic PEP and erythrose-4-phosphate (E4P) (Singh, 1998) as well as valine, which is synthesized from plastidic Pyr in plants (Singh, 1998), displayed substantial  $m+1$  abundances ( $> 11\%$ ) and significant  $m+2$  abundances (appendix **Table A.5**). All these observations are in accordance with the release of  $\text{CO}_2$  in the plastid from the  $\text{C}_4$  CCM.



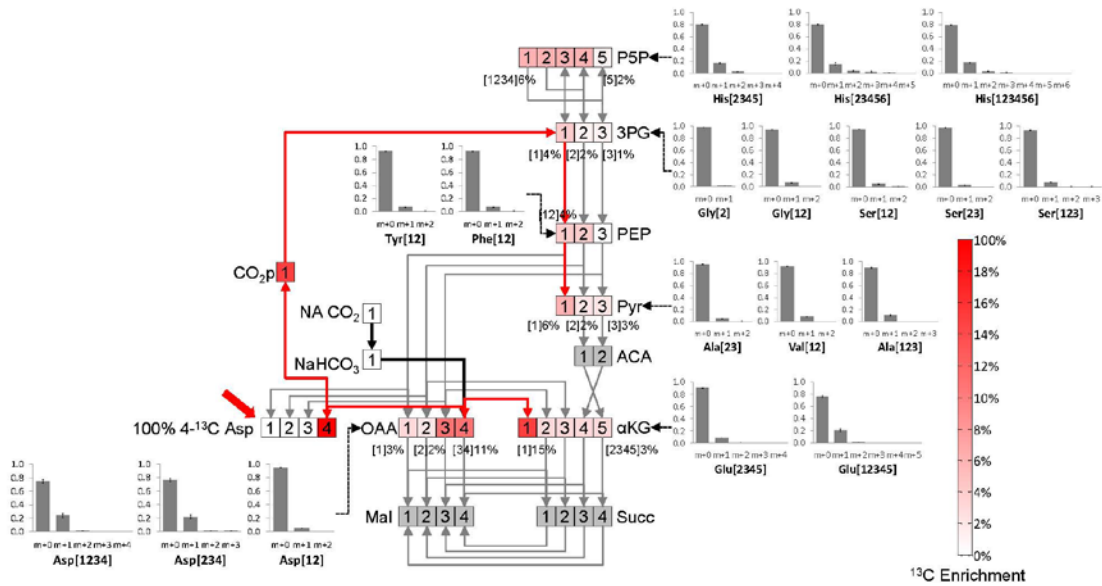


**Figure 3.12 Mixotrophic ILE feeding 4-<sup>13</sup>C Asp and unlabeled CO<sub>2</sub> evidences photosynthetic recapture of CO<sub>2</sub> released from a C<sub>4</sub> CCM.**

MIDs and <sup>13</sup>C enrichments, following the scheme of **Figure 3.10**. This ILE was very reproducible; all MIDs varied by ~1% across four biological replicates. The transfer of <sup>13</sup>C from C-4 of Asp (and OAA) to C-1 of αKG can be explained by the first reaction of the TCA cycle.

### 3.3.6. <sup>13</sup>C MFA Estimates that CO<sub>2</sub> Released from OAA C-4 Contributes a Minimum of 21% ± 3% of Photosynthetically Fixed CO<sub>2</sub>

The above observations are well explained by a scenario involving the release of CO<sub>2</sub> from OAA by the C<sub>4</sub> CCM and its photosynthetic re-assimilation (hereafter, “C<sub>4</sub> scenario”). However, an alternative scenario that may possibly explain the data is one involving carbon exchange between OAA C-4 and C-1 through the reversible steps of the TCA cycle: OAA ↔ Mal ↔ fumarate (Fum) ↔ succinate (Succ), followed by a reverse anaplerotic reaction that transfers <sup>13</sup>C from C-1 of OAA/Mal to C-1 of PEP/Pyr. This scenario (hereafter, “alternative scenario”) represents a C<sub>4</sub> CCM that is inefficient to the extreme: HCO<sub>3</sub><sup>-</sup> is captured into and CO<sub>2</sub> is released from

OAA C-4, but all the released CO<sub>2</sub> is expelled from the cell and is unavailable to RuBisCO. We employed <sup>13</sup>C MFA to determine which of these two scenarios is better supported by the labeling data. A compartmented metabolic model corresponding to the C<sub>4</sub> scenario (**Table 3.3**) featuring the cytosolic and plastidic compartments gave an acceptable statistical fit to the isotopomer data from this ILE. The fluxes evaluated using this model are depicted in **Figure 3.13a** and listed in **Table 3.3**; a goodness-of-fit plot comparing measured isotopomer abundances and simulated isotopomer abundances corresponding to the evaluated fluxes is shown in **Figure 3.13b**. We obtained a variance-weighted sum of squared residuals (SSR or the  $\chi^2$  metric) value of 91 between the (114) measured mass isotopomer abundances and the corresponding isotopomer abundances simulated from the evaluated fluxes (**Table 3.6**). The 95% confidence interval of SSR for 114 redundant measurements is [86, 145]; therefore, our fit is statistically acceptable. Additionally, slight variants of this metabolic model featuring an efflux of 3PG into the extracellular space also yielded acceptable SSRs less than 100 (models not shown). A metabolic model mimicking the alternative scenario (**Table 3.4**) did not explain the labeling data adequately. This model yielded an SSR of 169, greater than the acceptable upper limit of 145 (**Table 3.6**). Supplementary **Figure 3.13c,d** depicts the flux map and goodness-of-fit plot corresponding to this model. Thus we quantitatively demonstrated that amongst the two candidate metabolic models for this ILE, only a model incorporating the CO<sub>2</sub>-release and photosynthetic re-assimilation steps of the C<sub>4</sub> CCM can satisfactorily explain the labeling data.

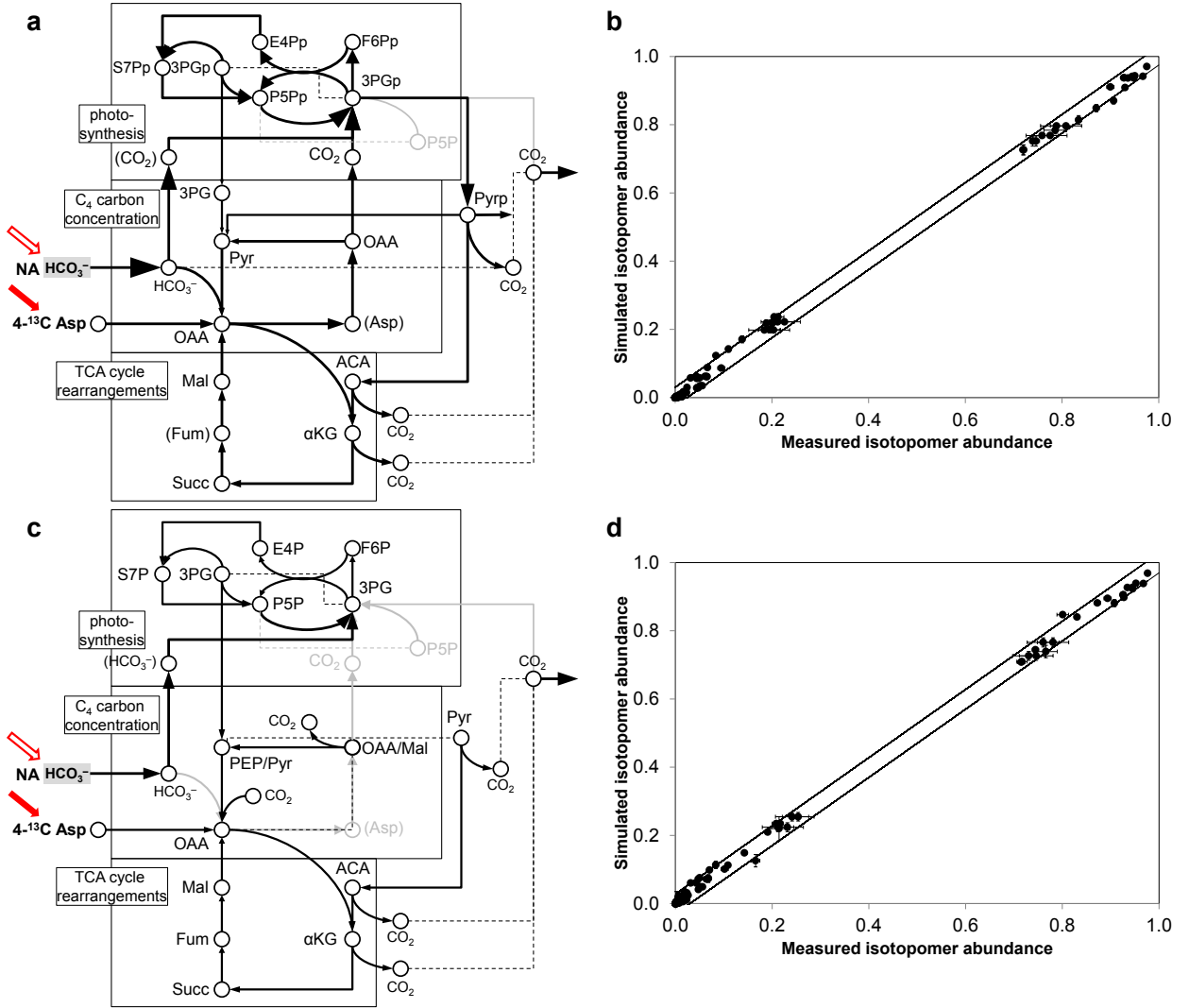


**Figure 3.13** The “C<sub>4</sub> scenario” and “alternative scenario” steady-state models for the 4-<sup>13</sup>C Asp ILE.

The flux map (a and c) depicts flux values with arrow thicknesses proportional to fluxes. Dashed lines connect multiple occurrences of the same metabolite on the map (shown thus to avoid excessive line intersections). Arrow widths are proportional to values of net fluxes. The parity plot (b and d) shows measured mass isotopomer abundances against simulated isotopomer abundances corresponding to the evaluated fluxes (their left panel). The SSR (91) for C<sub>4</sub> scenario model (a) fell well inside the acceptable 95% confidence interval of [86, 145]. The corresponding parity plot of measured isotopomers and simulated isotopomers corresponding to the evaluated fluxes (b; the band surrounding the 45° diagonal encloses 95% of the points) also shows that this model adequately explains the labeling data. The model mimicking the alternative scenario (c) did not explain the labeling data adequately and resulted in an SSR of 169.

**Table 3.6 Summary of metabolic scenarios used to model the 4-<sup>13</sup>C Asp ILE.**

Model	Source of CO <sub>2</sub> available to RuBisCO		SSR (χ <sup>2</sup> )	OAA C-4 contribution to CO <sub>2</sub> pool around RuBisCO
	OAA C-4	Diffusion, biophysical		
C <sub>4</sub> scenario (Figure 3.13a,b)	YES	YES	91	≥ 21.3% ± 3.3%
Alternative scenario (Figure 3.13c,d)	NO	YES	169	0.0% ± 0.0%
<b>Acceptable upper limit of SSR:</b>			<b>145</b>	

We found that in the C<sub>4</sub> scenario, segregation of metabolites into two compartments (cytosol and plastid) was necessary to obtain an acceptable SSR. An initial uncomparted model associated with a statistically unacceptable SSR simulated lower-than-observed <sup>13</sup>C labeling for His and Val. This problem was only corrected after assigning P5P to the plastid and designating plastidic Pyr as a precursor of valine, both of which are biologically accurate compartmental assignments for plant cells (Fujimori and Ohta, 1998; Singh, 1998). This is consistent with our observation that in this ILE, plastidic glycolytic metabolites are more <sup>13</sup>C-enriched than cytosolic ones. Combining this with the plastidic localization of photosynthesis and the requirement that all <sup>13</sup>C above natural abundance should originate in OAA C-4, this provides strong evidence for the photosynthetic fixation of CO<sub>2</sub> released from OAA C-4. Compartmentalization of metabolites was irrelevant (therefore not advantageous) to the alternative scenario, as that scenario assumed that CO<sub>2</sub> released from OAA is expelled instead of being transported to a RuBisCO-containing compartment.

An advantage of  $^{13}\text{C}$  MFA is that it permits the estimation of metabolic quantities not trivially calculable from MIDs or  $^{13}\text{C}$  enrichments. An interesting question that can be thus answered is: what fraction of  $\text{CO}_2$  released from the  $\text{C}_4$  CCM is re-assimilated photosynthetically? This fraction is an estimate of the extent to which the  $\text{C}_4$  CCM contributes to the pool of photosynthetically fixed  $\text{CO}_2$ . To estimate it, we obtained simulated  $^{13}\text{C}$  enrichments of OAA C-4 ( $15.4\% \pm 0.8\%$ ) and the plastidic  $\text{CO}_2$  pool available to RuBisCO ( $4.1\% \pm 0.3\%$ ) from the  $^{13}\text{C}$  MFA results. Using the formula:

$$\text{contribution of OAA C - 4 to plastidic CO}_2 \text{ pool} = \frac{\text{enrichment of plastidic CO}_2 - \text{NA}}{\text{enrichment of OAA C - 4} - \text{NA}} \quad (17)$$

where NA is natural abundance, we estimated that OAA C-4 (and therefore the  $\text{C}_4$  CCM) contributes at least  $21.3\% \pm 3.3\%$  of the  $\text{CO}_2$  available to photosynthesis. The rest is likely contributed by biophysical CCM or less likely, by  $\text{CO}_2$  diffusion. It is important to note that this estimated contribution is a minimum. This is because our model assumes proteinogenic Asp and cytosolic OAA to be equilibrated.

Consequently, the isotomeric composition of OAA (which we could not measure directly) would be identical to that of the  $\text{C}_4$  skeletons of proteinogenic Asp, Met and Thr (which we measured directly) in our model. However, it is likely that Asp and OAA do not equilibrate and that OAA, being downstream of the ingested  $4\text{-}^{13}\text{C}$  Asp, is less enriched at C-4 than Asp. This would decrease the denominator in Eq. (17), causing the fractional contribution of the  $\text{C}_4$  CCM to be higher. Additionally, the variants of the  $\text{C}_4$  scenario with 3PG effluxes (see above) estimated higher  $\text{C}_4$  CCM contributions to photosynthesis: a model with 3PG efflux and exchange between cytosolic and plastidic 3PG estimated  $26.9\% \pm 9.1\%$ , whereas a model with 3PG

efflux but no 3PG exchange between compartments estimated  $35.7\% \pm 12.9\%$ . Thus,  $21\% \pm 3\%$  is the minimal contribution of the C<sub>4</sub> CCM to photosynthesis.

### 3.4. Discussion

A small minority of plants and algae employ biophysical or biochemical (C<sub>4</sub>) CCMs to concentrate CO<sub>2</sub> around RuBisCO to enhance their photosynthetic rate. Investigating C<sub>4</sub> CCMs from a metabolic perspective, for instance by using isotope labeling and <sup>13</sup>C MFA, is essential to gain insights toward metabolic engineering of photosynthesis. Unicellular diatoms are an excellent testbed for probing single-cell C<sub>4</sub> CCMs because of their reported photosynthetic efficiency. Furthermore, the contrasting lines of evidence regarding the CCM used by *P. tricornutum* make this diatom an especially exciting subject for such a study.

Stable isotope labeling and <sup>13</sup>C MFA can provide stronger and more direct evidence for C<sub>4</sub> CCMs than traditionally used methods such as gene expression profiling, isotope discrimination or <sup>14</sup>C radiolabeling. Coordinated expression of genes encoding putative C<sub>4</sub> enzymes can only provide circumstantial evidence, as gene expression does not guarantee that the relevant metabolic pathways are operational. Isotope discrimination analysis is based on the premise that enzymes (e.g. RuBisCO and the putative C<sub>4</sub> enzyme PEP carboxylase) differ in their affinities for <sup>12</sup>C and <sup>13</sup>C on the order of a few parts per thousand (‰). Thus the measurement of <sup>12</sup>C:<sup>13</sup>C ratio in a biomass sample, such as by isotope ratio MS, can potentially be used to discern whether carbon in the biomass was first captured by RuBisCO or PEP

carboxylase. However, this interpretation can be complicated by the carbon isotope discrimination of thermodynamic processes (e.g. dissociation of  $\text{CO}_2$  to  $\text{HCO}_3^-$ ) and kinetic processes (e.g. intercompartmental transport of  $\text{HCO}_3^-$  or  $\text{CO}_2$ ) accompanying photosynthesis. Furthermore, the  $\text{C}_4$  CCM could use multiple carbon-capturing enzymes that differ in their  $^{12}\text{C}$  and  $^{13}\text{C}$  affinities.

In contrast, stable isotope labeling together with MFA directly estimates the metabolic fluxes that orchestrate a  $\text{C}_4$  CCM. In this methodology, the use of sufficient extents of  $^{13}\text{C}$  eliminates any effects of enzymatic discrimination of  $^{13}\text{C}$  over  $^{12}\text{C}$ .  $^{13}\text{C}$  labeling is also more informative than  $^{14}\text{C}$  radiolabeling because in conjunction with measurement techniques such as MS, it provides information not only on which metabolites contain the unusual isotope ( $^{13}\text{C}$ ) but also the precise carbon atom on which the isotope is located. For the first time, our study brings multiple lines of  $^{13}\text{C}$  isotope labeling evidence and  $^{13}\text{C}$  MFA to dissect a  $\text{C}_4$  CCM. Our ILEs used various carbon sources, steady-state and instationary dynamics as well as  $^{13}\text{C}$  MFA to quantify the fraction contribution of the  $\text{C}_4$  CCM to photosynthesis. We have also established a framework for isotope labeling studies in *P. tricornutum* that can be employed, for example, to assess the effects of environmental or genetic perturbations on the performance of the  $\text{C}_4$  CCM. Recently reported analytical methods (such as tandem MS to measure all isotopomers of Asp; Choi et al., 2012) should facilitate even further improvements in our methodology in the future.

Our principal hypothesis was that a  $\text{C}_4$  CCM was operational in *P. tricornutum* and that it contributes a significant amount of  $\text{CO}_2$  to photosynthesis. This hypothesis was confirmed by both mixotrophic and instationary ILEs. The

instationary ILE revealed that  $\text{HCO}_3^-$  is rapidly captured into Asp (**Figure 3.3**) and that Asp is more  $^{13}\text{C}$ -enriched than Mal for the first several minutes of the ILE (**Figure 3.3, Figure 3.5a, Figure 3.6a**). The  $\text{U-}^{13}\text{C}$  glucose and  $\text{U-}^{13}\text{C}$  acetate mixotrophic ILEs provided clear evidence for the capture of inorganic carbon into C-4 atoms of OAA or Mal (**Figure 3.10**). This suggests OAA and not Mal as the compound into which  $\text{HCO}_3^-$  is captured. Furthermore, our observation that plastidic and mitochondrial Pyr carboxylases are upregulated by light (**Figure 3.8**), points to the  $\text{Pyr} \leftrightarrow \text{OAA}$  reaction as the major mechanism of  $\text{HCO}_3^-$  capture. The  $4\text{-}^{13}\text{C}$  Asp ILE revealed metabolic signatures of  $\text{CO}_2$  release from the  $\text{C}_4$  CCM and its photosynthetic re-assimilation, especially into plastidic metabolites (**Figure 3.12**). Particularly, we were able to show that a metabolic scenario involving the  $\text{CO}_2$  release step and photosynthetic  $\text{CO}_2$  re-assimilation step of the  $\text{C}_4$  CCM (**Figure 3.13**) was able to statistically explain the isotopomer data from this ILE (**Figure 3.13** and **Table 3.6**). Importantly,  $^{13}\text{C}$  MFA of this ILE revealed that the  $\text{C}_4$  CCM contributes at least a fifth, if not more, of photosynthetically fixed  $\text{CO}_2$ .

The evidence from the mixotrophic ILEs was reinforced by results from an instationary  $\text{H}^{13}\text{CO}_3^-$  ILE (**Figure 3.3** and **Figure 3.5**). This experiment provided evidence for all three steps of the  $\text{C}_4$  CCM, in addition to giving insights on their relative timescales and the overall efficiency of the  $\text{C}_4$  CCM. The  $\text{HCO}_3^-$ -capture step was evidenced by the appearance of the supplied  $^{13}\text{C}$  first on Asp C-4 as against the carbon atoms of 3PG (**Figure 3.5 a-d,h**), the  $\text{CO}_2$ -release step was substantiated by the subsequent appearance of  $1\text{-}^{13}\text{C}$  Lac (**Figure 3.5 g**), and the photosynthetic  $\text{CO}_2$  re-assimilation step was evidenced by the ensuing labeling of 3PG (**Figure 3.5 h**) and



the eventual, approximately uniform labeling of biomass components (**Figure 3.3**). Our best attempt to model the instationary isotopomer data (**Figure 3.7**) showed that the C<sub>4</sub> CCM contributes two-thirds of photosynthetically fixed carbon. This is qualitatively consistent with the results from the analysis of the 4-<sup>13</sup>C Asp ILE. The numerical disagreement between the two results is likely because (i) the 4-<sup>13</sup>C Asp MFA provided a minimum value for the contribution of the C<sub>4</sub> CCM, (ii) the flux model for the instationary ILE did not provide a statistically acceptable fit, and (iii) metabolism could be slightly altered by the introduction of significant Asp into the medium. Overall, our results follow a very different metabolic trend compared to another recent report of photosynthetic MFA (Young et al., 2011b), where CO<sub>2</sub> appeared to be conveyed to RuBisCO either by diffusion or a biophysical CCM.

We performed the steady-state ILEs in batch for a significant duration (21 d) to prevent the initially present (“inoculum”) biomass to affect the labeling. Batch-grown *P. tricornutum* cells are in exponential growth through most of this period. From growth curves, we anticipated ~2% of the initial biomass to be present at 21 d of culture, so that any observed <sup>12</sup>C dilution in the glucose and acetate ILEs would be predominantly due to incorporation of <sup>12</sup>CO<sub>2</sub> from the headspace. We did verify that isotopic steady state was attained in these ILEs, by measuring isotopomer abundances on 20 d, 21 d and 22 d of a representative (U-<sup>13</sup>C glucose) ILE and finding them to be nearly identical by direct comparison and principal component analysis (data and analysis not shown). However, a possible criticism of such a long ILE is that the cultures may not have been at a single metabolic (steady) state during the experiment. Nonetheless, this criticism does not weaken our principal conclusions as the glucose,

acetate and Asp ILEs were designed to provide isotope labeling signatures of individual steps of the C<sub>4</sub> CCM, such as the appearance of <sup>12</sup>C on Asp C-4 and αKG C-1 in the glucose and acetate ILEs. Our observation of these signatures incontrovertibly demonstrates that the relevant step of the CCM was functional sometime during period of the ILE, if not uniformly throughout the experiment. Thus, the mixotrophic ILEs did accomplish their objective of stepwise confirmation of our hypothesis of a C<sub>4</sub> CCM. Furthermore, the labeling data from the instationary ILEs independently verified that these steps were operational.

Our flux model for the instationary ILE did provide an acceptable fit for the Asp isotopomer data. However, a closer look at the enrichment measurements (**Figure 3.5**), our metabolic model, the computationally estimated pool sizes (**Table 3.5**) and the cell culture itself brings out the reasons for unsatisfactory fit of TCA cycle metabolites. First, due to the excellent reproducibility of the instationary ILE, the standard deviations of the <sup>13</sup>C enrichments across three biological replicates were extremely small, often much less than 1% (see corresponding MIDs in appendix **Table A.1**). Second, the TCA cycle metabolites Mal and Fum exhibited labeling dynamics that were difficult to model (**Figure 3.6**). Thirdly, our model may not have accurately mimicked subcellular compartmentalization. The discrepancies between the simulated and measured values of at least two pool sizes (Fum and 3PG; **Table 3.5**) suggest we may have measured aggregate pool sizes of some compartmented metabolites. Finally, *P. tricornutum* cell cultures are slightly heterogeneous, unlike many microbial cultures. Microscope images showed that the cultures investigated in this work predominantly exhibit the fusiform morphotype (one of the three

morphotypes of this organism; Abdullahi et al., 2006) and stack together in groups of ~5 cells (images not shown). Thus, modeling the culture as a fully homogeneous suspension may not be accurate. The first three problems identified above can be corrected by a more detailed metabolic model, and efforts toward this are ongoing in our laboratory. Nevertheless, this experiment upholds the conclusions of the mixotrophic ILEs, viz. significant  $\text{HCO}_3^-$  capture (observed in U- $^{13}\text{C}$  glucose and acetate ILEs), significant  $\text{CO}_2$  release and photosynthetic incorporation (both observed in 4- $^{13}\text{C}$  Asp ILE). Additionally, the conclusion that the  $\text{C}_4$  CCM contributes partially to the  $\text{CO}_2$  pool around RuBisCO agreed with that obtained from the 4- $^{13}\text{C}$  Asp ILE. Furthermore, the instationary ILE revealed the relative timescales of  $\text{HCO}_3^-$  capture,  $\text{CO}_2$  release and photosynthetic incorporation.

Collectively, our isotope labeling and  $^{13}\text{C}$  MFA results support a working model of a  $\text{C}_4$  CCM (**Figure 3.4** and **Figure 3.7**) that captures  $\text{HCO}_3^-$  via the Pyr  $\leftrightarrow$  OAA reaction, transports either OAA, Asp or Mal to the vicinity of RuBisCO and finally decarboxylates OAA or Mal to Pyr. Our results also suggest the concomitant operation of a  $\text{C}_4$  and a biophysical CCM. How do our results fit into the context of previous work on CCMs in *P. tricornutum*? Our conclusions are consistent with previous bioinformatic analysis showing that *P. tricornutum* can operate both types of CCM in *P. tricornutum* (Kroth et al., 2008) and several previous gene expression profiles that supported a  $\text{C}_4$  CCM (Chauton et al., 2013; Maheswari et al., 2010; Nymark et al., 2009; Valenzuela et al., 2012). Importantly, our study offers direct, metabolic evidence of the various steps of the CCM as well as their relative timescales. One study used  $^{18}\text{O}$  labeling to measure  $\text{CO}_2$  fluxes between the medium,

cytoplasm and organelles of *P. tricornutum* (Hopkinson et al., 2011) and suggested a strong role for CA in concentrating CO<sub>2</sub>, thus pointing to a biophysical CCM. However, Hopkinson et al. did not rule out a C<sub>4</sub> CCM and actually suggested that a C<sub>4</sub> compound could be decarboxylated in the pyrenoid, the organelle within the cytosol where RuBisCO is localized. Hopkinson et al. did not report carbon metabolic fluxes as their objective was to measure CO<sub>2</sub> and HCO<sub>3</sub><sup>-</sup> fluxes through <sup>18</sup>O labeling. Our study addresses this gap through <sup>13</sup>C labeling. Finally, one study reported evidence against a C<sub>4</sub> CCM (Haimovich-Dayan et al., 2013). This study utilized RNAi to silence a gene encoding PPDK, which converts Pyr to PEP and could be a critical link in a C<sub>4</sub> CCM operating the cycle PEP (+ HCO<sub>3</sub><sup>-</sup>) → OAA → Pyr (+ CO<sub>2</sub>) → PEP. Haimovich-Dayan et al. found that silencing PPDK did not reduce the overall photosynthetic K<sub>1/2</sub> for CO<sub>2</sub>. However, this result can be explained despite the operation of a C<sub>4</sub> CCM if, according to our model, the C<sub>4</sub> CCM bypasses PEP and does not recruit PPDK.

Our elucidation of the C<sub>4</sub> CCM in *P. tricornutum* opens up further questions about the CCM, some of which are being investigated in our laboratory. For instance, whether the fractional contribution of the C<sub>4</sub> (and the biophysical) CCM to photosynthetically fixed CO<sub>2</sub> changes with environmental conditions will be crucial to understanding the relative roles of the two CCMs. Furthermore, unraveling the identities of all the metabolites and enzymes orchestrating the CCM will be crucial toward metabolic engineering. An interesting line of future investigation relates to the suggestion, from our work, that Asp may play an important role in the CCM. If Asp is indeed the C<sub>4</sub> species transported to the vicinity of RuBisCO, then each cycle of the

CCM will carry a nitrogen atom into the plastid. To balance nitrogen within organelles, this will need to be counteracted by the transport of a nitrogen-containing C<sub>3</sub> compound such as alanine from the plastid. This would give rise to the unusual carbon-concentrating cycle  $\text{Pyr}_c (+ \text{HCO}_3^-) \rightarrow \text{OAA}_c \rightarrow \text{Asp}_c \rightarrow \text{Asp}_p \rightarrow \text{OAA}_p \rightarrow \text{Pyr}_p (+ \text{CO}_2) \rightarrow \text{Ala}_p \rightarrow \text{Ala}_c \rightarrow \text{Pyr}_c$ . Finally, CCMs can require significant ATP expenditure, and C<sub>4</sub> CCMs more so than biophysical CCMs (Hopkinson et al., 2011). Therefore, the metabolic routes through which the organism meets this cost would be worthy of investigation.

## **4. Experimental Evidence and Isotopomer Analysis of Mixotrophic Glucose Metabolism in the Marine Diatom *Phaeodactylum tricornutum***

This chapter is part of a manuscript to *Microbial Cell Factories*, which is currently under editorial consideration after peer review and revision. If accepted for publication, copyright is likely to be held jointly by all the authors.

Yuting Zheng<sup>1,#</sup>, Andrew H. Quinn<sup>1,#</sup> and Ganesh Sriram<sup>1,2</sup>.

<sup>#</sup>These two authors contributed equally to this work and are listed in the order in which they joined the project. This chapter only describes Yuting Zheng's contribution. YZ wrote sections of Materials and Methods and Results and critically edited the Introduction.

<sup>1</sup>Department of Chemical and Biomolecular Engineering, University of Maryland

<sup>2</sup>Principal investigator and corresponding author

### **4.1. Introduction**

The search for robust platform organisms suitable for manufacturing economically valuable compounds such as fuels, commodity chemicals, pharmaceuticals and dietary supplements has increasingly turned to unicellular algae. These eukaryotes naturally synthesize many high-value compounds commonly found in plants whilst also displaying the high growth rates and scale-up characteristics of bacteria and yeast. One model species is the marine diatom *Phaeodactylum*

*tricornutum*. Apart from their unique capability to incorporate silica into their cell walls (Lopez et al., 2005), diatoms also synthesize copious amounts of lipids. *P. tricornutum* typically produces lipids up to 30% of its dry weight (Dunstan et al., 1993), nearly 40% of which is the nutritional supplement  $\omega$ -3-eicosapentaenoic acid (Alonso et al., 1996; Yongmanitchai and Ward, 1991). This high lipid content is indicative of significant reductive potential, which has been harnessed through genetic engineering to produce the bioplastic poly-3-hydroxybutyrate (PHB) in large quantities, up to 11% of dry weight (Hempel et al., 2011).

Evidencing the potential of *P. tricornutum* as a cell factory, recent research has suggested or uncovered unique metabolic pathways and combinations of pathways previously unseen in unicellular photosynthetic organisms (Andrew E. Allen et al., 2011; Bowler et al., 2008; Fabris et al., 2012; Zheng and Sriram, in review; Kroth et al., 2008). For instance, sequencing of the genome of *P. tricornutum* revealed that 7.5% of the genome is of bacterial origin, suggesting the acquisition of many pathways through lateral gene transfer (Bowler et al., 2008). An investigation of nitrogen metabolism in this diatom determined that this organism operates a urea cycle for nitrogen assimilation, contrasting with the nitrogen-eliminating function of the urea cycle in metazoans. However, despite recent advances in understanding and utilizing *P. tricornutum*, several fundamental biological questions still remain unanswered.

One question that first arose in the late 1950's is whether *P. tricornutum* can metabolize glucose. The answer is relevant for utilizing this marine diatom as a cell factory, because heterotrophic fermentation using simple sugars such as glucose

remains the most cost effective bioproduction strategy, largely due to the significant challenges in optimizing photobioreactors and race ponds for phototrophic growth (Morales-Sánchez et al., 2013; Simionato et al., n.d.; Wen and Chen, 2003). Multiple research groups have reported that *P. tricornutum* cannot grow heterotrophically on glucose in the dark, and that mixotrophic growth on glucose does not noticeably increase growth rates under light (Hayward, 1968; Lewin, 1958; Ukeles and Rose, 1976). On addition of  $^{14}\text{C}$  glucose under light and dark conditions minimal radioactivity was observed in the cell extract after 1-48 h, suggesting that it may be impermeable to glucose. These experiments give the impression that *P. tricornutum* does not uptake or metabolize glucose. On this basis, Zaslavskaja et al. (Zaslavskaja et al., 2001) engineered *P. tricornutum* to express the human *GLUT1* glucose transporter protein. The transformants exhibited glucose uptake as well as growth on glucose in both light and dark, in contrast to wild type or empty vector control lines that neither grew in the dark, nor appeared to consume glucose.

Conversely, many researchers have reported results suggesting that *P. tricornutum* may consume and metabolize glucose. For example, one study (Liu et al., 2009) found that the provision of glucose enhanced the growth rate by 27%, increased the respiration rate by 46% and decreased the net maximum photosynthetic rate by only 3%. This suggests that some glucose was respired for ATP production (Liu et al., 2009). A separate study (Ceron Garcia et al., 2006) found that the supply of 5 g L<sup>-1</sup> glucose increased maximum biomass productivity and maximum biomass concentration by 43% and 49%, respectively.



Given this conflicting evidence, the question of glucose metabolism by *P. tricornutum* needs to be addressed by convincing molecular evidence. A unique methodology available for resolving this problem is the isotope labeling experiment (ILE), wherein organic carbon sources such as glucose containing different isotopes (“labels”) of carbon (e.g.  $^{13}\text{C}$  and  $^{12}\text{C}$ ) are supplied to a cell culture. The incorporation of the labeled carbon source into metabolites and biomass components such as proteinogenic amino acids will produce unique  $^{13}\text{C}$ - $^{12}\text{C}$  patterns or isotopomers, which can be detected by measuring mass isotopomer distributions (MIDs) of the metabolites or biomass components. Furthermore, analysis of the isotopomer data by metabolic flux analysis (MFA) will also enable identification of carbon partitioning and flux through metabolic pathways (Crown et al., 2011; Feng et al., 2010a; Wiechert et al., 2001).

Apart from determining whether *P. tricornutum* consumes glucose, it is also necessary to identify the metabolic pathways it uses to convert glucose to biomass and products. Annotation of the genome revealed two alternate glycolytic pathways of bacterial origin in addition to the conventional reactions of the Embden-Meyerhof-Parnas (EMP) pathway (Fabris et al., 2012). Of these, the Entner-Doudoroff (ED) pathway splits one molecule of 6-phospho-D-gluconate to one molecule of pyruvate and one molecule of glyceraldehyde-3-phosphate, whereas the phosphoketolase (PPK) pathway converts one molecule xylulose-5-phosphate to glyceraldehyde-3-phosphate and acetylphosphate, which subsequently forms acetyl-CoA. It is important to resolve the carbon partitioning between these three pathways to develop genetic engineering strategies for improved product yield from organic carbon sources. As an

example of the potential benefits of the ED and PPK pathways for cell factories, these pathways have each been utilized to enhance production of PHB in bacteria (Hong et al., 2003) and yeast (Kocharin et al., 2013) by increasing the availability of acetyl-CoA and NADPH for PHB biosynthesis. Therefore, determining the role of the glycolytic pathways in *P. tricornerutum* could lead to strategies for enhanced production of PHB and other economically attractive compounds.

## **4.2. Materials and Methods**

### **4.2.1. Cell Culture and Counting**

*P. tricornerutum* (strain CCMP 632) was obtained from the Provasoli-Guillard National Center for Marine Algae and Microbiota (NCMA) (East Boothbay, ME), and maintained aseptically by subculturing biweekly. Cultures were grown at 24.5 °C under constant light in 125 mL Erlenmeyer flasks containing 50 mL L1 culture medium (NCMA) prepared in sea water (NCMA). Irradiance levels ranged between 40-80  $\mu\text{mol m}^{-2} \text{s}^{-1}$  of photons depending on the location of each flask in our shakers as measured using a MQ-100: Quantum integral sensor with handheld meter (Apogee Instruments) (Logan, UT). No changes in algal growth rates were observed across this range of light intensities (data not shown). The flasks were placed in refrigerated New Brunswick Innova 44R shakers (Eppendorf, Hauppauge, NY) with a 2-inch stroke and programmable temperature, light and photoperiod controls. Cell numbers were measured daily by aseptically transferring small aliquots (10  $\mu\text{L}$ ) of cell suspension from cultures to INCYTO C-Chip disposable hemacytometers

(ThermoFisher Scientific, Waltham, MA) and counting visible cells with an Axiovert 135 TV microscope (Zeiss Oberkochen, Germany) at 20X resolution. Three biological replicates each with two technical replicates were counted for each time point. During later stages of growth, cell suspensions were diluted in sea water to prevent overcrowding and to maintain cell densities at less than ~100 cells per chip. Glucose measurements were performed in triplicate by pipetting ~1 ml of media into a 2 ml microcentrifuge tube, and inserting the tube into YSI 2300 STAT Plus Glucose & Lactate Analyzer (YSI Life Sciences) (Yellow Springs, OH).

#### **4.2.2. Gene Expression Analysis by Quantitative Real-time Polymerase Chain Reaction (qRT-PCR)**

Cells were grown as described in the previous paragraph for 9 d to obtain sufficient biomass. The biomass was divided into eight groups: (i) dark/L1, (ii) light/L1, (iii) dark/ $\text{HCO}_3^-$  (iv) light/ $\text{HCO}_3^-$ , (v) dark/glucose, (vi) light/glucose, (vii) dark/urea and (viii) light/urea [same order as in figure], with each condition being represented by three biological replicates. The flasks in the L1 groups (L1) were incubated in (50 mL of) L1 medium, whereas the flasks in the  $\text{HCO}_3^-$ , glucose (Glc) and urea (Urea) groups were incubated in (50 mL of) L1 medium supplemented aseptically with 0.5 mL of 33 g L<sup>-1</sup> NaHCO<sub>3</sub> solution, 2 g L<sup>-1</sup> glucose solution and 3.7 g L<sup>-1</sup> urea, respectively. After incubation for 14 h under constant light, the flasks in the dark/L1, dark/ $\text{HCO}_3^-$ , dark/glucose and dark/urea groups were transferred to complete darkness and incubated for 90 min. Following this, the cell suspension from each flask was centrifuged at 8000 min<sup>-1</sup> for 5 min. The wet cell pellets, suspended in less than 0.5 mL medium, were transferred to separate 2 mL sterilized micro-

centrifuge tubes, which were quenched immediately with liquid nitrogen. RNA was extracted by using RNeasy Plant Mini Kits and RNase-Free DNase Set (QIAGEN, Valencia, CA). RNA concentrations in the extracts were quantified with a NanoDrop 2000 UV-Vis spectrophotometer (Thermo Scientific). cDNA was synthesized from RNA using a High Capacity RNA-to-cDNA Kit (Life Technologies, Grand Island, NY) and random primers. qRT-PCR analyses were conducted with Power SYBR Green PCR Master Mix (Life Technologies) on a 7500 Real-Time PCR System (Life Technologies). The genes encoding 18S rRNA (*18S*), histone 4 (*HIS4*) and elongation factor 1 $\alpha$  (*EF1 $\alpha$* ) were used as housekeeping genes (Siaut et al., 2007). The gene-specific primers used for amplification are listed in **Table 4.1**. The three biological replicates for each condition were each analyzed three times. For each of the eight conditions tested, gene expression fold changes relative to the dark/L1 condition were obtained by using the  $2^{-\Delta\Delta C_t}$  method (Livak and Schmittgen, 2001), and statistical significance was determined by using a Student's *t*-test.

**Table 4.1 Primers used for qRT-PCR**

Gene group	Gene name	Primer sequence	
Housekeeping genes	<i>18s</i>	Forward	5'-GATCCATTGGAGGGCAAGTC-3'
		Reverse	5'-ACAGCAACGGCCAACCTAAGG-3'
	<i>HIS4</i>	Forward	5'-AGGTCCTTCGCGACAATATC-3'
		Reverse	5'-ACGGAATCACGAATGACGTT-3'
	<i>EF1<math>\alpha</math></i>	Forward	5'-GCGGTCCTCGTCATTGACTC-3'
		Reverse	5'-TTCGGCGTACTTGACGGTCT-3'
Target genes	<i>Fba3</i>	Forward	5'-GGTGACAATCTCACGACGCT-3'
		Reverse	5'-GCCTCTTTCGACGAGACGAT-3'
	<i>GLUT1</i>	Forward	5'-CGCTCTACTCGGCCCTAAAG-3'
		Reverse	5'-AACCACAGCCGTTGCAATTC-3'
	<i>GLUT3</i>	Forward	5'-AATGGCGCGAAAGAATACGC-3'
		Reverse	5'-TGCCGCAATGGGTATCAGTT-3'

### 4.2.3. Mixotrophic ILEs, Cell Harvest, Protein Extraction, Hydrolysis and Derivatization

Steady-state, mixotrophic ILEs were performed by adding one of 100% U-<sup>13</sup>C glucose, 50% U-<sup>13</sup>C glucose (Glc), 100% 1-<sup>13</sup>C glucose, or 100% 2-<sup>13</sup>C glycerol to L1 medium. Only one isotopically labeled substrate was added in each experiment. The addition was performed aseptically before subculturing so as to result in the final concentration of 2 g L<sup>-1</sup> of substrate. Each mixotrophic ILE was represented by 3 to 4 biological replicates. Additionally, the 100 % U-<sup>13</sup>C Glc experiment was repeated with matching results (data not shown) on a second cell line of the identical strain of Pt purchased from the NCMA. Cells from the mixotrophic ILEs were harvested at 21 d of culture. Proof of isotopic steady state at this time point is shown in **Figure 4.1**. The cell suspensions were centrifuged at 8000 min<sup>-1</sup> for 30 min, and the supernatant was removed. The cell pellet was briefly resuspended in 50 mL deionized water to rinse out salts and then centrifuged again, after which the supernatant was removed. Cellular metabolism was quenched by immersing tubes containing the pellets in liquid nitrogen. The quenched cells were lyophilized overnight at room temperature and 133 μbar. The lyophilized pellet was hydrolyzed by adding 3 mL 6N HCl and incubating at 155 °C for 4 h to obtain proteinogenic amino acids. Before hydrolysis, the hydrolysis tube was evacuated, then flushed with nitrogen to remove residual oxygen, and then re-evacuated, followed by two more repetitions of these steps. The resulting hydrolysate was cooled to room temperature, filtered by glass wool and dried overnight in a RapidVap evaporator (Labconco, Kansas City, MO) at 55°C, 80 mbar, mixed with deionized water and lyophilized again. After lyophilization, this

mixture was reconstituted in 200  $\mu\text{L}$  dimethylformamide (DMF) and derivatized with 80  $\mu\text{L}$  *N*-(*tert*-butyldimethylsilyl)-*N*-methyltrifluoroacetamide MTBSTFA + 1% *tert*-butyldimethylchlorosilane (TBDMCS) (Thermo Scientific, Rockford, IL) at 70°C for 1.5 h. The derivatized sample was injected into a gas chromatograph (GC)- MS, using DMF as solvent.

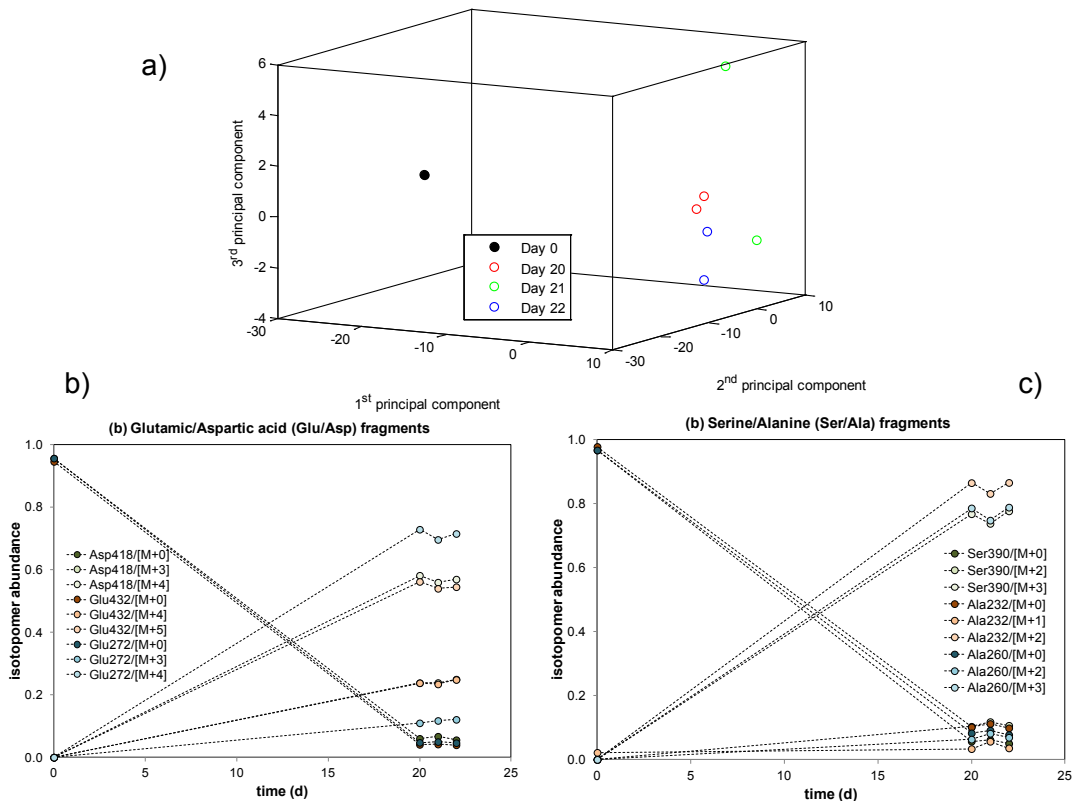


**Figure 4.1 Evidence for isotopic steady state from 20-22 d**

This analysis of *P. tricornutum* cells grown on 100%  $\text{U-}^{13}\text{C}$  glucose for 20, 21, and 22 d shows that the MIDs of the amino acid fragments remain nearly constant immediately before and after the standard harvesting time of 21 d. (a) A principal component analysis of 200 mass isotopomers from 38 amino acid fragments using a control sample at time zero and two biological replicates at each time-point shows that the 1<sup>st</sup> principle component explains 88% of the variance. The abundance of  $[\text{M}+0]$ ,  $[\text{M}+n-1]$ , and  $[\text{M}+n]$  mass isotopomers of key fragments of (b) aspartic acid and glutamic acid and (c) serine and alanine are plotted from time zero to 22 d. The abundances are noticeably different from time zero to 20 d, but remain constant over the following two days.

#### 4.2.4. Quantification of Mass Isotopomer Abundances by GC-MS

All GC-MS analyses were performed on a Varian 300MS quadrupole GC-MS unit (Bruker Corporation, Fremont, CA), equipped with an autoinjector and a VF5-ms column of dimensions 0.25 mm × 30 m × 0.25 μm. Typically, 1 μL of derivatized amino acids, in 3 technical replicates, was automatically injected at a split ratio of 1:15, with helium as the carrier gas at a constant flow rate of 1.0 mL min<sup>-1</sup>. The oven temperature was initially held at 150°C for 2 min, then increased at 3°C min<sup>-1</sup> to 250°C and then at 10°C min<sup>-1</sup> to 275°C, where it was held constant up to a run time of 43 min. The MS ran in electron ionization mode with a collection delay for 3 min. Mass spectra were recorded in the selected ion monitoring (SIM) mode. All mass spectral data were analyzed and quantified with the manufacturer's Varian MS Workstation software (Bruker, Billerica, MA). Raw mass spectral data were processed to filter out natural abundances of elements other than metabolic carbon, using a previously developed in-house MATLAB program (see Supplementary Material of Sriram et al., 2008), whose accuracy has been verified by us by processing a variety of amino acid isotopomer mixtures of known isotopomeric compositions (data not shown). The resulting mass isotopomer distribution data were converted to <sup>13</sup>C enrichments of individual amino acid fragments by using SVD. The accuracy of the SVD method for obtaining <sup>13</sup>C enrichments was verified by processing a synthetic set of amino acid MIDs and ensuring that the predicted enrichments were obtained (G. Sriram, unpublished calculations). MIDs obtained from steady-state ILEs are listed in appendix **Table A.2**, **Table A.6**, and **Table A.7**. Selected MIDs and <sup>13</sup>C enrichments are shown and discussed in Results. The MIDs

were adjusted to account for the presence of initially present unlabeled material that was used to inoculate each flask, so that the MIDs would reflect their true values if no unlabeled material were present. The corrected isotopomers were calculated (data not shown) using the equation  $C_i = (M_i - D * NA_i) / (1 - NA_i)$  for each mass isotopomer  $i = 0:n$ , where  $n$  is the number of carbon atoms,  $C$  is the corrected value,  $M$  is the measured value,  $NA$  is the natural abundance of that isotopomer, and  $D$  is the dilution factor from initially present material. The amount of initially present material was calculated as the ratio of the number of cells on day zero over the number of cells on the final day (data not shown). The calculation of a single dilution factor for all amino acids using the initial and final cell numbers is valid as long as both the weight percent of protein and the amino acid composition do not vary during the experiment. We calculated new dilution factors assuming the mass percent of protein could vary  $\pm 50\%$  over the timeframe of the experiment and we found that the new mass isotopomers fell within the standard deviations of our original calculations. We further analyzed the mass spectra of Pt cells grown on multiple substrates, including pure L1 media and L1 plus glucose, and found that changes in the percent composition of the amino acids again yielded smaller changes in the MID's than the standard deviations of our measurements.

#### **4.2.5. Evaluation of Metabolic Fluxes from Steady-State Isotopomer Data**

We used our computer program NMR2Flux+ (Nargund and Sriram, 2013; Sriram et al., 2004, 2008) to evaluate and compare the nine different pathway models



using corrected MIDs from the steady-state 100% 1-<sup>13</sup>C glucose ILE. Detail of the program is discussed in **Sec. 3.2.7**.

### **4.3. Results**

To test our hypothesis that *P. tricornutum* metabolizes glucose, cells were cultured for 21 d on media supplemented with U-<sup>13</sup>C glucose under both light and dark, and examined if the supplied <sup>13</sup>C label appeared in biomass components. In accordance with previously reported results (Hayward, 1968; Lewin, 1958; Ukeles and Rose, 1976), cultures kept in the dark exhibited no growth (**Supplemental Figure S1**); therefore, only cultures grown under light were analyzed for <sup>13</sup>C-enrichment. Toward this, we harvested biomass at the end of the 21-d ILE, acid-hydrolyzed the biomass to degrade cellular protein to amino acids and measured the <sup>13</sup>C enrichments of the amino acids by mass spectrometry (MS). Furthermore, on finding evidence of mixotrophic glucose metabolism, we employed MFA to identify the metabolic pathways through which glucose is metabolized (the detailed analysis of MFA will not be discussed in this work).

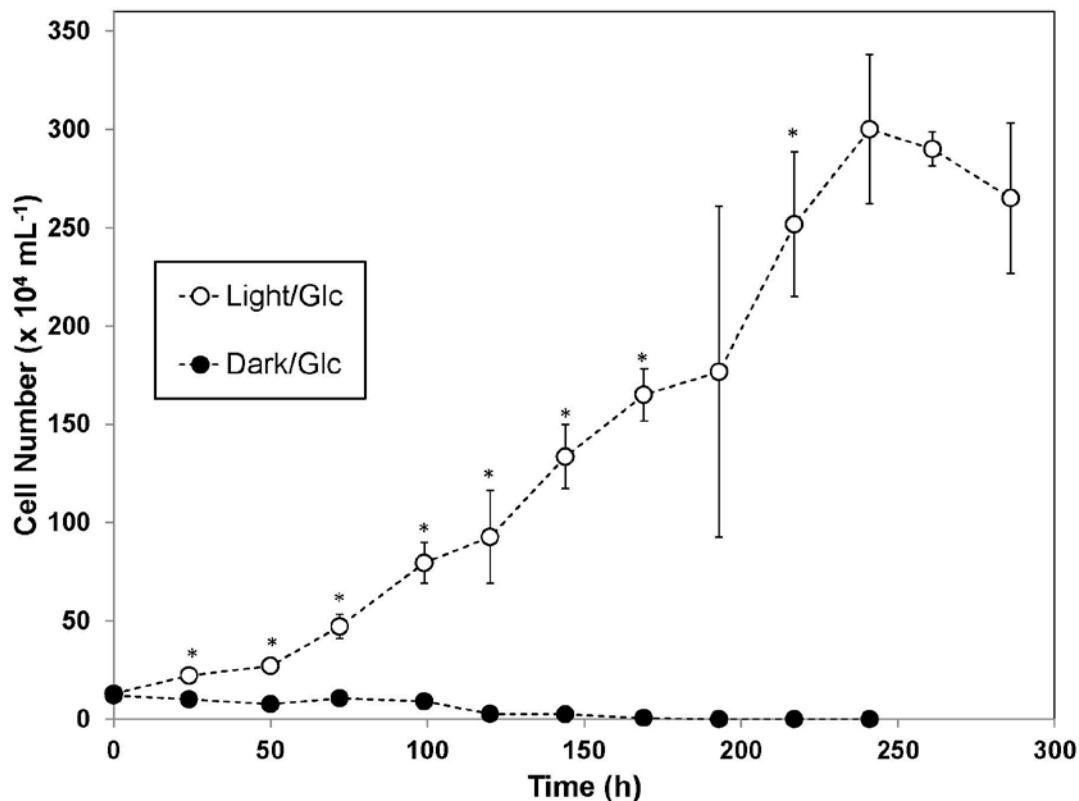


**Figure 4.2 Cell counts evidence that *Pt* grows on glucose under light but not under dark.**

*P. tricornutum* cells grown on L1 media supplemented with 2 g L<sup>-1</sup> glucose were sampled and counted on a hemacytometer over a 13 d growth period. Cell numbers increased under continuous light (open circles), but did not increase under continuous dark (closed circles). “\*” represents statistically significant differences between light-grown and dark-grown cells at the same time point with  $p < 0.05$ .

#### **4.3.1. Carbon from U-<sup>13</sup>C Glucose Appears in Proteinogenic Amino Acids of *P. tricornutum***

The ILEs on U-<sup>13</sup>C glucose supplied oppositely labeled glucose (100% U-<sup>13</sup>C or 50% U-<sup>13</sup>C) and dissolved inorganic carbon (naturally abundant; hence, 1.1% <sup>13</sup>C). Therefore, the <sup>13</sup>C enrichments of amino acid fragments from these experiments can be used as indicators of the extent to which the carbon atoms of glucose were

assimilated into the amino acids. Amino acid fragments from cells grown on 2 g L<sup>-1</sup> of 100% U-<sup>13</sup>C glucose were <sup>13</sup>C-enriched to 88% ± 3% (average across 38 fragments), whereas fragments from cultures grown on the same concentration of 50% U-<sup>13</sup>C glucose enriched to 45% ± 1% (average across 41 fragments) after consuming 50% of the glucose in the media (**Figure 4.3**). These enrichments are substantially higher than the 1.1% enrichment expected if *P. tricornutum* solely consumed dissolved inorganic carbon. In fact, these enrichments are close to those expected (100% and 50%) if it solely consumed glucose.

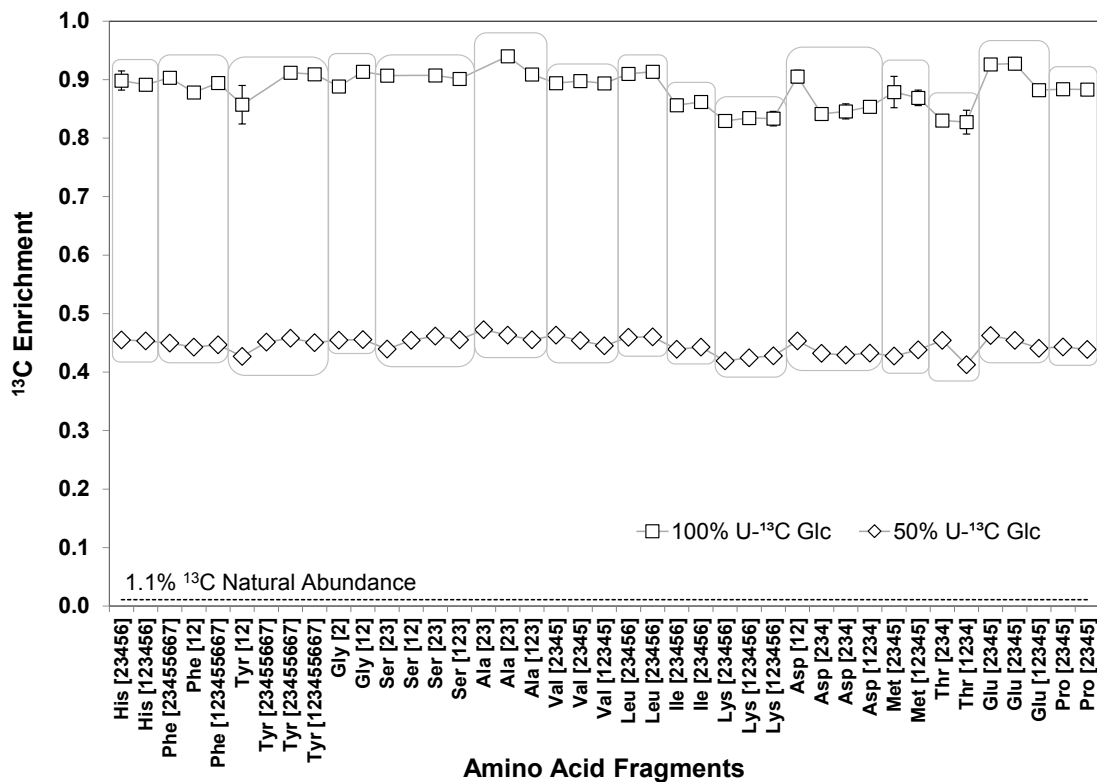


**Figure 4.3** <sup>13</sup>C enrichments of amino acid fragments synthesized from 100% and 50% U-<sup>13</sup>C glucose evidence significant glucose uptake

The 41 measured proteinogenic amino acid fragments in cell hydrolysates of *P. tricornutum* are grouped according to their metabolic precursor(s).

In these U-<sup>13</sup>C glucose ILEs, substantial metabolism of glucose can be expected to give a nearly uniform distribution of the <sup>13</sup>C label throughout the central metabolic network. In support of this, the ratios of the <sup>13</sup>C enrichments of different amino acid fragments in the 100% U-<sup>13</sup>C:50% U-<sup>13</sup>C glucose ILEs are generally equal to 100%:50% or 2:1. For example, the enrichment ratios of entire amino acid molecules originating in upper glycolysis and the PPP were 89%:45% (histidine) and 89%:45% (phenylalanine). For amino acids originating in lower glycolysis, the ratios were 91%:46% (alanine) and 89%:45% (valine). Amino acids originating in the TCA cycle displayed the ratios 87%:44% (methionine) and 88%:44% (glutamate).

Although a majority of the amino acid fragments showed nearly uniform <sup>13</sup>C enrichments in the two U-<sup>13</sup>C ILE, some fragments derived from oxaloacetate and  $\alpha$ -ketoglutarate were enriched to lower extents. Given that the initially present, unlabeled cell mass constituted 2% of the final mass (measurements not shown), the remaining ~10% of unlabeled carbon in the 100% U-<sup>13</sup>C glucose ILE could only have been assimilated from dissolved inorganic carbon, which was ultimately derived from atmospheric, naturally abundant CO<sub>2</sub>. *P. tricornutum* assimilates inorganic carbon through two mechanisms: direct, RuBisCO-mediated photosynthesis or anaplerotic fixation mediated by multiple reactions including phosphoenolpyruvate carboxylase. The latter mechanism incorporates naturally abundant carbon into the oxaloacetate C-4, which is then transferred to  $\alpha$ -ketoglutarate C-1 through the TCA cycle. This mechanism is discussed in this work in **Sec. 3**.

### 4.3.2. *Fba3* is Upregulated Significantly under Light while Glucose Transporters are Less Sensitive to Light and Carbon Substrates

By using qRT-PCR, we profiled genes encoding (i) the upper glycolysis enzyme *Fba3* (GenBank 7202915) catalyzing the reversible conversion of fructose-1,6-bisphosphate to glyceraldehyde-3-phosphate and dihydroxyacetone phosphate; and (ii) membrane glucose transporters *GLUT1* (GenBank 7198458) and *GLUT3* (GenBank NC\_011676). We performed qRT-PCR on cells in 4 different media solutions to measure changes in gene expression 1.5 h after switching from light to dark, resulting in 8 independent conditions: L1 medium under light (light/L1), L1 medium under dark (dark/L1), HCO<sub>3</sub><sup>-</sup>-supplemented L1 medium under light (light/HCO<sub>3</sub><sup>-</sup>), HCO<sub>3</sub><sup>-</sup>-supplemented L1 medium under dark (dark/ HCO<sub>3</sub><sup>-</sup>), glucose-supplemented L1 medium under light (light/Glc), glucose-supplemented L1 medium under dark (dark/Glc), urea-supplemented L1 medium under light (light/urea) and urea-supplemented L1 medium under dark (dark/urea), with the HCO<sub>3</sub><sup>-</sup> and urea samples acting as additional controls to gauge the relative transcription level changes due to light/dark versus changes caused by altering the carbon and nitrogen sources.

**Figure 4.4** depicts fold changes with respect to the housekeeping gene *18S* for all genes whose expression levels were consistent across three housekeeping genes (*18S*, *HIS4* and *EF1 $\alpha$* ; **Table 2.1**). Clearly, *Fba3* is repressed upon switching from light to dark, irrespective of carbon source supplementation. Exposure to light upregulated *Fba3* by  $7.7 \pm 1.7$ -fold ( $p < 0.01$ ) in unsupplemented L1 medium, by  $24 \pm 2.4$ -fold ( $p < 0.01$ ) in HCO<sub>3</sub><sup>-</sup>-supplemented L1 medium, by  $9.2 \pm 2.1$ -fold ( $p < 0.01$ ) in glucose-supplemented L1 medium and by  $18 \pm 1.9$ -fold ( $p < 0.05$ ) in urea-

supplemented L1 medium. Furthermore, urea repressed *Fba3* expression significantly. Under light, *Fba3* expression in urea-supplemented L1 medium was lower by  $4.1 \pm 0.2$ -fold ( $p < 0.05$ ) than in unsupplemented L1 medium. Under dark, *Fba3* expression in urea-supplemented L1 medium was lower by  $9.6 \pm 1.6$ -fold ( $p < 0.05$ ) than in unsupplemented L1 medium.

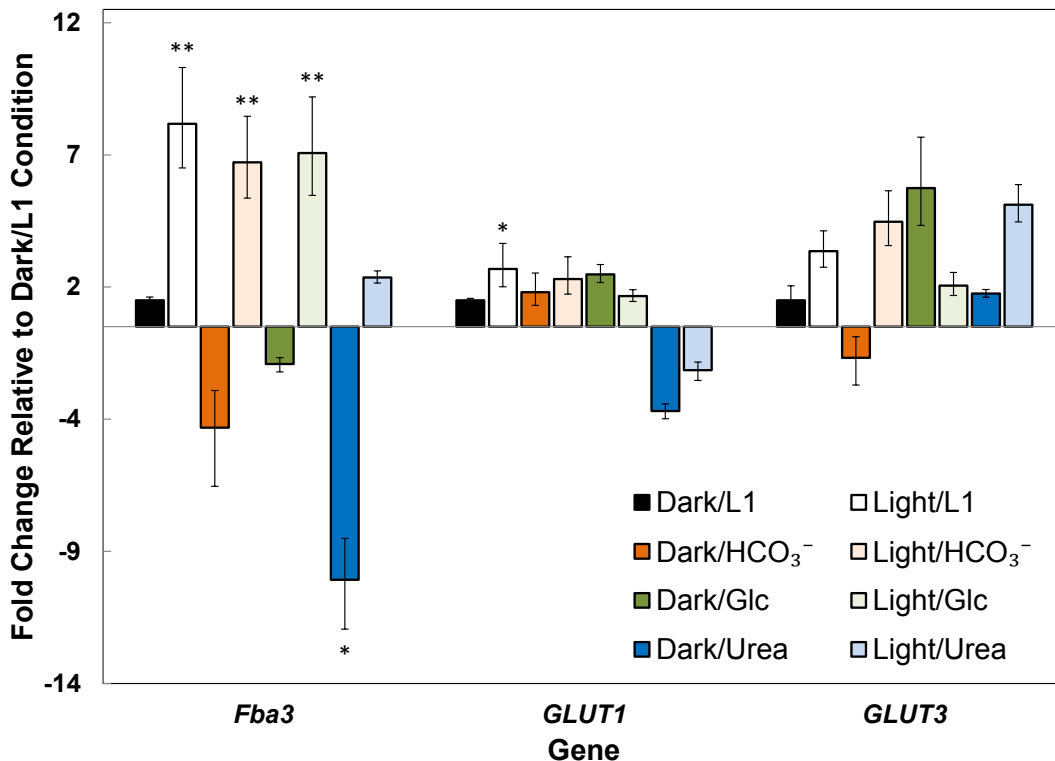


**Figure 4.4 Expression levels of key glucose-related and glycolytic genes under different environmental conditions**

Expression levels of genes under eight conditions (light/L1, dark/L1, light/HCO<sub>3</sub><sup>-</sup>, dark/HCO<sub>3</sub><sup>-</sup>, light/Glc, dark/Glc, light/urea, and dark urea, see **Sec. 4.2.2.** for details), as compared to the dark/L1 condition. Fold changes were calculated with respect to the housekeeping gene *18S* and were verified with respect to two other housekeeping genes. Results are presented as mean  $\pm$  SD of three biological and three technical replicates (a total of 9 replicates per gene and condition). \*:  $0.01 < p < 0.05$  when compared to the dark/L1 condition; \*\*:  $p \leq 0.01$  when compared to the dark/L1 condition.

In contrast to *Fba3*, transcription levels of genes encoding glucose transporters did not show consistent trends in light versus dark conditions. The only significant change was the  $2.4 \pm 1.1$ -fold ( $p < 0.05$ ) overexpression of *GLUT1* between the light and dark conditions in unsupplemented L1 medium (**Figure 4.4**).

In accordance with previous gene expression studies (Chauton et al., 2013), our results show that light transcriptionally activates genes encoding the cytosolic enzyme *Fba3*, which reversibly breaks down fructose 1,6-bisphosphate to three-carbon metabolites in Pt. This suggests that upper glycolysis rather than glucose transportation may be critical to glucose assimilation under light. In addition, urea inhibited expression of *Fba3* in *P. tricornutum* without effecting a significant change on the transcription level of glucose transporters.

#### **4.4. Discussion**

One of the goals for developing cell factories is finding flexible organisms that can be rapidly tailored to produce any of a large range of products using the most cost effective substrate available. Unicellular diatoms have the potential to meet this role due to their unique metabolic capabilities and the ease in which they can be genetically manipulated. While *P. tricornutum* has demonstrated a host of advantageous characteristics for cell factories, its utility has been limited by the perception that it cannot consume simple sugars such as glucose. The ILEs reported in this work have convincingly shown that *P. tricornutum* mixotrophically metabolizes glucose and uses the resulting carbon to synthesize each of the 15 amino

acids we measured. As these amino acids are synthesized from multiple nodes encompassing all of primary metabolism across at least three separate intracellular compartments (cytosol, plastid, mitochondrion), it is reasonable to generalize that *P. tricornutum* metabolizes glucose and uses its carbon for the full range of biosynthetic activities. Given this information, it is natural to question why this diatom mixotrophically consumes glucose only under light. Our gene expression analysis revealed that transcription level changes of membrane glucose transporters in *P. tricornutum* poorly correlate with exposure to light or glucose. This suggests that the inability of this species to grow on glucose in the dark is not due to insufficient expression of glucose transporters. However, we cannot discount the possibility that the products of either or both *GLUT1* and *GLUT3* does not transport glucose into the cell, but instead shuttles glucose from the vacuole to the cytosol.

In *P. tricornutum*, light availability has a significant effect over a 24 h period on the expression levels of many genes encoding enzymes in central carbon metabolism (Chauton et al., 2013). Of the genes encoding glycolysis and glucon biosynthesis, cytosolic *Fba3* is most strongly regulated by light, suggesting that its product may be a rate-limiting enzyme in this pathway. Our gene expression analysis assays confirmed that *Fba3* expression is upregulated by light and further showed that glucose has a negligible regulatory effect under light or dark. Allen et al. (Andrew E Allen et al., 2011) showed that of the five fructose biphosphate aldolase-3 genes in *P. tricornutum*, cytosolic *Fba3* is the only one actively involved in glycolysis and gluconeogenesis, facilitating synthesis of photosynthetically fixed triose phosphates into chrysolaminaran ( $\beta$ :1-3 and  $\beta$ :1-6 glucose polymers) (Kroth et al., 2008). Our



results taken together with previous work on the role of *Fba3*, suggest that in the dark, glucose metabolism is impeded either by the lack of sufficient *Fba3* expression or insufficient transport of glucose into the cell. Our ongoing work is focused on testing the hypothesis that glucose is not transported in the dark by elucidating a light-dependent mechanism for glucose transport and metabolism.

## 5. $^{13}\text{C}$ and $^{15}\text{N}$ Isotopes Labeling Experiments Reveal Nitrogen Assimilation Mechanism in *Phaeodactylum* *tricornutum*

Early draft of a manuscript to be submitted for publication.

Yuting Zheng<sup>1</sup> and Ganesh Sriram<sup>1,2</sup>.

<sup>1</sup>Department of Chemical and Biomolecular Engineering, University of Maryland

<sup>2</sup>Principal investigator and corresponding author

### 5.1. Introduction

As a crucial component of biomass synthesis, the assimilation of nitrogen determines the generation of protein, nucleotides, etc., and further influences cellular activities such as cellular enzymatic reactions and cell division (Allen and Arnon, 1955; Burns and Hardy, 1975). Although nitrogen constitutes 80% (by volume) of the atmosphere, little of this is *directly* involved in plant nitrogen assimilation. A miniscule amount of atmospheric nitrogen is converted to nitrogen oxides naturally through energetic processes such as lightning (Slosson, 1920), whereas a further amount is fixed by a group of prokaryotes called diazotrophs (Vitousek et al., 1997). The majority of nitrogen cycled within biological cycles is in the form of nitrate ( $\text{NO}_3^-$ ) and ammonia ( $\text{NH}_3$ ). Plants take nitrate or ammonia from soil, and accumulate this nitrogen as protein and nucleotides until natural biomass decomposition occurs or the plant biomass becomes a food source for animals. In plants, excess nitrogen is

removed by protein transportation to removable organs such as leaves in fall; in animals, excess nitrogen is expelled in the form of urine which contains a large amount of urea produced through the urea cycle.

The urea cycle is well known as a cycle produces nitrogen “waste” (urea) from decomposed proteins in vertebrates (Krebs and Henseleit, 1932). This cycle takes carbamoyl phosphate, which is the condensation product of free ammonia and bicarbonate, and then through a series of reactions with ornithine, finally produces urea and arginine (Arg). Although the urea cycle is known for elimination of nitrogen as urea, a recent study has shown that in the marine diatom *Phaeodactylum tricornutum*, this cycle may perform a contrasting, *biosynthetic* role by recycling nitrogen (Andrew E. Allen et al., 2011).

*Phaeodactylum tricornutum* is a model diatom with an efficient carbon concentrating mechanism (also known as “C<sub>4</sub> CCM”, see discussion in Chapter 3 in this work). This efficient photosynthetic process indicates a need for nitrogen sources for enzyme production. Previous studies have shown that nitrogen assimilation almost always associates with carbon assimilation, for the energy (e.g. ATP) and reducing agent (e.g. NADH/NAD<sup>+</sup>) produced from carbon assimilation are essentially necessary for nitrogen assimilation and they both participate biosynthesis of amino acids, the bricks of critical biomass, proteins (Eppley and Renger, 1974; Khamis et al., 1990; Lawlor and Cornic, 2002; Lawlor, 2002). The efficient photosynthetic mechanism, combined with a source recycling urea cycle, may explain the biological success of *P. tricornutum* in plant kingdom.

In this work, biosynthesis of  $^{15}\text{N}$  labeled urea will be compared with other nitrogen sources in the culture of *P. tricornutum*, followed with gene expression analysis on critical genes in nitrogen assimilation pathways, and we will further reveal role of urea in C and N assimilation pathways through  $^{13}\text{C}$  and  $^{15}\text{N}$  labeled instationary labeling experiments.

## 5.2. Materials and Methods

### 5.2.1. Instationary Parallel ILE, Intracellular Metabolite Extraction and Derivatization

Cells were cultured in L1 medium for six weeks to obtain sufficient biomass. After this period, cell suspensions were first centrifuged at  $8873 \times g$  for 5 min. Most of the supernatant medium was removed, leaving the cells suspended in  $\sim 1$  mL of medium. The cells were slightly mixed by shaking and transferred to 2 mL microcentrifuge tubes, after which the supernatant was removed by centrifugation at  $6200 \times g$  for 1 min. To set up the instationary parallel ILE, 0.5 mL of L1 medium containing i)  $0.027 \text{ g L}^{-1} \text{ }^{15}\text{N}$  urea, (ii)  $0.0472 \text{ g L}^{-1} \text{ }^{15}\text{N}$   $\text{NH}_4\text{Cl}$ , (iii)  $0.075 \text{ g L}^{-1} \text{ }^{15}\text{N}$   $\text{NaNO}_3$ , and (iv)  $0.036 \text{ g L}^{-1} \text{ }^{15}\text{N}$   $\text{NH}_4\text{NO}_3$  were each added to each microcentrifuge tube, respectively. One tube contains only one labeled nitrogen source and the amount of N equals to  $0.882 \text{ m mol L}^{-1}$  at each condition. Then cells were resuspended by shaking quickly under light with the photosynthetic photon flux density measured  $18 \pm 1 \mu\text{mol m}^{-2} \text{ s}^{-1}$  during the period of experiments. Enough tubes were set up so that four time points (5 min, 10 min, 15 min and 20 min) with one control time point (unlabeled nitrogen

source added for 10 min for each condition) could each be represented by three biological replicates. The time points were staggered so that the three replicates for each time point could be simultaneously and precisely quenched and harvested. At the appropriate time points, tubes were immediately dropped into liquid nitrogen to quench metabolism. To quantify metabolite pool sizes (concentrations), during the period the ILE was conducted, cells were separately grown for six weeks in three replicate flasks containing L1 medium, followed by quenching, metabolite extraction and quantification.

To isolate intracellular metabolites after quenching, 0.7 mL boiling methanol and 25  $\mu\text{L}$  deionized  $\text{H}_2\text{O}$  were added to the tubes, which were then incubated in a water bath at 30  $^\circ\text{C}$  to 35  $^\circ\text{C}$  for 30 min. When the liquid in the tubes turned green (due to secretion of chlorophyll from the ruptured cells) and white flocculent precipitates appeared, 0.7 mL deionized  $\text{H}_2\text{O}$  and 0.37 mL chloroform were added. After vortexing, the tubes were centrifuged at 17,000  $\times g$  at 4  $^\circ\text{C}$  for 10 min. The upper methanol/ $\text{H}_2\text{O}$  layer was collected and evaporated under  $\text{N}_2$  or He stream. The dried sample was dissolved in 80  $\mu\text{L}$  deionized  $\text{H}_2\text{O}$ , transferred to a 300  $\mu\text{L}$  GC vial and lyophilized overnight. The lyophilized residue was reconstituted in 50  $\mu\text{L}$  of a freshly made solution of 20  $\text{mg mL}^{-1}$  methoxyamine hydrochloride in pyridine, in a GC vial at 30  $^\circ\text{C}$  for 90 min. This sample was then derivatized with 50  $\mu\text{L}$  MTBSTFA + 1% TBDMCS at 70  $^\circ\text{C}$  for 30 min. The derivatized sample was injected into a GC-MS, using DMF as solvent. While samples added with labeled ammonium nitrate show unsatisfactory result, MIDs obtained from samples added with other

nitrogen sources in the instationary parallel ILE are listed in appendix **Table A.8** to **Table A.10**.

### **5.2.2. Gene Expression Analysis by Quantitative Real-time Polymerase Chain Reaction (qRT-PCR)**

Cells were grown as described in the **sec 3.2.5.** and **sec. 4.2.2.** Cells were grown for 9 d to obtain sufficient biomass. The biomass was divided into eight groups: (i) dark/L1, (ii) light/L1, (iii) dark/HCO<sub>3</sub><sup>-</sup> (iv) light/ HCO<sub>3</sub><sup>-</sup>, (v) dark/glucose, (vi) light/glucose, (vii) dark/urea and (viii) light/urea, with each condition being represented by three biological replicates. The flasks in the L1 groups (L1) were incubated in (50 mL of) L1 medium, whereas the flasks in the HCO<sub>3</sub><sup>-</sup>, glucose (Glc) and urea (Urea) groups were incubated in (50 mL of) L1 medium supplemented aseptically with 0.5 mL of 33 g L<sup>-1</sup> NaHCO<sub>3</sub> solution, 2 g L<sup>-1</sup> glucose solution and 3.7 g L<sup>-1</sup> urea, respectively. After incubation for 14 h under constant light, the flasks in the dark/L1, dark/ HCO<sub>3</sub><sup>-</sup>, dark/glucose and dark/urea groups were transferred to complete darkness and incubated for 90 min. Following this, the cell suspension from each flask was centrifuged at 8000 min<sup>-1</sup> for 5 min. The wet cell pellets, suspended in less than 0.5 mL medium, were transferred to separate 2 mL sterilized micro-centrifuge tubes, which were quenched immediately with liquid nitrogen. RNA was extracted by using RNeasy Plant Mini Kits and RNase-Free DNase Set (QIAGEN, Valencia, CA). RNA concentrations in the extracts were quantified with a NanoDrop 2000 UV-Vis spectrophotometer (Thermo Scientific). cDNA was synthesized from

RNA using a High Capacity RNA-to-cDNA Kit (Life Technologies, Grand Island, NY) and random primers. qRT-PCR analyses were conducted with Power SYBR Green PCR Master Mix (Life Technologies) on a 7500 Real-Time PCR System (Life Technologies). The genes encoding 18S rRNA (*18S*), histone 4 (*HIS4*) and elongation factor 1 $\alpha$  (*EF1 $\alpha$* ) were used as housekeeping genes (Siaut et al., 2007). The gene-specific primers used for amplification are listed in **Table 5.1**. The three biological replicates for each condition were each analyzed three times. For each of the eight conditions tested, gene expression fold changes relative to the dark/L1 condition were obtained by using the  $2^{-\Delta\Delta C_t}$  method (Livak and Schmittgen, 2001), and statistical significance was determined by using a Student's *t*-test.

### **5.2.3. Instationary Labeled Urea ILE, Intracellular Metabolite Extraction and Derivatization**

Cells were cultured and transferred to 2 mL micro-centrifuge tubes as described in **sec 5.2.1**. To set up the instationary labeled urea ILE, 0.5 mL of L1 medium containing 0.027 g L<sup>-1</sup> (i) <sup>15</sup>N urea, (ii) <sup>13</sup>C urea, and (iii) <sup>13</sup>C, <sup>15</sup>N urea were each added to each micro-centrifuge tube, respectively. One tube contains only one labeled urea source and the amount of urea equals to 0.44 m mol L<sup>-1</sup> at each condition. Then cells were resuspended by shaking quickly under light during the period of experiments. Enough tubes were set up so that eight time points (2 min, 5 min, 8 min, 12 min, 16 min, 20 min, 25 min, 30 min) with one control time point (unlabeled urea source with the same concentration added for 5 min for each condition) could each be represented by three biological replicates. Intracellular metabolites were quenched,

extracted and derivatized as described in **sec 5.2.1**. The derivatized sample was injected into a GC-MS, using DMF as solvent. MIDs obtained from the instationary parallel ILE are partially discussed in Sec 5.3.1.

**Table 5.1 Primers used for qRT-PCR**

Gene group	Gene name	Primer sequence	
Housekeeping genes	<i>18s</i>	Forward	5'-GATCCATTGGAGGGCAAGTC-3'
		Reverse	5'-ACAGCAACGGCCAACTAAGG-3'
	<i>HIS4</i>	Forward	5'-AGGTCCTTCGCGACAATATC-3'
		Reverse	5'-ACGGAATCACGAATGACGTT-3'
	<i>EF1<math>\alpha</math></i>	Forward	5'-GCGGTCCTCGTCATTGACTC-3'
		Reverse	5'-TTCGGCGTACTTGACGGTCT-3'
Target genes	<i>Ure</i>	Forward	5'-TGACGACCATGTTTGGAGGG-3'
		Reverse	5'-CTACCTTGCGGAAGATCGGA-3'
	<i>UTI</i>	Forward	5'-GACCGTTTCCGGCTTCAGTA-3'
		Reverse	5'-ACTTGCTTGGAGGGTACGTT-3'
	<i>NIT1</i>	Forward	5'-GTGAGGTCTTGACACACTCGT-3'
		Reverse	5'-GTTGAGTCTGGTGAACCCGT-3'
	<i>Nar1</i>	Forward	5'-CTTAGCATGCCGAGGGGAAT-3'
		Reverse	5'-AAGCGGAAGCTCACGTTGAT-3'
	<i>NiR</i>	Forward	5'-TCTCACACTCGACCATCCCT-3'
		Reverse	5'-ATCGCATTGGTTCGGCATTG-3'
	<i>Arg</i>	Forward	5'-AGAAAGACGCGGTCCATCAG-3'
		Reverse	5'-GAATCCGGAACATGCACGG-3'
	<i>AsuS</i>	Forward	5'-AACACCAAATCCCCTTGAC-3'
		Reverse	5'-TGGGGAGATACGGTCATTTT-3'
	<i>OCD</i>	Forward	5'-GTTTCGGGTTTGTCTGCGTC-3'
		Reverse	5'-CCGGAGATCCGTCATGTAGC-3'
	<i>CPS</i>	Forward	5'-GAGCTGACGATCTTCGGTGT-3'
		Reverse	5'-CTGCGCCGTCCAAATGTAAG-3'
	<i>HIS4</i>	Forward	5'-AGGTCCTTCGCGACAATATC-3'
		Reverse	5'-ACGGAATCACGAATGACGTT-3'
	<i>EF1<math>\alpha</math></i>	Forward	5'-GCGGTCCTCGTCATTGACTC-3'
		Reverse	5'-TTCGGCGTACTTGACGGTCT-3'



## 5.3. Results

### 5.3.1. Nitrogen Source Parallel Experiments reveal Pattern of Urea

#### Assimilation

This experiment examined the efficacy of nitrogen assimilation in *P. tricornutum* when nitrogen was supplied as urea, ammonium or nitrate. In general, the MIDs of soluble amino acids from other samples reveal the pattern of urea assimilation. The  $^{15}\text{N}$  enrichments of some amino acids, such as alanine (Ala, **Figure 5.1 a**), isoleucine (Ile, see appendix **Table A.8** to **Table A.10**), leucine (Leu) and valine (Val) increased linearly in  $^{15}\text{N}$  urea-containing medium, indicating a direct contribution of urea to their synthesis. A similar trend is also apparent in  $^{15}\text{NH}_4\text{Cl}$ -containing medium. However, the  $^{15}\text{N}$  enrichments of aspartic acid (Asp, **Figure 5.1 b**) and glutamic acid (Glu, **Figure 5.1 c**), were not identical between  $^{15}\text{N}$  urea-containing and  $^{15}\text{NH}_4\text{Cl}$ -containing media. Additionally, the rate of increase of  $^{15}\text{N}$  labeling in Ala was higher than that of Asp, but similar to that of Glu.

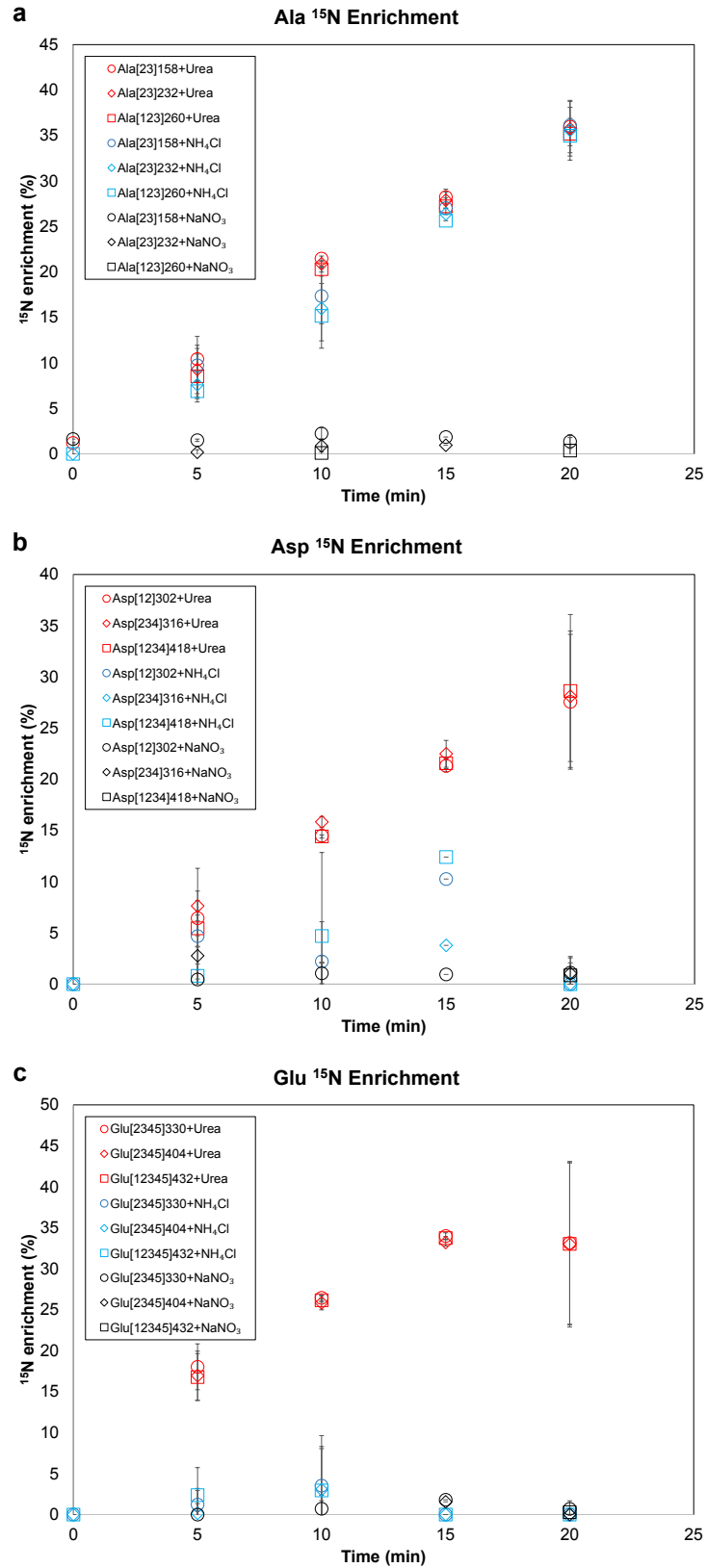


**Figure 5.1** Amino acid fragment <sup>15</sup>N enrichment in nitrogen source instationary parallel experiments.

### 5.3.2. Gene Expression Results Suggest Potential Participation of Urea Cycle in Urea Assimilation

To further investigate pathways that are potentially involved in nitrogen assimilation, especially urea assimilation in *P. tricornutum*, a series of gene expression experiments were conducted by using qRT-PCR. The genes examined are as shown in **Figure 5.2**. In this experiment, critical genes that putatively regulate urea cycle, nitrate assimilation, carbon assimilation (including C<sub>4</sub>-related pathway and glucose assimilation) were investigated under different carbon and nitrogen culture, as well as lighting conditions.

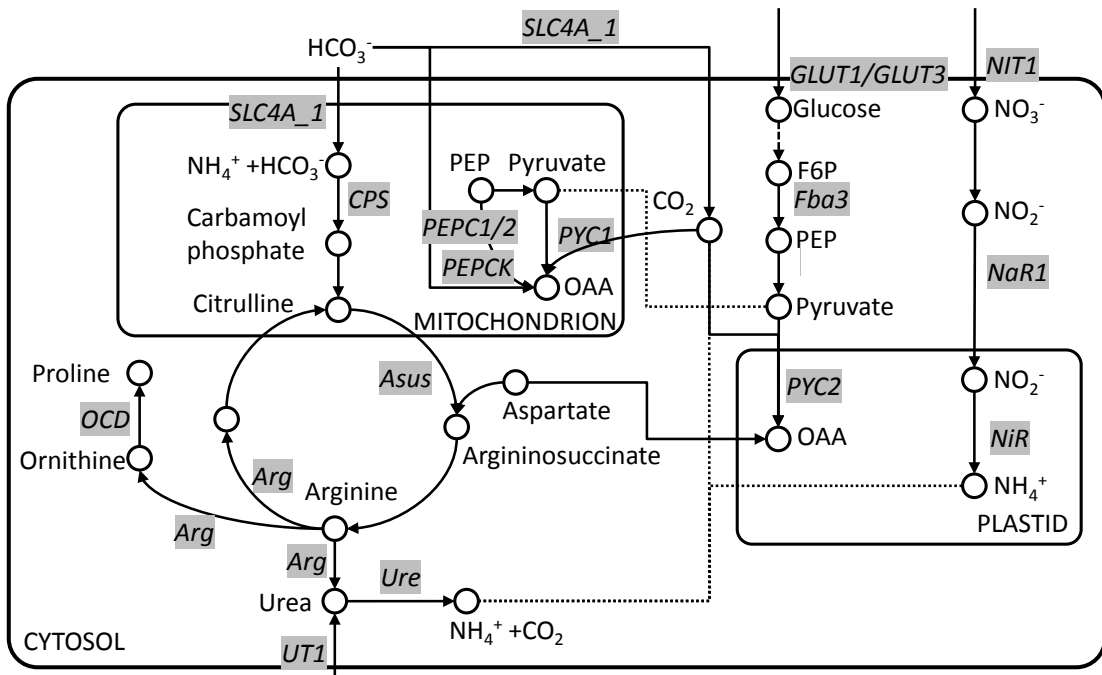


**Figure 5.2** Genes examined in gene expression experiments.

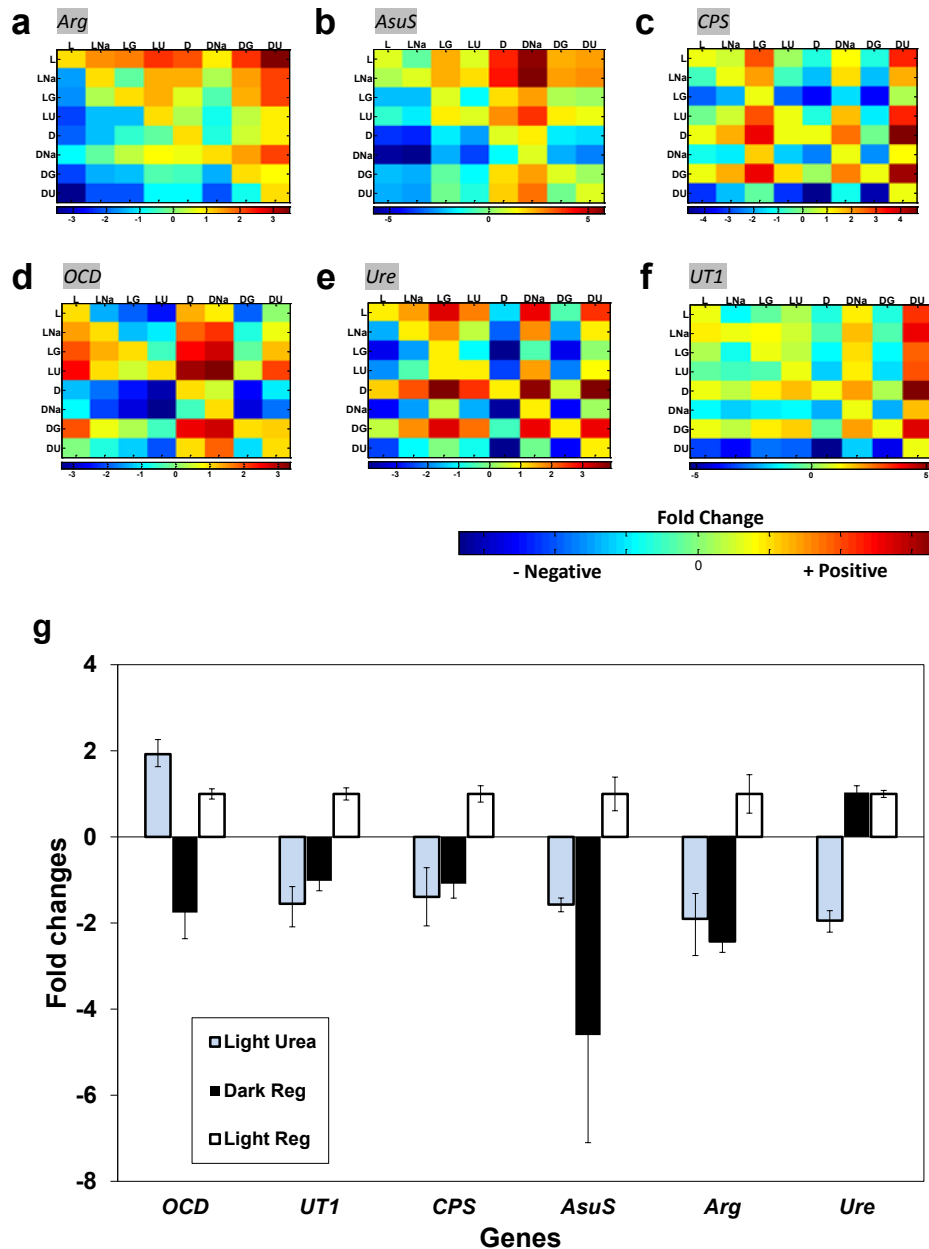


**Figure 5.3** Gene expression of those regulate urea cycle and related pathway.

Besides genes discussed in previous section (see sec 3.3.3 and sec. 4.3.2), six genes that regulate the urea cycle (**Figure 5.3**) and the nitrate assimilation pathway (**Table 5.1** and **Figure 5.2**) were further examined. **Figure 5.3** shows the relative fold changes between two conditions (**a-f**) and gene expression levels compared to

light/L1 condition under dark/L1 and light/urea conditions. From **Figure 5.3**, *OCD* gene was up-regulated  $2 \pm 0.3$  fold with adding of urea, while *Ure* gene was down-regulated  $2.1 \pm 0.2$  with presence of urea. Compared to nitrogen source alteration, light condition affects gene expression as well. When cells were in dark for 90 min, both *OCD* and *Arg* genes were significantly down-regulated ( $1.7 \pm 0.5$  fold and  $2.6 \pm 0.3$  fold, respectively).

#### **5.4. Discussion**

The instationary ILEs with  $^{15}\text{N}$ -labeled nitrogen sources (**Figure 5.1**) show that the assimilation of urea is remarkably different pattern as compared with that of  $\text{NH}_4\text{Cl}$  or  $\text{NaNO}_3$ . This uniqueness was further explored through gene expression experiments (**Figure 5.3**) and a series of instationary isotope labeling experiments employing urea (data not shown in this work, approach discussed in Sec 5.2.3).

From the parallel labeling experiments employing different nitrogen sources, the linear increase of labeling for certain amino acids may suggest diffusion transportation of urea into intracellular compartment and transamination may predominantly cause the labeling. However, transamination would not able to explain discrepancies of labeling patterns of Asp and Glu. Considering the complex role that Asp may play in the biological activities in *P. tricornutum* (as partially discussed in Sec. 3), the labeling of Asp may suggest participation of TCA cycle in urea assimilation, and could be further influenced by photosynthesis.

## 6. Conclusions and Future Work

### 6.1. Conclusions

In this work, we first test the hypothesis that *P. tricornutum* operates a C<sub>4</sub> CCM. To investigate this problem, we employed computer-aided isotope-assisted metabolic flux analysis (MFA) (Ahn and Antoniewicz, 2013; Alonso et al., 2011; Feng et al., 2010b; Sriram et al., 2004; Wiechert and Nöh, in press; Young et al., 2011b), which includes isotope labeling experiments and mathematical modeling on a core metabolic network. Toward this, by feeding several <sup>13</sup>C- and <sup>12</sup>C- labeled carbon sources including atmospheric CO<sub>2</sub>, dissolved HCO<sub>3</sub><sup>-</sup>, glucose, acetate and aspartic acid (Asp), individually or in combination to cell culture, and measuring biomass labeling patterns, flux-isotopomer models could be constructed. Both our steady-state and instationary experiments and analyses verified our hypothesis, for the first time indicating that a significant C<sub>4</sub> CCM is operational within this marine diatom. We further examined potential genes that may contribute to this mechanism, which showed that *PYCI* and *PYC2* were most up-regulated by light, with or without carbon sources.

That *P. tricornutum* assimilates glucose was revealed in steady-state labeling experiments, and this inspired us to further investigate this diatom's glucose assimilation, which was long-time debated among researchers. On basis of <sup>13</sup>C ILEs, our gene expression experiments suggested that the actual glucose assimilation step (upstream of glycolysis) rather than glucose transportation across cellular membrane might be the limiting step. Significant regulation of the *Fba3* gene by light condition

provided a possible explanation of why this assimilation could only happen under light.

Irrespective of carbon uptake through C<sub>4</sub> CCM or glucose assimilation, plants and algae require nitrogen to survive. Our nitrogen source instationary isotope labeling experiments employing <sup>15</sup>N-labeled nitrogen sources revealed that urea assimilation in *P. tricornutum* could be through a different pathway as compared to conventional nitrogen sources. Further investigation via qRT-PCR analysis suggested participation of urea cycle as well as TCA cycle, and certain amino acids may play a critical role during this process.

The novelty of this work lies in that it is the first application of isotope MFA to fundamentally investigate several processes in the model marine diatom *P. tricornutum*, including C<sub>4</sub> photosynthesis, glucose metabolism, and nitrogen metabolism. We anticipate that the metabolic flux analysis methodologies developed in this work will find widespread application to other biological systems. We also anticipate that our work on *P. tricornutum* unicellular C<sub>4</sub> CCM, glucose assimilation and nitrogen assimilation mechanisms will not only shed light on carbon and nitrogen assimilation in this model marine diatom, but also provide insights to further metabolic engineering on this unicellular organism.

## **6.2. Future Work**

### **6.2.1. C<sub>4</sub> CCM Enzyme Identification**

Our ILEs and analyses convincingly showed that *P. tricornutum* operated C<sub>4</sub> CCM when incorporating bicarbonate. Our gene expression studies also indicated that two pyruvate carboxylase genes were sensitive to light conditions and might participate in C<sub>4</sub> CCM regulation. However, more profound and targeted studies need to be done to verify the critical genes that involved in this process. One approach is to examine gene expression through microarray and collect information on clusters of genes that respond to stimulus (Ball et al., 2002; Schena et al., 1995). Another method is to conduct enzyme assay that may help locate the active enzymes in the photosynthetic pathway. Furthermore, gene silencing could be another powerful approach that could accurately understand gene's function and roles in the whole network (De Riso et al., 2009; Hammond et al., 2000; Smith et al., 2000). Combined with MFA, gene silencing could improve our understandings on C<sub>4</sub> CCM and provide direction on further modifications on *P. tricornutum*.

### **6.2.2. Identification of the Role of Urea Cycle in Urea Assimilation in *P. tricornutum***

Through <sup>15</sup>N and <sup>13</sup>C-<sup>15</sup>N combined instationary experiments we have revealed that urea assimilation in *P. tricornutum* may be different with nitrate or ammonium assimilation. Despite circumstantial evidence supported the hypothesis



that urea cycle may play a biosynthetic role in assimilation urea, direct evidence such as labeling on urea cycle metabolites yet were not found. One difficulty is the extraction on urea cycle metabolite was not always successful. Instability of many metabolites in this cycle, such as ornithine, citrulline and even arginine prevented successful extraction from this slow grow diatom. To possibly increase amount of urea cycle soluble metabolites, we may try i) modify extraction method including testing of pH and temperature and derivatization agent type and amount; ii) start with larger initial biomass and compensate nutrient (especially nitrogen) during batch culture; iii) measure samples with LC-MS to supplement GC-MS results.

## Appendices:

### **A.1. Table A.1 Mass Isotopomers from H<sup>13</sup>CO<sub>3</sub><sup>-</sup> Instationary ILE.**

Mass isotopomer distributions from instationary H<sup>13</sup>CO<sub>3</sub><sup>-</sup> ILE: intracellular metabolites (for time points 0 min, 1 min, 2 min, 5 min, 8 min, 12 min, 20 min, 8 h and 6 d) and proteinogenic amino acids from biomass (for 6 d time point). Mass isotopomers were obtained from GC-MS spectra by correcting for natural abundances of elements other than metabolic carbon as described in text. A few amino acids (mainly Arg and His) could not be detected in certain spectra due to their low abundance. The corresponding mass isotopomer abundances are marked as not determined (nd). Technical errors, e.g. between replicate GC-MS injections, were generally much smaller than errors between biological replicates. Some fragments were not considered because their enrichment in the control ( $t = 0$ ) time point deviated significantly from the natural abundance of <sup>13</sup>C. These fragments are indicated with a ~~strikethrough~~.

Table A.1 Mass isotopomers from H<sup>13</sup>CO<sub>2</sub> instationary ILE.

Metabolite	Fragment	m/z	Mass (n in m-n)	t = 0 min (control)										Overall	
				Intracellular metabolites: biological and technical (MS) replicates											
				Rep 1				Rep 2				Ave		SE	
Tech 1	Tech 2	Tech 3	Avg	SE	Tech 1	Tech 2	Tech 3	Avg	SE	Avg	SE				
AconiticAcid	[123456]	459	0	0.94	0.94	0.93	0.94	0.00	0.94	0.94	0.94	0.94	0.00	0.94	0.00
AconiticAcid	[123456]	459	1	0.05	0.05	0.06	0.05	0.00	0.04	0.06	0.05	0.05	0.01	0.05	0.01
AconiticAcid	[123456]	459	2	0.01	0.01	0.00	0.01	0.00	0.01	0.00	0.01	0.00	0.00	0.01	0.00
AconiticAcid	[123456]	459	3	0.00	0.01	0.00	0.00	0.00	0.00	0.00	0.00	0.00	0.00	0.00	0.00
AconiticAcid	[123456]	459	4	0.00	0.00	0.00	0.00	0.00	0.00	0.00	0.00	0.00	0.00	0.00	0.00
AconiticAcid	[123456]	459	5	0.00	0.00	0.00	0.00	0.00	0.00	0.00	0.00	0.00	0.00	0.00	0.00
AconiticAcid	[123456]	459	6	0.00	0.00	0.00	0.00	0.00	0.00	0.00	0.00	0.00	0.00	0.00	0.00
AconiticAcid	[12346]	327	0	0.80	0.79	0.76	0.79	0.01	0.79	0.82	0.81	0.81	0.01	0.80	0.01
AconiticAcid	[12346]	327	1	0.05	0.05	0.05	0.05	0.00	0.05	0.04	0.04	0.04	0.00	0.05	0.00
AconiticAcid	[12346]	327	2	0.07	0.08	0.10	0.08	0.01	0.08	0.08	0.10	0.09	0.01	0.08	0.01
AconiticAcid	[12346]	327	3	0.03	0.03	0.03	0.03	0.00	0.03	0.01	0.02	0.02	0.01	0.02	0.01
AconiticAcid	[12346]	327	4	0.04	0.05	0.05	0.05	0.00	0.04	0.04	0.03	0.04	0.00	0.04	0.00
AconiticAcid	[12346]	327	5	0.01	0.00	0.01	0.01	0.00	0.01	0.01	0.00	0.01	0.00	0.01	0.00
Asp	[12]	302	0	0.96	0.98	0.97	0.97	0.00	0.96	0.98	0.97	0.97	0.01	0.97	0.01
Asp	[12]	302	1	0.03	0.02	0.03	0.02	0.00	0.01	0.02	0.02	0.02	0.00	0.02	0.00
Asp	[12]	302	2	0.01	0.01	0.00	0.01	0.00	0.03	0.01	0.01	0.02	0.01	0.01	0.01
Asp	[234]	346	0	0.94	0.95	0.93	0.94	0.01	0.95	0.93	0.94	0.94	0.00	0.94	0.01
Asp	[234]	346	1	0.02	0.04	0.05	0.04	0.01	0.02	0.05	0.04	0.04	0.00	0.04	0.01
Asp	[234]	346	2	0.02	0.00	0.01	0.01	0.00	0.01	0.00	0.01	0.01	0.00	0.01	0.00
Asp	[234]	346	3	0.01	0.01	0.01	0.01	0.00	0.01	0.02	0.02	0.02	0.00	0.01	0.00
Asp	[12]	376	0	0.98	1.00	0.97	0.98	0.01	0.96	0.97	0.98	0.97	0.01	0.98	0.01
Asp	[12]	376	1	0.01	0.00	0.02	0.01	0.01	0.03	0.02	0.02	0.02	0.00	0.02	0.01
Asp	[12]	376	2	0.00	0.00	0.01	0.01	0.00	0.01	0.01	-0.01	0.00	0.01	0.00	0.01
Asp	[234]	390	0	0.97	0.98	0.97	0.97	0.00	0.98	0.97	0.99	0.98	0.00	0.98	0.00
Asp	[234]	390	1	0.02	0.02	0.03	0.02	0.00	0.02	0.02	0.01	0.01	0.00	0.02	0.00
Asp	[234]	390	2	0.01	0.00	0.00	0.00	0.00	0.00	0.00	0.00	0.00	0.00	0.00	0.00
Asp	[234]	390	3	0.00	0.00	0.00	0.00	0.00	0.00	0.01	0.00	0.01	0.00	0.00	0.00
Asp	[1234]	418	0	0.94	0.95	0.94	0.94	0.00	0.95	0.96	0.95	0.95	0.00	0.95	0.00
Asp	[1234]	418	1	0.04	0.04	0.04	0.04	0.00	0.04	0.04	0.04	0.04	0.00	0.04	0.00
Asp	[1234]	418	2	0.00	0.00	0.00	0.00	0.00	0.00	-0.01	0.01	0.00	0.00	0.00	0.00
Asp	[1234]	418	3	0.02	0.01	0.01	0.01	0.00	0.00	0.00	0.00	0.00	0.00	0.01	0.00
Asp	[1234]	418	4	0.00	0.00	0.00	0.00	0.00	0.00	0.00	0.00	0.00	0.00	0.00	0.00
C16D0FattyAcid	[1-16]	313	0	0.82	0.82	0.79	0.81	0.01	0.82	0.82	0.81	0.82	0.00	0.81	0.01
C16D0FattyAcid	[1-16]	313	1	0.13	0.13	0.13	0.13	0.00	0.13	0.13	0.13	0.13	0.00	0.13	0.00
C16D0FattyAcid	[1-16]	313	2	0.02	0.02	0.03	0.02	0.00	0.02	0.02	0.02	0.02	0.00	0.02	0.00
C16D0FattyAcid	[1-16]	313	3	0.01	0.00	0.01	0.01	0.00	0.00	0.00	0.00	0.00	0.00	0.00	0.00
C16D0FattyAcid	[1-16]	313	4	0.01	0.00	0.00	0.00	0.00	0.00	0.00	0.00	0.00	0.00	0.00	0.00
C16D0FattyAcid	[1-16]	313	5	0.00	0.00	0.00	0.00	0.00	0.00	0.00	0.00	0.00	0.00	0.00	0.00
C16D0FattyAcid	[1-16]	313	6	0.00	0.00	0.00	0.00	0.00	0.00	0.00	0.00	0.00	0.00	0.00	0.00
C16D0FattyAcid	[1-16]	313	7	0.00	0.00	0.00	0.00	0.00	0.00	0.00	0.00	0.00	0.00	0.00	0.00
C16D0FattyAcid	[1-16]	313	8	0.00	0.00	0.00	0.00	0.00	0.00	0.00	0.00	0.00	0.00	0.00	0.00
C16D0FattyAcid	[1-16]	313	9	0.00	0.00	0.00	0.00	0.00	0.00	0.00	0.00	0.00	0.00	0.00	0.00
C16D0FattyAcid	[1-16]	313	10	0.00	0.00	0.00	0.00	0.00	0.00	0.00	0.00	0.00	0.00	0.00	0.00
C16D0FattyAcid	[1-16]	313	11	0.00	0.00	0.00	0.00	0.00	0.00	0.00	0.00	0.00	0.00	0.00	0.00
C16D0FattyAcid	[1-16]	313	12	0.00	0.00	0.00	0.00	0.00	0.00	0.00	0.00	0.00	0.00	0.00	0.00
C16D0FattyAcid	[1-16]	313	13	0.00	0.00	0.00	0.00	0.00	0.00	0.00	0.00	0.00	0.00	0.00	0.00
C16D0FattyAcid	[1-16]	313	14	0.00	0.00	0.03	0.01	0.01	0.01	0.01	0.01	0.01	0.00	0.01	0.01
C16D0FattyAcid	[1-16]	313	15	0.00	0.00	0.01	0.00	0.00	0.00	0.00	0.00	0.00	0.00	0.00	0.00
C16D0FattyAcid	[1-16]	313	16	0.00	0.00	0.01	0.00	0.00	0.00	0.00	0.00	0.00	0.00	0.00	0.00
C16D1 FattyAcid	[1-16]	311	0	0.81	0.82	0.78	0.80	0.01	0.81	0.81	0.79	0.81	0.01	0.80	0.01
C16D1 FattyAcid	[1-16]	311	1	0.13	0.14	0.13	0.13	0.00	0.14	0.13	0.13	0.13	0.00	0.13	0.00
C16D1 FattyAcid	[1-16]	311	2	0.01	0.01	0.01	0.01	0.00	0.01	0.02	0.02	0.02	0.00	0.02	0.00
C16D1 FattyAcid	[1-16]	311	3	0.00	0.00	0.00	0.00	0.00	0.00	0.00	0.01	0.00	0.00	0.00	0.00
C16D1 FattyAcid	[1-16]	311	4	0.01	0.00	0.02	0.01	0.00	0.01	0.01	0.01	0.01	0.00	0.01	0.00
C16D1 FattyAcid	[1-16]	311	5	0.00	0.00	0.00	0.00	0.00	0.00	0.00	0.00	0.00	0.00	0.00	0.00
C16D1 FattyAcid	[1-16]	311	6	0.00	0.00	0.00	0.00	0.00	0.00	0.00	0.00	0.00	0.00	0.00	0.00
C16D1 FattyAcid	[1-16]	311	7	0.00	0.00	0.00	0.00	0.00	0.00	0.00	0.00	0.00	0.00	0.00	0.00
C16D1 FattyAcid	[1-16]	311	8	0.00	0.00	0.00	0.00	0.00	0.00	0.00	0.00	0.00	0.00	0.00	0.00
C16D1 FattyAcid	[1-16]	311	9	0.01	0.00	0.00	0.00	0.00	0.00	0.00	0.00	0.00	0.00	0.00	0.00
C16D1 FattyAcid	[1-16]	311	10	0.00	0.00	0.00	0.00	0.00	0.00	0.00	0.00	0.00	0.00	0.00	0.00
C16D1 FattyAcid	[1-16]	311	11	0.00	0.00	0.00	0.00	0.00	0.00	0.00	0.00	0.00	0.00	0.00	0.00
C16D1 FattyAcid	[1-16]	311	12	0.00	0.00	0.00	0.00	0.00	0.00	0.00	0.00	0.00	0.00	0.00	0.00
C16D1 FattyAcid	[1-16]	311	13	0.00	0.00	0.00	0.00	0.00	0.00	0.00	0.00	0.00	0.00	0.00	0.00
C16D1 FattyAcid	[1-16]	311	14	0.00	0.00	0.00	0.00	0.00	0.00	0.00	0.00	0.00	0.00	0.00	0.00
C16D1 FattyAcid	[1-16]	311	15	0.01	0.01	0.00	0.00	0.00	0.00	0.00	0.02	0.01	0.01	0.01	0.01
C16D1 FattyAcid	[1-16]	311	16	0.00	0.00	0.03	0.01	0.01	0.01	0.01	0.01	0.01	0.00	0.01	0.01
C18D0 FattyAcid	[1-18]	341	0	0.25	0.76	0.70	0.57	0.16	0.34	0.70	0.72	0.58	0.12	0.58	0.16
C18D0 FattyAcid	[1-18]	341	1	0.00	0.11	0.11	0.07	0.04	0.07	0.13	0.12	0.11	0.02	0.09	0.04
C18D0 FattyAcid	[1-18]	341	2	0.35	0.04	0.06	0.15	0.10	0.30	0.06	0.06	0.14	0.08	0.15	0.10
C18D0 FattyAcid	[1-18]	341	3	0.08	0.01	0.02	0.03	0.02	0.07	0.02	0.01	0.03	0.02	0.03	0.02
C18D0 FattyAcid	[1-18]	341	4	0.11	0.02	0.02	0.05	0.03	0.06	0.02	0.02	0.03	0.01	0.04	0.03
C18D0 FattyAcid	[1-18]	341	5	0.03	0.01	0.02	0.02	0.01	0.02	0.01	0.01	0.01	0.00	0.01	0.01
C18D0 FattyAcid	[1-18]	341	6	0.03	0.01	0.02	0.02	0.01	0.02	0.01	0.01	0.01	0.00	0.02	0.01
C18D0 FattyAcid	[1-18]	341	7	0.05	0.00	0.00	0.02	0.01	0.01	0.00	0.00	0.00	0.00	0.01	0.01
C18D0 FattyAcid	[1-18]	341	8	0.01	0.01	0.01	0.01	0.00	0.04	0.01	0.01	0.02	0.01	0.01	0.01
C18D0 FattyAcid	[1-18]	341	9	0.01	0.00	0.00	0.01	0.00	0.01	0.00	0.00	0.01	0.00	0.01	0.00
C18D0 FattyAcid	[1-18]	341	10	0.01	0.00	0.00	0.00	0.00	0.01	0.00	0.01	0.01	0.00	0.00	0.00
C18D0 FattyAcid	[1-18]	341	11	0.01	0.00	0.00	0.00	0.00	0.00	0.00	0.00	0.00	0.00	0.00	0.00
C18D0 FattyAcid	[1-18]	341	12	-0.01	0.00	0.00	0.00	0.00	0.01	0.00	0.00	0.00	0.00	0.00	0.00
C18D0 FattyAcid	[1-18]	341	13	0.04	0.01	0.00	0.02	0.01	0.00	0.00	0.00	0.00	0.00	0.01	0.01
C18D0 FattyAcid	[1-18]	341	14	0.02	0.00	0.01	0.01	0.00	0.02	0.01	0.02	0.02	0.00	0.01	0.00
C18D0 FattyAcid	[1-18]	341	15	0.00	0.00	0.01	0.00	0.							

t = 0 min (control)															
Metabolite	Fragment	m/z	Mass (n in m+n)	Intracellular metabolites: biological and technical (MS) replicates										Overall	
				Rep 1				Rep 2				Avg	SE	Avg	SE
				Tech 1	Tech 2	Tech 3	Avg	SE	Tech 1	Tech 2	Tech 3	Avg	SE	Avg	SE
Citrate	[123456]	591	2	-0.01	0.00	0.00	0.00	0.00	0.00	-0.01	0.00	0.00	0.00	0.00	0.00
Citrate	[123456]	591	3	0.00	0.00	0.00	0.00	0.00	0.00	0.00	0.00	0.00	0.00	0.00	0.00
Citrate	[123456]	591	4	0.00	0.00	0.00	0.00	0.00	0.00	0.00	0.00	0.00	0.00	0.00	0.00
Citrate	[123456]	591	5	0.00	0.00	0.00	0.00	0.00	0.00	0.00	0.00	0.00	0.00	0.00	0.00
Citrate	[123456]	591	6	0.00	0.00	0.00	0.00	0.00	0.00	0.00	0.00	0.00	0.00	0.00	0.00
Citrate	[12345]	431	0	0.97	0.96	0.97	0.96	0.00	0.97	0.96	0.96	0.96	0.00	0.96	0.00
Citrate	[12345]	431	1	0.03	0.04	0.03	0.03	0.00	0.03	0.04	0.04	0.04	0.00	0.03	0.00
Citrate	[12345]	431	2	0.00	0.00	0.00	0.00	0.00	0.00	0.00	0.00	0.00	0.00	0.00	0.00
Citrate	[12345]	431	3	0.00	0.00	0.00	0.00	0.00	0.00	0.00	0.00	0.00	0.00	0.00	0.00
Citrate	[12345]	431	4	0.00	0.00	0.00	0.00	0.00	0.00	0.00	0.00	0.00	0.00	0.00	0.00
Citrate	[12345]	431	5	0.00	0.00	0.00	0.00	0.00	0.00	0.00	0.00	0.00	0.00	0.00	0.00
Fumarate	[1234]	287	0	0.95	0.95	0.95	0.95	0.00	0.96	0.96	0.95	0.96	0.00	0.95	0.00
Fumarate	[1234]	287	1	0.04	0.04	0.04	0.04	0.00	0.04	0.04	0.04	0.04	0.00	0.04	0.00
Fumarate	[1234]	287	2	0.00	0.00	0.00	0.00	0.00	0.00	0.00	0.00	0.00	0.00	0.00	0.00
Fumarate	[1234]	287	3	0.00	0.00	0.00	0.00	0.00	0.00	0.00	0.00	0.00	0.00	0.00	0.00
Fumarate	[1234]	287	4	0.00	0.00	0.00	0.00	0.00	0.00	0.00	0.00	0.00	0.00	0.00	0.00
3PG	[2s]	231	0	0.98	0.98	0.98	0.98	0.00	0.98	0.98	0.98	0.98	0.00	0.98	0.00
3PG	[2s]	231	1	0.02	0.01	0.02	0.02	0.00	0.02	0.02	0.02	0.02	0.00	0.02	0.00
3PG	[2s]	231	2	0.01	0.01	0.01	0.01	0.00	0.01	0.01	0.01	0.01	0.00	0.01	0.00
3PG	[123]	391	0	0.98	0.98	0.97	0.98	0.00	0.98	0.98	0.98	0.98	0.00	0.98	0.00
3PG	[123]	391	1	0.02	0.02	0.03	0.02	0.00	0.02	0.02	0.02	0.02	0.00	0.02	0.00
3PG	[123]	391	2	0.00	0.00	0.00	0.00	0.00	0.00	0.00	0.00	0.00	0.00	0.00	0.00
3PG	[123]	391	3	0.00	0.00	0.00	0.00	0.00	0.00	0.00	0.00	0.00	0.00	0.00	0.00
Glu	[2345]	272	0	0.96	0.96	0.95	0.96	0.00	0.96	0.96	0.86	0.92	0.03	0.94	0.03
Glu	[2345]	272	1	0.02	0.03	0.03	0.03	0.00	0.03	0.03	0.13	0.06	0.03	0.04	0.03
Glu	[2345]	272	2	0.01	0.01	0.01	0.01	0.00	0.01	0.01	0.01	0.01	0.00	0.01	0.00
Glu	[2345]	272	3	0.00	0.00	0.01	0.00	0.00	0.00	0.00	0.00	0.00	0.00	0.00	0.00
Glu	[2345]	272	4	0.00	0.00	0.00	0.00	0.00	0.00	0.00	0.00	0.00	0.00	0.00	0.00
Glu	[2345]	330	0	0.97	0.96	0.96	0.96	0.00	0.96	0.96	0.96	0.96	0.00	0.96	0.00
Glu	[2345]	330	1	0.03	0.03	0.03	0.03	0.00	0.04	0.04	0.04	0.03	0.04	0.00	0.03
Glu	[2345]	330	2	0.00	0.00	0.00	0.00	0.00	0.00	0.00	0.00	0.00	0.00	0.00	0.00
Glu	[2345]	330	3	0.00	0.00	0.00	0.00	0.00	0.00	0.00	0.00	0.00	0.00	0.00	0.00
Glu	[2345]	330	4	0.00	0.00	0.00	0.00	0.00	0.00	0.00	0.00	0.00	0.00	0.00	0.00
Glu	[2345]	404	0	0.98	0.97	0.97	0.97	0.01	0.98	0.94	0.97	0.96	0.01	0.97	0.01
Glu	[2345]	404	1	0.02	0.03	0.03	0.02	0.00	0.02	0.02	0.02	0.02	0.00	0.02	0.00
Glu	[2345]	404	2	0.00	0.00	0.00	0.00	0.00	0.00	0.00	0.00	0.00	0.00	0.00	0.00
Glu	[2345]	404	3	0.00	0.00	0.00	0.00	0.00	0.00	0.00	0.00	0.00	0.00	0.00	0.00
Glu	[2345]	404	4	0.00	0.00	0.00	0.00	0.00	0.00	0.04	0.00	0.01	0.01	0.01	0.01
Glu	[12345]	432	0	0.98	0.98	0.98	0.98	0.00	0.99	0.98	0.98	0.98	0.00	0.98	0.00
Glu	[12345]	432	1	0.02	0.02	0.02	0.02	0.00	0.02	0.02	0.02	0.02	0.00	0.02	0.00
Glu	[12345]	432	2	-0.01	0.00	0.00	0.00	0.00	0.00	0.00	-0.01	0.00	0.00	0.00	0.00
Glu	[12345]	432	3	0.00	0.00	0.00	0.00	0.00	0.00	0.00	0.00	0.00	0.00	0.00	0.00
Glu	[12345]	432	4	0.00	0.00	0.00	0.00	0.00	0.00	0.00	0.00	0.00	0.00	0.00	0.00
Glu	[12345]	432	5	0.00	0.00	0.00	0.00	0.00	0.00	0.00	0.00	0.00	0.00	0.00	0.00
Glycerol	[123]	377	0	0.98	0.99	0.99	0.99	0.00	0.98	0.99	0.99	0.98	0.00	0.99	0.00
Glycerol	[123]	377	1	0.02	0.01	0.02	0.02	0.00	0.02	0.01	0.02	0.02	0.00	0.02	0.00
Glycerol	[123]	377	2	0.00	0.00	-0.01	0.00	0.00	0.00	0.00	-0.01	0.00	0.00	0.00	0.00
Glycerol	[123]	377	3	0.00	0.00	0.00	0.00	0.00	0.00	0.00	0.01	0.00	0.00	0.00	0.00
Lac	[23]	233	0	0.99	0.99	0.99	0.99	0.00	0.99	0.99	1.00	1.00	0.00	0.99	0.00
Lac	[23]	233	1	0.00	0.01	0.00	0.00	0.00	0.00	0.01	0.00	0.00	0.00	0.00	0.00
Lac	[23]	233	2	0.00	0.00	0.00	0.00	0.00	0.00	0.00	0.00	0.00	0.00	0.00	0.00
Lac	[123]	261	0	0.98	0.98	0.98	0.98	0.00	0.98	0.98	0.98	0.98	0.00	0.98	0.00
Lac	[123]	261	1	0.02	0.01	0.02	0.02	0.00	0.02	0.01	0.02	0.02	0.00	0.02	0.00
Lac	[123]	261	2	0.00	0.00	0.00	0.00	0.00	0.00	0.00	0.00	0.00	0.00	0.00	0.00
Lac	[123]	261	3	0.00	0.00	0.00	0.00	0.00	0.00	0.00	0.00	0.00	0.00	0.00	0.00
Leu	[23456]	200	0	0.86	0.88	0.87	0.87	0.01	0.88	0.89	0.88	0.88	0.01	0.88	0.01
Leu	[23456]	200	1	0.05	0.06	0.06	0.06	0.00	0.05	0.05	0.06	0.05	0.00	0.06	0.00
Leu	[23456]	200	2	0.03	0.02	0.02	0.02	0.00	0.02	0.02	0.02	0.02	0.00	0.02	0.00
Leu	[23456]	200	3	0.01	0.01	0.02	0.01	0.00	0.01	0.01	0.01	0.01	0.00	0.01	0.00
Leu	[23456]	200	4	0.01	0.00	0.00	0.01	0.00	0.00	0.00	0.02	0.01	0.00	0.01	0.00
Leu	[23456]	200	5	0.04	0.03	0.02	0.03	0.00	0.03	0.03	0.02	0.03	0.00	0.03	0.00
Leu	[23456]	274	0	0.89	0.91	0.88	0.89	0.01	0.90	0.89	0.90	0.89	0.00	0.89	0.01
Leu	[23456]	274	1	0.09	0.08	0.09	0.09	0.00	0.09	0.09	0.09	0.09	0.00	0.09	0.00
Leu	[23456]	274	2	0.01	0.00	0.00	0.00	0.00	0.00	0.01	0.00	0.01	0.00	0.00	0.00
Leu	[23456]	274	3	0.01	0.01	0.01	0.01	0.00	0.00	0.01	0.01	0.01	0.00	0.01	0.00
Leu	[23456]	274	4	0.00	0.00	0.00	0.00	0.00	0.00	0.00	0.00	0.00	0.00	0.00	0.00
Leu	[23456]	274	5	0.01	0.00	0.01	0.01	0.00	0.00	0.00	0.00	0.00	0.00	0.01	0.00
Leu	[123]	302	0	0.90	0.93	0.90	0.92	0.01	0.92	0.93	0.92	0.94	0.01	0.92	0.01
Leu	[123]	302	1	0.07	0.05	0.09	0.07	0.01	0.05	0.05	0.05	0.05	0.00	0.06	0.01
Leu	[123]	302	2	0.02	0.02	0.04	0.02	0.01	0.02	0.04	0.02	0.04	0.01	0.02	0.01
Malate	[1234]	419	0	0.97	0.97	0.97	0.97	0.00	0.97	0.96	0.97	0.97	0.00	0.97	0.00
Malate	[1234]	419	1	0.03	0.03	0.03	0.03	0.00	0.03	0.03	0.03	0.03	0.00	0.03	0.00
Malate	[1234]	419	2	0.00	0.00	0.00	0.00	0.00	0.00	0.00	0.00	0.00	0.00	0.00	0.00
Malate	[1234]	419	3	0.00	0.00	0.00	0.00	0.00	0.00	0.00	0.00	0.00	0.00	0.00	0.00
Malate	[1234]	419	4	0.00	0.00	0.00	0.00	0.00	0.00	0.00	0.00	0.00	0.00	0.00	0.00
Succinate	[1234]	289	0	0.96	0.96	0.97	0.96	0.00	0.97	0.96	0.97	0.97	0.00	0.97	0.00
Succinate	[1234]	289	1	0.03	0.04	0.03	0.03	0.00	0.03	0.03	0.03	0.03	0.00	0.03	0.00
Succinate	[1234]	289	2	0.00	0.00	0.00	0.00	0.00	0.00	0.00	0.00	0.00	0.00	0.00	0.00
Succinate	[1234]	289	3	0.00	0.00	0.00	0.00	0.00	0.00	0.00	0.00	0.00	0.00	0.00	0.00
Succinate	[1234]	289	4	0.00	0.00	0.00	0.00	0.00	0.00	0.00	0.00	0.00	0.00	0.00	0.00
Val	[2345]	186	0	0.80	0.84	0.83	0.82	0.01	0.82	0.85	0.82	0.83	0.01	0.83	0.01
Val	[2345]	186	1	0.09	0.05	0.06	0.07	0.01	0.07	0.05	0.06	0.06	0.01	0.06	0.01
Val	[2345]	186	2	0.01	0.01	0.00	0.00	0.00	0.01	0.01	0.01	0.01	0.00	0.01	0.00
Val	[2345]	186	3	0.09	0.09	0.10	0.09	0.00	0.09	0.08	0.10	0.09	0.01	0.09	0.01
Val	[2345]	18													





Table A.1 Mass isotopomers from H <sup>13</sup> CO <sub>2</sub> stationary JLE (Cont).																
t = 2 min																
Intracellular metabolites: biological and technical (MS) replicates																
Metabolite	Fragment	m/z	Mass (n in m-n)	Rep 1				Rep 2				Overall				
				Tech 1	Tech 2	Tech 3	Avg	SE	Tech 1	Tech 2	Tech 3	Avg	SE	Avg	SE	
AconiticAcid	[123456]	459	0	0.94	0.94	0.95	0.95	0.00	0.94	0.94	0.93	0.94	0.00	0.94	0.00	
AconiticAcid	[123456]	459	1	0.05	0.05	0.05	0.05	0.00	0.06	0.06	0.05	0.05	0.00	0.05	0.00	
AconiticAcid	[123456]	459	2	0.00	0.00	0.00	0.00	0.00	0.00	0.00	0.01	0.00	0.00	0.00	0.00	
AconiticAcid	[123456]	459	3	0.00	0.00	0.00	0.00	0.00	0.00	0.00	0.00	0.00	0.00	0.00	0.00	
AconiticAcid	[123456]	459	4	0.00	0.00	0.00	0.00	0.00	0.00	0.00	0.01	0.00	0.00	0.00	0.00	
AconiticAcid	[123456]	459	5	0.00	0.00	0.00	0.00	0.00	0.00	0.00	0.00	0.00	0.00	0.00	0.00	
AconiticAcid	[123456]	459	6	0.00	0.00	0.00	0.00	0.00	0.00	0.00	0.00	0.00	0.00	0.00	0.00	
AconiticAcid	[12346]	327	0	0.89	0.90	0.91	0.90	0.00	0.88	0.90	nd	0.89	0.01	0.90	0.01	
AconiticAcid	[12346]	327	1	0.05	0.04	0.04	0.04	0.00	0.05	0.04	nd	0.04	0.00	0.04	0.00	
AconiticAcid	[12346]	327	2	0.04	0.04	0.03	0.04	0.00	0.05	0.04	nd	0.04	0.00	0.04	0.00	
AconiticAcid	[12346]	327	3	0.01	0.01	0.01	0.01	0.00	0.01	0.01	nd	0.01	0.00	0.01	0.00	
AconiticAcid	[12346]	327	4	0.01	0.01	0.01	0.01	0.00	0.01	0.01	nd	0.01	0.00	0.01	0.00	
AconiticAcid	[12346]	327	5	0.00	0.00	0.00	0.00	0.00	0.01	0.00	nd	0.00	0.00	0.00	0.00	
Asp	[12]	302	0	0.92	0.92	0.90	0.91	0.01	0.90	0.92	nd	0.91	0.01	0.91	0.01	
Asp	[12]	302	1	0.07	0.07	0.07	0.07	0.00	0.08	0.07	nd	0.07	0.00	0.07	0.00	
Asp	[12]	302	2	0.02	0.02	0.03	0.02	0.00	0.02	0.01	nd	0.02	0.00	0.02	0.00	
Asp	[234]	316	0	0.86	0.87	0.85	0.86	0.01	0.85	0.88	nd	0.86	0.01	0.86	0.01	
Asp	[234]	316	1	0.12	0.11	0.12	0.12	0.00	0.12	0.10	nd	0.11	0.01	0.11	0.01	
Asp	[234]	316	2	0.00	0.01	0.01	0.01	0.00	0.01	0.01	nd	0.01	0.00	0.01	0.00	
Asp	[234]	316	3	0.02	0.01	0.02	0.02	0.00	0.02	0.01	nd	0.02	0.00	0.02	0.00	
Asp	[12]	376	0	0.92	0.92	0.91	0.92	0.00	0.89	0.90	nd	0.90	0.00	0.91	0.01	
Asp	[12]	376	1	0.07	0.06	0.07	0.06	0.00	0.09	0.08	nd	0.09	0.00	0.08	0.01	
Asp	[12]	376	2	0.01	0.01	0.02	0.01	0.00	0.02	0.02	nd	0.02	0.00	0.02	0.00	
Asp	[234]	390	0	0.88	0.88	0.85	0.87	0.01	0.87	0.90	nd	0.89	0.01	0.88	0.01	
Asp	[234]	390	1	0.11	0.11	0.13	0.12	0.01	0.11	0.09	nd	0.10	0.01	0.11	0.01	
Asp	[234]	390	2	0.01	0.01	0.01	0.01	0.00	0.01	0.01	nd	0.01	0.00	0.01	0.00	
Asp	[234]	390	3	0.00	0.00	0.01	0.01	0.00	0.01	0.00	nd	0.01	0.00	0.01	0.00	
Asp	[1234]	418	0	0.83	0.83	0.81	0.82	0.01	0.81	0.83	nd	0.82	0.01	0.82	0.01	
Asp	[1234]	418	1	0.14	0.14	0.15	0.14	0.00	0.15	0.14	nd	0.14	0.00	0.14	0.00	
Asp	[1234]	418	2	0.03	0.03	0.03	0.03	0.00	0.03	0.02	nd	0.02	0.00	0.03	0.00	
Asp	[1234]	418	3	0.00	0.00	0.00	0.00	0.00	0.01	0.00	nd	0.00	0.00	0.00	0.00	
Asp	[1234]	418	4	0.00	0.00	0.01	0.00	0.00	0.01	0.00	nd	0.00	0.00	0.00	0.00	
C16D0FattyAcid	[1-16]	313	0	0.84	0.84	0.84	0.84	0.00	0.84	0.84	0.83	0.83	0.00	0.84	0.00	
C16D0FattyAcid	[1-16]	313	1	0.14	0.14	0.15	0.15	0.00	0.14	0.14	0.15	0.15	0.00	0.15	0.00	
C16D0FattyAcid	[1-16]	313	2	0.01	0.01	0.01	0.01	0.00	0.01	0.01	0.01	0.01	0.00	0.01	0.00	
C16D0FattyAcid	[1-16]	313	3	0.00	0.00	0.00	0.00	0.00	0.00	0.00	0.00	0.00	0.00	0.00	0.00	
C16D0FattyAcid	[1-16]	313	4	0.00	0.00	0.00	0.00	0.00	0.00	0.00	0.00	0.00	0.00	0.00	0.00	
C16D0FattyAcid	[1-16]	313	5	0.00	0.00	0.00	0.00	0.00	0.00	0.00	0.00	0.00	0.00	0.00	0.00	
C16D0FattyAcid	[1-16]	313	6	0.00	0.00	0.00	0.00	0.00	0.00	0.00	0.00	0.00	0.00	0.00	0.00	
C16D0FattyAcid	[1-16]	313	7	0.00	0.00	0.00	0.00	0.00	0.00	0.00	0.00	0.00	0.00	0.00	0.00	
C16D0FattyAcid	[1-16]	313	8	0.00	0.00	0.00	0.00	0.00	0.00	0.00	0.00	0.00	0.00	0.00	0.00	
C16D0FattyAcid	[1-16]	313	9	0.00	0.00	0.00	0.00	0.00	0.00	0.00	0.00	0.00	0.00	0.00	0.00	
C16D0FattyAcid	[1-16]	313	10	0.00	0.00	0.00	0.00	0.00	0.00	0.00	0.00	0.00	0.00	0.00	0.00	
C16D0FattyAcid	[1-16]	313	11	0.00	0.00	0.00	0.00	0.00	0.00	0.00	0.00	0.00	0.00	0.00	0.00	
C16D0FattyAcid	[1-16]	313	12	0.00	0.00	0.00	0.00	0.00	0.00	0.00	0.00	0.00	0.00	0.00	0.00	
C16D0FattyAcid	[1-16]	313	13	0.00	0.00	0.00	0.00	0.00	0.00	0.00	0.00	0.00	0.00	0.00	0.00	
C16D0FattyAcid	[1-16]	313	14	0.00	0.00	0.00	0.00	0.00	0.00	0.00	0.00	0.00	0.00	0.00	0.00	
C16D0FattyAcid	[1-16]	313	15	0.00	0.00	0.00	0.00	0.00	0.00	0.00	0.00	0.00	0.00	0.00	0.00	
C16D0FattyAcid	[1-16]	313	16	0.00	0.00	0.00	0.00	0.00	0.00	0.00	0.00	0.00	0.00	0.00	0.00	
C16D1 FattyAcid	[1-16]	311	0	0.84	0.84	0.84	0.84	0.00	0.84	0.83	0.83	0.83	0.00	0.84	0.00	
C16D1 FattyAcid	[1-16]	311	1	0.15	0.14	0.14	0.14	0.00	0.15	0.15	0.14	0.15	0.00	0.15	0.00	
C16D1 FattyAcid	[1-16]	311	2	0.01	0.01	0.01	0.01	0.00	0.01	0.01	0.01	0.01	0.00	0.01	0.00	
C16D1 FattyAcid	[1-16]	311	3	0.00	0.00	0.00	0.00	0.00	0.00	0.00	0.00	0.00	0.00	0.00	0.00	
C16D1 FattyAcid	[1-16]	311	4	0.00	0.00	0.00	0.00	0.00	0.00	0.00	0.00	0.00	0.00	0.00	0.00	
C16D1 FattyAcid	[1-16]	311	5	0.00	0.00	0.00	0.00	0.00	0.00	0.00	0.00	0.00	0.00	0.00	0.00	
C16D1 FattyAcid	[1-16]	311	6	0.00	0.00	0.00	0.00	0.00	0.00	0.00	0.00	0.00	0.00	0.00	0.00	
C16D1 FattyAcid	[1-16]	311	7	0.00	0.00	0.00	0.00	0.00	0.00	0.00	0.00	0.00	0.00	0.00	0.00	
C16D1 FattyAcid	[1-16]	311	8	0.00	0.00	0.00	0.00	0.00	0.00	0.00	0.00	0.00	0.00	0.00	0.00	
C16D1 FattyAcid	[1-16]	311	9	0.00	0.00	0.00	0.00	0.00	0.00	0.00	0.00	0.00	0.00	0.00	0.00	
C16D1 FattyAcid	[1-16]	311	10	0.00	0.00	0.00	0.00	0.00	0.00	0.00	0.00	0.00	0.00	0.00	0.00	
C16D1 FattyAcid	[1-16]	311	11	0.00	0.00	0.00	0.00	0.00	0.00	0.00	0.00	0.00	0.00	0.00	0.00	
C16D1 FattyAcid	[1-16]	311	12	0.00	0.00	0.00	0.00	0.00	0.00	0.00	0.00	0.00	0.00	0.00	0.00	
C16D1 FattyAcid	[1-16]	311	13	0.00	0.00	0.00	0.00	0.00	0.00	0.00	0.00	0.00	0.00	0.00	0.00	
C16D1 FattyAcid	[1-16]	311	14	0.00	0.00	0.00	0.00	0.00	0.00	0.00	0.00	0.00	0.00	0.00	0.00	
C16D1 FattyAcid	[1-16]	311	15	0.00	0.00	0.00	0.00	0.00	0.00	0.00	0.00	0.00	0.00	0.00	0.00	
C16D1 FattyAcid	[1-16]	311	16	0.00	0.00	0.00	0.00	0.00	0.00	0.00	0.00	0.00	0.00	0.00	0.00	
C18D0FattyAcid	[1-18]	341	0	0.84	0.84	0.84	0.84	0.00	0.84	0.83	0.82	0.83	0.01	0.83	0.01	
C18D0FattyAcid	[1-18]	341	1	0.14	0.14	0.14	0.14	0.00	0.14	0.14	0.13	0.14	0.00	0.14	0.00	
C18D0FattyAcid	[1-18]	341	2	0.01	0.01	0.02	0.01	0.00	0.01	0.02	0.02	0.02	0.00	0.02	0.00	
C18D0FattyAcid	[1-18]	341	3	0.00	0.00	0.00	0.00	0.00	0.00	0.00	0.00	0.00	0.00	0.00	0.00	
C18D0FattyAcid	[1-18]	341	4	0.00	0.00	0.00	0.00	0.00	0.00	0.00	0.00	0.00	0.00	0.00	0.00	
C18D0FattyAcid	[1-18]	341	5	0.00	0.00	0.00	0.00	0.00	0.00	0.00	0.00	0.00	0.00	0.00	0.00	
C18D0FattyAcid	[1-18]	341	6	0.00	0.00	0.00	0.00	0.00	0.00	0.00	0.00	0.00	0.00	0.00	0.00	
C18D0FattyAcid	[1-18]	341	7	0.00	0.00	0.00	0.00	0.00	0.00	0.00	0.00	0.00	0.00	0.00	0.00	
C18D0FattyAcid	[1-18]	341	8	0.00	0.00	0.00	0.00	0.00	0.00	0.00	0.00	0.00	0.00	0.00	0.00	
C18D0FattyAcid	[1-18]	341	9	0.00	0.00	0.00	0.00	0.00	0.00	0.00	0.00	0.00	0.00	0.00	0.00	
C18D0FattyAcid	[1-18]	341	10	0.00	0.00	0.00	0.00	0.00	0.00	0.00	0.00	0.00	0.00	0.00	0.00	
C18D0FattyAcid	[1-18]	341	11	0.00	0.00	0.00	0.00	0.00	0.00	0.00	0.00	0.00	0.00	0.00	0.00	
C18D0FattyAcid	[1-18]	341	12	0.00	0.00	0.00	0.00	0.00	0.00	0.00	0.01	0.00	0.00	0.00	0.00	
C18D0FattyAcid	[1-18]	341	13	0.00	0.00	0.00	0.00	0.00	0.00	0.00	0.00	0.00	0.00	0.00	0.00	
C18D0FattyAcid	[1-18]	341	14	0.00	0.00	0.00	0.00	0.00	0.00	0.00	0.00	0.00	0.00	0.00	0.00	
C18D0FattyAcid	[1-18]	341	15	0.00	0.00	0.00	0.00	0.00	0.00	0.00	0.00	0.00	0.00	0.00	0.00	
C18D0FattyAcid	[1-18]	341	16	0.00												







Table A.1 Mass isotopomers from H <sup>13</sup> CO <sub>2</sub> ; instationary ILE (Cont).																			
t = 5 min																			
Metabolite	Fragment	m/z	Mass (n in m+n)	Intracellular metabolites: biological and technical (MS) replicates															
				Rep 1				Rep 2				Rep 3				Overall			
				Tech 1	Tech 2	Tech 3	Avg	SE	Tech 1	Tech 2	Tech 3	Avg	SE	Tech 1	Tech 2	Tech 3	Avg	SE	Avg
Citrate	[123456]	591	2	-0.01	0.00	0.00	0.00	0.00	0.00	-0.01	0.00	0.00	0.00	0.00	0.00	0.00	0.00	0.00	0.00
Citrate	[123456]	591	3	0.00	0.00	0.00	0.00	0.00	0.00	0.00	0.00	0.00	0.00	0.00	0.00	0.00	0.00	0.00	0.00
Citrate	[123456]	591	4	0.00	0.00	0.00	0.00	0.00	0.00	0.00	0.00	0.00	0.00	0.00	0.00	0.00	0.00	0.00	0.00
Citrate	[123456]	591	5	0.00	0.00	0.00	0.00	0.00	0.00	0.00	0.00	0.00	0.00	0.00	0.00	0.00	0.00	0.00	0.00
Citrate	[123456]	591	6	0.00	0.00	0.00	0.00	0.00	0.00	0.00	0.00	0.00	0.00	0.00	0.00	0.00	0.00	0.00	0.00
Citrate	[12345]	431	0	0.96	0.96	0.97	0.96	0.00	0.97	0.96	0.96	0.96	0.00	0.96	0.96	0.96	0.96	0.00	0.96
Citrate	[12345]	431	1	0.04	0.03	0.03	0.03	0.00	0.03	0.03	0.03	0.03	0.00	0.03	0.03	0.03	0.03	0.00	0.03
Citrate	[12345]	431	2	0.00	0.00	0.00	0.00	0.00	0.00	0.00	0.01	0.00	0.00	0.00	0.00	0.01	0.00	0.00	0.00
Citrate	[12345]	431	3	0.00	0.00	0.00	0.00	0.00	0.00	0.00	0.00	0.00	0.00	0.00	0.00	0.00	0.00	0.00	0.00
Citrate	[12345]	431	4	0.00	0.00	0.00	0.00	0.00	0.00	0.00	0.00	0.00	0.00	0.00	0.00	0.00	0.00	0.00	0.00
Citrate	[12345]	431	5	0.00	0.00	0.00	0.00	0.00	0.00	0.00	0.00	0.00	0.00	0.00	0.00	0.00	0.00	0.00	0.00
Fumarate	[1234]	287	0	0.93	0.93	0.93	0.93	0.00	0.93	0.92	0.93	0.93	0.00	0.92	0.92	0.92	0.92	0.00	0.92
Fumarate	[1234]	287	1	0.07	0.06	0.07	0.07	0.00	0.06	0.07	0.07	0.07	0.00	0.07	0.07	0.07	0.07	0.00	0.07
Fumarate	[1234]	287	2	0.01	0.01	0.01	0.01	0.00	0.01	0.01	0.01	0.01	0.00	0.01	0.01	0.01	0.01	0.00	0.01
Fumarate	[1234]	287	3	0.00	0.00	0.00	0.00	0.00	0.00	0.00	0.00	0.00	0.00	0.00	0.00	0.00	0.00	0.00	0.00
Fumarate	[1234]	287	4	0.00	0.00	0.00	0.00	0.00	0.00	0.00	0.00	0.00	0.00	0.00	0.00	0.00	0.00	0.00	0.00
3PG	[2x]	231	0	0.98	0.97	0.98	0.98	0.00	0.97	0.98	0.97	0.97	0.00	0.98	0.97	0.97	0.97	0.00	0.97
3PG	[2x]	231	1	0.01	0.02	0.02	0.02	0.00	0.02	0.01	0.02	0.02	0.00	0.01	0.02	0.01	0.02	0.00	0.02
3PG	[2x]	231	2	0.01	0.01	0.01	0.01	0.00	0.01	0.01	0.01	0.01	0.00	0.01	0.01	0.01	0.01	0.00	0.01
3PG	[123]	391	0	0.98	0.98	0.98	0.98	0.00	0.98	0.98	0.98	0.98	0.00	0.97	0.98	0.98	0.98	0.00	0.98
3PG	[123]	391	1	0.02	0.02	0.02	0.02	0.00	0.02	0.02	0.02	0.02	0.00	0.02	0.02	0.02	0.02	0.00	0.02
3PG	[123]	391	2	0.00	-0.01	0.00	0.00	0.00	0.00	0.00	0.00	0.00	0.00	0.00	0.00	0.00	0.00	0.00	0.00
3PG	[123]	391	3	0.00	0.00	0.00	0.00	0.00	0.00	0.00	0.00	0.00	0.00	0.00	0.00	0.00	0.00	0.00	0.00
Glucose	[2345]	272	0	0.94	0.93	0.94	0.94	0.00	0.94	0.94	0.94	0.94	0.00	0.94	0.93	0.93	0.93	0.00	0.94
Glucose	[2345]	272	1	0.04	0.05	0.05	0.05	0.00	0.04	0.05	0.05	0.05	0.00	0.05	0.05	0.05	0.05	0.00	0.05
Glucose	[2345]	272	2	0.01	0.01	0.01	0.01	0.00	0.01	0.01	0.01	0.01	0.00	0.01	0.01	0.01	0.01	0.00	0.01
Glucose	[2345]	272	3	0.00	0.00	0.00	0.00	0.00	0.00	0.00	0.00	0.00	0.00	0.00	0.01	0.01	0.01	0.00	0.00
Glucose	[2345]	272	4	0.00	0.00	0.00	0.00	0.00	0.00	0.00	0.00	0.00	0.00	0.00	0.00	0.00	0.00	0.00	0.00
Glucose	[2345]	330	0	0.96	0.96	0.96	0.96	0.00	0.96	0.96	0.96	0.96	0.00	0.96	0.96	0.96	0.96	0.00	0.96
Glucose	[2345]	330	1	0.04	0.03	0.04	0.04	0.00	0.03	0.03	0.03	0.03	0.00	0.04	0.04	0.04	0.04	0.00	0.03
Glucose	[2345]	330	2	0.00	0.00	0.00	0.00	0.00	0.00	0.00	0.00	0.00	0.00	0.00	0.00	0.00	0.00	0.00	0.00
Glucose	[2345]	330	3	0.00	0.00	0.00	0.00	0.00	0.00	0.00	0.00	0.00	0.00	0.00	0.00	0.00	0.00	0.00	0.00
Glucose	[2345]	330	4	0.00	0.00	0.00	0.00	0.00	0.00	0.00	0.00	0.00	0.00	0.00	0.00	0.00	0.00	0.00	0.00
Glucose	[2345]	404	0	0.97	0.97	0.97	0.97	0.00	0.98	0.97	0.97	0.97	0.00	0.97	0.97	0.97	0.96	0.00	0.97
Glucose	[2345]	404	1	0.02	0.02	0.03	0.02	0.00	0.02	0.03	0.02	0.02	0.00	0.02	0.03	0.03	0.03	0.00	0.02
Glucose	[2345]	404	2	0.00	0.00	0.00	0.00	0.00	0.00	0.00	0.00	0.00	0.00	0.01	0.00	0.00	0.00	0.00	0.00
Glucose	[2345]	404	3	0.00	0.00	0.00	0.00	0.00	0.00	0.00	0.00	0.00	0.00	0.00	0.00	0.00	0.00	0.00	0.00
Glucose	[2345]	404	4	0.00	0.00	0.00	0.00	0.00	0.00	0.00	0.00	0.00	0.00	0.00	0.00	0.00	0.00	0.00	0.00
Glucose	[12345]	432	0	0.97	0.95	0.94	0.95	0.01	0.95	0.94	0.93	0.94	0.00	0.96	0.92	0.92	0.93	0.01	0.94
Glucose	[12345]	432	1	0.03	0.05	0.06	0.05	0.01	0.05	0.06	0.06	0.06	0.01	0.04	0.08	0.08	0.06	0.01	0.06
Glucose	[12345]	432	2	0.00	0.00	0.00	0.00	0.00	0.00	0.00	0.00	0.00	0.00	0.00	0.00	0.00	0.00	0.00	0.00
Glucose	[12345]	432	3	0.00	0.00	0.00	0.00	0.00	0.00	0.00	0.00	0.00	0.00	0.00	0.00	0.00	0.00	0.00	0.00
Glucose	[12345]	432	4	0.00	0.00	0.00	0.00	0.00	0.00	0.00	0.00	0.00	0.00	0.00	0.00	0.00	0.00	0.00	0.00
Glucose	[12345]	432	5	0.00	0.00	0.00	0.00	0.00	0.00	0.00	0.00	0.00	0.00	0.00	0.00	0.00	0.00	0.00	0.00
Glycerol	[123]	377	0	0.98	0.99	0.98	0.98	0.00	0.98	0.99	0.98	0.98	0.00	0.99	0.99	0.99	0.99	0.00	0.98
Glycerol	[123]	377	1	0.02	0.01	0.02	0.02	0.00	0.02	0.02	0.03	0.02	0.00	0.01	0.01	0.01	0.01	0.00	0.02
Glycerol	[123]	377	2	0.00	-0.01	0.00	0.00	0.00	0.00	0.00	0.00	0.00	0.00	0.00	0.00	0.00	0.00	0.00	0.00
Glycerol	[123]	377	3	0.00	0.00	0.00	0.00	0.00	0.00	0.00	0.00	0.00	0.00	0.00	0.00	0.00	0.00	0.00	0.00
Lactate	[23]	233	0	0.98	0.98	0.99	0.98	0.00	0.99	0.98	0.98	0.98	0.00	0.98	0.98	0.98	0.98	0.00	0.98
Lactate	[23]	233	1	0.01	0.02	0.01	0.02	0.00	0.01	0.02	0.01	0.01	0.00	0.02	0.02	0.01	0.02	0.00	0.02
Lactate	[23]	233	2	0.00	0.00	0.00	0.00	0.00	0.00	0.00	0.00	0.00	0.00	0.00	0.00	0.00	0.00	0.00	0.00
Lactate	[123]	261	0	0.93	0.93	0.93	0.93	0.00	0.92	0.92	0.93	0.92	0.00	nd	nd	nd	nd	0.00	0.93
Lactate	[123]	261	1	0.06	0.06	0.06	0.06	0.00	0.07	0.07	0.07	0.07	0.00	nd	nd	nd	nd	0.00	0.07
Lactate	[123]	261	2	0.00	0.00	0.00	0.00	0.00	0.00	0.00	0.00	0.00	0.00	nd	nd	nd	nd	0.00	0.00
Lactate	[123]	261	3	0.00	0.00	0.00	0.00	0.00	0.00	0.00	0.00	0.00	0.00	nd	nd	nd	nd	0.00	0.00
Leucine	[23456]	200	0	0.88	0.83	0.83	0.85	0.02	0.90	0.89	0.90	0.90	0.01	0.89	0.89	0.89	0.89	0.00	0.88
Leucine	[23456]	200	1	0.07	0.06	0.07	0.06	0.00	0.06	0.06	0.06	0.06	0.00	0.07	0.06	0.06	0.06	0.00	0.06
Leucine	[23456]	200	2	0.02	0.02	0.02	0.02	0.00	0.01	0.02	0.01	0.02	0.00	0.02	0.02	0.02	0.02	0.00	0.02
Leucine	[23456]	200	3	0.01	0.01	0.01	0.01	0.00	0.01	0.01	0.01	0.01	0.00	0.01	0.01	0.01	0.01	0.00	0.01
Leucine	[23456]	200	4	0.00	0.02	0.01	0.01	0.01	0.01	0.00	0.00	0.00	0.00	0.00	0.00	0.00	0.00	0.00	0.01
Leucine	[23456]	200	5	0.02	0.06	0.07	0.05	0.01	0.02	0.02	0.02	0.02	0.00	0.02	0.02	0.02	0.02	0.00	0.03
Leucine	[23456]	274	0	0.89	0.90	0.89	0.89	0.00	0.90	0.90	0.90	0.90	0.00	0.90	0.90	0.90	0.90	0.00	0.90
Leucine	[23456]	274	1	0.08	0.08	0.08	0.08	0.00	0.09	0.08	0.09	0.08	0.00	0.09	0.09	0.09	0.09	0.00	0.08
Leucine	[23456]	274	2	0.01	0.01	0.01	0.01	0.00	0.01	0.01	0.01	0.01	0.00	0.01	0.01	0.01	0.01	0.00	0.01
Leucine	[23456]	274	3	0.00	0.01	0.00	0.00	0.00	0.00	0.00	0.00	0.00	0.00	0.00	0.00	0.01	0.00	0.00	0.00
Leucine	[23456]	274	4	0.00	0.00	0.00	0.00	0.00	0.00	0.00	0.00	0.00	0.00	0.00	0.00	0.00	0.00	0.00	0.00
Leucine	[23456]	274	5	0.02	0.01	0.02	0.02	0.00	0.01	0.01	0.01	0.01	0.00	0.01	0.01	0.01	0.01	0.00	0.01
Leucine	[123]	302</																	

Table A.1 Mass isotopomers from H<sup>13</sup>CO<sub>2</sub> stationary ILE (Cont).

Metabolite	Fragment	m/z	Mass (n in m-n)	Intracellular metabolites: biological and technical (MS) replicates												Overall	
				t = 8 min													
				Rep 1						Rep 2							
				Tech 1	Tech 2	Avg	SE	Tech 1	Tech 2	Avg	SE	Avg	SE				
AconiticAcid	[123456]	459	0	0.94	0.95	0.94	0.00	0.94	0.95	0.95	0.00	0.95	0.00	0.95	0.00		
AconiticAcid	[123456]	459	1	0.05	0.05	0.05	0.00	0.06	0.05	0.05	0.00	0.05	0.00	0.05	0.00		
AconiticAcid	[123456]	459	2	0.00	0.00	0.00	0.00	0.00	0.00	0.00	0.00	0.00	0.00	0.00	0.00		
AconiticAcid	[123456]	459	3	0.00	0.00	0.00	0.00	0.00	0.00	0.00	0.00	0.00	0.00	0.00	0.00		
AconiticAcid	[123456]	459	4	0.00	0.00	0.00	0.00	0.00	0.00	0.00	0.00	0.00	0.00	0.00	0.00		
AconiticAcid	[123456]	459	5	0.00	0.00	0.00	0.00	0.00	0.00	0.00	0.00	0.00	0.00	0.00	0.00		
AconiticAcid	[123456]	459	6	0.00	0.00	0.00	0.00	0.00	0.00	0.00	0.00	0.00	0.00	0.00	0.00		
AconiticAcid	[12346]	327	0	0.90	0.90	0.90	0.00	0.90	0.90	0.90	0.00	0.90	0.00	0.90	0.00		
AconiticAcid	[12346]	327	1	0.04	0.04	0.04	0.00	0.04	0.04	0.04	0.00	0.04	0.00	0.04	0.00		
AconiticAcid	[12346]	327	2	0.03	0.03	0.03	0.00	0.04	0.04	0.04	0.00	0.04	0.00	0.04	0.00		
AconiticAcid	[12346]	327	3	0.01	0.01	0.01	0.00	0.01	0.01	0.01	0.00	0.01	0.00	0.01	0.00		
AconiticAcid	[12346]	327	4	0.01	0.01	0.01	0.00	0.01	0.01	0.01	0.00	0.01	0.00	0.01	0.00		
AconiticAcid	[12346]	327	5	0.00	0.00	0.00	0.00	0.00	0.00	0.00	0.00	0.00	0.00	0.00	0.00		
Asp	[12]	302	0	nd	nd	nd	nd	0.86	0.87	0.88	0.87	0.01	0.87	0.01	0.87	0.01	
Asp	[12]	302	1	nd	nd	nd	nd	0.13	0.12	0.12	0.13	0.01	0.13	0.01	0.13	0.01	
Asp	[12]	302	2	nd	nd	nd	nd	0.00	0.01	0.00	0.00	0.00	0.00	0.00	0.00	0.00	
Asp	[234]	346	0	0.29	0.80	0.29	0.00	0.80	0.82	0.81	0.81	0.00	0.80	0.00	0.80	0.00	
Asp	[234]	346	1	0.17	0.17	0.17	0.00	0.17	0.17	0.18	0.17	0.00	0.17	0.00	0.17	0.00	
Asp	[234]	346	2	0.01	0.01	0.01	0.00	0.01	0.01	0.00	0.01	0.00	0.01	0.00	0.01	0.00	
Asp	[234]	346	3	0.03	0.03	0.03	0.00	0.02	0.01	0.01	0.01	0.00	0.02	0.00	0.02	0.00	
Asp	[12]	376	0	0.88	0.87	0.88	0.00	0.85	0.88	0.89	0.87	0.01	0.88	0.01	0.88	0.01	
Asp	[12]	376	1	0.11	0.11	0.11	0.00	0.13	0.13	0.10	0.12	0.01	0.12	0.01	0.12	0.01	
Asp	[12]	376	2	0.01	0.01	0.01	0.00	0.02	-0.01	0.01	0.01	0.01	0.01	0.01	0.01	0.01	
Asp	[234]	390	0	0.83	0.83	0.83	0.00	0.84	0.82	0.84	0.84	0.01	0.83	0.01	0.83	0.01	
Asp	[234]	390	1	0.17	0.16	0.16	0.00	0.17	0.17	0.15	0.16	0.01	0.16	0.01	0.16	0.01	
Asp	[234]	390	2	0.00	0.00	0.00	0.00	-0.01	0.00	0.00	0.00	0.00	0.01	0.00	0.01	0.00	
Asp	[234]	390	3	0.01	0.01	0.01	0.00	0.01	0.01	0.00	0.01	0.00	0.01	0.00	0.01	0.00	
Asp	[1234]	418	0	0.75	0.76	0.75	0.00	0.74	0.75	0.77	0.75	0.01	0.75	0.01	0.75	0.01	
Asp	[1234]	418	1	0.20	0.20	0.20	0.00	0.23	0.20	0.19	0.21	0.01	0.20	0.01	0.20	0.01	
Asp	[1234]	418	2	0.04	0.04	0.04	0.00	0.04	0.04	0.03	0.04	0.00	0.04	0.00	0.04	0.00	
Asp	[1234]	418	3	0.00	0.00	0.00	0.00	0.01	0.00	0.00	0.00	0.00	0.00	0.00	0.00	0.00	
Asp	[1234]	418	4	0.00	0.01	0.00	0.00	-0.01	0.00	0.00	0.00	0.00	0.00	0.00	0.00	0.00	
C16:0 Fatty Acid	[1-16]	313	0	0.84	0.83	0.83	0.00	0.83	0.83	0.83	0.83	0.00	0.83	0.00	0.83	0.00	
C16:0 Fatty Acid	[1-16]	313	1	0.14	0.15	0.15	0.00	0.14	0.14	0.14	0.14	0.00	0.14	0.00	0.14	0.00	
C16:0 Fatty Acid	[1-16]	313	2	0.01	0.01	0.01	0.00	0.02	0.02	0.02	0.02	0.00	0.02	0.00	0.02	0.00	
C16:0 Fatty Acid	[1-16]	313	3	0.00	0.00	0.00	0.00	0.00	0.00	0.00	0.00	0.00	0.00	0.00	0.00	0.00	
C16:0 Fatty Acid	[1-16]	313	4	0.00	0.00	0.00	0.00	0.00	0.00	0.00	0.00	0.00	0.00	0.00	0.00	0.00	
C16:0 Fatty Acid	[1-16]	313	5	0.00	0.00	0.00	0.00	0.00	0.00	0.00	0.00	0.00	0.00	0.00	0.00	0.00	
C16:0 Fatty Acid	[1-16]	313	6	0.00	0.00	0.00	0.00	0.00	0.00	0.00	0.00	0.00	0.00	0.00	0.00	0.00	
C16:0 Fatty Acid	[1-16]	313	7	0.00	0.00	0.00	0.00	0.00	0.00	0.00	0.00	0.00	0.00	0.00	0.00	0.00	
C16:0 Fatty Acid	[1-16]	313	8	0.00	0.00	0.00	0.00	0.00	0.00	0.00	0.00	0.00	0.00	0.00	0.00	0.00	
C16:0 Fatty Acid	[1-16]	313	9	0.00	0.00	0.00	0.00	0.00	0.00	0.00	0.00	0.00	0.00	0.00	0.00	0.00	
C16:0 Fatty Acid	[1-16]	313	10	0.00	0.00	0.00	0.00	0.00	0.00	0.00	0.00	0.00	0.00	0.00	0.00	0.00	
C16:0 Fatty Acid	[1-16]	313	11	0.00	0.00	0.00	0.00	0.00	0.00	0.00	0.00	0.00	0.00	0.00	0.00	0.00	
C16:0 Fatty Acid	[1-16]	313	12	0.00	0.00	0.00	0.00	0.00	0.00	0.00	0.00	0.00	0.00	0.00	0.00	0.00	
C16:0 Fatty Acid	[1-16]	313	13	0.00	0.00	0.00	0.00	0.00	0.00	0.00	0.00	0.00	0.00	0.00	0.00	0.00	
C16:0 Fatty Acid	[1-16]	313	14	0.00	0.00	0.00	0.00	0.00	0.00	0.00	0.00	0.00	0.00	0.00	0.00	0.00	
C16:0 Fatty Acid	[1-16]	313	15	0.00	0.00	0.00	0.00	0.00	0.00	0.00	0.00	0.00	0.00	0.00	0.00	0.00	
C16:0 Fatty Acid	[1-16]	313	16	0.00	0.00	0.00	0.00	0.00	0.00	0.00	0.00	0.00	0.00	0.00	0.00	0.00	
C16:1 Fatty Acid	[1-16]	311	0	0.84	0.84	0.84	0.00	0.82	0.82	0.83	0.83	0.00	0.83	0.00	0.83	0.00	
C16:1 Fatty Acid	[1-16]	311	1	0.15	0.14	0.14	0.00	0.14	0.14	0.14	0.14	0.00	0.14	0.00	0.14	0.00	
C16:1 Fatty Acid	[1-16]	311	2	0.01	0.01	0.01	0.00	0.01	0.01	0.01	0.01	0.00	0.01	0.00	0.01	0.00	
C16:1 Fatty Acid	[1-16]	311	3	0.00	0.00	0.00	0.00	0.00	0.00	0.00	0.00	0.00	0.00	0.00	0.00	0.00	
C16:1 Fatty Acid	[1-16]	311	4	0.00	0.00	0.00	0.00	0.01	0.01	0.00	0.01	0.00	0.01	0.00	0.01	0.00	
C16:1 Fatty Acid	[1-16]	311	5	0.00	0.00	0.00	0.00	0.00	0.00	0.00	0.00	0.00	0.00	0.00	0.00	0.00	
C16:1 Fatty Acid	[1-16]	311	6	0.00	0.00	0.00	0.00	0.00	0.00	0.00	0.00	0.00	0.00	0.00	0.00	0.00	
C16:1 Fatty Acid	[1-16]	311	7	0.00	0.00	0.00	0.00	0.00	0.00	0.00	0.00	0.00	0.00	0.00	0.00	0.00	
C16:1 Fatty Acid	[1-16]	311	8	0.00	0.00	0.00	0.00	0.00	0.00	0.00	0.00	0.00	0.00	0.00	0.00	0.00	
C16:1 Fatty Acid	[1-16]	311	9	0.00	0.00	0.00	0.00	0.00	0.00	0.00	0.00	0.00	0.00	0.00	0.00	0.00	
C16:1 Fatty Acid	[1-16]	311	10	0.00	0.00	0.00	0.00	0.00	0.00	0.00	0.00	0.00	0.00	0.00	0.00	0.00	
C16:1 Fatty Acid	[1-16]	311	11	0.00	0.00	0.00	0.00	0.00	0.00	0.00	0.00	0.00	0.00	0.00	0.00	0.00	
C16:1 Fatty Acid	[1-16]	311	12	0.00	0.00	0.00	0.00	0.00	0.00	0.00	0.00	0.00	0.00	0.00	0.00	0.00	
C16:1 Fatty Acid	[1-16]	311	13	0.00	0.00	0.00	0.00	0.00	0.00	0.00	0.00	0.00	0.00	0.00	0.00	0.00	
C16:1 Fatty Acid	[1-16]	311	14	0.00	0.00	0.00	0.00	0.00	0.00	0.00	0.00	0.00	0.00	0.00	0.00	0.00	
C16:1 Fatty Acid	[1-16]	311	15	0.00	0.00	0.00	0.00	0.00	0.00	0.00	0.00	0.00	0.00	0.00	0.00	0.00	
C16:1 Fatty Acid	[1-16]	311	16	0.00	0.00	0.00	0.00	0.00	0.00	0.00	0.00	0.00	0.00	0.00	0.00	0.00	
C18:0 Fatty Acid	[1-18]	341	0	0.84	0.84	0.84	0.00	0.77	0.76	0.75	0.76	0.00	0.80	0.00	0.80	0.00	
C18:0 Fatty Acid	[1-18]	341	1	0.14	0.14	0.14	0.00	0.13	0.13	0.13	0.13	0.00	0.13	0.00	0.13	0.00	
C18:0 Fatty Acid	[1-18]	341	2	0.01	0.02	0.01	0.00	0.03	0.04	0.04	0.04	0.00	0.03	0.00	0.03	0.01	
C18:0 Fatty Acid	[1-18]	341	3	0.00	0.00	0.00	0.00	0.01	0.01	0.01	0.01	0.00	0.01	0.00	0.01	0.00	
C18:0 Fatty Acid	[1-18]	341	4	0.00	0.00	0.00	0.00	0.01	0.01	0.01	0.01	0.00	0.01	0.00	0.01	0.00	
C18:0 Fatty Acid	[1-18]	341	5	0.00	0.00	0.00	0.00	0.01	0.00	0.00	0.00	0.00	0.00	0.00	0.00	0.00	
C18:0 Fatty Acid	[1-18]	341	6	0.00	0.00	0.00	0.00	0.00	0.00	0.00	0.00	0.00	0.00	0.00	0.00	0.00	
C18:0 Fatty Acid	[1-18]	341	7	0.00	0.00	0.00	0.00	0.00	0.00	0.00	0.00	0.00	0.00	0.00	0.00	0.00	
C18:0 Fatty Acid	[1-18]	341	8	0.00	0.00	0.00	0.00	0.00	0.00	0.00	0.00	0.00	0.00	0.00	0.00	0.00	
C18:0 Fatty Acid	[1-18]	341	9	0.00	0.00	0.00	0.00	0.00	0.00	0.00	0.00	0.00	0.00	0.00	0.00	0.00	
C18:0 Fatty Acid	[1-18]	341	10	0.00	0.00	0.00	0.00	0.00	0.00	0.00	0.00	0.00	0.00	0.00	0.00	0.00	
C18:0 Fatty Acid	[1-18]	341	11	0.00	0.00	0.00	0.00	0.00	0.00	0.00	0.00	0.00	0.00	0.00	0.00	0.00	
C18:0 Fatty Acid	[1-18]	341	12	0.00	0.00	0.00											

		Table A.1 Mass isotopomers from H <sup>13</sup> CO <sub>2</sub> stationary ILE (Cont).														
		t = 8 min														
Metabolite	Fragment	m/z	Mass (n in m+n)	Intracellular metabolites: biological and technical (MS) replicates										Overall		
				Rep 1				Rep 2								
				Tech 1	Tech 2	Avg	SE	Tech 1	Tech 2	Tech 3	Avg	SE	Avg	SE		
Citrate	[123456]	591	2	0.00	0.00	0.00	0.00	0.00	0.00	0.00	0.01	0.00	0.00	0.00	0.00	0.00
Citrate	[123456]	591	3	0.00	0.00	0.00	0.00	0.00	0.00	0.00	0.00	0.00	0.00	0.00	0.00	0.00
Citrate	[123456]	591	4	0.00	0.00	0.00	0.00	0.00	0.00	0.00	0.00	0.00	0.00	0.00	0.00	0.00
Citrate	[123456]	591	5	0.00	0.00	0.00	0.00	0.00	0.00	0.00	0.00	0.00	0.00	0.00	0.00	0.00
Citrate	[123456]	591	6	0.00	0.00	0.00	0.00	0.00	0.00	0.00	0.00	0.00	0.00	0.00	0.00	0.00
Citrate	[12345]	431	0	0.96	0.96	0.96	0.00	0.96	0.96	0.96	0.96	0.96	0.00	0.96	0.00	0.00
Citrate	[12345]	431	1	0.04	0.03	0.04	0.00	0.04	0.03	0.04	0.03	0.04	0.00	0.03	0.00	0.00
Citrate	[12345]	431	2	0.00	0.00	0.00	0.00	0.00	0.00	0.00	0.00	0.00	0.00	0.00	0.00	0.00
Citrate	[12345]	431	3	0.00	0.00	0.00	0.00	0.00	0.00	0.00	0.00	0.00	0.00	0.00	0.00	0.00
Citrate	[12345]	431	4	0.00	0.00	0.00	0.00	0.00	0.00	0.00	0.00	0.00	0.00	0.00	0.00	0.00
Citrate	[12345]	431	5	0.00	0.00	0.00	0.00	0.00	0.00	0.00	0.00	0.00	0.00	0.00	0.00	0.00
Fumarate	[1234]	287	0	0.92	0.92	0.92	0.00	0.91	0.91	0.91	0.91	0.00	0.92	0.00	0.00	0.00
Fumarate	[1234]	287	1	0.07	0.07	0.07	0.00	0.08	0.08	0.08	0.08	0.00	0.07	0.00	0.00	0.00
Fumarate	[1234]	287	2	0.01	0.01	0.01	0.00	0.01	0.01	0.01	0.01	0.00	0.01	0.00	0.00	0.00
Fumarate	[1234]	287	3	0.00	0.00	0.00	0.00	0.00	0.00	0.00	0.00	0.00	0.00	0.00	0.00	0.00
Fumarate	[1234]	287	4	0.00	0.00	0.00	0.00	0.00	0.00	0.00	0.00	0.00	0.00	0.00	0.00	0.00
3PG	[2x]	231	0	0.98	0.97	0.97	0.00	0.97	0.98	0.97	0.97	0.00	0.97	0.00	0.00	0.00
3PG	[2x]	231	1	0.02	0.02	0.02	0.00	0.02	0.02	0.02	0.02	0.00	0.02	0.00	0.00	0.00
3PG	[2x]	231	2	0.01	0.01	0.01	0.00	0.01	0.01	0.01	0.01	0.00	0.01	0.00	0.00	0.00
3PG	[123]	391	0	0.98	0.98	0.98	0.00	0.97	0.98	0.97	0.98	0.00	0.98	0.00	0.00	0.00
3PG	[123]	391	1	0.02	0.03	0.02	0.00	0.02	0.02	0.02	0.02	0.00	0.02	0.00	0.00	0.00
3PG	[123]	391	2	0.00	0.00	0.00	0.00	0.00	0.00	0.00	0.00	0.00	0.00	0.00	0.00	0.00
3PG	[123]	391	3	0.00	0.00	0.00	0.00	0.00	0.00	0.00	0.00	0.00	0.00	0.00	0.00	0.00
Glu	[2345]	272	0	0.94	0.94	0.94	0.00	0.93	0.92	0.94	0.93	0.00	0.93	0.00	0.00	0.00
Glu	[2345]	272	1	0.05	0.05	0.05	0.00	0.05	0.06	0.05	0.05	0.00	0.05	0.00	0.00	0.00
Glu	[2345]	272	2	0.01	0.01	0.01	0.00	0.01	0.01	0.01	0.01	0.00	0.01	0.00	0.00	0.00
Glu	[2345]	272	3	0.00	0.00	0.00	0.00	0.01	0.01	0.00	0.01	0.00	0.01	0.00	0.00	0.00
Glu	[2345]	272	4	0.00	0.00	0.00	0.00	0.00	0.00	0.00	0.00	0.00	0.00	0.00	0.00	0.00
Glu	[2345]	330	0	0.96	0.96	0.96	0.00	0.96	0.95	0.96	0.96	0.00	0.96	0.00	0.00	0.00
Glu	[2345]	330	1	0.04	0.03	0.04	0.00	0.04	0.04	0.03	0.04	0.00	0.04	0.00	0.00	0.00
Glu	[2345]	330	2	0.00	0.00	0.00	0.00	0.00	0.00	0.00	0.00	0.00	0.00	0.00	0.00	0.00
Glu	[2345]	330	3	0.00	0.00	0.00	0.00	0.00	0.00	0.00	0.00	0.00	0.00	0.00	0.00	0.00
Glu	[2345]	330	4	0.00	0.00	0.00	0.00	0.00	0.00	0.00	0.00	0.00	0.00	0.00	0.00	0.00
Glu	[2345]	404	0	0.97	0.96	0.97	0.01	0.97	0.96	0.97	0.96	0.00	0.96	0.00	0.00	0.01
Glu	[2345]	404	1	0.02	0.04	0.03	0.01	0.02	0.04	0.03	0.03	0.00	0.03	0.00	0.00	0.01
Glu	[2345]	404	2	0.00	0.00	0.00	0.00	0.00	0.00	0.00	0.00	0.00	0.00	0.00	0.00	0.00
Glu	[2345]	404	3	0.00	0.00	0.00	0.00	0.00	0.00	0.00	0.00	0.00	0.00	0.00	0.00	0.00
Glu	[2345]	404	4	0.00	0.01	0.00	0.00	0.00	0.00	0.00	0.00	0.00	0.00	0.00	0.00	0.00
Glu	[12345]	432	0	0.97	0.95	0.96	0.01	0.96	0.94	0.93	0.94	0.01	0.95	0.01	0.01	0.01
Glu	[12345]	432	1	0.03	0.05	0.04	0.01	0.04	0.06	0.07	0.05	0.01	0.05	0.01	0.01	0.01
Glu	[12345]	432	2	0.00	0.00	0.00	0.00	0.00	0.00	0.00	0.00	0.00	0.00	0.00	0.00	0.00
Glu	[12345]	432	3	0.00	0.00	0.00	0.00	0.00	0.00	0.00	0.00	0.00	0.00	0.00	0.00	0.00
Glu	[12345]	432	4	0.00	0.00	0.00	0.00	0.00	0.00	0.00	0.00	0.00	0.00	0.00	0.00	0.00
Glu	[12345]	432	5	0.00	0.00	0.00	0.00	0.00	0.00	0.00	0.00	0.00	0.00	0.00	0.00	0.00
Glycerol	[123]	377	0	0.98	0.98	0.98	0.00	0.99	0.98	0.98	0.98	0.00	0.98	0.00	0.00	0.00
Glycerol	[123]	377	1	0.01	0.02	0.01	0.00	0.01	0.02	0.01	0.01	0.00	0.01	0.00	0.00	0.00
Glycerol	[123]	377	2	0.00	0.00	0.00	0.00	0.00	0.00	0.00	0.00	0.00	0.00	0.00	0.00	0.00
Glycerol	[123]	377	3	0.00	0.00	0.00	0.00	0.00	0.00	0.00	0.00	0.00	0.00	0.00	0.00	0.00
Lac	[23]	233	0	0.98	0.98	0.98	0.00	0.98	0.98	0.98	0.98	0.00	0.98	0.00	0.00	0.00
Lac	[23]	233	1	0.02	0.02	0.02	0.00	0.02	0.02	0.02	0.02	0.00	0.02	0.00	0.00	0.00
Lac	[23]	233	2	0.00	0.00	0.00	0.00	0.00	0.00	0.00	0.00	0.00	0.00	0.00	0.00	0.00
Lac	[123]	261	0	0.93	0.93	0.93	0.00	0.92	0.93	0.93	0.92	0.00	0.93	0.00	0.00	0.00
Lac	[123]	261	1	0.07	0.07	0.07	0.00	0.08	0.07	0.07	0.07	0.00	0.07	0.00	0.00	0.00
Lac	[123]	261	2	0.00	0.00	0.00	0.00	0.00	0.00	0.00	0.00	0.00	0.00	0.00	0.00	0.00
Lac	[123]	261	3	0.00	0.00	0.00	0.00	0.00	0.00	0.00	0.00	0.00	0.00	0.00	0.00	0.00
Leu	[23456]	200	0	0.77	0.77	0.77	0.00	0.88	0.86	0.88	0.88	0.01	0.82	0.05	0.05	0.05
Leu	[23456]	200	1	0.08	0.08	0.08	0.00	0.06	0.06	0.06	0.06	0.00	0.07	0.01	0.01	0.01
Leu	[23456]	200	2	0.04	0.04	0.04	0.00	0.02	0.02	0.02	0.02	0.00	0.03	0.01	0.01	0.01
Leu	[23456]	200	3	0.02	0.02	0.02	0.00	0.01	0.01	0.01	0.01	0.00	0.01	0.00	0.00	0.00
Leu	[23456]	200	4	0.00	0.01	0.00	0.00	0.00	0.02	0.00	0.01	0.01	0.01	0.01	0.01	0.01
Leu	[23456]	200	5	0.08	0.08	0.08	0.00	0.02	0.03	0.03	0.03	0.00	0.05	0.03	0.03	0.03
Leu	[23456]	274	0	0.82	0.77	0.80	0.02	0.88	0.89	0.90	0.89	0.01	0.84	0.05	0.05	0.05
Leu	[23456]	274	1	0.16	0.18	0.17	0.01	0.10	0.09	0.08	0.09	0.00	0.13	0.04	0.04	0.04
Leu	[23456]	274	2	0.00	0.01	0.01	0.01	0.01	0.00	0.00	0.00	0.00	0.01	0.01	0.01	0.01
Leu	[23456]	274	3	0.02	0.00	0.01	0.01	0.00	0.00	0.00	0.00	0.00	0.00	0.01	0.01	0.01
Leu	[23456]	274	4	0.03	0.01	0.02	0.01	0.00	0.00	0.00	0.00	0.00	0.00	0.01	0.01	0.01
Leu	[23456]	274	5	-0.03	0.03	0.00	0.03	0.01	0.01	0.01	0.01	0.00	0.01	0.00	0.01	0.03
Leu	[123]	302	0	0.78	0.75	0.77	0.01	0.94	0.92	0.92	0.94	0.00	0.85	0.09	0.09	0.09
Leu	[123]	302	1	0.12	0.14	0.13	0.01	0.05	0.07	0.06	0.06	0.00	0.10	0.04	0.04	0.04
Leu	[123]	302	2	0.10	0.10	0.10	0.00	0.01	0.00	0.01	0.00	0.00	0.05	0.05	0.05	0.05
Malate	[1234]	419	0	0.92	0.92	0.92	0.00	0.90	0.90	0.90	0.90	0.00	0.91	0.00	0.00	0.00
Malate	[1234]	419	1	0.07	0.07	0.07	0.00	0.09	0.08	0.08	0.08	0.00	0.08	0.00	0.00	0.00
Malate	[1234]	419	2	0.01	0.01	0.01	0.00	0.01	0.01	0.01	0.01	0.00	0.01	0.00	0.00	0.00
Malate	[1234]	419	3	0.00	0.00	0.00	0.00	0.00	0.00	0.00	0.00	0.00	0.00	0.00	0.00	0.00
Malate	[1234]	419	4	0.00	0.00	0.00	0.00	0.00	0.00	0.00	0.00	0.00	0.00	0.00	0.00	0.00
Succinate	[1234]	289	0	0.78	0.79	0.78	0.01	0.73	0.73	0.73	0.73	0.00	0.76	0.03	0.03	0.03
Succinate	[1234]	289	1	0.19	0.18	0.18	0.01	0.23	0.23	0.23	0.23	0.00	0.21	0.00	0.00	0.00
Succinate	[1234]	289	2	0.03	0.03	0.03	0.00	0.04	0.04	0.04	0.04	0.00	0.03	0.00	0.00	0.00
Succinate	[1234]	289	3	0.00	0.00	0.00	0.00	0.00	0.00	0.00	0.00	0.00	0.00	0.00	0.00	0.00
Succinate	[1234]	289	4	0.00	0.00</											

Table A.1 Mass isotopomers from H <sup>13</sup> CO <sub>2</sub> instationary JLE (Cont.)																	
t = 12 min																	
Metabolite	Fragment	m/z	Mass (n in m-n)	Intracellular metabolites: biological and technical (MS) replicates												Overall	
				Rep 1				Rep 2				Avg	SE	Avg	SE		
				Tech 1	Tech 2	Tech 3	Avg	SE	Tech 1	Tech 2	Tech 3					Avg	SE
AconiticAcid	[123456]	459	0	0.94	0.95	0.95	0.94	0.00	0.94	0.95	0.94	0.95	0.00	0.94	0.00		
AconiticAcid	[123456]	459	1	0.06	0.05	0.05	0.05	0.00	0.06	0.05	0.05	0.05	0.00	0.05	0.00		
AconiticAcid	[123456]	459	2	0.00	0.00	0.00	0.00	0.00	0.00	0.00	0.00	0.00	0.00	0.00	0.00		
AconiticAcid	[123456]	459	3	0.00	0.00	0.00	0.00	0.00	0.00	0.00	0.00	0.00	0.00	0.00	0.00		
AconiticAcid	[123456]	459	4	0.00	0.00	0.00	0.00	0.00	0.00	0.00	0.00	0.00	0.00	0.00	0.00		
AconiticAcid	[123456]	459	5	0.00	0.00	0.00	0.00	0.00	0.00	0.00	0.00	0.00	0.00	0.00	0.00		
AconiticAcid	[123456]	459	6	0.00	0.00	0.00	0.00	0.00	0.00	0.00	0.00	0.00	0.00	0.00	0.00		
AconiticAcid	[12346]	327	0	0.84	0.88	0.89	0.87	0.01	0.91	0.90	0.89	0.90	0.01	0.88	0.02		
AconiticAcid	[12346]	327	1	0.06	0.05	0.05	0.05	0.00	0.04	0.04	0.04	0.04	0.00	0.05	0.00		
AconiticAcid	[12346]	327	2	0.07	0.05	0.04	0.05	0.01	0.04	0.04	0.04	0.04	0.00	0.05	0.01		
AconiticAcid	[12346]	327	3	0.01	0.01	0.01	0.01	0.00	0.00	0.01	0.01	0.01	0.00	0.01	0.00		
AconiticAcid	[12346]	327	4	0.02	0.01	0.01	0.01	0.00	0.01	0.01	0.02	0.01	0.00	0.01	0.00		
AconiticAcid	[12346]	327	5	0.01	0.00	0.00	0.00	0.00	0.00	0.00	0.00	0.00	0.00	0.00	0.00		
Asp	[12]	302	0	0.84	0.85	0.84	0.84	0.00	0.88	0.88	0.88	0.88	0.00	0.86	0.02		
Asp	[12]	302	1	0.16	0.15	0.15	0.15	0.01	0.11	0.12	0.11	0.11	0.00	0.13	0.02		
Asp	[12]	302	2	0.00	0.01	0.01	0.00	0.00	0.01	0.01	0.01	0.01	0.00	0.00	0.00		
Asp	[234]	346	0	0.76	0.79	0.77	0.78	0.01	0.84	0.84	0.84	0.84	0.00	0.79	0.02		
Asp	[234]	346	1	0.22	0.19	0.21	0.24	0.01	0.17	0.17	0.17	0.17	0.00	0.19	0.02		
Asp	[234]	346	2	0.00	0.01	0.00	0.00	0.00	0.01	0.01	0.00	0.00	0.00	0.00	0.00		
Asp	[234]	346	3	0.02	0.02	0.01	0.02	0.00	0.01	0.01	0.01	0.01	0.00	0.01	0.00		
Asp	[12]	376	0	nd	0.89	0.88	0.88	0.00	0.88	0.88	0.88	0.88	0.00	0.88	0.00		
Asp	[12]	376	1	nd	0.10	0.13	0.12	0.01	0.11	0.12	0.12	0.12	0.00	0.12	0.01		
Asp	[12]	376	2	nd	0.01	0.00	0.00	0.01	0.01	0.01	0.00	0.01	0.00	0.00	0.01		
Asp	[234]	390	0	0.81	0.81	0.83	0.82	0.01	0.82	0.82	0.82	0.82	0.00	0.82	0.01		
Asp	[234]	390	1	0.18	0.19	0.17	0.18	0.00	0.18	0.18	0.18	0.18	0.00	0.18	0.00		
Asp	[234]	390	2	0.00	0.00	-0.01	-0.01	0.00	0.00	0.00	0.00	0.00	0.00	0.00	0.00		
Asp	[234]	390	3	0.01	0.01	0.01	0.01	0.00	0.00	0.00	0.00	0.00	0.00	0.00	0.00		
Asp	[1234]	418	0	0.74	0.75	0.75	0.75	0.00	0.74	0.74	0.74	0.74	0.00	0.74	0.00		
Asp	[1234]	418	1	0.20	0.20	0.20	0.20	0.00	0.21	0.21	0.21	0.21	0.00	0.20	0.00		
Asp	[1234]	418	2	0.05	0.04	0.06	0.05	0.00	0.05	0.05	0.05	0.05	0.00	0.05	0.00		
Asp	[1234]	418	3	0.01	0.00	0.00	0.00	0.00	0.00	0.00	0.00	0.00	0.00	0.00	0.00		
Asp	[1234]	418	4	0.00	0.00	0.00	0.00	0.00	0.00	0.00	0.00	0.00	0.00	0.00	0.00		
C16D0FattyAcid	[1-16]	313	0	0.83	0.83	0.83	0.83	0.00	0.84	0.84	0.83	0.84	0.00	0.83	0.00		
C16D0FattyAcid	[1-16]	313	1	0.14	0.14	0.14	0.14	0.00	0.14	0.15	0.15	0.15	0.00	0.14	0.00		
C16D0FattyAcid	[1-16]	313	2	0.02	0.02	0.02	0.02	0.00	0.01	0.01	0.01	0.01	0.00	0.01	0.00		
C16D0FattyAcid	[1-16]	313	3	0.00	0.00	0.00	0.00	0.00	0.00	0.00	0.00	0.00	0.00	0.00	0.00		
C16D0FattyAcid	[1-16]	313	4	0.00	0.00	0.00	0.00	0.00	0.00	0.00	0.00	0.00	0.00	0.00	0.00		
C16D0FattyAcid	[1-16]	313	5	0.00	0.00	0.00	0.00	0.00	0.00	0.00	0.00	0.00	0.00	0.00	0.00		
C16D0FattyAcid	[1-16]	313	6	0.00	0.00	0.00	0.00	0.00	0.00	0.00	0.00	0.00	0.00	0.00	0.00		
C16D0FattyAcid	[1-16]	313	7	0.00	0.00	0.00	0.00	0.00	0.00	0.00	0.00	0.00	0.00	0.00	0.00		
C16D0FattyAcid	[1-16]	313	8	0.00	0.00	0.00	0.00	0.00	0.00	0.00	0.00	0.00	0.00	0.00	0.00		
C16D0FattyAcid	[1-16]	313	9	0.00	0.00	0.00	0.00	0.00	0.00	0.00	0.00	0.00	0.00	0.00	0.00		
C16D0FattyAcid	[1-16]	313	10	0.00	0.00	0.00	0.00	0.00	0.00	0.00	0.00	0.00	0.00	0.00	0.00		
C16D0FattyAcid	[1-16]	313	11	0.00	0.00	0.00	0.00	0.00	0.00	0.00	0.00	0.00	0.00	0.00	0.00		
C16D0FattyAcid	[1-16]	313	12	0.00	0.00	0.00	0.00	0.00	0.00	0.00	0.00	0.00	0.00	0.00	0.00		
C16D0FattyAcid	[1-16]	313	13	0.00	0.00	0.00	0.00	0.00	0.00	0.00	0.00	0.00	0.00	0.00	0.00		
C16D0FattyAcid	[1-16]	313	14	0.00	0.00	0.00	0.00	0.00	0.00	0.00	0.00	0.00	0.00	0.00	0.00		
C16D0FattyAcid	[1-16]	313	15	0.00	0.00	0.00	0.00	0.00	0.00	0.00	0.00	0.00	0.00	0.00	0.00		
C16D0FattyAcid	[1-16]	313	16	0.00	0.00	0.00	0.00	0.00	0.00	0.00	0.00	0.00	0.00	0.00	0.00		
C16D1FattyAcid	[1-16]	311	0	0.83	0.83	0.83	0.83	0.00	0.84	0.83	0.83	0.84	0.00	0.83	0.00		
C16D1FattyAcid	[1-16]	311	1	0.14	0.14	0.14	0.14	0.00	0.15	0.15	0.15	0.15	0.00	0.14	0.00		
C16D1FattyAcid	[1-16]	311	2	0.01	0.01	0.01	0.01	0.00	0.01	0.01	0.01	0.01	0.00	0.01	0.00		
C16D1FattyAcid	[1-16]	311	3	0.00	0.00	0.00	0.00	0.00	0.00	0.00	0.00	0.00	0.00	0.00	0.00		
C16D1FattyAcid	[1-16]	311	4	0.01	0.00	0.01	0.01	0.00	0.00	0.00	0.00	0.00	0.00	0.00	0.00		
C16D1FattyAcid	[1-16]	311	5	0.00	0.00	0.00	0.00	0.00	0.00	0.00	0.00	0.00	0.00	0.00	0.00		
C16D1FattyAcid	[1-16]	311	6	0.00	0.00	0.00	0.00	0.00	0.00	0.00	0.00	0.00	0.00	0.00	0.00		
C16D1FattyAcid	[1-16]	311	7	0.00	0.00	0.00	0.00	0.00	0.00	0.00	0.00	0.00	0.00	0.00	0.00		
C16D1FattyAcid	[1-16]	311	8	0.00	0.00	0.00	0.00	0.00	0.00	0.00	0.00	0.00	0.00	0.00	0.00		
C16D1FattyAcid	[1-16]	311	9	0.00	0.00	0.00	0.00	0.00	0.00	0.00	0.00	0.00	0.00	0.00	0.00		
C16D1FattyAcid	[1-16]	311	10	0.00	0.00	0.00	0.00	0.00	0.00	0.00	0.00	0.00	0.00	0.00	0.00		
C16D1FattyAcid	[1-16]	311	11	0.00	0.00	0.00	0.00	0.00	0.00	0.00	0.00	0.00	0.00	0.00	0.00		
C16D1FattyAcid	[1-16]	311	12	0.00	0.00	0.00	0.00	0.00	0.00	0.00	0.00	0.00	0.00	0.00	0.00		
C16D1FattyAcid	[1-16]	311	13	0.00	0.00	0.00	0.00	0.00	0.00	0.00	0.00	0.00	0.00	0.00	0.00		
C16D1FattyAcid	[1-16]	311	14	0.00	0.00	0.00	0.00	0.00	0.00	0.00	0.00	0.00	0.00	0.00	0.00		
C16D1FattyAcid	[1-16]	311	15	0.00	0.00	0.00	0.00	0.00	0.00	0.00	0.00	0.00	0.00	0.00	0.00		
C16D1FattyAcid	[1-16]	311	16	0.00	0.00	0.00	0.00	0.00	0.00	0.00	0.00	0.00	0.00	0.00	0.00		
C18D0FattyAcid	[1-18]	341	0	0.73	0.71	0.68	0.70	0.01	0.84	0.83	0.82	0.83	0.01	0.77	0.06		
C18D0FattyAcid	[1-18]	341	1	0.12	0.12	0.11	0.12	0.00	0.14	0.14	0.13	0.14	0.00	0.13	0.01		
C18D0FattyAcid	[1-18]	341	2	0.05	0.06	0.07	0.06	0.01	0.02	0.02	0.03	0.02	0.00	0.04	0.02		
C18D0FattyAcid	[1-18]	341	3	0.01	0.01	0.01	0.01	0.00	0.00	0.00	0.00	0.00	0.00	0.01	0.00		
C18D0FattyAcid	[1-18]	341	4	0.00	0.01	0.01	0.01	0.00	0.00	0.00	0.00	0.00	0.00	0.00	0.00		
C18D0FattyAcid	[1-18]	341	5	0.01	0.01	0.01	0.01	0.00	0.00	0.00	0.00	0.00	0.00	0.01	0.00		
C18D0FattyAcid	[1-18]	341	6	0.01	0.01	0.01	0.01	0.00	0.00	0.00	0.00	0.00	0.00	0.01	0.01		
C18D0FattyAcid	[1-18]	341	7	0.00	0.00	0.00	0.00	0.00	0.00	0.00	0.00	0.00	0.00	0.00	0.00		
C18D0FattyAcid	[1-18]	341	8	0.00	0.01	0.01	0.01	0.00	0.00	0.00	0.00	0.00	0.00	0.00	0.00		
C18D0FattyAcid	[1-18]	341	9	0.00	0.00	0.00	0.00	0.00	0.00	0.00	0.00	0.00	0.00	0.00	0.00		
C18D0FattyAcid	[1-18]	341	10	0.00	0.00	0.00	0.00	0.00	0.00	0.00	0.00	0.00	0.00	0.00	0.00		
C18D0FattyAcid	[1-18]	341	11	0.01	0.01	0.01	0.01	0.00	0.00	0.00	0.00	0.00	0.00	0.00	0.00		
C18D0FattyAcid	[1-18]	341	12	0.00	0.00	0.00	0.00	0.00	0.00	0.00	0.00	0.00	0.00	0.00	0.00		
C18D0FattyAcid	[1-18]	341	13	0.00	0.00	0.01	0.01	0.00	0.00	0.00	0.00	0.00	0.00	0.00	0.00		
C18D0FattyAcid	[1-18]	341	14	0.01	0.01	0.04	0.02	0.01	0.00	0.00	0.00	0.00	0.00	0.01	0.01		
C18D0FattyAcid	[1-18]	341	15	0.02	0.03	0.01	0.02	0.00	0.00	0.00							

Table A.1 Mass isotopomers from H<sup>13</sup>CO<sub>2</sub> instationary ILE (Cont.)

Metabolite	Fragment	m/z	Mass (n in m+n)	t = 12 min												Overall		
				Intracellular metabolites: biological and technical (MS) replicates														
				Rep 1				Rep 2				Rep 3				Avg	SE	
				Tech 1	Tech 2	Tech 3	Avg	SE	Tech 1	Tech 2	Tech 3	Avg	SE	Tech 1	Tech 2			Tech 3
Citrate	[123456]	591	2	0.00	0.00	0.00	0.00	0.00	0.00	0.00	0.00	0.00	0.00	0.00	0.00	0.00	0.00	0.00
Citrate	[123456]	591	3	0.00	0.00	0.00	0.00	0.00	0.00	0.00	0.00	0.00	0.00	0.00	0.00	0.00	0.00	0.00
Citrate	[123456]	591	4	0.00	0.00	0.00	0.00	0.00	0.00	0.00	0.00	0.00	0.00	0.00	0.00	0.00	0.00	0.00
Citrate	[123456]	591	5	0.00	0.00	0.00	0.00	0.00	0.00	0.00	0.00	0.00	0.00	0.00	0.00	0.00	0.00	0.00
Citrate	[123456]	591	6	0.00	0.00	0.00	0.00	0.00	0.00	0.00	0.00	0.00	0.00	0.00	0.00	0.00	0.00	0.00
Citrate	[12345]	431	0	0.96	0.96	0.96	0.96	0.00	0.96	0.96	0.96	0.96	0.96	0.00	0.96	0.00	0.96	0.00
Citrate	[12345]	431	1	0.04	0.03	0.03	0.03	0.03	0.00	0.04	0.03	0.04	0.04	0.00	0.04	0.00	0.03	0.00
Citrate	[12345]	431	2	0.00	0.01	0.00	0.00	0.00	0.00	0.00	0.00	0.00	0.00	0.00	0.00	0.00	0.00	0.00
Citrate	[12345]	431	3	0.00	0.00	0.00	0.00	0.00	0.00	0.00	0.00	0.00	0.00	0.00	0.00	0.00	0.00	0.00
Citrate	[12345]	431	4	0.00	0.00	0.00	0.00	0.00	0.00	0.00	0.00	0.00	0.00	0.00	0.00	0.00	0.00	0.00
Citrate	[12345]	431	5	0.00	0.00	0.00	0.00	0.00	0.00	0.00	0.00	0.00	0.00	0.00	0.00	0.00	0.00	0.00
Fumarate	[1234]	287	0	0.91	0.90	0.90	0.90	0.00	0.89	0.90	0.90	0.90	0.00	0.90	0.00	0.90	0.00	0.00
Fumarate	[1234]	287	1	0.08	0.08	0.08	0.08	0.00	0.09	0.08	0.08	0.08	0.00	0.09	0.00	0.08	0.00	0.00
Fumarate	[1234]	287	2	0.01	0.02	0.02	0.02	0.00	0.02	0.02	0.02	0.02	0.00	0.02	0.00	0.02	0.00	0.00
Fumarate	[1234]	287	3	0.00	0.00	0.00	0.00	0.00	0.00	0.00	0.00	0.00	0.00	0.00	0.00	0.00	0.00	0.00
Fumarate	[1234]	287	4	0.00	0.00	0.00	0.00	0.00	0.00	0.00	0.00	0.00	0.00	0.00	0.00	0.00	0.00	0.00
3PG	[2x]	231	0	0.97	0.98	0.97	0.97	0.00	0.98	0.97	0.97	0.97	0.00	0.97	0.00	0.97	0.00	0.00
3PG	[2x]	231	1	0.02	0.02	0.02	0.02	0.00	0.02	0.02	0.02	0.02	0.00	0.02	0.00	0.02	0.00	0.00
3PG	[2x]	231	2	0.01	0.01	0.01	0.01	0.00	0.01	0.01	0.01	0.01	0.00	0.01	0.00	0.01	0.00	0.00
3PG	[123]	391	0	0.98	0.98	0.98	0.98	0.00	0.97	0.97	0.97	0.97	0.00	0.97	0.00	0.97	0.00	0.00
3PG	[123]	391	1	0.02	0.02	0.03	0.02	0.00	0.03	0.03	0.03	0.03	0.00	0.03	0.00	0.03	0.00	0.00
3PG	[123]	391	2	0.00	0.00	0.00	0.00	0.00	0.00	0.00	0.00	0.00	0.00	0.00	0.00	0.00	0.00	0.00
3PG	[123]	391	3	0.00	0.00	0.00	0.00	0.00	0.00	0.00	0.00	0.00	0.00	0.00	0.00	0.00	0.00	0.00
Glu	[2345]	272	0	0.94	0.93	0.93	0.93	0.00	0.94	0.94	0.94	0.94	0.00	0.94	0.00	0.94	0.00	0.00
Glu	[2345]	272	1	0.04	0.05	0.05	0.05	0.00	0.05	0.05	0.05	0.05	0.00	0.05	0.00	0.05	0.00	0.00
Glu	[2345]	272	2	0.01	0.01	0.01	0.01	0.00	0.01	0.01	0.01	0.01	0.00	0.01	0.00	0.01	0.00	0.00
Glu	[2345]	272	3	0.01	0.01	0.01	0.01	0.00	0.00	0.00	0.00	0.00	0.00	0.00	0.00	0.01	0.00	0.00
Glu	[2345]	272	4	0.00	0.00	0.00	0.00	0.00	0.00	0.00	0.00	0.00	0.00	0.00	0.00	0.00	0.00	0.00
Glu	[2345]	330	0	0.96	0.95	0.96	0.96	0.00	0.96	0.96	0.96	0.96	0.00	0.96	0.00	0.96	0.00	0.00
Glu	[2345]	330	1	0.04	0.04	0.04	0.04	0.00	0.04	0.03	0.03	0.03	0.00	0.03	0.00	0.03	0.00	0.00
Glu	[2345]	330	2	0.00	0.00	0.00	0.00	0.00	0.00	0.00	0.00	0.00	0.00	0.00	0.00	0.00	0.00	0.00
Glu	[2345]	330	3	0.00	0.00	0.00	0.00	0.00	0.00	0.00	0.00	0.00	0.00	0.00	0.00	0.00	0.00	0.00
Glu	[2345]	330	4	0.00	0.00	0.00	0.00	0.00	0.00	0.00	0.00	0.00	0.00	0.00	0.00	0.00	0.00	0.00
Glu	[2345]	404	0	0.98	0.96	0.97	0.97	0.01	0.97	0.96	0.95	0.96	0.01	0.97	0.01	0.97	0.01	0.01
Glu	[2345]	404	1	0.01	0.03	0.02	0.02	0.01	0.02	0.04	0.03	0.03	0.00	0.03	0.00	0.03	0.01	0.01
Glu	[2345]	404	2	0.00	0.00	0.00	0.00	0.00	0.00	0.00	0.00	0.00	0.00	0.00	0.00	0.00	0.00	0.00
Glu	[2345]	404	3	0.00	0.00	0.00	0.00	0.00	0.00	0.00	0.00	0.00	0.00	0.00	0.00	0.00	0.00	0.00
Glu	[2345]	404	4	0.00	0.00	0.00	0.00	0.00	0.00	0.01	0.02	0.01	0.01	0.01	0.01	0.01	0.01	0.01
Glu	[12345]	432	0	0.94	0.91	0.91	0.92	0.01	0.95	0.92	0.91	0.93	0.01	0.93	0.01	0.92	0.01	0.01
Glu	[12345]	432	1	0.05	0.08	0.08	0.07	0.01	0.05	0.08	0.08	0.07	0.01	0.07	0.01	0.07	0.01	0.01
Glu	[12345]	432	2	0.00	0.01	0.00	0.00	0.00	0.00	0.00	0.00	0.00	0.00	0.00	0.00	0.00	0.00	0.00
Glu	[12345]	432	3	0.00	0.00	0.00	0.00	0.00	0.00	0.00	0.00	0.00	0.00	0.00	0.00	0.00	0.00	0.00
Glu	[12345]	432	4	0.00	0.00	0.00	0.00	0.00	0.00	0.00	0.00	0.00	0.00	0.00	0.00	0.00	0.00	0.00
Glu	[12345]	432	5	0.00	0.00	0.00	0.00	0.00	0.00	0.00	0.00	0.00	0.00	0.00	0.00	0.00	0.00	0.00
Glycerol	[123]	377	0	0.99	0.99	1.00	0.99	0.00	0.99	0.98	0.98	0.99	0.00	0.99	0.00	0.99	0.00	0.00
Glycerol	[123]	377	1	0.02	0.02	0.01	0.02	0.00	0.01	0.02	0.01	0.01	0.00	0.01	0.00	0.01	0.00	0.00
Glycerol	[123]	377	2	0.00	-0.02	-0.01	-0.01	0.00	0.00	0.00	0.00	0.00	0.00	0.00	0.00	0.00	0.00	0.00
Glycerol	[123]	377	3	0.00	0.00	0.00	0.00	0.00	0.00	0.00	0.00	0.00	0.00	0.00	0.00	0.00	0.00	0.00
Lac	[23]	233	0	0.99	0.98	0.98	0.99	0.00	0.98	0.99	0.99	0.98	0.00	0.98	0.00	0.99	0.00	0.00
Lac	[23]	233	1	0.00	0.02	0.02	0.01	0.00	0.02	0.01	0.01	0.02	0.00	0.02	0.00	0.01	0.00	0.00
Lac	[23]	233	2	0.00	0.00	0.00	0.00	0.00	0.00	0.00	0.00	0.00	0.00	0.00	0.00	0.00	0.00	0.00
Lac	[123]	261	0	0.93	0.93	0.93	0.93	0.00	0.93	0.93	0.93	0.93	0.00	0.93	0.00	0.93	0.00	0.00
Lac	[123]	261	1	0.07	0.07	0.07	0.07	0.00	0.07	0.07	0.07	0.07	0.00	0.07	0.00	0.07	0.00	0.00
Lac	[123]	261	2	0.00	0.00	0.00	0.00	0.00	0.00	0.00	0.00	0.00	0.00	0.00	0.00	0.00	0.00	0.00
Lac	[123]	261	3	0.00	0.00	0.00	0.00	0.00	0.00	0.00	0.00	0.00	0.00	0.00	0.00	0.00	0.00	0.00
Leu	[23456]	200	0	0.88	0.88	0.84	0.87	0.01	0.85	0.84	0.84	0.85	0.00	0.86	0.00	0.86	0.01	0.01
Leu	[23456]	200	1	0.07	0.06	0.06	0.06	0.00	0.06	0.07	0.06	0.06	0.00	0.06	0.00	0.06	0.00	0.00
Leu	[23456]	200	2	0.02	0.02	0.02	0.02	0.00	0.02	0.03	0.03	0.03	0.00	0.03	0.00	0.02	0.01	0.01
Leu	[23456]	200	3	0.01	0.01	0.01	0.01	0.00	0.01	0.01	0.01	0.01	0.00	0.01	0.00	0.01	0.00	0.00
Leu	[23456]	200	4	0.00	0.00	0.01	0.01	0.00	0.00	0.00	0.00	0.00	0.00	0.00	0.00	0.00	0.00	0.00
Leu	[23456]	200	5	0.02	0.03	0.06	0.04	0.01	0.05	0.05	0.05	0.05	0.00	0.04	0.00	0.04	0.01	0.01
Leu	[23456]	274	0	0.88	0.88	0.87	0.88	0.00	0.89	0.88	0.87	0.88	0.00	0.88	0.00	0.88	0.00	0.00
Leu	[23456]	274	1	0.10	0.10	0.11	0.10	0.00	0.10	0.10	0.11	0.10	0.00	0.10	0.00	0.10	0.00	0.00
Leu	[23456]	274	2	0.00	0.01	0.01	0.01	0.00	0.01	0.00	0.01	0.01	0.00	0.01	0.00	0.01	0.00	0.00
Leu	[23456]	274	3	0.00	0.01	0.00	0.00	0.00	0.00	0.00	0.01	0.00	0.00	0.00	0.00	0.00	0.00	0.00
Leu	[23456]	274	4	0.00	0.00	0.00	0.00	0.00	0.00	0.00	0.00	0.00	0.00	0.00	0.00	0.00	0.00	0.00
Leu	[23456]	274	5	0.01	0.01	0.01	0.01	0.00	0.00	0.00	0.00	0.00	0.00	0.00	0.00	0.01	0.00	0.00
Leu	[123]	302	0	0.92	0.92	0.91	0.92	0.00	0.88	0.86	0.85	0.86	0.01	0.89	0.01	0.89	0.02	0.02
Leu	[123]	302	1	0.07	0.09	0.09	0.08	0.01	0.07	0.08	0.10	0.08	0.01	0.08	0.01	0.08	0.01	0.01
Leu	[123]	302	2	0.01	0.01	0.01	0.01	0.00	0.01	0.01	0.01	0.01	0.00	0.01	0.00	0.01	0.00	0.00
Malate	[1234]	419	0	0.87	0.87	0.87	0.87	0.00	0.8									



Table A.1 Mass isotopomers from H<sup>13</sup>CO<sub>2</sub>; instationary ILE (Cont).

Metabolite	Fragment	m/z	Mass (n in m+n)	t = 20 min															
				Intracellular metabolites: biological and technical (MS) replicates															
				Rep 1				Rep 2				Rep 3				Overall			
				Tech 1	Tech 2	Tech 3	Avg	SE	Tech 1	Tech 2	Tech 3	Avg	SE	Tech 1	Tech 2	Tech 3	Avg	SE	Avg
Citrate	[123456]	591	2	0.00	0.00	0.01	0.00	0.00	0.00	0.00	0.00	0.00	0.01	0.00	0.00	0.00	0.00	0.00	
Citrate	[123456]	591	3	0.00	0.00	0.00	0.00	0.00	0.00	0.00	0.00	0.00	0.00	0.00	0.00	0.00	0.00	0.00	
Citrate	[123456]	591	4	0.00	0.00	0.00	0.00	0.00	0.00	0.00	0.00	0.00	0.00	0.00	0.00	0.00	0.00	0.00	
Citrate	[123456]	591	5	0.00	0.00	0.00	0.00	0.00	0.00	0.00	0.00	0.00	0.00	0.00	0.00	0.00	0.00	0.00	
Citrate	[123456]	591	6	0.00	0.00	0.00	0.00	0.00	0.00	0.00	0.00	0.00	0.00	0.00	0.00	0.00	0.00	0.00	
Citrate	[12345]	431	0	0.96	0.96	0.97	0.96	0.00	0.96	0.96	0.97	0.96	0.00	0.96	0.96	0.97	0.96	0.00	
Citrate	[12345]	431	1	0.03	0.03	0.03	0.03	0.00	0.04	0.04	0.03	0.03	0.00	0.04	0.04	0.04	0.04	0.00	
Citrate	[12345]	431	2	0.00	0.00	0.00	0.00	0.00	0.00	0.00	0.00	0.00	0.00	0.00	0.00	-0.01	0.00	0.00	
Citrate	[12345]	431	3	0.00	0.00	0.00	0.00	0.00	0.00	0.00	0.00	0.00	0.00	0.00	0.00	0.00	0.00	0.00	
Citrate	[12345]	431	4	0.00	0.00	0.00	0.00	0.00	0.00	0.00	0.00	0.00	0.00	0.00	0.00	0.00	0.00	0.00	
Citrate	[12345]	431	5	0.00	0.00	0.00	0.00	0.00	0.00	0.00	0.00	0.00	0.00	0.00	0.00	0.00	0.00	0.00	
Fumarate	[1234]	287	0	nd	nd	nd	nd	nd	0.81	0.80	0.80	0.80	0.00	0.84	0.84	0.83	0.83	0.00	
Fumarate	[1234]	287	1	nd	nd	nd	nd	nd	0.15	0.15	0.15	0.15	0.00	0.13	0.13	0.14	0.13	0.00	
Fumarate	[1234]	287	2	nd	nd	nd	nd	nd	0.04	0.04	0.04	0.04	0.00	0.03	0.03	0.03	0.03	0.00	
Fumarate	[1234]	287	3	nd	nd	nd	nd	nd	0.00	0.00	0.00	0.00	0.00	0.00	0.00	0.00	0.00	0.00	
Fumarate	[1234]	287	4	nd	nd	nd	nd	nd	0.00	0.00	0.00	0.00	0.00	0.00	0.00	0.00	0.00	0.00	
3PG	[2x]	231	0	0.98	0.98	0.97	0.97	0.00	0.98	0.98	0.98	0.98	0.00	0.98	0.97	0.98	0.98	0.00	
3PG	[2x]	231	1	0.01	0.02	0.02	0.02	0.00	0.02	0.02	0.02	0.02	0.00	0.01	0.02	0.01	0.01	0.00	
3PG	[2x]	231	2	0.01	0.01	0.01	0.01	0.00	0.01	0.01	0.01	0.01	0.00	0.01	0.01	0.01	0.01	0.00	
3PG	[123]	391	0	0.97	0.98	0.98	0.98	0.00	0.98	0.98	0.98	0.98	0.00	0.98	0.98	0.97	0.98	0.00	
3PG	[123]	391	1	0.02	0.02	0.03	0.02	0.00	0.02	0.02	0.02	0.02	0.00	0.02	0.02	0.02	0.02	0.00	
3PG	[123]	391	2	0.00	0.00	0.00	0.00	0.00	0.00	0.00	0.00	0.00	0.00	0.00	0.00	0.00	0.00	0.00	
3PG	[123]	391	3	0.00	0.00	0.00	0.00	0.00	0.00	0.00	0.00	0.00	0.00	0.00	0.00	0.00	0.00	0.00	
Glu	[2345]	272	0	0.94	0.93	0.93	0.93	0.00	0.94	0.94	0.94	0.94	0.00	0.93	0.92	0.93	0.93	0.00	
Glu	[2345]	272	1	0.05	0.05	0.05	0.05	0.00	0.05	0.05	0.05	0.05	0.00	0.05	0.06	0.06	0.05	0.00	
Glu	[2345]	272	2	0.01	0.01	0.01	0.01	0.00	0.01	0.01	0.01	0.01	0.00	0.01	0.01	0.01	0.01	0.00	
Glu	[2345]	272	3	0.01	0.01	0.01	0.01	0.00	0.00	0.00	0.00	0.00	0.00	0.01	0.01	0.01	0.01	0.00	
Glu	[2345]	272	4	0.00	0.00	0.00	0.00	0.00	0.00	0.00	0.00	0.00	0.00	0.00	0.00	0.00	0.00	0.00	
Glu	[2345]	330	0	0.96	0.96	0.96	0.96	0.00	0.96	0.96	0.96	0.96	0.00	0.95	0.95	0.95	0.95	0.00	
Glu	[2345]	330	1	0.03	0.04	0.04	0.04	0.00	0.03	0.03	0.03	0.03	0.00	0.04	0.04	0.04	0.04	0.00	
Glu	[2345]	330	2	0.01	0.00	0.00	0.00	0.00	0.00	0.00	0.00	0.00	0.00	0.00	0.00	0.00	0.00	0.00	
Glu	[2345]	330	3	0.00	0.00	0.00	0.00	0.00	0.00	0.00	0.00	0.00	0.00	0.00	0.00	0.00	0.00	0.00	
Glu	[2345]	330	4	0.00	0.00	0.00	0.00	0.00	0.00	0.00	0.00	0.00	0.00	0.00	0.00	0.00	0.00	0.00	
Glu	[2345]	404	0	0.96	0.97	0.96	0.96	0.00	0.96	0.96	0.96	0.96	0.00	0.96	0.96	0.96	0.96	0.00	
Glu	[2345]	404	1	0.03	0.03	0.02	0.03	0.00	0.03	0.03	0.03	0.03	0.00	0.03	0.03	0.03	0.03	0.00	
Glu	[2345]	404	2	0.00	0.00	0.00	0.00	0.00	0.00	0.00	0.00	0.00	0.00	0.00	0.00	0.00	0.00	0.00	
Glu	[2345]	404	3	0.00	0.00	0.00	0.00	0.00	0.00	0.00	0.00	0.00	0.00	0.00	0.00	0.00	0.00	0.00	
Glu	[2345]	404	4	0.00	0.00	0.02	0.01	0.01	0.01	0.01	0.01	0.01	0.00	0.00	0.00	0.00	0.00	0.01	
Glu	[12345]	432	0	0.95	0.94	0.95	0.94	0.00	0.95	0.93	0.92	0.93	0.01	0.93	0.92	0.93	0.93	0.00	
Glu	[12345]	432	1	0.05	0.06	0.05	0.05	0.00	0.04	0.07	0.07	0.06	0.01	0.06	0.07	0.06	0.06	0.00	
Glu	[12345]	432	2	0.00	0.00	0.00	0.00	0.00	0.00	0.00	0.00	0.00	0.00	0.01	0.00	0.01	0.01	0.00	
Glu	[12345]	432	3	0.00	0.00	0.00	0.00	0.00	0.00	0.00	0.00	0.00	0.00	0.00	0.00	0.00	0.00	0.00	
Glu	[12345]	432	4	0.00	0.00	0.00	0.00	0.00	0.00	0.00	0.00	0.00	0.00	0.00	0.00	0.00	0.00	0.00	
Glu	[12345]	432	5	0.00	0.00	0.00	0.00	0.00	0.00	0.00	0.00	0.00	0.00	0.00	0.00	0.00	0.00	0.00	
Glycerol	[123]	377	0	0.99	0.98	0.98	0.98	0.00	0.99	0.98	0.98	0.98	0.00	0.98	0.99	0.98	0.98	0.00	
Glycerol	[123]	377	1	0.01	0.02	0.02	0.01	0.00	0.01	0.02	0.02	0.01	0.00	0.02	0.02	0.02	0.02	0.00	
Glycerol	[123]	377	2	0.00	0.00	0.00	0.00	0.00	0.00	0.00	0.00	0.00	0.00	0.01	-0.01	0.00	0.00	0.00	
Glycerol	[123]	377	3	0.00	0.00	0.00	0.00	0.00	0.00	0.00	0.00	0.00	0.00	0.00	0.00	0.00	0.00	0.00	
Lac	[23]	233	0	0.99	0.98	0.98	0.98	0.00	0.98	0.98	0.98	0.98	0.00	0.99	0.98	0.98	0.98	0.00	
Lac	[23]	233	1	0.01	0.02	0.02	0.02	0.00	0.02	0.02	0.02	0.02	0.00	0.01	0.02	0.01	0.01	0.00	
Lac	[23]	233	2	0.00	0.00	0.00	0.00	0.00	0.00	0.00	0.00	0.00	0.00	0.00	0.00	0.00	0.00	0.00	
Lac	[123]	261	0	0.94	0.94	0.94	0.94	0.00	0.94	0.94	0.94	0.94	0.00	0.93	0.93	0.93	0.93	0.00	
Lac	[123]	261	1	0.06	0.06	0.06	0.06	0.00	0.06	0.06	0.06	0.06	0.00	0.07	0.07	0.07	0.07	0.00	
Lac	[123]	261	2	0.00	0.00	0.00	0.00	0.00	0.00	0.00	0.00	0.00	0.00	0.00	0.00	0.00	0.00	0.00	
Lac	[123]	261	3	0.00	0.00	0.00	0.00	0.00	0.00	0.00	0.00	0.00	0.00	0.00	0.00	0.00	0.00	0.00	
Leu	[23456]	200	0	0.88	0.87	0.90	0.88	0.01	0.87	0.88	0.88	0.88	0.00	0.90	0.89	0.89	0.89	0.00	
Leu	[23456]	200	1	0.06	0.06	0.07	0.06	0.00	0.06	0.06	0.06	0.06	0.00	0.06	0.06	0.06	0.06	0.00	
Leu	[23456]	200	2	0.01	0.02	0.01	0.01	0.00	0.02	0.02	0.02	0.02	0.00	0.03	0.03	0.03	0.03	0.00	
Leu	[23456]	200	3	0.01	0.01	0.01	0.01	0.00	0.01	0.01	0.01	0.01	0.00	0.01	0.01	0.01	0.01	0.00	
Leu	[23456]	200	4	0.01	0.01	0.00	0.01	0.00	0.00	0.00	0.00	0.00	0.00	0.00	0.01	0.00	0.00	0.00	
Leu	[23456]	200	5	0.03	0.04	0.02	0.03	0.01	0.04	0.03	0.03	0.03	0.00	0.01	0.00	0.01	0.00	0.02	
Leu	[23456]	274	0	0.91	0.89	0.91	0.90	0.01	0.90	0.90	0.90	0.90	0.00	0.90	0.89	0.90	0.90	0.00	
Leu	[23456]	274	1	0.07	0.09	0.08	0.08	0.01	0.08	0.09	0.08	0.08	0.00	0.09	0.08	0.10	0.09	0.01	
Leu	[23456]	274	2	0.00	0.01	0.00	0.00	0.00	0.00	0.01	0.00	0.00	0.00	0.00	0.00	0.00	0.00	0.00	
Leu	[23456]	274	3	0.01	0.00	0.00	0.00	0.00	0.00	0.00	0.00	0.00	0.00	0.00	0.00	0.00	0.00	0.00	
Leu	[23456]	274	4	0.00	0.00	0.00	0.00	0.00	0.00	0.00	0.00	0.00	0.00	0.00	0.00	0.00	0.00	0.00	
Leu	[23456]	274	5	0.01	0.01	0.01	0.01	0.00	0.01	0.00	0.01	0.01	0.00	0.01	0.01	0.01	0.01	0.00	
Leu	[123]	302	0	0.92	0.95	0.94	0.94	0.01	0.90	0.89	0.89	0.89	0.00	0.94	0.94	0.94	0.94	0.00	
Leu	[123]	302	1	0.07	0.06	0.06	0.07	0.01	0.06	0.06	0.06	0.06	0.00	0.06	0.06	0.06	0.06	0.00	
Leu	[123]	302	2	0.00	0.01	0.01	0.01	0.01	0.01	0.01	0.01	0.01	0.00	0.01	0.01	0.01	0.01	0.00	
Malate	[1234]	419	0	0.87	0.87	0.87	0.87	0.00	0.87	0.77	0.77	0.77	0.00	0.76	0.77	0.77	0.77	0.00	







**Table A.1 Mass isotopomers from H<sup>13</sup>CO<sub>3</sub><sup>-</sup> instationary ILE (Cont).**

AA	Fragment	m/z	Mass (n in m+n)	t = 6 d				
				Proteinogenic amino acids: biological replicates				
				Biological Replicates			Overall	
				Rep 1	Rep 2	Rep 3	Avg	SE
Ala	[23]	158	0	0.24	0.23	0.23	0.23	0.01
Ala	[23]	158	1	0.42	0.42	0.43	0.42	0.00
Ala	[23]	158	2	0.34	0.35	0.35	0.34	0.00
Ala	[23]	232	0	0.24	0.23	0.23	0.23	0.00
Ala	[23]	232	1	0.42	0.43	0.44	0.43	0.00
Ala	[23]	232	2	0.34	0.34	0.34	0.34	0.00
Ala	[123]	260	0	0.15	0.14	0.15	0.15	0.00
Ala	[123]	260	1	0.27	0.27	0.26	0.27	0.00
Ala	[123]	260	2	0.37	0.38	0.38	0.38	0.00
Ala	[123]	260	3	0.21	0.21	0.21	0.21	0.00
Asp	[12]	302	0	0.24	0.23	0.23	0.23	0.00
Asp	[12]	302	1	0.42	0.42	0.42	0.42	0.00
Asp	[12]	302	2	0.34	0.36	0.35	0.35	0.00
Asp	[234]	316	0	0.12	0.13	0.12	0.13	0.00
Asp	[234]	316	1	0.28	0.28	0.28	0.28	0.00
Asp	[234]	316	2	0.37	0.37	0.38	0.38	0.00
Asp	[234]	316	3	0.23	0.22	0.22	0.22	0.00
Asp	[12]	376	0	0.24	0.25	0.23	0.24	0.00
Asp	[12]	376	1	0.41	0.41	0.41	0.41	0.00
Asp	[12]	376	2	0.35	0.34	0.36	0.35	0.00
Asp	[234]	390	0	0.13	0.13	0.13	0.13	0.00
Asp	[234]	390	1	0.27	0.28	0.28	0.28	0.00
Asp	[234]	390	2	0.38	0.37	0.38	0.38	0.00
Asp	[234]	390	3	0.21	0.23	0.21	0.22	0.01
Asp	[1234]	418	0	0.09	0.09	0.09	0.09	0.00
Asp	[1234]	418	1	0.17	0.17	0.17	0.17	0.00
Asp	[1234]	418	2	0.30	0.30	0.30	0.30	0.00
Asp	[1234]	418	3	0.30	0.31	0.31	0.31	0.00
Asp	[1234]	418	4	0.14	0.13	0.13	0.13	0.00
Glu	[2345]	272	0	0.10	0.11	0.10	0.10	0.00
Glu	[2345]	272	1	0.15	0.15	0.15	0.15	0.00
Glu	[2345]	272	2	0.30	0.29	0.29	0.29	0.00
Glu	[2345]	272	3	0.30	0.32	0.32	0.31	0.01
Glu	[2345]	272	4	0.14	0.14	0.14	0.14	0.00
Glu	[2345]	330	0	0.11	0.11	0.11	0.11	0.00
Glu	[2345]	330	1	0.16	0.15	0.15	0.15	0.00
Glu	[2345]	330	2	0.29	0.29	0.29	0.29	0.00
Glu	[2345]	330	3	0.31	0.31	0.31	0.31	0.00
Glu	[2345]	330	4	0.13	0.14	0.14	0.13	0.00
Glu	[2345]	404	0	0.09	0.07	0.10	0.09	0.01
Glu	[2345]	404	1	0.14	0.18	0.15	0.16	0.01
Glu	[2345]	404	2	0.29	0.32	0.29	0.30	0.01
Glu	[2345]	404	3	0.35	0.31	0.32	0.32	0.01
Glu	[2345]	404	4	0.14	0.12	0.14	0.13	0.01
Glu	[12345]	432	0	0.07	0.07	0.06	0.07	0.00
Glu	[12345]	432	1	0.10	0.10	0.10	0.10	0.00
Glu	[12345]	432	2	0.21	0.21	0.21	0.21	0.00
Glu	[12345]	432	3	0.29	0.29	0.29	0.29	0.00
Glu	[12345]	432	4	0.23	0.23	0.23	0.23	0.00
Glu	[12345]	432	5	0.09	0.09	0.10	0.09	0.00
Gly	[2]	218	0	0.45	0.44	0.44	0.44	0.00
Gly	[2]	218	1	0.55	0.56	0.56	0.56	0.00
Gly	[12]	246	0	0.23	0.22	0.22	0.22	0.00
Gly	[12]	246	1	0.42	0.42	0.42	0.42	0.00
Gly	[12]	246	2	0.35	0.36	0.36	0.36	0.00
Ile	[23456]	200	0	0.08	0.08	0.07	0.08	0.00
Ile	[23456]	200	1	0.08	0.09	0.09	0.09	0.00
Ile	[23456]	200	2	0.17	0.18	0.18	0.18	0.00
Ile	[23456]	200	3	0.26	0.27	0.28	0.27	0.01
Ile	[23456]	200	4	0.23	0.24	0.25	0.24	0.00
Ile	[23456]	200	5	0.18	0.14	0.12	0.15	0.02
Ile	[23456]	274	0	0.08	0.07	0.07	0.07	0.00
Ile	[23456]	274	1	0.09	0.07	0.09	0.08	0.00
Ile	[23456]	274	2	0.18	0.17	0.17	0.18	0.00
Ile	[23456]	274	3	0.28	0.29	0.28	0.28	0.00

Table A.1 Mass isotopomers from H<sup>13</sup>CO<sub>3</sub><sup>-</sup> instationary ILE (Cont).

AA	Fragment	m/z	Mass (n in m+n)	t = 6 d				
				Proteinogenic amino acids: biological replicates				
				Biological Replicates			Overall	
				Rep 1	Rep 2	Rep 3	Avg	SE
Ile	[23456]	274	4	0.24	0.26	0.25	0.25	0.01
Ile	[23456]	274	5	0.13	0.13	0.14	0.13	0.00
Ile	[12]	302	0	0.23	0.20	0.22	0.22	0.01
Ile	[12]	302	1	0.32	0.33	0.33	0.33	0.01
Ile	[12]	302	2	0.45	0.46	0.44	0.45	0.01
Leu	[23456]	200	0	0.09	0.09	0.09	0.09	0.00
Leu	[23456]	200	1	0.08	0.08	0.08	0.08	0.00
Leu	[23456]	200	2	0.19	0.19	0.18	0.19	0.00
Leu	[23456]	200	3	0.28	0.28	0.28	0.28	0.00
Leu	[23456]	200	4	0.24	0.24	0.25	0.24	0.00
Leu	[23456]	200	5	0.13	0.12	0.12	0.12	0.00
Leu	[23456]	274	0	0.09	0.09	0.09	0.09	0.00
Leu	[23456]	274	1	0.08	0.07	0.08	0.08	0.00
Leu	[23456]	274	2	0.19	0.18	0.19	0.19	0.00
Leu	[23456]	274	3	0.28	0.29	0.28	0.28	0.00
Leu	[23456]	274	4	0.24	0.25	0.24	0.24	0.00
Leu	[23456]	274	5	0.11	0.12	0.11	0.11	0.00
Leu	[12]	302	0	0.24	0.22	0.24	0.23	0.01
Leu	[12]	302	1	0.22	0.21	0.20	0.21	0.00
Leu	[12]	302	2	0.54	0.57	0.56	0.56	0.01
Met	[2345]	218	0	0.07	0.07	0.08	0.07	0.00
Met	[2345]	218	1	0.15	0.16	0.16	0.16	0.00
Met	[2345]	218	2	0.23	0.30	0.30	0.28	0.02
Met	[2345]	218	3	0.36	0.32	0.30	0.33	0.02
Met	[2345]	218	4	0.18	0.15	0.16	0.16	0.01
Met	[2345]	292	0	0.07	0.08	0.07	0.08	0.00
Met	[2345]	292	1	0.16	0.17	0.16	0.16	0.00
Met	[2345]	292	2	0.30	0.30	0.30	0.30	0.00
Met	[2345]	292	3	0.32	0.31	0.32	0.32	0.00
Met	[2345]	292	4	0.14	0.15	0.15	0.15	0.00
Met	[12345]	320	0	0.06	0.04	0.04	0.05	0.01
Met	[12345]	320	1	0.06	0.09	0.12	0.09	0.02
Met	[12345]	320	2	0.18	0.22	0.24	0.22	0.02
Met	[12345]	320	3	0.31	0.32	0.31	0.31	0.00
Met	[12345]	320	4	0.26	0.24	0.22	0.24	0.01
Met	[12345]	320	5	0.12	0.09	0.07	0.09	0.01
Phe	[23455667]	234	0	0.07	0.07	0.07	0.07	0.00
Phe	[23455667]	234	1	0.03	0.02	0.03	0.02	0.00
Phe	[23455667]	234	2	0.04	0.04	0.04	0.04	0.00
Phe	[23455667]	234	3	0.10	0.09	0.10	0.10	0.00
Phe	[23455667]	234	4	0.18	0.17	0.17	0.17	0.00
Phe	[23455667]	234	5	0.22	0.22	0.21	0.22	0.00
Phe	[23455667]	234	6	0.20	0.21	0.21	0.21	0.00
Phe	[23455667]	234	7	0.13	0.12	0.12	0.12	0.00
Phe	[23455667]	234	8	0.04	0.05	0.04	0.04	0.00
Phe	[12]	302	0	0.22	0.21	0.21	0.22	0.00
Phe	[12]	302	1	0.41	0.42	0.42	0.42	0.00
Phe	[12]	302	2	0.36	0.37	0.36	0.36	0.00
Phe	[23455667]	308	0	0.11	0.11	0.11	0.11	0.00
Phe	[23455667]	308	1	0.03	0.04	0.05	0.04	0.01
Phe	[23455667]	308	2	-0.02	-0.04	-0.01	-0.02	0.01
Phe	[23455667]	308	3	0.01	-0.02	-0.02	-0.01	0.01
Phe	[23455667]	308	4	0.13	0.11	0.10	0.11	0.01
Phe	[23455667]	308	5	0.24	0.26	0.25	0.25	0.01
Phe	[23455667]	308	6	0.26	0.29	0.29	0.28	0.01
Phe	[23455667]	308	7	0.18	0.19	0.19	0.19	0.00
Phe	[23455667]	308	8	0.06	0.05	0.05	0.05	0.00
Phe	[123455667]	336	0	0.07	0.06	0.06	0.06	0.00
Phe	[123455667]	336	1	0.03	0.02	0.02	0.02	0.00
Phe	[123455667]	336	2	0.04	0.02	0.03	0.03	0.00
Phe	[123455667]	336	3	0.08	0.07	0.07	0.07	0.00
Phe	[123455667]	336	4	0.14	0.12	0.14	0.13	0.00
Phe	[123455667]	336	5	0.20	0.19	0.19	0.20	0.00
Phe	[123455667]	336	6	0.20	0.22	0.20	0.21	0.00
Phe	[123455667]	336	7	0.15	0.17	0.17	0.16	0.01

**Table A.1 Mass isotopomers from H<sup>13</sup>CO<sub>3</sub><sup>-</sup> instationary ILE (Cont).**

AA	Fragment	m/z	Mass (n in m+n)	t = 6 d				
				Proteinogenic amino acids: biological replicates				
				Biological Replicates			Overall	
				Rep 1	Rep 2	Rep 3	Avg	SE
Phe	[123455667]	336	8	0.08	0.10	0.08	0.09	0.01
Phe	[123455667]	336	9	0.02	0.02	0.03	0.02	0.00
Pro	[2345]	184	0	0.10	0.10	0.11	0.10	0.00
Pro	[2345]	184	1	0.13	0.13	0.14	0.13	0.00
Pro	[2345]	184	2	0.27	0.27	0.28	0.27	0.00
Pro	[2345]	184	3	0.31	0.31	0.31	0.31	0.00
Pro	[2345]	184	4	0.18	0.17	0.17	0.17	0.00
Pro	[2345]	258	0	0.11	0.10	0.11	0.10	0.00
Pro	[2345]	258	1	0.14	0.14	0.14	0.14	0.00
Pro	[2345]	258	2	0.27	0.28	0.28	0.28	0.00
Pro	[2345]	258	3	0.32	0.31	0.31	0.31	0.00
Pro	[2345]	258	4	0.17	0.17	0.16	0.17	0.00
Pro	[12345]	286	0	0.19	0.26	0.21	0.22	0.02
Pro	[12345]	286	1	0.05	0.10	0.08	0.08	0.02
Pro	[12345]	286	2	-0.01	-0.04	0.00	-0.02	0.01
Pro	[12345]	286	3	0.22	0.14	0.18	0.18	0.02
Pro	[12345]	286	4	0.34	0.31	0.33	0.33	0.01
Pro	[12345]	286	5	0.21	0.22	0.21	0.21	0.00
Ser	[23]	288	0	0.23	0.23	0.24	0.23	0.00
Ser	[23]	288	1	0.44	0.43	0.43	0.43	0.00
Ser	[23]	288	2	0.33	0.34	0.33	0.33	0.00
Ser	[12]	302	0	0.25	0.24	0.23	0.24	0.00
Ser	[12]	302	1	0.44	0.43	0.43	0.43	0.00
Ser	[12]	302	2	0.32	0.33	0.34	0.33	0.01
Ser	[23]	362	0	0.23	0.23	0.23	0.23	0.00
Ser	[23]	362	1	0.43	0.44	0.44	0.44	0.00
Ser	[23]	362	2	0.33	0.33	0.33	0.33	0.00
Ser	[123]	390	0	0.14	0.14	0.15	0.14	0.00
Ser	[123]	390	1	0.27	0.27	0.27	0.27	0.00
Ser	[123]	390	2	0.37	0.38	0.37	0.37	0.00
Ser	[123]	390	3	0.22	0.21	0.21	0.21	0.00
Thr	[234]	376	0	0.13	0.12	0.13	0.13	0.00
Thr	[234]	376	1	0.27	0.28	0.27	0.27	0.00
Thr	[234]	376	2	0.38	0.38	0.39	0.38	0.00
Thr	[234]	376	3	0.22	0.22	0.21	0.22	0.00
Thr	[1234]	404	0	0.09	0.09	0.09	0.09	0.00
Thr	[1234]	404	1	0.16	0.16	0.16	0.16	0.00
Thr	[1234]	404	2	0.30	0.28	0.30	0.29	0.01
Thr	[1234]	404	3	0.30	0.32	0.29	0.30	0.01
Thr	[1234]	404	4	0.15	0.15	0.16	0.15	0.00
Tyr	[12]	302	0	0.22	0.21	0.22	0.22	0.00
Tyr	[12]	302	1	0.42	0.42	0.43	0.42	0.00
Tyr	[12]	302	2	0.36	0.37	0.35	0.36	0.00
Tyr	[23455667]	364	0	0.06	0.06	0.06	0.06	0.00
Tyr	[23455667]	364	1	0.03	0.03	0.04	0.03	0.00
Tyr	[23455667]	364	2	0.05	0.06	0.05	0.05	0.00
Tyr	[23455667]	364	3	0.09	0.12	0.09	0.10	0.01
Tyr	[23455667]	364	4	0.20	0.18	0.19	0.19	0.00
Tyr	[23455667]	364	5	0.26	0.27	0.27	0.27	0.00
Tyr	[23455667]	364	6	0.14	0.19	0.17	0.17	0.02
Tyr	[23455667]	364	7	0.14	0.10	0.07	0.11	0.02
Tyr	[23455667]	364	8	0.03	-0.01	0.05	0.02	0.02
Tyr	[23455667]	438	0	0.06	0.06	0.05	0.06	0.00
Tyr	[23455667]	438	1	0.03	0.01	0.03	0.02	0.01
Tyr	[23455667]	438	2	0.05	0.05	0.06	0.05	0.00
Tyr	[23455667]	438	3	0.11	0.09	0.13	0.11	0.01
Tyr	[23455667]	438	4	0.19	0.20	0.20	0.20	0.00
Tyr	[23455667]	438	5	0.24	0.22	0.24	0.24	0.01
Tyr	[23455667]	438	6	0.20	0.20	0.17	0.19	0.01
Tyr	[23455667]	438	7	0.10	0.12	0.11	0.11	0.01
Tyr	[23455667]	438	8	0.03	0.05	0.02	0.03	0.01
Tyr	[123455667]	466	0	0.05	0.05	0.07	0.05	0.01
Tyr	[123455667]	466	1	0.02	0.01	0.02	0.02	0.00
Tyr	[123455667]	466	2	0.03	0.02	0.01	0.02	0.01
Tyr	[123455667]	466	3	0.07	0.06	0.10	0.07	0.01

**Table A.1 Mass isotopomers from H<sup>13</sup>CO<sub>3</sub><sup>-</sup> instationary ILE (Cont).**

t = 6 d								
Proteinogenic amino acids: biological replicates								
AA	Fragment	m/z	Mass (n in m+n)	Biological Replicates			Overall	
				Rep 1	Rep 2	Rep 3	Avg	SE
Tyr	[123455667]	466	4	0.16	0.16	0.16	0.16	0.00
Tyr	[123455667]	466	5	0.16	0.18	0.18	0.17	0.01
Tyr	[123455667]	466	6	0.13	0.22	0.22	0.19	0.03
Tyr	[123455667]	466	7	0.24	0.19	0.17	0.20	0.02
Tyr	[123455667]	466	8	0.10	0.07	0.04	0.07	0.02
Tyr	[123455667]	466	9	0.04	0.03	0.03	0.03	0.00
Val	[2345]	186	0	0.10	0.10	0.10	0.10	0.00
Val	[2345]	186	1	0.14	0.14	0.14	0.14	0.00
Val	[2345]	186	2	0.27	0.27	0.27	0.27	0.00
Val	[2345]	186	3	0.31	0.32	0.32	0.32	0.00
Val	[2345]	186	4	0.17	0.17	0.16	0.17	0.00
Val	[2345]	260	0	0.11	0.11	0.11	0.11	0.00
Val	[2345]	260	1	0.14	0.14	0.14	0.14	0.00
Val	[2345]	260	2	0.28	0.28	0.27	0.28	0.00
Val	[2345]	260	3	0.30	0.31	0.31	0.31	0.00
Val	[2345]	260	4	0.16	0.16	0.17	0.16	0.00
Val	[12345]	288	0	0.09	0.08	0.08	0.09	0.00
Val	[12345]	288	1	0.09	0.08	0.09	0.09	0.00
Val	[12345]	288	2	0.19	0.19	0.19	0.19	0.00
Val	[12345]	288	3	0.28	0.29	0.29	0.29	0.00
Val	[12345]	288	4	0.24	0.25	0.25	0.25	0.00
Val	[12345]	288	5	0.11	0.11	0.10	0.10	0.00
Val	[12]	302	0	0.23	0.22	0.22	0.22	0.00
Val	[12]	302	1	0.38	0.40	0.39	0.39	0.00
Val	[12]	302	2	0.39	0.39	0.39	0.39	0.00

## **A.2. Table A.2 Mass Isotopomers from 100% U-<sup>13</sup>C Glc ILE.**

Mass isotopomer distributions from 100% U-<sup>13</sup>C glucose ILE (**Table A.2**).

This table follows the scheme of **Table A.1**.

Table A.2 Mass isotopomers from 100% U-13C Glc ILE.

AA	Fragment	m/z	Mass (n in m+n)	Biological Replicates				Consider Replicate				Overall	
				Rep 1	Rep 2	Rep 3	Rep 4	1	2	3	4	Avg	SD
Ala	[23]	158	0	0.09	0.08	0.10	0.09	Y	Y	Y	Y	0.09	0.01
Ala	[23]	158	1	0.09	0.07	0.09	0.08	Y	Y	Y	Y	0.08	0.01
Ala	[23]	158	2	0.82	0.86	0.81	0.83	Y	Y	Y	Y	0.83	0.02
Ala	[23]	232	0	0.10	0.08	0.11	0.10	Y	Y	Y	Y	0.10	0.01
Ala	[23]	232	1	0.04	0.00	0.04	0.03	Y	Y	Y	Y	0.04	0.00
Ala	[23]	232	2	0.87	0.91	0.85	0.87	Y	Y	Y	Y	0.86	0.01
Ala	[123]	260	0	0.08	0.07	0.09	0.08	Y	Y	Y	Y	0.08	0.01
Ala	[123]	260	1	0.07	0.05	0.07	0.06	Y	Y	Y	Y	0.06	0.01
Ala	[123]	260	2	0.07	0.06	0.07	0.06	Y	Y	Y	Y	0.06	0.01
Ala	[123]	260	3	0.79	0.82	0.77	0.80	Y	Y	Y	Y	0.79	0.02
Arg	[2345]	340	0	0.09	0.07	0.08	0.08	Y	Y	Y	Y	0.08	0.00
Arg	[2345]	340	1	0.06	0.05	0.06	0.05	Y	Y	Y	Y	0.06	0.00
Arg	[2345]	340	2	0.07	0.05	0.07	0.06	Y	Y	Y	Y	0.06	0.01
Arg	[2345]	340	3	0.13	0.12	0.13	0.12	Y	Y	Y	Y	0.13	0.00
Arg	[2345]	340	4	0.66	0.72	0.66	0.68	Y	Y	Y	Y	0.67	0.01
Arg	[12345]	442	0	0.07	0.06	0.07	0.07	Y	Y	Y	Y	0.07	0.00
Arg	[12345]	442	1	0.04	0.04	0.02	0.04	Y	Y	Y	Y	0.04	0.01
Arg	[12345]	442	2	0.05	0.03	0.03	0.05	Y	Y	Y	Y	0.04	0.01
Arg	[12345]	442	3	0.06	0.04	0.05	0.05	Y	Y	Y	Y	0.05	0.01
Arg	[12345]	442	4	0.22	0.22	0.23	0.22	Y	Y	Y	Y	0.22	0.01
Arg	[12345]	442	5	0.55	0.60	0.60	0.57	Y	Y	Y	Y	0.58	0.02
Asp	[12]	302	0	0.08	0.07	0.09	0.08	Y	Y	Y	Y	0.08	0.01
Asp	[12]	302	1	0.11	0.09	0.11	0.10	Y	Y	Y	Y	0.10	0.01
Asp	[12]	302	2	0.81	0.84	0.80	0.82	Y	Y	Y	Y	0.82	0.02
Asp	[234]	316	0	0.07	0.06	0.08	0.07	Y	Y	Y	Y	0.07	0.01
Asp	[234]	316	1	0.07	0.05	0.07	0.06	Y	Y	Y	Y	0.06	0.01
Asp	[234]	316	2	0.23	0.23	0.22	0.23	Y	Y	Y	Y	0.23	0.01
Asp	[234]	316	3	0.63	0.66	0.63	0.64	Y	Y	Y	Y	0.64	0.02
Asp	[234]	390	0	0.07	0.06	0.08	0.07	Y	Y	Y	Y	0.07	0.01
Asp	[234]	390	1	0.07	0.05	0.07	0.07	Y	Y	Y	Y	0.07	0.01
Asp	[234]	390	2	0.24	0.23	0.23	0.23	Y	Y	Y	Y	0.23	0.01
Asp	[234]	390	3	0.62	0.65	0.62	0.63	Y	Y	Y	Y	0.63	0.01
Asp	[1234]	418	0	0.06	0.05	0.06	0.06	Y	Y	Y	Y	0.06	0.01
Asp	[1234]	418	1	0.05	0.04	0.06	0.05	Y	Y	Y	Y	0.05	0.01
Asp	[1234]	418	2	0.07	0.06	0.07	0.06	Y	Y	Y	Y	0.06	0.01
Asp	[1234]	418	3	0.24	0.24	0.23	0.24	Y	Y	Y	Y	0.24	0.00
Asp	[1234]	418	4	0.58	0.61	0.58	0.59	Y	Y	Y	Y	0.59	0.02
Glu	[2345]	272	0	0.04	0.03	0.05	0.04	Y	Y	Y	Y	0.04	0.01
Glu	[2345]	272	1	0.04	0.03	0.05	0.04	Y	Y	Y	Y	0.04	0.01
Glu	[2345]	272	2	0.07	0.05	0.07	0.06	Y	Y	Y	Y	0.06	0.01
Glu	[2345]	272	3	0.12	0.10	0.11	0.11	Y	Y	Y	Y	0.11	0.01
Glu	[2345]	272	4	0.74	0.78	0.73	0.75	Y	Y	Y	Y	0.75	0.02
Glu	[2345]	330	0	0.04	0.04	0.05	0.05	Y	Y	Y	Y	0.04	0.01
Glu	[2345]	330	1	0.04	0.03	0.05	0.04	Y	Y	Y	Y	0.04	0.01
Glu	[2345]	330	2	0.07	0.06	0.07	0.07	Y	Y	Y	Y	0.07	0.01
Glu	[2345]	330	3	0.12	0.10	0.11	0.11	Y	Y	Y	Y	0.11	0.01
Glu	[2345]	330	4	0.73	0.77	0.72	0.74	Y	Y	Y	Y	0.74	0.02
Glu	[12345]	432	0	0.04	0.03	0.04	0.04	Y	Y	Y	Y	0.04	0.00
Glu	[12345]	432	1	0.03	0.03	0.04	0.04	Y	Y	Y	Y	0.03	0.01
Glu	[12345]	432	2	0.05	0.04	0.05	0.05	Y	Y	Y	Y	0.05	0.01
Glu	[12345]	432	3	0.07	0.06	0.06	0.06	Y	Y	Y	Y	0.06	0.01
Glu	[12345]	432	4	0.24	0.24	0.23	0.24	Y	Y	Y	Y	0.24	0.01
Glu	[12345]	432	5	0.57	0.60	0.57	0.58	Y	Y	Y	Y	0.58	0.02
Gly	[2]	218	0	0.14	0.10	0.14	0.12	Y	Y	Y	Y	0.13	0.02
Gly	[2]	218	1	0.86	0.90	0.86	0.88	Y	Y	Y	Y	0.87	0.02
Gly	[12]	246	0	0.09	0.08	0.11	0.08	Y	Y	Y	Y	0.09	0.01
Gly	[12]	246	1	0.07	0.05	0.07	0.06	Y	Y	Y	Y	0.06	0.01
Gly	[12]	246	2	0.84	0.86	0.82	0.85	Y	Y	Y	Y	0.84	0.02
His	[2345]	195	0	0.01	0.01	0.01	0.01	Y	Y	Y	Y	0.01	0.00
His	[2345]	195	1	0.13	0.11	0.11	0.12	Y	Y	Y	Y	0.12	0.01
His	[2345]	195	2	0.13	0.11	0.15	0.13	Y	Y	Y	Y	0.14	0.01
His	[2345]	195	3	0.21	0.20	0.22	0.21	Y	Y	Y	Y	0.21	0.00
His	[2345]	195	4	0.52	0.57	0.50	0.52	Y	Y	Y	Y	0.51	0.01
His	[23456]	338	0	0.06	0.05	0.05	0.05	Y	Y	Y	Y	0.05	0.00
His	[23456]	338	1	0.04	0.02	0.03	0.04	Y	Y	Y	Y	0.03	0.01
His	[23456]	338	2	0.06	0.03	0.04	0.05	Y	Y	Y	Y	0.05	0.01
His	[23456]	338	3	0.06	0.04	0.03	0.07	Y	Y	Y	Y	0.05	0.02
His	[23456]	338	4	0.09	0.09	0.05	0.09	Y	Y	Y	Y	0.08	0.02
His	[23456]	338	5	0.70	0.77	0.81	0.70	Y	Y	Y	Y	0.74	0.05
His	[123456]	440	0	0.05	0.04	nd	0.05	Y	Y	Y	Y	0.05	0.00
His	[123456]	440	1	0.03	0.02	nd	0.03	Y	Y	Y	Y	0.03	0.00
His	[123456]	440	2	0.04	0.03	nd	0.04	Y	Y	Y	Y	0.04	0.01
His	[123456]	440	3	0.05	0.03	nd	0.05	Y	Y	Y	Y	0.04	0.01
His	[123456]	440	4	0.05	0.03	nd	0.05	Y	Y	Y	Y	0.04	0.01
His	[123456]	440	5	0.09	0.08	nd	0.08	Y	Y	Y	Y	0.08	0.00
His	[123456]	440	6	0.69	0.76	nd	0.71	Y	Y	Y	Y	0.72	0.03
Ile	[23456]	200	0	0.05	0.04	0.05	0.05	Y	Y	Y	Y	0.05	0.00
Ile	[23456]	200	1	0.03	0.02	0.03	0.03	Y	Y	Y	Y	0.03	0.00
Ile	[23456]	200	2	0.05	0.04	0.05	0.04	Y	Y	Y	Y	0.04	0.01
Ile	[23456]	200	3	0.06	0.05	0.06	0.05	Y	Y	Y	Y	0.06	0.01
Ile	[23456]	200	4	0.19	0.20	0.19	0.19	Y	Y	Y	Y	0.19	0.00
Ile	[23456]	200	5	0.61	0.65	0.62	0.63	Y	Y	Y	Y	0.63	0.02
Ile	[23456]	274	0	0.05	0.04	0.05	0.05	Y	Y	Y	Y	0.05	0.00
Ile	[23456]	274	1	0.03	0.02	0.03	0.03	Y	Y	Y	Y	0.03	0.00
Ile	[23456]	274	2	0.05	0.04	0.05	0.04	Y	Y	Y	Y	0.04	0.01



Table A.2 Mass isotopomers from 100% U-<sup>13</sup>C Glc ILE.

AA	Fragment	m/z	Mass (n in m+n)	Biological Replicates				Consider Replicate				Overall	
				Rep 1	Rep 2	Rep 3	Rep 4	1	2	3	4	Avg	SD
Ile	[23456]	274	3	0.06	0.06	0.06	0.05	Y	Y	Y	Y	0.05	0.01
Ile	[23456]	274	4	0.20	0.20	0.20	0.20	Y	Y	Y	Y	0.20	0.00
Ile	[23456]	274	5	0.61	0.65	0.62	0.63	Y	Y	Y	Y	0.63	0.02
Ile	[12]	302	0	0.16	0.13	0.15	0.15	Y	Y	Y	Y	0.15	0.01
Ile	[12]	302	1	0.10	0.08	0.10	0.09	Y	Y	Y	Y	0.09	0.01
Ile	[12]	302	2	0.74	0.79	0.75	0.76	Y	Y	Y	Y	0.76	0.02
Leu	[23456]	200	0	0.04	0.03	0.05	0.04	Y	Y	Y	Y	0.04	0.00
Leu	[23456]	200	1	0.04	0.03	0.04	0.04	Y	Y	Y	Y	0.04	0.01
Leu	[23456]	200	2	0.05	0.03	0.05	0.04	Y	Y	Y	Y	0.04	0.01
Leu	[23456]	200	3	0.05	0.04	0.05	0.05	Y	Y	Y	Y	0.05	0.01
Leu	[23456]	200	4	0.09	0.08	0.08	0.08	Y	Y	Y	Y	0.08	0.00
Leu	[23456]	200	5	0.73	0.79	0.73	0.75	Y	Y	Y	Y	0.75	0.02
Leu	[23456]	274	0	0.04	0.03	0.04	0.04	Y	Y	Y	Y	0.04	0.00
Leu	[23456]	274	1	0.04	0.03	0.04	0.04	Y	Y	Y	Y	0.04	0.01
Leu	[23456]	274	2	0.05	0.03	0.05	0.04	Y	Y	Y	Y	0.04	0.01
Leu	[23456]	274	3	0.05	0.04	0.05	0.04	Y	Y	Y	Y	0.05	0.01
Leu	[23456]	274	4	0.09	0.09	0.08	0.08	Y	Y	Y	Y	0.08	0.00
Leu	[23456]	274	5	0.74	0.78	0.74	0.76	Y	Y	Y	Y	0.75	0.02
Leu	[12]	302	0	0.23	0.21	0.23	0.24	Y	Y	Y	Y	0.23	0.01
Leu	[12]	302	1	0.16	0.14	0.17	0.17	Y	Y	Y	Y	0.16	0.01
Leu	[12]	302	2	0.61	0.65	0.60	0.59	Y	Y	Y	Y	0.61	0.02
Lys	[23456]	329	0	0.07	0.05	0.06	0.06	Y	Y	Y	Y	0.06	0.01
Lys	[23456]	329	1	0.04	0.04	0.04	0.04	Y	Y	Y	Y	0.04	0.00
Lys	[23456]	329	2	0.06	0.06	0.07	0.06	Y	Y	Y	Y	0.06	0.00
Lys	[23456]	329	3	0.06	0.06	0.06	0.06	Y	Y	Y	Y	0.06	0.00
Lys	[23456]	329	4	0.23	0.23	0.22	0.23	Y	Y	Y	Y	0.23	0.00
Lys	[23456]	329	5	0.53	0.56	0.55	0.54	Y	Y	Y	Y	0.55	0.01
Lys	[123456]	431	0	0.06	0.05	0.05	0.06	Y	Y	Y	Y	0.06	0.01
Lys	[123456]	431	1	0.03	0.02	0.02	0.03	Y	Y	Y	Y	0.02	0.00
Lys	[123456]	431	2	0.03	0.02	0.03	0.03	Y	Y	Y	Y	0.03	0.00
Lys	[123456]	431	3	0.04	0.03	0.04	0.04	Y	Y	Y	Y	0.04	0.00
Lys	[123456]	431	4	0.07	0.06	0.06	0.06	Y	Y	Y	Y	0.06	0.00
Lys	[123456]	431	5	0.24	0.24	0.23	0.24	Y	Y	Y	Y	0.24	0.00
Lys	[123456]	431	6	0.54	0.57	0.57	0.55	Y	Y	Y	Y	0.56	0.02
Lys	[123456]	488	0	0.06	0.05	0.05	0.06	Y	Y	Y	Y	0.06	0.01
Lys	[123456]	488	1	0.03	0.02	0.03	0.03	Y	Y	Y	Y	0.02	0.00
Lys	[123456]	488	2	0.03	0.02	0.03	0.03	Y	Y	Y	Y	0.03	0.01
Lys	[123456]	488	3	0.03	0.03	0.03	0.03	Y	Y	Y	Y	0.03	0.00
Lys	[123456]	488	4	0.06	0.05	0.04	0.05	Y	Y	Y	Y	0.05	0.01
Lys	[123456]	488	5	0.23	0.24	0.23	0.23	Y	Y	Y	Y	0.23	0.00
Lys	[123456]	488	6	0.56	0.60	0.58	0.57	Y	Y	Y	Y	0.58	0.02
Met	[2345]	218	0	0.05	0.04	0.05	0.05	Y	Y	Y	Y	0.05	0.00
Met	[2345]	218	1	0.07	0.07	0.08	0.07	Y	Y	Y	Y	0.07	0.01
Met	[2345]	218	2	0.00	-0.02	0.01	-0.03	Y	Y	Y	Y	-0.01	0.02
Met	[2345]	218	3	0.22	0.16	0.19	0.19	Y	Y	Y	Y	0.20	0.02
Met	[2345]	218	4	0.67	0.77	0.69	0.72	Y	Y	Y	Y	0.69	0.02
Met	[2345]	292	0	0.04	0.03	0.04	0.04	Y	Y	Y	Y	0.04	0.00
Met	[2345]	292	1	0.07	0.05	0.07	0.06	Y	Y	Y	Y	0.06	0.01
Met	[2345]	292	2	0.08	0.06	0.08	0.07	Y	Y	Y	Y	0.07	0.01
Met	[2345]	292	3	0.24	0.24	0.24	0.25	Y	Y	Y	Y	0.24	0.01
Met	[2345]	292	4	0.57	0.62	0.58	0.59	Y	Y	Y	Y	0.59	0.02
Met	[12345]	320	0	0.03	0.03	0.02	0.03	Y	Y	Y	Y	0.03	0.00
Met	[12345]	320	1	0.06	0.05	0.06	0.06	Y	Y	Y	Y	0.06	0.00
Met	[12345]	320	2	0.07	0.06	0.08	0.07	Y	Y	Y	Y	0.07	0.01
Met	[12345]	320	3	0.07	0.04	0.07	0.05	Y	Y	Y	Y	0.06	0.01
Met	[12345]	320	4	0.20	0.19	0.20	0.19	Y	Y	Y	Y	0.19	0.00
Met	[12345]	320	5	0.57	0.63	0.57	0.60	Y	Y	Y	Y	0.58	0.02
Phe	[23455667]	234	0	0.04	0.04	0.04	0.04	Y	Y	Y	Y	0.04	0.00
Phe	[23455667]	234	1	0.02	0.02	0.03	0.02	Y	Y	Y	Y	0.02	0.00
Phe	[23455667]	234	2	0.03	0.02	0.03	0.03	Y	Y	Y	Y	0.03	0.00
Phe	[23455667]	234	3	0.03	0.03	0.04	0.03	Y	Y	Y	Y	0.03	0.01
Phe	[23455667]	234	4	0.03	0.02	0.03	0.02	Y	Y	Y	Y	0.03	0.00
Phe	[23455667]	234	5	0.02	0.02	0.02	0.02	Y	Y	Y	Y	0.02	0.00
Phe	[23455667]	234	6	0.03	0.02	0.02	0.03	Y	Y	Y	Y	0.02	0.00
Phe	[23455667]	234	7	0.05	0.04	0.06	-0.01	Y	Y	Y	Y	0.05	0.00
Phe	[23455667]	234	8	0.75	0.79	0.73	0.81	Y	Y	Y	Y	0.74	0.01
Phe	[12]	302	0	0.11	0.09	0.11	0.11	Y	Y	Y	Y	0.10	0.01
Phe	[12]	302	1	0.06	0.05	0.07	0.06	Y	Y	Y	Y	0.06	0.01
Phe	[12]	302	2	0.83	0.85	0.82	0.83	Y	Y	Y	Y	0.83	0.01
Phe	[123455667]	336	0	0.04	0.04	0.04	0.04	Y	Y	Y	Y	0.04	0.00
Phe	[123455667]	336	1	0.02	0.02	0.02	0.02	Y	Y	Y	Y	0.02	0.00
Phe	[123455667]	336	2	0.02	0.02	0.03	0.02	Y	Y	Y	Y	0.02	0.00
Phe	[123455667]	336	3	0.03	0.02	0.03	0.03	Y	Y	Y	Y	0.03	0.00
Phe	[123455667]	336	4	0.03	0.02	0.03	0.03	Y	Y	Y	Y	0.03	0.00
Phe	[123455667]	336	5	0.02	0.02	0.03	0.02	Y	Y	Y	Y	0.02	0.00
Phe	[123455667]	336	6	0.02	0.02	0.02	0.02	Y	Y	Y	Y	0.02	0.00
Phe	[123455667]	336	7	0.02	0.02	0.02	0.02	Y	Y	Y	Y	0.02	0.00
Phe	[123455667]	336	8	0.08	0.08	0.07	0.08	Y	Y	Y	Y	0.07	0.00
Phe	[123455667]	336	9	0.71	0.74	0.71	0.71	Y	Y	Y	Y	0.72	0.01
Pro	[2345]	184	0	0.08	0.06	0.07	0.07	Y	Y	Y	Y	0.07	0.00
Pro	[2345]	184	1	0.04	0.03	0.05	0.04	Y	Y	Y	Y	0.05	0.00
Pro	[2345]	184	2	0.07	0.05	0.08	0.06	Y	Y	Y	Y	0.07	0.01
Pro	[2345]	184	3	0.10	0.09	0.10	0.10	Y	Y	Y	Y	0.10	0.00
Pro	[2345]	184	4	0.70	0.76	0.70	0.73	Y	Y	Y	Y	0.71	0.01
Pro	[2345]	258	0	0.08	0.06	0.07	0.07	Y	Y	Y	Y	0.07	0.00

Table A.2 Mass isotopomers from 100% U-13C Glc ILE.

AA	Fragment	m/z	Mass (n in m+n)	Biological Replicates				Consider Replicate				Overall	
				Rep 1	Rep 2	Rep 3	Rep 4	1	2	3	4	Avg	SD
Pro	[2345]	258	1	0.04	0.03	0.05	0.04	Y		Y	Y	0.04	0.00
Pro	[2345]	258	2	0.08	0.06	0.08	0.07	Y		Y	Y	0.08	0.01
Pro	[2345]	258	3	0.10	0.08	0.09	0.09	Y		Y	Y	0.09	0.01
Pro	[2345]	258	4	0.70	0.76	0.71	0.73	Y		Y	Y	0.71	0.01
Pro	[12345]	286	0	0.08	0.08	0.12	0.12	Y		Y	Y	0.11	0.02
Pro	[12345]	286	1	0.04	0.04	0.06	0.06	Y		Y	Y	0.05	0.01
Pro	[12345]	286	2	0.06	0.04	0.05	0.05	Y		Y	Y	0.05	0.00
Pro	[12345]	286	3	0.07	0.05	0.06	0.05	Y		Y	Y	0.06	0.01
Pro	[12345]	286	4	0.20	0.17	0.12	0.14	Y		Y	Y	0.15	0.04
Pro	[12345]	286	5	0.56	0.62	0.59	0.59	Y		Y	Y	0.58	0.02
Ser	[23]	288	0	0.07	0.06	0.08	0.07	Y	Y	Y	Y	0.07	0.01
Ser	[23]	288	1	0.12	0.10	0.12	0.11	Y	Y	Y	Y	0.11	0.01
Ser	[23]	288	2	0.81	0.83	0.80	0.82	Y	Y	Y	Y	0.82	0.02
Ser	[12]	302	0	0.07	0.06	0.08	0.06	Y	Y	Y	Y	0.07	0.01
Ser	[12]	302	1	0.18	0.18	0.16	0.18	Y	Y	Y	Y	0.17	0.01
Ser	[12]	302	2	0.75	0.76	0.77	0.76	Y	Y	Y	Y	0.76	0.01
Ser	[23]	362	0	0.07	0.06	0.08	0.07	Y	Y	Y	Y	0.07	0.01
Ser	[23]	362	1	0.12	0.10	0.13	0.10	Y	Y	Y	Y	0.11	0.01
Ser	[23]	362	2	0.81	0.83	0.79	0.83	Y	Y	Y	Y	0.82	0.02
Ser	[123]	390	0	0.06	0.05	0.06	0.05	Y	Y	Y	Y	0.06	0.01
Ser	[123]	390	1	0.08	0.06	0.08	0.07	Y	Y	Y	Y	0.07	0.01
Ser	[123]	390	2	0.11	0.10	0.11	0.10	Y	Y	Y	Y	0.11	0.01
Ser	[123]	390	3	0.76	0.79	0.75	0.78	Y	Y	Y	Y	0.77	0.02
Thr	[234]	376	0	0.09	0.07	0.08	0.07	Y	Y	Y	Y	0.08	0.01
Thr	[234]	376	1	0.08	0.06	0.08	0.07	Y	Y	Y	Y	0.07	0.01
Thr	[234]	376	2	0.25	0.25	0.24	0.25	Y	Y	Y	Y	0.25	0.01
Thr	[234]	376	3	0.58	0.62	0.60	0.61	Y	Y	Y	Y	0.61	0.02
Thr	[1234]	404	0	0.07	0.05	0.06	0.06	Y	Y	Y	Y	0.06	0.01
Thr	[1234]	404	1	0.05	0.04	0.05	0.04	Y	Y	Y	Y	0.05	0.01
Thr	[1234]	404	2	0.07	0.06	0.06	0.06	Y	Y	Y	Y	0.06	0.01
Thr	[1234]	404	3	0.24	0.24	0.23	0.24	Y	Y	Y	Y	0.24	0.00
Thr	[1234]	404	4	0.57	0.61	0.58	0.60	Y	Y	Y	Y	0.59	0.02
Tyr	[12]	302	0	0.07	0.06	0.07	0.06	Y	Y	Y	Y	0.06	0.00
Tyr	[12]	302	1	0.16	0.20	0.15	0.17	Y	Y	Y	Y	0.17	0.02
Tyr	[12]	302	2	0.77	0.74	0.78	0.76	Y	Y	Y	Y	0.76	0.02
Tyr	[23455667]	364	0	0.03	0.03	0.03	0.03	Y	Y	Y	Y	0.03	0.00
Tyr	[23455667]	364	1	0.03	0.02	0.03	0.02	Y	Y	Y	Y	0.02	0.00
Tyr	[23455667]	364	2	0.03	0.03	0.03	0.03	Y	Y	Y	Y	0.03	0.00
Tyr	[23455667]	364	3	0.03	0.03	0.04	0.03	Y	Y	Y	Y	0.03	0.00
Tyr	[23455667]	364	4	0.03	0.02	0.03	0.03	Y	Y	Y	Y	0.03	0.00
Tyr	[23455667]	364	5	0.02	0.02	0.02	0.02	Y	Y	Y	Y	0.02	0.00
Tyr	[23455667]	364	6	0.03	0.03	0.03	0.03	Y	Y	Y	Y	0.03	0.00
Tyr	[23455667]	364	7	0.08	0.09	0.08	0.08	Y	Y	Y	Y	0.09	0.00
Tyr	[23455667]	364	8	0.71	0.74	0.71	0.72	Y	Y	Y	Y	0.72	0.02
Tyr	[23455667]	438	0	0.03	0.03	0.03	0.03	Y	Y	Y	Y	0.03	0.00
Tyr	[23455667]	438	1	0.02	0.02	0.03	0.02	Y	Y	Y	Y	0.02	0.00
Tyr	[23455667]	438	2	0.03	0.02	0.04	0.03	Y	Y	Y	Y	0.03	0.00
Tyr	[23455667]	438	3	0.03	0.02	0.03	0.03	Y	Y	Y	Y	0.03	0.00
Tyr	[23455667]	438	4	0.03	0.02	0.03	0.03	Y	Y	Y	Y	0.03	0.00
Tyr	[23455667]	438	5	0.02	0.01	0.02	0.02	Y	Y	Y	Y	0.02	0.01
Tyr	[23455667]	438	6	0.02	0.02	0.02	0.02	Y	Y	Y	Y	0.02	0.00
Tyr	[23455667]	438	7	0.08	0.08	0.07	0.07	Y	Y	Y	Y	0.08	0.00
Tyr	[23455667]	438	8	0.73	0.78	0.74	0.75	Y	Y	Y	Y	0.75	0.02
Tyr	[123455667]	466	0	0.03	0.02	0.03	0.03	Y	Y	Y	Y	0.03	0.00
Tyr	[123455667]	466	1	0.02	0.02	0.02	0.02	Y	Y	Y	Y	0.02	0.00
Tyr	[123455667]	466	2	0.03	0.02	0.03	0.03	Y	Y	Y	Y	0.03	0.00
Tyr	[123455667]	466	3	0.03	0.03	0.04	0.03	Y	Y	Y	Y	0.03	0.00
Tyr	[123455667]	466	4	0.03	0.02	0.03	0.03	Y	Y	Y	Y	0.03	0.00
Tyr	[123455667]	466	5	0.02	0.02	0.02	0.02	Y	Y	Y	Y	0.02	0.00
Tyr	[123455667]	466	6	0.02	0.02	0.02	0.02	Y	Y	Y	Y	0.02	0.00
Tyr	[123455667]	466	7	0.03	0.03	0.03	0.03	Y	Y	Y	Y	0.03	0.00
Tyr	[123455667]	466	8	0.08	0.08	0.08	0.08	Y	Y	Y	Y	0.08	0.00
Tyr	[123455667]	466	9	0.70	0.75	0.71	0.72	Y	Y	Y	Y	0.72	0.02
Val	[2345]	186	0	0.06	0.05	0.06	0.06	Y	Y	Y	Y	0.06	0.01
Val	[2345]	186	1	0.04	0.03	0.04	0.04	Y	Y	Y	Y	0.04	0.01
Val	[2345]	186	2	0.06	0.05	0.06	0.05	Y	Y	Y	Y	0.05	0.01
Val	[2345]	186	3	0.11	0.11	0.12	0.11	Y	Y	Y	Y	0.11	0.00
Val	[2345]	186	4	0.72	0.76	0.72	0.74	Y	Y	Y	Y	0.74	0.02
Val	[2345]	260	0	0.06	0.05	0.06	0.06	Y	Y	Y	Y	0.06	0.01
Val	[2345]	260	1	0.05	0.04	0.05	0.04	Y	Y	Y	Y	0.04	0.01
Val	[2345]	260	2	0.06	0.05	0.06	0.05	Y	Y	Y	Y	0.06	0.01
Val	[2345]	260	3	0.08	0.06	0.07	0.07	Y	Y	Y	Y	0.07	0.01
Val	[2345]	260	4	0.75	0.80	0.76	0.78	Y	Y	Y	Y	0.77	0.02
Val	[12345]	288	0	0.06	0.05	0.06	0.05	Y	Y	Y	Y	0.05	0.01
Val	[12345]	288	1	0.04	0.03	0.04	0.04	Y	Y	Y	Y	0.04	0.01
Val	[12345]	288	2	0.05	0.03	0.05	0.04	Y	Y	Y	Y	0.04	0.01
Val	[12345]	288	3	0.05	0.04	0.05	0.04	Y	Y	Y	Y	0.05	0.01
Val	[12345]	288	4	0.08	0.07	0.07	0.07	Y	Y	Y	Y	0.07	0.00
Val	[12345]	288	5	0.73	0.78	0.73	0.75	Y	Y	Y	Y	0.75	0.02
Val	[12]	302	0	0.12	0.09	0.12	0.11	Y	Y	Y	Y	0.11	0.01
Val	[12]	302	1	0.09	0.08	0.09	0.08	Y	Y	Y	Y	0.08	0.01
Val	[12]	302	2	0.79	0.83	0.79	0.81	Y	Y	Y	Y	0.80	0.02

### **A.3. Table A.3 Mass Isotopomers from 100% U-<sup>13</sup>C Ace ILE.**

Mass isotopomer distributions from 100% U-<sup>13</sup>C acetate ILE (**Table A.3**).

This table follows the scheme of **Table A.1**.

AA	Fragment	m/z	Mass (n in m+n)	Biological Replicates			Consider			Overall	
				Rep 1	Rep 2	Rep 3	1	2	3	Avg	SD
Ala	[23]	158	0	0.33	0.34	0.35	Y	Y	Y	0.34	0.01
Ala	[23]	158	1	0.13	0.14	0.12	Y	Y	Y	0.13	0.01
Ala	[23]	158	2	0.55	0.53	0.53	Y	Y	Y	0.53	0.01
Ala	[23]	232	0	0.33	0.35	0.35	Y	Y	Y	0.34	0.01
Ala	[23]	232	1	0.12	0.13	0.12	Y	Y	Y	0.12	0.01
Ala	[23]	232	2	0.55	0.52	0.53	Y	Y	Y	0.53	0.01
Ala	[123]	260	0	0.30	0.31	0.33	Y	Y	Y	0.31	0.01
Ala	[123]	260	1	0.10	0.11	0.10	Y	Y	Y	0.10	0.01
Ala	[123]	260	2	0.09	0.08	0.08	Y	Y	Y	0.08	0.00
Ala	[123]	260	3	0.51	0.49	0.50	Y	Y	Y	0.50	0.01
Arg	[2345]	340	0	nd	nd	nd	Y	Y	Y	nd	nd
Arg	[2345]	340	1	nd	nd	nd	Y	Y	Y	nd	nd
Arg	[2345]	340	2	nd	nd	nd	Y	Y	Y	nd	nd
Arg	[2345]	340	3	nd	nd	nd	Y	Y	Y	nd	nd
Arg	[2345]	340	4	nd	nd	nd	Y	Y	Y	nd	nd
Arg	[12345]	442	0	nd	nd	nd	Y	Y	Y	nd	nd
Arg	[12345]	442	1	nd	nd	nd	Y	Y	Y	nd	nd
Arg	[12345]	442	2	nd	nd	nd	Y	Y	Y	nd	nd
Arg	[12345]	442	3	nd	nd	nd	Y	Y	Y	nd	nd
Arg	[12345]	442	4	nd	nd	nd	Y	Y	Y	nd	nd
Arg	[12345]	442	5	nd	nd	nd	Y	Y	Y	nd	nd
Asp	[12]	302	0	<del>0.28</del>	0.32	0.33	Y	Y	Y	0.32	0.00
Asp	[12]	302	1	<del>0.15</del>	0.14	0.13	Y	Y	Y	0.14	0.01
Asp	[12]	302	2	<del>0.57</del>	0.53	0.54	Y	Y	Y	0.54	0.01
Asp	[234]	316	0	0.26	0.29	0.29	Y	Y	Y	0.28	0.02
Asp	[234]	316	1	0.12	0.12	0.11	Y	Y	Y	0.12	0.00
Asp	[234]	316	2	0.17	0.15	0.16	Y	Y	Y	0.16	0.01
Asp	[234]	316	3	0.46	0.44	0.43	Y	Y	Y	0.44	0.01
Asp	[234]	390	0	0.26	0.28	0.29	Y	Y	Y	0.28	0.02
Asp	[234]	390	1	0.12	0.13	0.12	Y	Y	Y	0.12	0.01
Asp	[234]	390	2	0.17	0.16	0.16	Y	Y	Y	0.16	0.01
Asp	[234]	390	3	0.45	0.43	0.44	Y	Y	Y	0.44	0.01
Asp	[1234]	418	0	0.23	0.26	0.27	Y	Y	Y	0.25	0.02
Asp	[1234]	418	1	0.10	0.11	0.10	Y	Y	Y	0.11	0.01
Asp	[1234]	418	2	0.10	0.10	0.09	Y	Y	Y	0.09	0.01
Asp	[1234]	418	3	0.16	0.14	0.14	Y	Y	Y	0.15	0.01
Asp	[1234]	418	4	0.42	0.39	0.40	Y	Y	Y	0.40	0.01
Glu	[2345]	272	0	0.24	0.25	0.27	Y	Y	Y	0.25	0.01
Glu	[2345]	272	1	0.10	0.12	0.10	Y	Y	Y	0.11	0.01
Glu	[2345]	272	2	0.08	0.09	0.08	Y	Y	Y	0.08	0.01
Glu	[2345]	272	3	0.09	0.09	0.08	Y	Y	Y	0.09	0.00
Glu	[2345]	272	4	0.49	0.45	0.47	Y	Y	Y	0.47	0.02
Glu	[2345]	330	0	0.23	0.25	0.28	Y	Y	Y	0.25	0.02
Glu	[2345]	330	1	0.10	0.12	0.10	Y	Y	Y	0.11	0.01
Glu	[2345]	330	2	0.08	0.09	0.08	Y	Y	Y	0.08	0.00
Glu	[2345]	330	3	0.09	0.09	0.09	Y	Y	Y	0.09	0.00
Glu	[2345]	330	4	0.49	0.46	0.46	Y	Y	Y	0.47	0.02
Glu	[12345]	432	0	0.22	0.22	0.25	Y	Y	Y	0.23	0.02
Glu	[12345]	432	1	0.09	0.11	0.10	Y	Y	Y	0.10	0.01
Glu	[12345]	432	2	0.07	0.08	0.06	Y	Y	Y	0.07	0.01
Glu	[12345]	432	3	0.07	0.07	0.06	Y	Y	Y	0.07	0.00
Glu	[12345]	432	4	0.13	0.12	0.12	Y	Y	Y	0.13	0.01
Glu	[12345]	432	5	0.42	0.39	0.40	Y	Y	Y	0.40	0.01
Gly	[2]	218	0	0.40	0.44	0.42	Y	Y	Y	0.42	0.02
Gly	[2]	218	1	0.60	0.56	0.58	Y	Y	Y	0.58	0.02
Gly	[12]	246	0	0.34	0.37	0.37	Y	Y	Y	0.36	0.02
Gly	[12]	246	1	0.13	0.14	0.12	Y	Y	Y	0.13	0.01
Gly	[12]	246	2	0.53	0.49	0.51	Y	Y	Y	0.51	0.02
His	[2345]	195	0	nd	nd	nd	Y	Y	Y	nd	nd
His	[2345]	195	1	nd	nd	nd	Y	Y	Y	nd	nd
His	[2345]	195	2	nd	nd	nd	Y	Y	Y	nd	nd
His	[2345]	195	3	nd	nd	nd	Y	Y	Y	nd	nd
His	[2345]	195	4	nd	nd	nd	Y	Y	Y	nd	nd
His	[23456]	338	0	nd	nd	nd	Y	Y	Y	nd	nd
His	[23456]	338	1	nd	nd	nd	Y	Y	Y	nd	nd
His	[23456]	338	2	nd	nd	nd	Y	Y	Y	nd	nd
His	[23456]	338	3	nd	nd	nd	Y	Y	Y	nd	nd
His	[23456]	338	4	nd	nd	nd	Y	Y	Y	nd	nd
His	[23456]	338	5	nd	nd	nd	Y	Y	Y	nd	nd
His	[123456]	440	0	nd	nd	nd	Y	Y	Y	nd	nd
His	[123456]	440	1	nd	nd	nd	Y	Y	Y	nd	nd
His	[123456]	440	2	nd	nd	nd	Y	Y	Y	nd	nd
His	[123456]	440	3	nd	nd	nd	Y	Y	Y	nd	nd
His	[123456]	440	4	nd	nd	nd	Y	Y	Y	nd	nd
His	[123456]	440	5	nd	nd	nd	Y	Y	Y	nd	nd
His	[123456]	440	6	nd	nd	nd	Y	Y	Y	nd	nd
Ile	[23456]	200	0	0.14	0.17	0.17	Y	Y	Y	0.16	0.02
Ile	[23456]	200	1	0.09	0.11	0.10	Y	Y	Y	0.10	0.01
Ile	[23456]	200	2	0.09	0.10	0.09	Y	Y	Y	0.09	0.00
Ile	[23456]	200	3	0.10	0.10	0.09	Y	Y	Y	0.10	0.00
Ile	[23456]	200	4	0.15	0.13	0.14	Y	Y	Y	0.14	0.01
Ile	[23456]	200	5	0.43	0.39	0.41	Y	Y	Y	0.41	0.02
Ile	[23456]	274	0	0.14	0.17	0.17	Y	Y	Y	0.16	0.02
Ile	[23456]	274	1	0.09	0.11	0.10	Y	Y	Y	0.10	0.01
Ile	[23456]	274	2	0.09	0.10	0.09	Y	Y	Y	0.09	0.01

Table A.3 Mass isotopomers from 100% U-13C Ace ILE.

AA	Fragment	m/z	Mass (n in m+n)	Biological Replicates			Consider			Overall	
				Rep 1	Rep 2	Rep 3	1	2	3	Avg	SD
Ile	[23456]	274	3	0.10	0.09	0.09	Y	Y	Y	0.10	0.00
Ile	[23456]	274	4	0.15	0.13	0.14	Y	Y	Y	0.14	0.01
Ile	[23456]	274	5	0.44	0.39	0.42	Y	Y	Y	0.42	0.02
Ile	[12]	302	0	<del>0.28</del>	0.33	0.33	Y	Y	Y	0.33	0.00
Ile	[12]	302	1	<del>0.20</del>	0.22	0.20	Y	Y	Y	0.21	0.01
Ile	[12]	302	2	<del>0.54</del>	0.45	0.47	Y	Y	Y	0.46	0.01
Leu	[23456]	200	0	0.18	0.20	0.21	Y	Y	Y	0.20	0.02
Leu	[23456]	200	1	0.08	0.11	0.10	Y	Y	Y	0.10	0.01
Leu	[23456]	200	2	0.07	0.08	0.07	Y	Y	Y	0.07	0.01
Leu	[23456]	200	3	0.08	0.08	0.07	Y	Y	Y	0.08	0.00
Leu	[23456]	200	4	0.10	0.09	0.09	Y	Y	Y	0.09	0.01
Leu	[23456]	200	5	0.49	0.44	0.46	Y	Y	Y	0.47	0.02
Leu	[23456]	274	0	<del>0.18</del>	0.20	0.21	Y	Y	Y	0.20	0.01
Leu	[23456]	274	1	<del>0.08</del>	0.11	0.10	Y	Y	Y	0.10	0.01
Leu	[23456]	274	2	<del>0.06</del>	0.08	0.07	Y	Y	Y	0.07	0.01
Leu	[23456]	274	3	<del>0.07</del>	0.08	0.07	Y	Y	Y	0.07	0.00
Leu	[23456]	274	4	<del>0.10</del>	0.09	0.09	Y	Y	Y	0.09	0.00
Leu	[23456]	274	5	<del>0.50</del>	0.45	0.47	Y	Y	Y	0.46	0.01
Leu	[12]	302	0	0.45	0.45	0.49	Y	Y	Y	0.46	0.02
Leu	[12]	302	1	0.22	0.24	0.22	Y	Y	Y	0.23	0.01
Leu	[12]	302	2	0.33	0.31	0.29	Y	Y	Y	0.31	0.02
Lys	[23456]	329	0	nd	nd	nd	Y	Y	Y	nd	nd
Lys	[23456]	329	1	nd	nd	nd	Y	Y	Y	nd	nd
Lys	[23456]	329	2	nd	nd	nd	Y	Y	Y	nd	nd
Lys	[23456]	329	3	nd	nd	nd	Y	Y	Y	nd	nd
Lys	[23456]	329	4	nd	nd	nd	Y	Y	Y	nd	nd
Lys	[23456]	329	5	nd	nd	nd	Y	Y	Y	nd	nd
Lys	[123456]	431	0	nd	nd	nd	Y	Y	Y	nd	nd
Lys	[123456]	431	1	nd	nd	nd	Y	Y	Y	nd	nd
Lys	[123456]	431	2	nd	nd	nd	Y	Y	Y	nd	nd
Lys	[123456]	431	3	nd	nd	nd	Y	Y	Y	nd	nd
Lys	[123456]	431	4	nd	nd	nd	Y	Y	Y	nd	nd
Lys	[123456]	431	5	nd	nd	nd	Y	Y	Y	nd	nd
Lys	[123456]	431	6	nd	nd	nd	Y	Y	Y	nd	nd
Lys	[123456]	488	0	nd	nd	nd	Y	Y	Y	nd	nd
Lys	[123456]	488	1	nd	nd	nd	Y	Y	Y	nd	nd
Lys	[123456]	488	2	nd	nd	nd	Y	Y	Y	nd	nd
Lys	[123456]	488	3	nd	nd	nd	Y	Y	Y	nd	nd
Lys	[123456]	488	4	nd	nd	nd	Y	Y	Y	nd	nd
Lys	[123456]	488	5	nd	nd	nd	Y	Y	Y	nd	nd
Lys	[123456]	488	6	nd	nd	nd	Y	Y	Y	nd	nd
Met	[2345]	218	0	<del>0.24</del>	0.27	0.28	Y	Y	Y	0.27	0.01
Met	[2345]	218	1	<del>0.14</del>	0.16	0.14	Y	Y	Y	0.15	0.01
Met	[2345]	218	2	<del>0.07</del>	0.09	0.07	Y	Y	Y	0.08	0.01
Met	[2345]	218	3	<del>0.14</del>	0.12	0.13	Y	Y	Y	0.13	0.01
Met	[2345]	218	4	<del>0.44</del>	0.36	0.38	Y	Y	Y	0.37	0.02
Met	[2345]	292	0	<del>0.23</del>	0.26	0.26	Y	Y	Y	0.26	0.00
Met	[2345]	292	1	<del>0.12</del>	0.15	0.13	Y	Y	Y	0.14	0.01
Met	[2345]	292	2	<del>0.09</del>	0.10	0.09	Y	Y	Y	0.09	0.01
Met	[2345]	292	3	<del>0.14</del>	0.13	0.13	Y	Y	Y	0.13	0.00
Met	[2345]	292	4	<del>0.44</del>	0.35	0.39	Y	Y	Y	0.37	0.03
Met	[12345]	320	0	nd	nd	nd	Y	Y	Y	nd	nd
Met	[12345]	320	1	nd	nd	nd	Y	Y	Y	nd	nd
Met	[12345]	320	2	nd	nd	nd	Y	Y	Y	nd	nd
Met	[12345]	320	3	nd	nd	nd	Y	Y	Y	nd	nd
Met	[12345]	320	4	nd	nd	nd	Y	Y	Y	nd	nd
Met	[12345]	320	5	nd	nd	nd	Y	Y	Y	nd	nd
Phe	[23455667]	234	0	0.15	0.16	0.17	Y	Y	Y	0.16	0.01
Phe	[23455667]	234	1	0.08	0.10	0.09	Y	Y	Y	0.09	0.01
Phe	[23455667]	234	2	0.05	0.07	0.05	Y	Y	Y	0.05	0.01
Phe	[23455667]	234	3	0.04	0.06	0.05	Y	Y	Y	0.05	0.01
Phe	[23455667]	234	4	0.05	0.06	0.05	Y	Y	Y	0.05	0.00
Phe	[23455667]	234	5	0.07	0.06	0.06	Y	Y	Y	0.06	0.00
Phe	[23455667]	234	6	0.06	0.06	0.06	Y	Y	Y	0.06	0.00
Phe	[23455667]	234	7	0.09	0.08	0.08	Y	Y	Y	0.08	0.00
Phe	[23455667]	234	8	0.41	0.37	0.39	Y	Y	Y	0.39	0.02
Phe	[12]	302	0	<del>0.26</del>	0.32	0.30	Y	Y	Y	0.31	0.01
Phe	[12]	302	1	<del>0.17</del>	0.18	0.16	Y	Y	Y	0.17	0.02
Phe	[12]	302	2	<del>0.57</del>	0.50	0.54	Y	Y	Y	0.52	0.03
Phe	[123455667]	336	0	0.14	0.15	0.16	Y	Y	Y	0.15	0.01
Phe	[123455667]	336	1	0.07	0.09	0.08	Y	Y	Y	0.08	0.01
Phe	[123455667]	336	2	0.04	0.06	0.05	Y	Y	Y	0.05	0.01
Phe	[123455667]	336	3	0.04	0.05	0.04	Y	Y	Y	0.04	0.01
Phe	[123455667]	336	4	0.04	0.05	0.04	Y	Y	Y	0.05	0.00
Phe	[123455667]	336	5	0.05	0.05	0.05	Y	Y	Y	0.05	0.00
Phe	[123455667]	336	6	0.06	0.05	0.05	Y	Y	Y	0.06	0.01
Phe	[123455667]	336	7	0.07	0.05	0.05	Y	Y	Y	0.06	0.01
Phe	[123455667]	336	8	0.09	0.08	0.08	Y	Y	Y	0.08	0.01
Phe	[123455667]	336	9	0.40	0.35	0.39	Y	Y	Y	0.38	0.02
Pro	[2345]	184	0	<del>0.25</del>	0.28	0.30	Y	Y	Y	0.29	0.01
Pro	[2345]	184	1	<del>0.12</del>	0.13	0.12	Y	Y	Y	0.13	0.01
Pro	[2345]	184	2	<del>0.09</del>	0.10	0.08	Y	Y	Y	0.09	0.01
Pro	[2345]	184	3	<del>0.09</del>	0.09	0.08	Y	Y	Y	0.09	0.01
Pro	[2345]	184	4	<del>0.46</del>	0.40	0.42	Y	Y	Y	0.41	0.02
Pro	[2345]	258	0	<del>0.24</del>	0.27	0.29	Y	Y	Y	0.28	0.02

Table A.3 Mass isotopomers from 100% U-<sup>13</sup>C Ace ILE.

AA	Fragment	m/z	Mass (n in m+n)	Biological Replicates			Consider			Overall	
				Rep 1	Rep 2	Rep 3	1	2	3	Avg	SD
Pro	[2345]	258	1	<del>0.12</del>	0.13	0.12		Y	Y	0.13	0.01
Pro	[2345]	258	2	<del>0.09</del>	0.10	0.08		Y	Y	0.09	0.01
Pro	[2345]	258	3	<del>0.09</del>	0.09	0.08		Y	Y	0.08	0.01
Pro	[2345]	258	4	<del>0.46</del>	0.41	0.43		Y	Y	0.42	0.02
Pro	[12345]	286	0	0.25	0.26	0.27	Y	Y	Y	0.26	0.01
Pro	[12345]	286	1	0.13	0.14	0.13	Y	Y	Y	0.13	0.00
Pro	[12345]	286	2	0.06	0.07	0.06	Y	Y	Y	0.07	0.01
Pro	[12345]	286	3	0.09	0.09	0.08	Y	Y	Y	0.09	0.01
Pro	[12345]	286	4	0.09	0.10	0.09	Y	Y	Y	0.09	0.00
Pro	[12345]	286	5	0.37	0.34	0.36	Y	Y	Y	0.36	0.02
Ser	[23]	288	0	0.36	0.38	0.38	Y	Y	Y	0.37	0.01
Ser	[23]	288	1	0.15	0.16	0.14	Y	Y	Y	0.15	0.01
Ser	[23]	288	2	0.49	0.46	0.48	Y	Y	Y	0.48	0.02
Ser	[12]	302	0	0.34	0.37	0.37	Y	Y	Y	0.36	0.02
Ser	[12]	302	1	0.16	0.16	0.15	Y	Y	Y	0.16	0.01
Ser	[12]	302	2	0.50	0.46	0.48	Y	Y	Y	0.48	0.02
Ser	[23]	362	0	0.34	0.37	0.37	Y	Y	Y	0.36	0.02
Ser	[23]	362	1	0.16	0.17	0.14	Y	Y	Y	0.15	0.01
Ser	[23]	362	2	0.50	0.46	0.48	Y	Y	Y	0.48	0.02
Ser	[123]	390	0	0.32	0.34	0.35	Y	Y	Y	0.33	0.01
Ser	[123]	390	1	0.12	0.13	0.11	Y	Y	Y	0.12	0.01
Ser	[123]	390	2	0.11	0.10	0.09	Y	Y	Y	0.10	0.01
Ser	[123]	390	3	0.46	0.42	0.45	Y	Y	Y	0.44	0.02
Thr	[234]	376	0	0.25	0.27	0.27	Y	Y	Y	0.26	0.01
Thr	[234]	376	1	0.12	0.14	0.12	Y	Y	Y	0.13	0.01
Thr	[234]	376	2	0.17	0.16	0.16	Y	Y	Y	0.17	0.01
Thr	[234]	376	3	0.46	0.43	0.45	Y	Y	Y	0.44	0.01
Thr	[1234]	404	0	0.22	0.25	0.25	Y	Y	Y	0.24	0.02
Thr	[1234]	404	1	0.10	0.12	0.11	Y	Y	Y	0.11	0.01
Thr	[1234]	404	2	0.09	0.09	0.08	Y	Y	Y	0.09	0.00
Thr	[1234]	404	3	0.16	0.14	0.15	Y	Y	Y	0.15	0.01
Thr	[1234]	404	4	0.44	0.40	0.41	Y	Y	Y	0.42	0.02
Tyr	[12]	302	0	0.25	0.28	0.27	Y	Y	Y	0.27	0.02
Tyr	[12]	302	1	0.15	0.15	0.14	Y	Y	Y	0.15	0.01
Tyr	[12]	302	2	0.60	0.57	0.58	Y	Y	Y	0.58	0.02
Tyr	[23455667]	364	0	nd	nd	nd	Y	Y	Y	nd	nd
Tyr	[23455667]	364	1	nd	nd	nd	Y	Y	Y	nd	nd
Tyr	[23455667]	364	2	nd	nd	nd	Y	Y	Y	nd	nd
Tyr	[23455667]	364	3	nd	nd	nd	Y	Y	Y	nd	nd
Tyr	[23455667]	364	4	nd	nd	nd	Y	Y	Y	nd	nd
Tyr	[23455667]	364	5	nd	nd	nd	Y	Y	Y	nd	nd
Tyr	[23455667]	364	6	nd	nd	nd	Y	Y	Y	nd	nd
Tyr	[23455667]	364	7	nd	nd	nd	Y	Y	Y	nd	nd
Tyr	[23455667]	364	8	nd	nd	nd	Y	Y	Y	nd	nd
Tyr	[23455667]	438	0	nd	nd	nd	Y	Y	Y	nd	nd
Tyr	[23455667]	438	1	nd	nd	nd	Y	Y	Y	nd	nd
Tyr	[23455667]	438	2	nd	nd	nd	Y	Y	Y	nd	nd
Tyr	[23455667]	438	3	nd	nd	nd	Y	Y	Y	nd	nd
Tyr	[23455667]	438	4	nd	nd	nd	Y	Y	Y	nd	nd
Tyr	[23455667]	438	5	nd	nd	nd	Y	Y	Y	nd	nd
Tyr	[23455667]	438	6	nd	nd	nd	Y	Y	Y	nd	nd
Tyr	[23455667]	438	7	nd	nd	nd	Y	Y	Y	nd	nd
Tyr	[23455667]	438	8	nd	nd	nd	Y	Y	Y	nd	nd
Tyr	[123455667]	466	0	nd	nd	nd	Y	Y	Y	nd	nd
Tyr	[123455667]	466	1	nd	nd	nd	Y	Y	Y	nd	nd
Tyr	[123455667]	466	2	nd	nd	nd	Y	Y	Y	nd	nd
Tyr	[123455667]	466	3	nd	nd	nd	Y	Y	Y	nd	nd
Tyr	[123455667]	466	4	nd	nd	nd	Y	Y	Y	nd	nd
Tyr	[123455667]	466	5	nd	nd	nd	Y	Y	Y	nd	nd
Tyr	[123455667]	466	6	nd	nd	nd	Y	Y	Y	nd	nd
Tyr	[123455667]	466	7	nd	nd	nd	Y	Y	Y	nd	nd
Tyr	[123455667]	466	8	nd	nd	nd	Y	Y	Y	nd	nd
Tyr	[123455667]	466	9	nd	nd	nd	Y	Y	Y	nd	nd
Val	[2345]	186	0	0.20	0.24	0.24	Y	Y	Y	0.23	0.02
Val	[2345]	186	1	0.10	0.12	0.11	Y	Y	Y	0.11	0.01
Val	[2345]	186	2	0.09	0.09	0.08	Y	Y	Y	0.09	0.00
Val	[2345]	186	3	0.14	0.12	0.12	Y	Y	Y	0.13	0.01
Val	[2345]	186	4	0.47	0.43	0.45	Y	Y	Y	0.45	0.02
Val	[2345]	260	0	0.21	0.24	0.23	Y	Y	Y	0.23	0.01
Val	[2345]	260	1	0.11	0.13	0.11	Y	Y	Y	0.12	0.01
Val	[2345]	260	2	0.09	0.09	0.09	Y	Y	Y	0.09	0.00
Val	[2345]	260	3	0.11	0.10	0.10	Y	Y	Y	0.10	0.01
Val	[2345]	260	4	0.48	0.44	0.47	Y	Y	Y	0.46	0.02
Val	[12345]	288	0	0.20	0.22	0.22	Y	Y	Y	0.21	0.01
Val	[12345]	288	1	0.10	0.12	0.10	Y	Y	Y	0.11	0.01
Val	[12345]	288	2	0.07	0.08	0.07	Y	Y	Y	0.08	0.00
Val	[12345]	288	3	0.08	0.07	0.07	Y	Y	Y	0.07	0.00
Val	[12345]	288	4	0.09	0.08	0.08	Y	Y	Y	0.09	0.01
Val	[12345]	288	5	0.46	0.42	0.45	Y	Y	Y	0.44	0.02
Val	[12]	302	0	<del>0.30</del>	0.35	0.34		Y	Y	0.34	0.01
Val	[12]	302	1	<del>0.17</del>	0.18	0.16		Y	Y	0.17	0.01
Val	[12]	302	2	<del>0.53</del>	0.48	0.51		Y	Y	0.49	0.02

#### **A.4. Table A.4 Mass Isotopomers from 100% 1-<sup>13</sup>C Ace ILE.**

Mass isotopomer distributions from 100% 1-<sup>13</sup>C acetate ILE (**Table A.4**). This table follows the scheme of **Table A.1**.

Table A.4 Mass isotopomers from 100%  $1^{13}\text{C}$  Ace ILE.

AA	Fragment	m/z	Mass (n in m+n)	Biological Replicates				Consider Replicate				Overall	
				Rep 1	Rep 2	Rep 3	Rep 4	1	2	3	4	Avg	SD
Ala	[23]	158	0	0.88	0.87	0.89	0.88	Y	Y	Y	Y	0.88	0.01
Ala	[23]	158	1	0.08	0.07	0.08	0.08	Y	Y	Y	Y	0.08	0.01
Ala	[23]	158	2	0.04	0.04	0.04	0.04	Y	Y	Y	Y	0.04	0.00
Ala	[23]	232	0	0.89	0.90	0.89	0.91	Y	Y	Y	Y	0.90	0.01
Ala	[23]	232	1	0.09	0.08	0.09	0.08	Y	Y	Y	Y	0.09	0.01
Ala	[23]	232	2	0.02	0.01	0.01	0.01	Y	Y	Y	Y	0.01	0.00
Ala	[123]	260	0	0.61	0.57	0.60	0.55	Y	Y	Y	Y	0.58	0.02
Ala	[123]	260	1	0.36	0.40	0.37	0.42	Y	Y	Y	Y	0.39	0.03
Ala	[123]	260	2	0.03	0.03	0.03	0.03	Y	Y	Y	Y	0.03	0.00
Ala	[123]	260	3	0.00	0.00	0.00	0.00	Y	Y	Y	Y	0.00	0.00
Arg	[2345]	340	0	0.27	nd	nd	nd	Y	Y	Y	Y	0.27	nd
Arg	[2345]	340	1	0.46	nd	nd	nd	Y	Y	Y	Y	0.46	nd
Arg	[2345]	340	2	0.22	nd	nd	nd	Y	Y	Y	Y	0.22	nd
Arg	[2345]	340	3	0.04	nd	nd	nd	Y	Y	Y	Y	0.04	nd
Arg	[2345]	340	4	0.02	nd	nd	nd	Y	Y	Y	Y	0.02	nd
Arg	[12345]	442	0	0.24	nd	nd	nd	Y	Y	Y	Y	0.24	nd
Arg	[12345]	442	1	0.30	nd	nd	nd	Y	Y	Y	Y	0.30	nd
Arg	[12345]	442	2	0.32	nd	nd	nd	Y	Y	Y	Y	0.32	nd
Arg	[12345]	442	3	0.12	nd	nd	nd	Y	Y	Y	Y	0.12	nd
Arg	[12345]	442	4	0.02	nd	nd	nd	Y	Y	Y	Y	0.02	nd
Arg	[12345]	442	5	0.00	nd	nd	nd	Y	Y	Y	Y	0.00	nd
Asp	[12]	302	0	0.63	0.59	0.61	0.58	Y	Y	Y	Y	0.60	0.02
Asp	[12]	302	1	0.35	0.39	0.37	0.40	Y	Y	Y	Y	0.38	0.02
Asp	[12]	302	2	0.02	0.02	0.02	0.02	Y	Y	Y	Y	0.02	0.00
Asp	[234]	316	0	0.60	0.57	0.60	0.56	Y	Y	Y	Y	0.58	0.02
Asp	[234]	316	1	0.35	0.38	0.36	0.39	Y	Y	Y	Y	0.37	0.02
Asp	[234]	316	2	0.04	0.03	0.04	0.03	Y	Y	Y	Y	0.03	0.00
Asp	[234]	316	3	0.01	0.01	0.01	0.01	Y	Y	Y	Y	0.01	0.00
Asp	[234]	390	0	0.61	0.59	0.60	0.58	Y	Y	Y	Y	0.60	0.02
Asp	[234]	390	1	0.35	0.38	0.36	0.39	Y	Y	Y	Y	0.37	0.02
Asp	[234]	390	2	0.03	0.03	0.03	0.03	Y	Y	Y	Y	0.03	0.00
Asp	[234]	390	3	0.01	0.00	0.00	0.00	Y	Y	Y	Y	0.00	0.00
Asp	[1234]	418	0	0.41	0.36	0.39	0.34	Y	Y	Y	Y	0.38	0.03
Asp	[1234]	418	1	0.45	0.50	0.46	0.51	Y	Y	Y	Y	0.48	0.03
Asp	[1234]	418	2	0.12	0.13	0.13	0.13	Y	Y	Y	Y	0.13	0.00
Asp	[1234]	418	3	0.02	0.01	0.01	0.01	Y	Y	Y	Y	0.01	0.00
Asp	[1234]	418	4	0.00	0.00	0.00	0.00	Y	Y	Y	Y	0.00	0.00
Glu	[2345]	272	0	0.39	0.33	0.37	0.31	Y	Y	Y		0.36	0.03
Glu	[2345]	272	1	0.54	0.60	0.56	0.62	Y	Y	Y		0.56	0.03
Glu	[2345]	272	2	0.06	0.05	0.06	0.05	Y	Y	Y		0.05	0.00
Glu	[2345]	272	3	0.02	0.02	0.02	0.01	Y	Y	Y		0.02	0.00
Glu	[2345]	272	4	0.00	0.00	0.00	0.00	Y	Y	Y		0.00	0.00
Glu	[2345]	330	0	0.39	0.32	0.36	0.28	Y	Y	Y		0.36	0.03
Glu	[2345]	330	1	0.56	0.63	0.58	0.66	Y	Y	Y		0.59	0.04
Glu	[2345]	330	2	0.04	0.04	0.04	0.04	Y	Y	Y		0.04	0.00
Glu	[2345]	330	3	0.01	0.01	0.01	0.01	Y	Y	Y		0.01	0.00
Glu	[2345]	330	4	0.00	0.00	0.00	0.00	Y	Y	Y		0.00	0.00
Glu	[12345]	432	0	0.35	0.29	0.33	0.27	Y	Y	Y		0.32	0.03
Glu	[12345]	432	1	0.35	0.37	0.35	0.38	Y	Y	Y		0.36	0.01
Glu	[12345]	432	2	0.27	0.31	0.28	0.32	Y	Y	Y		0.29	0.02
Glu	[12345]	432	3	0.02	0.02	0.03	0.02	Y	Y	Y		0.02	0.00
Glu	[12345]	432	4	0.01	0.01	0.00	0.00	Y	Y	Y		0.00	0.00
Glu	[12345]	432	5	0.00	0.00	0.00	0.00	Y	Y	Y		0.00	0.00
Gly	[2]	218	0	0.95	0.95	0.95	0.95	Y	Y	Y		0.95	0.00
Gly	[2]	218	1	0.05	0.05	0.05	0.05	Y	Y	Y		0.05	0.00
Gly	[12]	246	0	0.65	0.61	0.62	0.58	Y	Y	Y		0.63	0.02
Gly	[12]	246	1	0.34	0.37	0.36	0.41	Y	Y	Y		0.36	0.02
Gly	[12]	246	2	0.01	0.01	0.02	0.01	Y	Y	Y		0.02	0.00
His	[2345]	195	0	nd	nd	nd	nd	Y	Y	Y	Y	nd	nd
His	[2345]	195	1	nd	nd	nd	nd	Y	Y	Y	Y	nd	nd
His	[2345]	195	2	nd	nd	nd	nd	Y	Y	Y	Y	nd	nd
His	[2345]	195	3	nd	nd	nd	nd	Y	Y	Y	Y	nd	nd
His	[2345]	195	4	nd	nd	nd	nd	Y	Y	Y	Y	nd	nd
His	[23456]	338	0	nd	nd	nd	nd	Y	Y	Y	Y	nd	nd
His	[23456]	338	1	nd	nd	nd	nd	Y	Y	Y	Y	nd	nd
His	[23456]	338	2	nd	nd	nd	nd	Y	Y	Y	Y	nd	nd
His	[23456]	338	3	nd	nd	nd	nd	Y	Y	Y	Y	nd	nd
His	[23456]	338	4	nd	nd	nd	nd	Y	Y	Y	Y	nd	nd
His	[23456]	338	5	nd	nd	nd	nd	Y	Y	Y	Y	nd	nd
His	[123456]	440	0	nd	nd	nd	nd	Y	Y	Y	Y	nd	nd
His	[123456]	440	1	nd	nd	nd	nd	Y	Y	Y	Y	nd	nd
His	[123456]	440	2	nd	nd	nd	nd	Y	Y	Y	Y	nd	nd
His	[123456]	440	3	nd	nd	nd	nd	Y	Y	Y	Y	nd	nd
His	[123456]	440	4	nd	nd	nd	nd	Y	Y	Y	Y	nd	nd
His	[123456]	440	5	nd	nd	nd	nd	Y	Y	Y	Y	nd	nd
His	[123456]	440	6	nd	nd	nd	nd	Y	Y	Y	Y	nd	nd
Ile	[23456]	200	0	0.48	0.48	0.48	0.47	Y	Y	Y	Y	0.48	0.00
Ile	[23456]	200	1	0.37	0.39	0.38	0.40	Y	Y	Y	Y	0.38	0.01
Ile	[23456]	200	2	0.10	0.08	0.09	0.08	Y	Y	Y	Y	0.09	0.01
Ile	[23456]	200	3	0.04	0.03	0.04	0.03	Y	Y	Y	Y	0.04	0.00
Ile	[23456]	200	4	0.01	0.01	0.01	0.01	Y	Y	Y	Y	0.01	0.00
Ile	[23456]	200	5	0.00	0.00	0.00	0.00	Y	Y	Y	Y	0.00	0.00
Ile	[23456]	274	0	0.46	0.47	0.47	0.47	Y	Y	Y	Y	0.47	0.00
Ile	[23456]	274	1	0.37	0.39	0.38	0.41	Y	Y	Y	Y	0.39	0.01
Ile	[23456]	274	2	0.10	0.09	0.10	0.08	Y	Y	Y	Y	0.09	0.01



Table A.4 Mass isotopomers from 100% 1-13C Ace ILE.

AA	Fragment	m/z	Mass (n in m+n)	Biological Replicates				Consider Replicate				Overall	
				Rep 1	Rep 2	Rep 3	Rep 4	1	2	3	4	Avg	SD
Ile	[23456]	274	3	0.05	0.04	0.04	0.04	Y	Y	Y	Y	0.04	0.00
Ile	[23456]	274	4	0.01	0.01	0.01	0.01	Y	Y	Y	Y	0.01	0.00
Ile	[23456]	274	5	0.00	0.00	0.00	0.00	Y	Y	Y	Y	0.00	0.00
Ile	[12]	302	0	0.40	0.38	0.40	0.35	Y	Y	Y	Y	0.38	0.02
Ile	[12]	302	1	0.48	0.51	0.49	0.54	Y	Y	Y	Y	0.50	0.02
Ile	[12]	302	2	0.12	0.11	0.11	0.11	Y	Y	Y	Y	0.11	0.00
Leu	[23456]	200	0	0.73	0.77	0.75	0.79	Y	Y	Y	Y	0.76	0.02
Leu	[23456]	200	1	0.14	0.13	0.14	0.12	Y	Y	Y	Y	0.13	0.01
Leu	[23456]	200	2	0.07	0.06	0.07	0.05	Y	Y	Y	Y	0.06	0.01
Leu	[23456]	200	3	0.04	0.03	0.03	0.03	Y	Y	Y	Y	0.03	0.00
Leu	[23456]	200	4	0.01	0.01	0.01	0.01	Y	Y	Y	Y	0.01	0.00
Leu	[23456]	200	5	0.00	0.00	0.00	0.00	Y	Y	Y	Y	0.00	0.00
Leu	[23456]	274	0	0.74	0.78	0.77	0.80	Y	Y	Y	Y	0.77	0.02
Leu	[23456]	274	1	0.14	0.12	0.13	0.11	Y	Y	Y	Y	0.13	0.01
Leu	[23456]	274	2	0.07	0.06	0.06	0.05	Y	Y	Y	Y	0.06	0.01
Leu	[23456]	274	3	0.04	0.03	0.03	0.03	Y	Y	Y	Y	0.03	0.00
Leu	[23456]	274	4	0.01	0.01	0.01	0.01	Y	Y	Y	Y	0.01	0.00
Leu	[23456]	274	5	0.00	0.00	0.00	0.00	Y	Y	Y	Y	0.00	0.00
Leu	[12]	302	0	0.29	0.25	0.28	<del>0.21</del>	Y	Y	Y		0.28	0.02
Leu	[12]	302	1	0.63	0.69	0.65	<del>0.73</del>	Y	Y	Y		0.66	0.03
Leu	[12]	302	2	0.08	0.06	0.07	<del>0.06</del>	Y	Y	Y		0.07	0.01
Lys	[23456]	329	0	0.48	0.48	0.49	0.48	Y	Y	Y	Y	0.48	0.01
Lys	[23456]	329	1	0.35	0.40	0.36	0.41	Y	Y	Y	Y	0.38	0.03
Lys	[23456]	329	2	0.10	0.08	0.09	0.06	Y	Y	Y	Y	0.08	0.02
Lys	[23456]	329	3	0.05	0.03	0.04	0.04	Y	Y	Y	Y	0.04	0.01
Lys	[23456]	329	4	0.01	0.01	0.01	0.01	Y	Y	Y	Y	0.01	0.00
Lys	[23456]	329	5	0.00	0.00	0.00	0.00	Y	Y	Y	Y	0.00	0.00
Lys	[123456]	431	0	0.32	0.29	0.31	0.25	Y	Y	Y	Y	0.29	0.03
Lys	[123456]	431	1	0.39	0.44	0.40	0.46	Y	Y	Y	Y	0.42	0.03
Lys	[123456]	431	2	0.20	0.21	0.21	0.23	Y	Y	Y	Y	0.21	0.01
Lys	[123456]	431	3	0.05	0.04	0.05	0.04	Y	Y	Y	Y	0.04	0.01
Lys	[123456]	431	4	0.02	0.02	0.02	0.02	Y	Y	Y	Y	0.02	0.00
Lys	[123456]	431	5	0.01	0.01	0.01	0.00	Y	Y	Y	Y	0.01	0.00
Lys	[123456]	431	6	0.00	0.00	0.00	0.00	Y	Y	Y	Y	0.00	0.00
Lys	[123456]	488	0	0.34	0.31	0.33	0.30	Y	Y	Y	Y	0.32	0.02
Lys	[123456]	488	1	0.39	0.43	0.40	0.43	Y	Y	Y	Y	0.41	0.02
Lys	[123456]	488	2	0.19	0.20	0.19	0.21	Y	Y	Y	Y	0.20	0.01
Lys	[123456]	488	3	0.06	0.04	0.05	0.04	Y	Y	Y	Y	0.05	0.01
Lys	[123456]	488	4	0.02	0.02	0.02	0.02	Y	Y	Y	Y	0.02	0.00
Lys	[123456]	488	5	0.00	0.01	0.00	0.00	Y	Y	Y	Y	0.00	0.00
Lys	[123456]	488	6	0.00	0.00	0.00	0.00	Y	Y	Y	Y	0.00	0.00
Met	[2345]	218	0	0.57	0.55	0.56	0.54	Y	Y	Y	Y	0.55	0.01
Met	[2345]	218	1	0.36	0.39	0.37	0.40	Y	Y	Y	Y	0.38	0.02
Met	[2345]	218	2	0.06	0.05	0.05	0.05	Y	Y	Y	Y	0.05	0.00
Met	[2345]	218	3	0.01	0.01	0.01	0.01	Y	Y	Y	Y	0.01	0.00
Met	[2345]	218	4	0.00	0.00	0.00	0.00	Y	Y	Y	Y	0.00	0.00
Met	[2345]	292	0	0.56	0.55	0.56	0.54	Y	Y	Y	Y	0.55	0.01
Met	[2345]	292	1	0.37	0.39	0.38	0.40	Y	Y	Y	Y	0.38	0.01
Met	[2345]	292	2	0.06	0.06	0.05	0.05	Y	Y	Y	Y	0.05	0.00
Met	[2345]	292	3	0.01	0.01	0.01	0.01	Y	Y	Y	Y	0.01	0.00
Met	[2345]	292	4	0.00	0.00	0.00	0.00	Y	Y	Y	Y	0.00	0.00
Met	[12345]	320	0	0.38	0.34	0.36	0.31	Y	Y	Y	Y	0.35	0.03
Met	[12345]	320	1	0.45	0.49	0.46	0.50	Y	Y	Y	Y	0.47	0.02
Met	[12345]	320	2	0.14	0.15	0.15	0.16	Y	Y	Y	Y	0.15	0.01
Met	[12345]	320	3	0.02	0.02	0.03	0.03	Y	Y	Y	Y	0.02	0.00
Met	[12345]	320	4	0.01	0.01	0.01	0.00	Y	Y	Y	Y	0.01	0.00
Met	[12345]	320	5	0.00	0.00	0.00	0.00	Y	Y	Y	Y	0.00	0.00
Phe	[23455667]	234	0	0.34	0.33	0.34	0.31	Y	Y	Y	Y	0.33	0.01
Phe	[23455667]	234	1	0.34	0.36	0.34	0.38	Y	Y	Y	Y	0.36	0.02
Phe	[23455667]	234	2	0.18	0.19	0.18	0.19	Y	Y	Y	Y	0.19	0.00
Phe	[23455667]	234	3	0.07	0.06	0.06	0.06	Y	Y	Y	Y	0.06	0.00
Phe	[23455667]	234	4	0.04	0.03	0.04	0.03	Y	Y	Y	Y	0.04	0.00
Phe	[23455667]	234	5	0.02	0.02	0.02	0.02	Y	Y	Y	Y	0.02	0.00
Phe	[23455667]	234	6	0.01	0.01	0.01	0.01	Y	Y	Y	Y	0.01	0.00
Phe	[23455667]	234	7	0.00	0.00	0.00	0.00	Y	Y	Y	Y	0.00	0.00
Phe	[23455667]	234	8	0.00	0.00	0.00	0.00	Y	Y	Y	Y	0.00	0.00
Phe	[12]	302	0	0.58	0.56	0.57	0.54	Y	Y	Y	Y	0.57	0.02
Phe	[12]	302	1	0.39	0.41	0.40	0.43	Y	Y	Y	Y	0.41	0.02
Phe	[12]	302	2	0.03	0.03	0.03	0.03	Y	Y	Y	Y	0.03	0.00
Phe	[123455667]	336	0	0.27	0.24	0.26	0.23	Y	Y	Y	Y	0.25	0.02
Phe	[123455667]	336	1	0.27	0.29	0.28	0.30	Y	Y	Y	Y	0.29	0.01
Phe	[123455667]	336	2	0.24	0.26	0.25	0.27	Y	Y	Y	Y	0.26	0.01
Phe	[123455667]	336	3	0.12	0.12	0.12	0.13	Y	Y	Y	Y	0.12	0.00
Phe	[123455667]	336	4	0.05	0.04	0.05	0.04	Y	Y	Y	Y	0.05	0.00
Phe	[123455667]	336	5	0.03	0.02	0.03	0.02	Y	Y	Y	Y	0.02	0.00
Phe	[123455667]	336	6	0.01	0.01	0.01	0.01	Y	Y	Y	Y	0.01	0.00
Phe	[123455667]	336	7	0.00	0.00	0.00	0.00	Y	Y	Y	Y	0.00	0.00
Phe	[123455667]	336	8	0.00	0.00	0.00	0.00	Y	Y	Y	Y	0.00	0.00
Phe	[123455667]	336	9	0.00	0.00	0.00	0.00	Y	Y	Y	Y	0.00	0.00
Pro	[2345]	184	0	0.38	0.32	0.36	<del>0.30</del>	Y	Y	Y		0.35	0.03
Pro	[2345]	184	1	0.53	0.59	0.55	<del>0.62</del>	Y	Y	Y		0.56	0.03
Pro	[2345]	184	2	0.07	0.06	0.07	<del>0.06</del>	Y	Y	Y		0.07	0.00
Pro	[2345]	184	3	0.02	0.02	0.02	<del>0.02</del>	Y	Y	Y		0.02	0.00
Pro	[2345]	184	4	0.00	0.00	0.00	<del>0.00</del>	Y	Y	Y		0.00	0.00
Pro	[2345]	258	0	0.38	0.32	0.36	<del>0.29</del>	Y	Y	Y		0.35	0.03

Table A.4 Mass isotopomers from 100% <sup>13</sup>C Ace ILE.

AA	Fragment	m/z	Mass (n in m+n)	Biological Replicates				Consider Replicate				Overall	
				Rep 1	Rep 2	Rep 3	Rep 4	1	2	3	4	Avg	SD
Pro	[2345]	258	1	0.53	0.59	0.55	0.63	Y	Y	Y		0.56	0.03
Pro	[2345]	258	2	0.07	0.07	0.07	0.06	Y	Y	Y		0.07	0.00
Pro	[2345]	258	3	0.02	0.02	0.02	0.02	Y	Y	Y		0.02	0.00
Pro	[2345]	258	4	0.00	0.00	0.00	0.00	Y	Y	Y		0.00	0.00
Pro	[12345]	286	0	0.34	0.29	0.31	0.26	Y	Y	Y	Y	0.30	0.03
Pro	[12345]	286	1	0.33	0.35	0.34	0.36	Y	Y	Y	Y	0.35	0.01
Pro	[12345]	286	2	0.26	0.29	0.27	0.29	Y	Y	Y	Y	0.28	0.02
Pro	[12345]	286	3	0.05	0.05	0.05	0.06	Y	Y	Y	Y	0.05	0.00
Pro	[12345]	286	4	0.02	0.02	0.02	0.02	Y	Y	Y	Y	0.02	0.00
Pro	[12345]	286	5	0.00	0.00	0.00	0.01	Y	Y	Y	Y	0.00	0.00
Ser	[23]	288	0	0.91	0.92	0.92	0.92	Y	Y	Y	Y	0.92	0.00
Ser	[23]	288	1	0.08	0.07	0.07	0.07	Y	Y	Y	Y	0.07	0.01
Ser	[23]	288	2	0.01	0.01	0.01	0.01	Y	Y	Y	Y	0.01	0.00
Ser	[12]	302	0	0.65	0.61	0.64	0.59	Y	Y	Y	Y	0.62	0.03
Ser	[12]	302	1	0.34	0.37	0.34	0.40	Y	Y	Y	Y	0.36	0.03
Ser	[12]	302	2	0.02	0.01	0.02	0.02	Y	Y	Y	Y	0.02	0.00
Ser	[23]	362	0	0.91	0.92	0.91	0.91	Y	Y	Y	Y	0.91	0.00
Ser	[23]	362	1	0.08	0.08	0.08	0.08	Y	Y	Y	Y	0.08	0.00
Ser	[23]	362	2	0.01	0.01	0.01	0.01	Y	Y	Y	Y	0.01	0.00
Ser	[123]	390	0	0.62	0.58	0.61	0.56	Y	Y	Y	Y	0.59	0.03
Ser	[123]	390	1	0.35	0.39	0.36	0.41	Y	Y	Y	Y	0.38	0.03
Ser	[123]	390	2	0.03	0.03	0.03	0.03	Y	Y	Y	Y	0.03	0.00
Ser	[123]	390	3	0.00	0.00	0.00	0.00	Y	Y	Y	Y	0.00	0.00
Thr	[234]	376	0	0.58	0.56	0.57	0.55	Y	Y	Y	Y	0.57	0.02
Thr	[234]	376	1	0.36	0.40	0.38	0.41	Y	Y	Y	Y	0.39	0.02
Thr	[234]	376	2	0.04	0.04	0.04	0.04	Y	Y	Y	Y	0.04	0.00
Thr	[234]	376	3	0.01	0.01	0.01	0.01	Y	Y	Y	Y	0.01	0.00
Thr	[1234]	404	0	0.38	0.32	0.36	0.29	Y	Y	Y		0.35	0.03
Thr	[1234]	404	1	0.46	0.52	0.48	0.53	Y	Y	Y		0.48	0.03
Thr	[1234]	404	2	0.15	0.14	0.14	0.16	Y	Y	Y		0.14	0.00
Thr	[1234]	404	3	0.02	0.02	0.02	0.02	Y	Y	Y		0.02	0.00
Thr	[1234]	404	4	0.00	0.00	0.00	0.00	Y	Y	Y		0.00	0.00
Tyr	[12]	302	0	0.58	0.56	0.57	0.54	Y	Y	Y	Y	0.56	0.02
Tyr	[12]	302	1	0.40	0.42	0.41	0.44	Y	Y	Y	Y	0.42	0.02
Tyr	[12]	302	2	0.02	0.02	0.02	0.02	Y	Y	Y	Y	0.02	0.00
Tyr	[23455667]	364	0	0.34	0.34	0.34	0.32	Y	Y	Y	Y	0.34	0.01
Tyr	[23455667]	364	1	0.36	0.38	0.37	0.38	Y	Y	Y	Y	0.37	0.01
Tyr	[23455667]	364	2	0.19	0.20	0.19	0.22	Y	Y	Y	Y	0.20	0.02
Tyr	[23455667]	364	3	0.06	0.04	0.06	0.04	Y	Y	Y	Y	0.05	0.01
Tyr	[23455667]	364	4	0.04	0.03	0.03	0.02	Y	Y	Y	Y	0.03	0.01
Tyr	[23455667]	364	5	0.01	0.01	0.02	0.01	Y	Y	Y	Y	0.01	0.01
Tyr	[23455667]	364	6	0.00	0.00	0.00	0.00	Y	Y	Y	Y	0.00	0.00
Tyr	[23455667]	364	7	0.00	0.00	0.00	0.00	Y	Y	Y	Y	0.00	0.00
Tyr	[23455667]	364	8	0.00	0.00	0.00	0.00	Y	Y	Y	Y	0.00	0.00
Tyr	[23455667]	438	0	0.35	0.33	0.35	0.35	Y	Y	Y	Y	0.34	0.01
Tyr	[23455667]	438	1	0.36	0.38	0.37	0.34	Y	Y	Y	Y	0.36	0.02
Tyr	[23455667]	438	2	0.18	0.21	0.19	0.21	Y	Y	Y	Y	0.20	0.02
Tyr	[23455667]	438	3	0.06	0.03	0.05	0.06	Y	Y	Y	Y	0.05	0.02
Tyr	[23455667]	438	4	0.03	0.04	0.03	0.03	Y	Y	Y	Y	0.03	0.00
Tyr	[23455667]	438	5	0.02	0.01	0.01	0.01	Y	Y	Y	Y	0.01	0.00
Tyr	[23455667]	438	6	0.00	0.00	0.00	0.00	Y	Y	Y	Y	0.00	0.00
Tyr	[23455667]	438	7	0.00	0.00	0.00	0.00	Y	Y	Y	Y	0.00	0.00
Tyr	[23455667]	438	8	0.00	0.00	0.00	0.00	Y	Y	Y	Y	0.00	0.00
Tyr	[123455667]	466	0	0.26	0.24	0.26	0.24	Y	Y	Y	Y	0.25	0.01
Tyr	[123455667]	466	1	0.29	0.32	0.29	0.29	Y	Y	Y	Y	0.30	0.01
Tyr	[123455667]	466	2	0.25	0.27	0.27	0.30	Y	Y	Y	Y	0.27	0.02
Tyr	[123455667]	466	3	0.12	0.11	0.12	0.13	Y	Y	Y	Y	0.12	0.01
Tyr	[123455667]	466	4	0.04	0.04	0.04	0.03	Y	Y	Y	Y	0.04	0.01
Tyr	[123455667]	466	5	0.02	0.02	0.02	0.01	Y	Y	Y	Y	0.02	0.00
Tyr	[123455667]	466	6	0.01	0.01	0.00	0.01	Y	Y	Y	Y	0.01	0.00
Tyr	[123455667]	466	7	0.00	0.00	0.00	0.00	Y	Y	Y	Y	0.00	0.00
Tyr	[123455667]	466	8	0.00	0.00	0.00	0.00	Y	Y	Y	Y	0.00	0.00
Tyr	[123455667]	466	9	0.00	0.00	0.00	0.00	Y	Y	Y	Y	0.00	0.00
Val	[2345]	186	0	0.75	0.78	0.75	0.77	Y	Y	Y	Y	0.76	0.01
Val	[2345]	186	1	0.14	0.13	0.13	0.12	Y	Y	Y	Y	0.13	0.01
Val	[2345]	186	2	0.06	0.05	0.06	0.05	Y	Y	Y	Y	0.06	0.01
Val	[2345]	186	3	0.04	0.04	0.05	0.05	Y	Y	Y	Y	0.05	0.01
Val	[2345]	186	4	0.01	0.01	0.01	0.01	Y	Y	Y	Y	0.01	0.00
Val	[2345]	260	0	0.75	0.78	0.76	0.80	Y	Y	Y	Y	0.77	0.02
Val	[2345]	260	1	0.16	0.14	0.15	0.12	Y	Y	Y	Y	0.14	0.02
Val	[2345]	260	2	0.07	0.06	0.07	0.05	Y	Y	Y	Y	0.06	0.01
Val	[2345]	260	3	0.02	0.02	0.02	0.02	Y	Y	Y	Y	0.02	0.00
Val	[2345]	260	4	0.00	0.00	0.01	0.01	Y	Y	Y	Y	0.01	0.00
Val	[12345]	288	0	0.49	0.47	0.48	0.46	Y	Y	Y	Y	0.48	0.01
Val	[12345]	288	1	0.38	0.42	0.39	0.43	Y	Y	Y	Y	0.41	0.02
Val	[12345]	288	2	0.08	0.07	0.08	0.07	Y	Y	Y	Y	0.08	0.01
Val	[12345]	288	3	0.03	0.03	0.03	0.03	Y	Y	Y	Y	0.03	0.00
Val	[12345]	288	4	0.01	0.01	0.01	0.01	Y	Y	Y	Y	0.01	0.00
Val	[12345]	288	5	0.00	0.00	0.00	0.00	Y	Y	Y	Y	0.00	0.00
Val	[12]	302	0	0.62	0.61	0.62	0.60	Y	Y	Y	Y	0.61	0.01
Val	[12]	302	1	0.35	0.36	0.35	0.38	Y	Y	Y	Y	0.36	0.01
Val	[12]	302	2	0.03	0.03	0.03	0.02	Y	Y	Y	Y	0.03	0.00

### **A.5. Table A.5 Mass Isotopomers from 100% 4-<sup>13</sup>C Asp ILE.**

Mass isotopomer distributions from 100% 4-<sup>13</sup>C aspartate ILE (**Table A.5**).

This table follows the scheme of **Table A.1**.

Table A.5 Mass isotopomers from 100% 4-<sup>13</sup>C Asp ILE.

AA	Fragment	m/z	Mass (n in m+n)	Biological Replicates				Consider Replicate				Overall	
				Rep 1	Rep 2	Rep 3	Rep 4	1	2	3	4	Avg	SD
Ala	[23]	158	0	0.92	0.92	0.92	0.92	Y	Y	Y	Y	0.92	0.00
Ala	[23]	158	1	0.04	0.05	0.05	0.05	Y	Y	Y	Y	0.05	0.00
Ala	[23]	158	2	0.03	0.03	0.03	0.03	Y	Y	Y	Y	0.03	0.00
Ala	[23]	232	0	0.95	0.95	0.95	0.95	Y	Y	Y	Y	0.95	0.00
Ala	[23]	232	1	0.04	0.04	0.04	0.05	Y	Y	Y	Y	0.04	0.00
Ala	[23]	232	2	0.00	0.00	0.00	0.00	Y	Y	Y	Y	0.00	0.00
Ala	[123]	260	0	0.89	0.89	0.90	0.90	Y	Y	Y	Y	0.89	0.01
Ala	[123]	260	1	0.11	0.11	0.09	0.10	Y	Y	Y	Y	0.10	0.01
Ala	[123]	260	2	0.00	0.01	0.00	0.00	Y	Y	Y	Y	0.00	0.00
Ala	[123]	260	3	0.00	0.00	0.00	0.00	Y	Y	Y	Y	0.00	0.00
Arg	[2345]	340	0	0.81	0.80	0.81	0.81	Y	Y	Y	Y	0.81	0.01
Arg	[2345]	340	1	0.15	0.16	0.14	0.15	Y	Y	Y	Y	0.15	0.00
Arg	[2345]	340	2	0.02	0.02	0.02	0.02	Y	Y	Y	Y	0.02	0.00
Arg	[2345]	340	3	0.01	0.01	0.01	0.01	Y	Y	Y	Y	0.01	0.00
Arg	[2345]	340	4	0.01	0.01	0.01	0.01	Y	Y	Y	Y	0.01	0.00
Arg	[12345]	442	0	0.69	0.69	0.73	0.72	Y	Y	Y	Y	0.71	0.02
Arg	[12345]	442	1	0.26	0.25	0.22	0.23	Y	Y	Y	Y	0.24	0.02
Arg	[12345]	442	2	0.05	0.05	0.04	0.04	Y	Y	Y	Y	0.05	0.01
Arg	[12345]	442	3	0.00	0.00	0.00	0.00	Y	Y	Y	Y	0.00	0.00
Arg	[12345]	442	4	0.00	0.00	0.00	0.00	Y	Y	Y	Y	0.00	0.00
Arg	[12345]	442	5	0.00	0.00	0.00	0.00	Y	Y	Y	Y	0.00	0.00
Asp	[12]	302	0	0.94	0.95	0.95	0.94	Y	Y	Y	Y	0.95	0.00
Asp	[12]	302	1	0.05	0.05	0.05	0.05	Y	Y	Y	Y	0.05	0.00
Asp	[12]	302	2	0.00	0.01	0.00	0.00	Y	Y	Y	Y	0.00	0.00
Asp	[234]	316	0	0.73	0.75	0.79	0.79	Y	Y	Y	Y	0.76	0.03
Asp	[234]	316	1	0.26	0.23	0.19	0.19	Y	Y	Y	Y	0.22	0.03
Asp	[234]	316	2	0.01	0.01	0.01	0.01	Y	Y	Y	Y	0.01	0.00
Asp	[234]	316	3	0.01	0.01	0.01	0.01	Y	Y	Y	Y	0.01	0.00
Asp	[234]	390	0	0.75	0.76	0.81	0.81	Y	Y	Y	Y	0.78	0.03
Asp	[234]	390	1	0.25	0.23	0.18	0.19	Y	Y	Y	Y	0.21	0.03
Asp	[234]	390	2	0.01	0.01	0.01	0.01	Y	Y	Y	Y	0.01	0.00
Asp	[234]	390	3	0.00	0.00	0.00	0.00	Y	Y	Y	Y	0.00	0.00
Asp	[1234]	418	0	0.71	0.73	0.78	0.77	Y	Y	Y	Y	0.75	0.03
Asp	[1234]	418	1	0.28	0.26	0.21	0.21	Y	Y	Y	Y	0.24	0.03
Asp	[1234]	418	2	0.01	0.01	0.01	0.01	Y	Y	Y	Y	0.01	0.00
Asp	[1234]	418	3	0.00	0.00	0.00	0.00	Y	Y	Y	Y	0.00	0.00
Asp	[1234]	418	4	0.00	0.00	0.00	0.00	Y	Y	Y	Y	0.00	0.00
Glu	[2345]	272	0	0.89	0.89	0.89	0.89	Y	Y	Y	Y	0.89	0.00
Glu	[2345]	272	1	0.09	0.09	0.09	0.09	Y	Y	Y	Y	0.09	0.00
Glu	[2345]	272	2	0.01	0.01	0.01	0.02	Y	Y	Y	Y	0.01	0.00
Glu	[2345]	272	3	0.00	0.00	0.00	0.00	Y	Y	Y	Y	0.00	0.00
Glu	[2345]	272	4	0.00	0.00	0.00	0.00	Y	Y	Y	Y	0.00	0.00
Glu	[2345]	330	0	0.91	0.91	0.91	0.91	Y	Y	Y	Y	0.91	0.00
Glu	[2345]	330	1	0.08	0.08	0.08	0.08	Y	Y	Y	Y	0.08	0.00
Glu	[2345]	330	2	0.01	0.01	0.01	0.01	Y	Y	Y	Y	0.01	0.00
Glu	[2345]	330	3	0.00	0.00	0.00	0.00	Y	Y	Y	Y	0.00	0.00
Glu	[2345]	330	4	0.00	0.00	0.00	0.00	Y	Y	Y	Y	0.00	0.00
Glu	[12345]	432	0	0.74	0.75	0.79	0.79	Y	Y	Y	Y	0.77	0.02
Glu	[12345]	432	1	0.24	0.23	0.19	0.20	Y	Y	Y	Y	0.21	0.02
Glu	[12345]	432	2	0.02	0.02	0.02	0.02	Y	Y	Y	Y	0.02	0.00
Glu	[12345]	432	3	0.00	0.00	0.00	0.00	Y	Y	Y	Y	0.00	0.00
Glu	[12345]	432	4	0.00	0.00	0.00	0.00	Y	Y	Y	Y	0.00	0.00
Glu	[12345]	432	5	0.00	0.00	0.00	0.00	Y	Y	Y	Y	0.00	0.00
Gly	[2]	218	0	0.98	0.98	0.98	0.97	Y	Y	Y	Y	0.98	0.00
Gly	[2]	218	1	0.02	0.02	0.02	0.03	Y	Y	Y	Y	0.02	0.00
Gly	[12]	246	0	0.93	0.93	0.94	0.93	Y	Y	Y	Y	0.93	0.00
Gly	[12]	246	1	0.07	0.07	0.06	0.06	Y	Y	Y	Y	0.06	0.00
Gly	[12]	246	2	0.00	0.00	0.00	0.00	Y	Y	Y	Y	0.00	0.00
His	[2345]	195	0	0.81	0.78	0.81	0.80	Y	Y	Y	Y	0.80	0.01
His	[2345]	195	1	0.16	0.18	0.16	0.16	Y	Y	Y	Y	0.17	0.01
His	[2345]	195	2	0.02	0.03	0.02	0.03	Y	Y	Y	Y	0.03	0.00
His	[2345]	195	3	0.00	0.01	0.00	0.01	Y	Y	Y	Y	0.00	0.00
His	[2345]	195	4	0.00	0.00	0.00	0.00	Y	Y	Y	Y	0.00	0.00
His	[23456]	338	0	0.81	0.81	nd	0.79	Y	Y	Y	Y	0.80	0.01
His	[23456]	338	1	0.14	0.20	nd	0.14	Y	Y	Y	Y	0.16	0.04
His	[23456]	338	2	0.03	0.02	nd	0.04	Y	Y	Y	Y	0.03	0.01
His	[23456]	338	3	0.02	-0.04	nd	0.03	Y	Y	Y	Y	0.00	0.04
His	[23456]	338	4	0.00	0.00	nd	0.01	Y	Y	Y	Y	0.00	0.00
His	[23456]	338	5	0.00	0.00	nd	-0.01	Y	Y	Y	Y	0.00	0.00
His	[123456]	440	0	0.80	0.78	0.80	0.79	Y	Y	Y	Y	0.79	0.01
His	[123456]	440	1	0.17	0.18	0.17	0.17	Y	Y	Y	Y	0.17	0.01
His	[123456]	440	2	0.03	0.02	0.03	0.03	Y	Y	Y	Y	0.03	0.01
His	[123456]	440	3	0.01	0.02	0.01	0.01	Y	Y	Y	Y	0.01	0.01
His	[123456]	440	4	0.00	0.00	0.00	0.00	Y	Y	Y	Y	0.00	0.00
His	[123456]	440	5	0.00	0.00	0.00	0.00	Y	Y	Y	Y	0.00	0.00
His	[123456]	440	6	0.00	0.00	0.00	0.00	Y	Y	Y	Y	0.00	0.00
Ile	[23456]	200	0	0.67	0.68	0.72	0.71	Y	Y	Y	Y	0.69	0.02
Ile	[23456]	200	1	0.29	0.28	0.25	0.25	Y	Y	Y	Y	0.27	0.02
Ile	[23456]	200	2	0.03	0.03	0.03	0.03	Y	Y	Y	Y	0.03	0.00
Ile	[23456]	200	3	0.00	0.01	0.00	0.00	Y	Y	Y	Y	0.00	0.00
Ile	[23456]	200	4	0.00	0.00	0.00	0.00	Y	Y	Y	Y	0.00	0.00
Ile	[23456]	200	5	0.00	0.00	0.00	0.00	Y	Y	Y	Y	0.00	0.00
Ile	[23456]	274	0	0.68	0.68	0.72	0.72	Y	Y	Y	Y	0.70	0.02
Ile	[23456]	274	1	0.29	0.28	0.24	0.25	Y	Y	Y	Y	0.26	0.02
Ile	[23456]	274	2	0.03	0.03	0.03	0.03	Y	Y	Y	Y	0.03	0.00

Table A.5 Mass isotopomers from 100% 4-<sup>13</sup>C Asp ILE.

AA	Fragment	m/z	Mass (n in m+n)	Biological Replicates				Consider Replicate				Overall	
				Rep 1	Rep 2	Rep 3	Rep 4	1	2	3	4	Avg	SD
Ile	[23456]	274	3	0.00	0.00	0.00	0.01	Y	Y	Y	Y	0.00	0.00
Ile	[23456]	274	4	0.00	0.00	0.00	0.00	Y	Y	Y	Y	0.00	0.00
Ile	[23456]	274	5	0.00	0.00	0.00	0.00	Y	Y	Y	Y	0.00	0.00
Ile	[12]	302	0	0.78	0.78	0.81	0.81	Y	Y	Y	Y	0.80	0.01
Ile	[12]	302	1	0.20	0.20	0.17	0.18	Y	Y	Y	Y	0.19	0.02
Ile	[12]	302	2	0.02	0.02	0.02	0.02	Y	Y	Y	Y	0.02	0.00
Leu	[23456]	200	0	0.85	0.84	0.84	0.84	Y	Y	Y	Y	0.84	0.01
Leu	[23456]	200	1	0.12	0.13	0.13	0.13	Y	Y	Y	Y	0.12	0.01
Leu	[23456]	200	2	0.03	0.03	0.03	0.03	Y	Y	Y	Y	0.03	0.00
Leu	[23456]	200	3	0.00	0.00	0.00	0.00	Y	Y	Y	Y	0.00	0.00
Leu	[23456]	200	4	0.00	0.00	0.00	0.00	Y	Y	Y	Y	0.00	0.00
Leu	[23456]	200	5	0.00	0.00	0.00	0.00	Y	Y	Y	Y	0.00	0.00
Leu	[23456]	274	0	0.87	0.85	0.85	0.85	Y	Y	Y	Y	0.86	0.01
Leu	[23456]	274	1	0.12	0.12	0.12	0.13	Y	Y	Y	Y	0.12	0.01
Leu	[23456]	274	2	0.02	0.02	0.02	0.02	Y	Y	Y	Y	0.02	0.00
Leu	[23456]	274	3	0.00	0.00	0.00	0.00	Y	Y	Y	Y	0.00	0.00
Leu	[23456]	274	4	0.00	0.00	0.00	0.00	Y	Y	Y	Y	0.00	0.00
Leu	[23456]	274	5	0.00	0.00	0.00	0.00	Y	Y	Y	Y	0.00	0.00
Leu	[12]	302	0	0.89	0.87	0.88	0.87	Y	Y	Y	Y	0.88	0.01
Leu	[12]	302	1	0.10	0.11	0.10	0.11	Y	Y	Y	Y	0.10	0.01
Leu	[12]	302	2	0.02	0.02	0.02	0.02	Y	Y	Y	Y	0.02	0.00
Lys	[23456]	329	0	0.69	0.69	0.72	0.72	Y	Y	Y	Y	0.71	0.02
Lys	[23456]	329	1	0.27	0.27	0.23	0.24	Y	Y	Y	Y	0.25	0.02
Lys	[23456]	329	2	0.03	0.03	0.03	0.03	Y	Y	Y	Y	0.03	0.00
Lys	[23456]	329	3	0.01	0.01	0.01	0.01	Y	Y	Y	Y	0.01	0.00
Lys	[23456]	329	4	0.00	0.00	0.00	0.00	Y	Y	Y	Y	0.00	0.00
Lys	[23456]	329	5	0.00	0.00	0.00	0.00	Y	Y	Y	Y	0.00	0.00
Lys	[123456]	431	0	0.67	0.67	0.71	0.71	Y	Y	Y	Y	0.69	0.02
Lys	[123456]	431	1	0.27	0.27	0.23	0.23	Y	Y	Y	Y	0.25	0.02
Lys	[123456]	431	2	0.05	0.05	0.04	0.05	Y	Y	Y	Y	0.05	0.00
Lys	[123456]	431	3	0.01	0.01	0.01	0.01	Y	Y	Y	Y	0.01	0.00
Lys	[123456]	431	4	0.00	0.00	0.00	0.00	Y	Y	Y	Y	0.00	0.00
Lys	[123456]	431	5	0.00	0.00	0.00	0.00	Y	Y	Y	Y	0.00	0.00
Lys	[123456]	431	6	0.00	0.00	0.00	0.00	Y	Y	Y	Y	0.00	0.00
Lys	[123456]	488	0	0.67	0.68	0.71	0.71	Y	Y	Y	Y	0.69	0.02
Lys	[123456]	488	1	0.27	0.26	0.24	0.24	Y	Y	Y	Y	0.25	0.02
Lys	[123456]	488	2	0.05	0.05	0.05	0.05	Y	Y	Y	Y	0.05	0.00
Lys	[123456]	488	3	0.01	0.01	0.01	0.01	Y	Y	Y	Y	0.01	0.00
Lys	[123456]	488	4	0.00	0.00	0.00	0.00	Y	Y	Y	Y	0.00	0.00
Lys	[123456]	488	5	0.00	0.00	0.00	0.00	Y	Y	Y	Y	0.00	0.00
Lys	[123456]	488	6	0.00	0.00	0.00	0.00	Y	Y	Y	Y	0.00	0.00
Met	[2345]	218	0	0.72	0.73	0.78	0.77	Y	Y	Y	Y	0.75	0.03
Met	[2345]	218	1	0.26	0.25	0.21	0.21	Y	Y	Y	Y	0.23	0.03
Met	[2345]	218	2	0.02	0.02	0.01	0.01	Y	Y	Y	Y	0.01	0.00
Met	[2345]	218	3	0.00	0.00	0.00	0.00	Y	Y	Y	Y	0.00	0.00
Met	[2345]	218	4	0.00	0.00	0.00	0.00	Y	Y	Y	Y	0.00	0.00
Met	[2345]	292	0	0.72	0.73	0.78	0.78	Y	Y	Y	Y	0.75	0.03
Met	[2345]	292	1	0.27	0.25	0.21	0.21	Y	Y	Y	Y	0.23	0.03
Met	[2345]	292	2	0.01	0.01	0.01	0.01	Y	Y	Y	Y	0.01	0.00
Met	[2345]	292	3	0.00	0.00	0.00	0.00	Y	Y	Y	Y	0.00	0.00
Met	[2345]	292	4	0.00	0.00	0.00	0.00	Y	Y	Y	Y	0.00	0.00
Met	[12345]	320	0	0.69	0.70	0.75	0.75	Y	Y	Y	Y	0.72	0.03
Met	[12345]	320	1	0.29	0.27	0.23	0.23	Y	Y	Y	Y	0.26	0.03
Met	[12345]	320	2	0.02	0.02	0.02	0.02	Y	Y	Y	Y	0.02	0.00
Met	[12345]	320	3	0.00	0.00	0.00	0.00	Y	Y	Y	Y	0.00	0.00
Met	[12345]	320	4	0.00	0.00	0.00	0.00	Y	Y	Y	Y	0.00	0.00
Met	[12345]	320	5	0.00	0.00	0.00	0.00	Y	Y	Y	Y	0.00	0.00
Phe	[23455667]	234	0	0.75	0.73	0.74	0.74	Y	Y	Y	Y	0.74	0.01
Phe	[23455667]	234	1	0.20	0.21	0.20	0.20	Y	Y	Y	Y	0.20	0.00
Phe	[23455667]	234	2	0.04	0.05	0.04	0.05	Y	Y	Y	Y	0.04	0.00
Phe	[23455667]	234	3	0.01	0.01	0.01	0.01	Y	Y	Y	Y	0.01	0.00
Phe	[23455667]	234	4	0.00	0.00	0.00	0.00	Y	Y	Y	Y	0.00	0.00
Phe	[23455667]	234	5	0.00	0.00	0.00	0.00	Y	Y	Y	Y	0.00	0.00
Phe	[23455667]	234	6	0.00	0.00	0.00	0.00	Y	Y	Y	Y	0.00	0.00
Phe	[23455667]	234	7	0.00	0.00	0.00	0.00	Y	Y	Y	Y	0.00	0.00
Phe	[23455667]	234	8	0.00	0.00	0.00	0.00	Y	Y	Y	Y	0.00	0.00
Phe	[12]	302	0	0.93	0.92	0.93	0.93	Y	Y	Y	Y	0.93	0.00
Phe	[12]	302	1	0.07	0.07	0.06	0.07	Y	Y	Y	Y	0.07	0.00
Phe	[12]	302	2	0.01	0.01	0.01	0.01	Y	Y	Y	Y	0.01	0.00
Phe	[123455667]	336	0	0.72	0.70	0.72	0.72	Y	Y	Y	Y	0.72	0.01
Phe	[123455667]	336	1	0.20	0.22	0.21	0.20	Y	Y	Y	Y	0.21	0.01
Phe	[123455667]	336	2	0.05	0.06	0.05	0.06	Y	Y	Y	Y	0.06	0.00
Phe	[123455667]	336	3	0.01	0.02	0.01	0.02	Y	Y	Y	Y	0.01	0.00
Phe	[123455667]	336	4	0.00	0.00	0.00	0.00	Y	Y	Y	Y	0.00	0.00
Phe	[123455667]	336	5	0.00	0.00	0.00	0.00	Y	Y	Y	Y	0.00	0.00
Phe	[123455667]	336	6	0.00	0.00	0.00	0.00	Y	Y	Y	Y	0.00	0.00
Phe	[123455667]	336	7	0.00	0.00	0.00	0.00	Y	Y	Y	Y	0.00	0.00
Phe	[123455667]	336	8	0.00	0.00	0.00	0.00	Y	Y	Y	Y	0.00	0.00
Phe	[123455667]	336	9	0.00	0.00	0.00	0.00	Y	Y	Y	Y	0.00	0.00
Pro	[2345]	184	0	0.89	0.88	0.88	0.88	Y	Y	Y	Y	0.88	0.00
Pro	[2345]	184	1	0.10	0.11	0.11	0.11	Y	Y	Y	Y	0.11	0.00
Pro	[2345]	184	2	0.01	0.01	0.01	0.01	Y	Y	Y	Y	0.01	0.00
Pro	[2345]	184	3	0.00	0.00	0.00	0.00	Y	Y	Y	Y	0.00	0.00
Pro	[2345]	184	4	0.00	0.00	0.00	0.00	Y	Y	Y	Y	0.00	0.00
Pro	[2345]	258	0	0.89	0.88	0.88	0.89	Y	Y	Y	Y	0.89	0.00

Table A.5 Mass isotopomers from 100% 4-<sup>13</sup>C Asp ILE.

AA	Fragment	m/z	Mass (n in m+n)	Biological Replicates				Consider Replicate				Overall	
				Rep 1	Rep 2	Rep 3	Rep 4	1	2	3	4	Avg	SD
Pro	[2345]	258	1	0.09	0.10	0.10	0.10	Y	Y	Y	Y	0.10	0.00
Pro	[2345]	258	2	0.01	0.02	0.01	0.01	Y	Y	Y	Y	0.01	0.00
Pro	[2345]	258	3	0.00	0.00	0.00	0.00	Y	Y	Y	Y	0.00	0.00
Pro	[2345]	258	4	0.00	0.00	0.00	0.00	Y	Y	Y	Y	0.00	0.00
Pro	[12345]	286	0	0.72	0.72	0.73	0.74	Y	Y	Y	Y	0.73	0.01
Pro	[12345]	286	1	0.21	0.20	0.17	0.17	Y	Y	Y	Y	0.19	0.02
Pro	[12345]	286	2	0.02	0.02	0.02	0.02	Y	Y	Y	Y	0.02	0.00
Pro	[12345]	286	3	0.05	0.05	0.06	0.06	Y	Y	Y	Y	0.05	0.01
Pro	[12345]	286	4	0.01	0.01	0.01	0.01	Y	Y	Y	Y	0.01	0.00
Pro	[12345]	286	5	0.00	0.00	0.00	0.00	Y	Y	Y	Y	0.00	0.00
Ser	[23]	288	0	0.97	0.97	0.97	0.97	Y	Y	Y	Y	0.97	0.00
Ser	[23]	288	1	0.03	0.03	0.03	0.03	Y	Y	Y	Y	0.03	0.00
Ser	[23]	288	2	0.00	0.00	0.00	0.00	Y	Y	Y	Y	0.00	0.00
Ser	[12]	302	0	0.94	0.94	0.95	0.95	Y	Y	Y	Y	0.94	0.00
Ser	[12]	302	1	0.05	0.05	0.04	0.04	Y	Y	Y	Y	0.05	0.00
Ser	[12]	302	2	0.01	0.01	0.01	0.01	Y	Y	Y	Y	0.01	0.00
Ser	[23]	362	0	0.97	0.97	0.97	0.97	Y	Y	Y	Y	0.97	0.00
Ser	[23]	362	1	0.03	0.03	0.03	0.03	Y	Y	Y	Y	0.03	0.00
Ser	[23]	362	2	0.00	0.00	0.00	0.00	Y	Y	Y	Y	0.00	0.00
Ser	[123]	390	0	0.92	0.92	0.93	0.93	Y	Y	Y	Y	0.93	0.00
Ser	[123]	390	1	0.07	0.07	0.07	0.07	Y	Y	Y	Y	0.07	0.00
Ser	[123]	390	2	0.00	0.00	0.00	0.00	Y	Y	Y	Y	0.00	0.00
Ser	[123]	390	3	0.00	0.00	0.00	0.00	Y	Y	Y	Y	0.00	0.00
Thr	[234]	376	0	0.72	0.74	0.79	0.79	Y	Y	Y	Y	0.76	0.03
Thr	[234]	376	1	0.27	0.25	0.20	0.20	Y	Y	Y	Y	0.23	0.03
Thr	[234]	376	2	0.01	0.01	0.01	0.01	Y	Y	Y	Y	0.01	0.00
Thr	[234]	376	3	0.00	0.00	0.00	0.00	Y	Y	Y	Y	0.00	0.00
Thr	[1234]	404	0	0.69	0.71	0.76	0.76	Y	Y	Y	Y	0.73	0.03
Thr	[1234]	404	1	0.29	0.27	0.23	0.23	Y	Y	Y	Y	0.25	0.03
Thr	[1234]	404	2	0.02	0.02	0.01	0.01	Y	Y	Y	Y	0.01	0.00
Thr	[1234]	404	3	0.00	0.00	0.00	0.00	Y	Y	Y	Y	0.00	0.00
Thr	[1234]	404	4	0.00	0.00	0.00	0.00	Y	Y	Y	Y	0.00	0.00
Tyr	[12]	302	0	0.93	0.92	0.93	0.93	Y	Y	Y	Y	0.93	0.00
Tyr	[12]	302	1	0.07	0.07	0.06	0.07	Y	Y	Y	Y	0.07	0.00
Tyr	[12]	302	2	0.01	0.01	0.01	0.01	Y	Y	Y	Y	0.01	0.00
Tyr	[23455667]	364	0	0.75	0.74	0.75	0.74	Y	Y	Y	Y	0.74	0.01
Tyr	[23455667]	364	1	0.19	0.20	0.19	0.19	Y	Y	Y	Y	0.19	0.00
Tyr	[23455667]	364	2	0.04	0.05	0.05	0.05	Y	Y	Y	Y	0.05	0.00
Tyr	[23455667]	364	3	0.01	0.01	0.01	0.01	Y	Y	Y	Y	0.01	0.00
Tyr	[23455667]	364	4	0.00	0.00	0.00	0.00	Y	Y	Y	Y	0.00	0.00
Tyr	[23455667]	364	5	0.00	0.00	0.00	0.00	Y	Y	Y	Y	0.00	0.00
Tyr	[23455667]	364	6	0.00	0.00	0.00	0.00	Y	Y	Y	Y	0.00	0.00
Tyr	[23455667]	364	7	0.00	0.00	0.00	0.00	Y	Y	Y	Y	0.00	0.00
Tyr	[23455667]	364	8	0.00	0.00	0.00	0.00	Y	Y	Y	Y	0.00	0.00
Tyr	[23455667]	438	0	0.75	0.73	0.74	0.74	Y	Y	Y	Y	0.74	0.01
Tyr	[23455667]	438	1	0.21	0.22	0.20	0.21	Y	Y	Y	Y	0.21	0.01
Tyr	[23455667]	438	2	0.04	0.04	0.04	0.04	Y	Y	Y	Y	0.04	0.00
Tyr	[23455667]	438	3	0.01	0.01	0.01	0.01	Y	Y	Y	Y	0.01	0.00
Tyr	[23455667]	438	4	0.00	0.00	0.00	0.00	Y	Y	Y	Y	0.00	0.00
Tyr	[23455667]	438	5	0.00	0.00	0.00	0.00	Y	Y	Y	Y	0.00	0.00
Tyr	[23455667]	438	6	0.00	0.00	0.00	0.00	Y	Y	Y	Y	0.00	0.00
Tyr	[23455667]	438	7	0.00	0.00	0.00	0.00	Y	Y	Y	Y	0.00	0.00
Tyr	[23455667]	438	8	0.00	0.00	0.00	0.00	Y	Y	Y	Y	0.00	0.00
Tyr	[123455667]	466	0	0.72	0.70	0.72	0.72	Y	Y	Y	Y	0.72	0.01
Tyr	[123455667]	466	1	0.22	0.22	0.21	0.21	Y	Y	Y	Y	0.22	0.01
Tyr	[123455667]	466	2	0.05	0.05	0.05	0.05	Y	Y	Y	Y	0.05	0.00
Tyr	[123455667]	466	3	0.01	0.01	0.01	0.01	Y	Y	Y	Y	0.01	0.00
Tyr	[123455667]	466	4	0.00	0.00	0.00	0.00	Y	Y	Y	Y	0.00	0.00
Tyr	[123455667]	466	5	0.00	0.00	0.00	0.00	Y	Y	Y	Y	0.00	0.00
Tyr	[123455667]	466	6	0.00	0.00	0.00	0.00	Y	Y	Y	Y	0.00	0.00
Tyr	[123455667]	466	7	0.00	0.00	0.00	0.00	Y	Y	Y	Y	0.00	0.00
Tyr	[123455667]	466	8	0.00	0.00	0.00	0.00	Y	Y	Y	Y	0.00	0.00
Val	[2345]	186	0	0.86	0.85	0.85	0.85	Y	Y	Y	Y	0.85	0.01
Val	[2345]	186	1	0.10	0.11	0.11	0.11	Y	Y	Y	Y	0.11	0.00
Val	[2345]	186	2	0.01	0.02	0.02	0.02	Y	Y	Y	Y	0.02	0.00
Val	[2345]	186	3	0.02	0.03	0.02	0.02	Y	Y	Y	Y	0.02	0.00
Val	[2345]	186	4	0.00	0.00	0.00	0.00	Y	Y	Y	Y	0.00	0.00
Val	[2345]	260	0	0.88	0.87	0.87	0.87	Y	Y	Y	Y	0.87	0.01
Val	[2345]	260	1	0.10	0.11	0.11	0.11	Y	Y	Y	Y	0.11	0.00
Val	[2345]	260	2	0.01	0.02	0.02	0.02	Y	Y	Y	Y	0.02	0.00
Val	[2345]	260	3	0.00	0.00	0.00	0.00	Y	Y	Y	Y	0.00	0.00
Val	[2345]	260	4	0.00	0.00	0.00	0.00	Y	Y	Y	Y	0.00	0.00
Val	[12345]	288	0	0.83	0.82	0.84	0.83	Y	Y	Y	Y	0.83	0.01
Val	[12345]	288	1	0.14	0.15	0.14	0.14	Y	Y	Y	Y	0.14	0.01
Val	[12345]	288	2	0.02	0.02	0.02	0.02	Y	Y	Y	Y	0.02	0.00
Val	[12345]	288	3	0.00	0.00	0.00	0.00	Y	Y	Y	Y	0.00	0.00
Val	[12345]	288	4	0.00	0.00	0.00	0.00	Y	Y	Y	Y	0.00	0.00
Val	[12345]	288	5	0.00	0.00	0.00	0.00	Y	Y	Y	Y	0.00	0.00
Val	[12]	302	0	0.91	0.91	0.92	0.92	Y	Y	Y	Y	0.91	0.00
Val	[12]	302	1	0.09	0.09	0.08	0.08	Y	Y	Y	Y	0.08	0.00
Val	[12]	302	2	0.00	0.00	0.00	0.00	Y	Y	Y	Y	0.00	0.00

### **A.6. Table A.6 Mass Isotopomers from 50% U-<sup>13</sup>C Glc ILE.**

Mass isotopomer distributions from 50% U-<sup>13</sup>C glucose ILE (**Table A.6**). This table follows the scheme of **Table A.1**.

Table A.6 Mass isotopomers from 50% U-<sup>13</sup>C Glc ILE.

AA	Fragment	m/z	Mass (n in m+n)	Biological Replicates				Consider Replicate				Overall	
				Rep 1	Rep 2	Rep 3	Rep 4	1	2	3	4	Avg	SD
Ala	[23]	158	0	0.44	0.44	0.45	0.44	Y	Y	Y	Y	0.44	0.00
Ala	[23]	158	1	0.17	0.17	0.17	0.17	Y	Y	Y	Y	0.17	0.00
Ala	[23]	158	2	0.39	0.39	0.38	0.39	Y	Y	Y	Y	0.39	0.00
Ala	[23]	232	0	0.45	0.45	0.46	0.45	Y	Y	Y	Y	0.45	0.00
Ala	[23]	232	1	0.17	0.17	0.17	0.17	Y	Y	Y	Y	0.17	0.00
Ala	[23]	232	2	0.38	0.38	0.37	0.39	Y	Y	Y	Y	0.38	0.01
Ala	[123]	260	0	0.42	0.42	0.43	0.43	Y	Y	Y	Y	0.42	0.00
Ala	[123]	260	1	0.13	0.13	0.13	0.12	Y	Y	Y	Y	0.13	0.00
Ala	[123]	260	2	0.11	0.11	0.10	0.10	Y	Y	Y	Y	0.11	0.00
Ala	[123]	260	3	0.34	0.34	0.34	0.35	Y	Y	Y	Y	0.34	0.01
Arg	[2345]	340	0	0.17	0.18	0.17	0.17	Y	Y	Y	Y	0.17	0.00
Arg	[2345]	340	1	0.19	0.19	0.16	0.20	Y	Y	Y	Y	0.18	0.02
Arg	[2345]	340	2	0.27	0.28	0.30	0.28	Y	Y	Y	Y	0.28	0.01
Arg	[2345]	340	3	0.21	0.20	0.21	0.21	Y	Y	Y	Y	0.21	0.00
Arg	[2345]	340	4	0.17	0.15	0.17	0.15	Y	Y	Y	Y	0.16	0.01
Arg	[12345]	442	0	0.14	0.14	0.14	0.13	Y	Y	Y	Y	0.14	0.00
Arg	[12345]	442	1	0.17	0.16	0.17	0.16	Y	Y	Y	Y	0.17	0.00
Arg	[12345]	442	2	0.24	0.24	0.24	0.25	Y	Y	Y	Y	0.24	0.00
Arg	[12345]	442	3	0.22	0.22	0.22	0.22	Y	Y	Y	Y	0.22	0.00
Arg	[12345]	442	4	0.15	0.16	0.15	0.16	Y	Y	Y	Y	0.15	0.00
Arg	[12345]	442	5	0.08	0.08	0.08	0.08	Y	Y	Y	Y	0.08	0.00
Asp	[12]	302	0	0.45	0.45	0.45	0.45	Y	Y	Y	Y	0.45	0.00
Asp	[12]	302	1	0.19	0.19	0.21	0.19	Y	Y	Y	Y	0.20	0.01
Asp	[12]	302	2	0.36	0.36	0.34	0.36	Y	Y	Y	Y	0.36	0.01
Asp	[234]	316	0	0.28	0.28	0.28	0.28	Y	Y	Y	Y	0.28	0.00
Asp	[234]	316	1	0.28	0.28	0.29	0.28	Y	Y	Y	Y	0.28	0.01
Asp	[234]	316	2	0.29	0.29	0.29	0.29	Y	Y	Y	Y	0.29	0.00
Asp	[234]	316	3	0.14	0.15	0.14	0.15	Y	Y	Y	Y	0.14	0.00
Asp	[234]	390	0	0.29	0.29	0.29	0.29	Y	Y	Y	Y	0.29	0.00
Asp	[234]	390	1	0.28	0.28	0.29	0.28	Y	Y	Y	Y	0.28	0.00
Asp	[234]	390	2	0.29	0.29	0.29	0.29	Y	Y	Y	Y	0.29	0.00
Asp	[234]	390	3	0.15	0.14	0.14	0.15	Y	Y	Y	Y	0.14	0.00
Asp	[1234]	418	0	0.24	0.24	0.24	0.24	Y	Y	Y	Y	0.24	0.00
Asp	[1234]	418	1	0.21	0.21	0.22	0.21	Y	Y	Y	Y	0.21	0.00
Asp	[1234]	418	2	0.21	0.21	0.22	0.22	Y	Y	Y	Y	0.22	0.00
Asp	[1234]	418	3	0.22	0.22	0.22	0.22	Y	Y	Y	Y	0.22	0.00
Asp	[1234]	418	4	0.11	0.11	0.10	0.11	Y	Y	Y	Y	0.11	0.00
Glu	[2345]	272	0	0.17	0.18	0.18	0.18	Y	Y	Y	Y	0.18	0.00
Glu	[2345]	272	1	0.21	0.21	0.22	0.21	Y	Y	Y	Y	0.21	0.01
Glu	[2345]	272	2	0.31	0.31	0.31	0.31	Y	Y	Y	Y	0.31	0.00
Glu	[2345]	272	3	0.18	0.18	0.18	0.18	Y	Y	Y	Y	0.18	0.00
Glu	[2345]	272	4	0.12	0.12	0.11	0.12	Y	Y	Y	Y	0.12	0.00
Glu	[2345]	330	0	0.18	0.18	0.18	0.18	Y	Y	Y	Y	0.18	0.00
Glu	[2345]	330	1	0.21	0.21	0.23	0.21	Y	Y	Y	Y	0.22	0.01
Glu	[2345]	330	2	0.32	0.31	0.31	0.32	Y	Y	Y	Y	0.31	0.00
Glu	[2345]	330	3	0.18	0.17	0.18	0.17	Y	Y	Y	Y	0.18	0.00
Glu	[2345]	330	4	0.12	0.11	0.10	0.11	Y	Y	Y	Y	0.11	0.01
Glu	[12345]	432	0	0.14	0.14	0.14	0.14	Y	Y	Y	Y	0.14	0.00
Glu	[12345]	432	1	0.17	0.17	0.18	0.17	Y	Y	Y	Y	0.18	0.00
Glu	[12345]	432	2	0.28	0.27	0.27	0.28	Y	Y	Y	Y	0.28	0.00
Glu	[12345]	432	3	0.22	0.22	0.22	0.22	Y	Y	Y	Y	0.22	0.00
Glu	[12345]	432	4	0.14	0.14	0.13	0.14	Y	Y	Y	Y	0.14	0.00
Glu	[12345]	432	5	0.06	0.06	0.05	0.06	Y	Y	Y	Y	0.06	0.00
Gly	[2]	218	0	0.54	0.54	0.55	0.54	Y	Y	Y	Y	0.55	0.00
Gly	[2]	218	1	0.46	0.46	0.45	0.46	Y	Y	Y	Y	0.45	0.00
Gly	[12]	246	0	0.50	0.50	0.50	0.50	Y	Y	Y	Y	0.50	0.00
Gly	[12]	246	1	0.09	0.09	0.10	0.09	Y	Y	Y	Y	0.09	0.01
Gly	[12]	246	2	0.41	0.41	0.40	0.41	Y	Y	Y	Y	0.41	0.01
His	[2345]	195	0	0.01	0.01	0.01	0.01	Y	Y	Y	Y	0.01	0.00
His	[2345]	195	1	0.19	0.19	0.18	0.19	Y	Y	Y	Y	0.19	0.00
His	[2345]	195	2	0.28	0.28	0.28	0.28	Y	Y	Y	Y	0.28	0.00
His	[2345]	195	3	0.27	0.27	0.27	0.27	Y	Y	Y	Y	0.27	0.00
His	[2345]	195	4	0.25	0.25	0.25	0.25	Y	Y	Y	Y	0.25	0.00
His	[23456]	338	0	0.17	0.17	0.17	0.17	Y	Y	Y	Y	0.17	0.00
His	[23456]	338	1	0.16	0.16	0.17	0.16	Y	Y	Y	Y	0.16	0.01
His	[23456]	338	2	0.23	0.23	0.23	0.23	Y	Y	Y	Y	0.23	0.00
His	[23456]	338	3	0.21	0.20	0.21	0.22	Y	Y	Y	Y	0.21	0.01
His	[23456]	338	4	0.12	0.12	0.12	0.13	Y	Y	Y	Y	0.12	0.00
His	[23456]	338	5	0.11	0.11	0.10	0.10	Y	Y	Y	Y	0.11	0.01
His	[123456]	440	0	0.16	0.16	0.16	0.16	Y	Y	Y	Y	0.16	0.00
His	[123456]	440	1	0.16	0.15	0.16	0.15	Y	Y	Y	Y	0.16	0.00
His	[123456]	440	2	0.15	0.15	0.15	0.15	Y	Y	Y	Y	0.15	0.00
His	[123456]	440	3	0.20	0.20	0.20	0.20	Y	Y	Y	Y	0.20	0.00
His	[123456]	440	4	0.12	0.12	0.12	0.12	Y	Y	Y	Y	0.12	0.00
His	[123456]	440	5	0.12	0.12	0.11	0.12	Y	Y	Y	Y	0.12	0.00
His	[123456]	440	6	0.11	0.10	0.09	0.09	Y	Y	Y	Y	0.10	0.01
Ile	[23456]	200	0	0.15	0.15	0.15	0.15	Y	Y	Y	Y	0.15	0.00
Ile	[23456]	200	1	0.17	0.17	0.17	0.17	Y	Y	Y	Y	0.17	0.00
Ile	[23456]	200	2	0.27	0.27	0.27	0.27	Y	Y	Y	Y	0.27	0.00
Ile	[23456]	200	3	0.21	0.21	0.21	0.21	Y	Y	Y	Y	0.21	0.00
Ile	[23456]	200	4	0.14	0.14	0.14	0.14	Y	Y	Y	Y	0.14	0.00
Ile	[23456]	200	5	0.06	0.06	0.06	0.06	Y	Y	Y	Y	0.06	0.00
Ile	[23456]	274	0	0.15	0.15	0.15	0.15	Y	Y	Y	Y	0.15	0.00
Ile	[23456]	274	1	0.17	0.17	0.17	0.17	Y	Y	Y	Y	0.17	0.00



Table A.6 Mass isotopomers from 50% U-<sup>13</sup>C Glc ILE.

AA	Fragment	m/z	Mass (n in m+n)	Biological Replicates				Consider Replicate				Overall	
				Rep 1	Rep 2	Rep 3	Rep 4	1	2	3	4	Avg	SD
Ile	[23456]	274	2	0.27	0.27	0.26	0.27	Y	Y	Y	Y	0.27	0.00
Ile	[23456]	274	3	0.21	0.22	0.22	0.22	Y	Y	Y	Y	0.22	0.00
Ile	[23456]	274	4	0.14	0.14	0.14	0.14	Y	Y	Y	Y	0.14	0.00
Ile	[23456]	274	5	0.06	0.06	0.06	0.06	Y	Y	Y	Y	0.06	0.00
Leu	[23456]	200	0	0.13	0.13	0.14	0.13	Y	Y	Y	Y	0.13	0.00
Leu	[23456]	200	1	0.17	0.17	0.17	0.17	Y	Y	Y	Y	0.17	0.00
Leu	[23456]	200	2	0.25	0.26	0.25	0.26	Y	Y	Y	Y	0.26	0.00
Leu	[23456]	200	3	0.23	0.23	0.23	0.23	Y	Y	Y	Y	0.23	0.00
Leu	[23456]	200	4	0.14	0.14	0.13	0.14	Y	Y	Y	Y	0.14	0.00
Leu	[23456]	200	5	0.08	0.07	0.08	0.08	Y	Y	Y	Y	0.08	0.00
Leu	[23456]	274	0	0.13	0.13	0.13	0.13	Y	Y	Y	Y	0.13	0.00
Leu	[23456]	274	1	0.17	0.17	0.17	0.17	Y	Y	Y	Y	0.17	0.00
Leu	[23456]	274	2	0.25	0.25	0.25	0.25	Y	Y	Y	Y	0.25	0.00
Leu	[23456]	274	3	0.24	0.24	0.23	0.24	Y	Y	Y	Y	0.23	0.00
Leu	[23456]	274	4	0.14	0.14	0.13	0.14	Y	Y	Y	Y	0.14	0.00
Leu	[23456]	274	5	0.07	0.07	0.07	0.08	Y	Y	Y	Y	0.08	0.00
Lys	[23456]	329	0	0.18	0.18	0.17	0.18	Y	Y	Y	Y	0.18	0.01
Lys	[23456]	329	1	0.17	0.17	0.18	0.17	Y	Y	Y	Y	0.17	0.00
Lys	[23456]	329	2	0.26	0.26	0.26	0.26	Y	Y	Y	Y	0.26	0.00
Lys	[23456]	329	3	0.20	0.20	0.21	0.20	Y	Y	Y	Y	0.20	0.00
Lys	[23456]	329	4	0.13	0.13	0.13	0.13	Y	Y	Y	Y	0.13	0.00
Lys	[23456]	329	5	0.05	0.05	0.05	0.06	Y	Y	Y	Y	0.05	0.00
Lys	[123456]	431	0	0.16	0.16	0.15	0.16	Y	Y	Y	Y	0.16	0.01
Lys	[123456]	431	1	0.14	0.15	0.15	0.14	Y	Y	Y	Y	0.15	0.00
Lys	[123456]	431	2	0.19	0.19	0.19	0.19	Y	Y	Y	Y	0.19	0.00
Lys	[123456]	431	3	0.20	0.20	0.20	0.21	Y	Y	Y	Y	0.20	0.00
Lys	[123456]	431	4	0.14	0.14	0.15	0.15	Y	Y	Y	Y	0.15	0.00
Lys	[123456]	431	5	0.11	0.11	0.11	0.11	Y	Y	Y	Y	0.11	0.00
Lys	[123456]	431	6	0.04	0.04	0.05	0.05	Y	Y	Y	Y	0.05	0.00
Lys	[123456]	488	0	0.16	0.16	0.15	0.16	Y	Y	Y	Y	0.16	0.01
Lys	[123456]	488	1	0.14	0.14	0.14	0.14	Y	Y	Y	Y	0.14	0.00
Lys	[123456]	488	2	0.19	0.19	0.19	0.19	Y	Y	Y	Y	0.19	0.00
Lys	[123456]	488	3	0.20	0.20	0.21	0.20	Y	Y	Y	Y	0.20	0.00
Lys	[123456]	488	4	0.15	0.15	0.15	0.15	Y	Y	Y	Y	0.15	0.00
Lys	[123456]	488	5	0.11	0.11	0.11	0.11	Y	Y	Y	Y	0.11	0.00
Lys	[123456]	488	6	0.05	0.05	0.05	0.05	Y	Y	Y	Y	0.05	0.00
Met	[2345]	218	0	0.18	0.18	0.18	0.18	Y	Y	Y	Y	0.18	0.00
Met	[2345]	218	1	0.28	0.27	0.28	0.27	Y	Y	Y	Y	0.28	0.01
Met	[2345]	218	2	0.27	0.27	0.27	0.28	Y	Y	Y	Y	0.27	0.00
Met	[2345]	218	3	0.21	0.21	0.20	0.21	Y	Y	Y	Y	0.21	0.00
Met	[2345]	218	4	0.07	0.07	0.06	0.07	Y	Y	Y	Y	0.07	0.00
Met	[2345]	292	0	0.18	0.18	0.18	0.17	Y	Y	Y	Y	0.18	0.00
Met	[2345]	292	1	0.27	0.27	0.28	0.27	Y	Y	Y	Y	0.28	0.00
Met	[2345]	292	2	0.28	0.28	0.27	0.28	Y	Y	Y	Y	0.27	0.00
Met	[2345]	292	3	0.21	0.21	0.21	0.21	Y	Y	Y	Y	0.21	0.00
Met	[2345]	292	4	0.07	0.06	0.06	0.07	Y	Y	Y	Y	0.06	0.00
Met	[12345]	320	0	0.15	0.15	0.15	0.15	Y	Y	Y	Y	0.15	0.00
Met	[12345]	320	1	0.22	0.22	0.23	0.22	Y	Y	Y	Y	0.22	0.00
Met	[12345]	320	2	0.20	0.20	0.20	0.20	Y	Y	Y	Y	0.20	0.00
Met	[12345]	320	3	0.21	0.21	0.20	0.21	Y	Y	Y	Y	0.21	0.00
Met	[12345]	320	4	0.17	0.17	0.17	0.17	Y	Y	Y	Y	0.17	0.00
Met	[12345]	320	5	0.05	0.06	0.05	0.06	Y	Y	Y	Y	0.06	0.00
Phe	[23455667]	234	0	0.12	0.12	0.12	0.12	Y	Y	Y	Y	0.12	0.00
Phe	[23455667]	234	1	0.07	0.07	0.08	0.07	Y	Y	Y	Y	0.07	0.01
Phe	[23455667]	234	2	0.17	0.17	0.17	0.17	Y	Y	Y	Y	0.17	0.00
Phe	[23455667]	234	3	0.13	0.13	0.13	0.12	Y	Y	Y	Y	0.13	0.00
Phe	[23455667]	234	4	0.16	0.16	0.16	0.16	Y	Y	Y	Y	0.16	0.00
Phe	[23455667]	234	5	0.11	0.11	0.11	0.11	Y	Y	Y	Y	0.11	0.00
Phe	[23455667]	234	6	0.14	0.14	0.13	0.14	Y	Y	Y	Y	0.14	0.00
Phe	[23455667]	234	7	0.04	0.04	0.04	0.04	Y	Y	Y	Y	0.04	0.00
Phe	[23455667]	234	8	0.06	0.06	0.06	0.06	Y	Y	Y	Y	0.06	0.00
Phe	[12]	302	0	0.52	0.52	0.53	0.52	Y	Y	Y	Y	0.52	0.00
Phe	[12]	302	1	0.07	0.06	0.07	0.06	Y	Y	Y	Y	0.07	0.00
Phe	[12]	302	2	0.41	0.41	0.40	0.41	Y	Y	Y	Y	0.41	0.01
Phe	[123455667]	336	0	0.11	0.11	0.11	0.11	Y	Y	Y	Y	0.11	0.00
Phe	[123455667]	336	1	0.07	0.07	0.08	0.07	Y	Y	Y	Y	0.07	0.00
Phe	[123455667]	336	2	0.11	0.10	0.11	0.10	Y	Y	Y	Y	0.11	0.00
Phe	[123455667]	336	3	0.16	0.16	0.16	0.16	Y	Y	Y	Y	0.16	0.00
Phe	[123455667]	336	4	0.13	0.13	0.13	0.13	Y	Y	Y	Y	0.13	0.00
Phe	[123455667]	336	5	0.12	0.12	0.12	0.12	Y	Y	Y	Y	0.12	0.00
Phe	[123455667]	336	6	0.13	0.13	0.13	0.13	Y	Y	Y	Y	0.13	0.00
Phe	[123455667]	336	7	0.08	0.08	0.08	0.08	Y	Y	Y	Y	0.08	0.00
Phe	[123455667]	336	8	0.04	0.04	0.04	0.04	Y	Y	Y	Y	0.04	0.00
Phe	[123455667]	336	9	0.06	0.06	0.06	0.06	Y	Y	Y	Y	0.06	0.00
Pro	[2345]	184	0	0.21	0.22	0.22	0.21	Y	Y	Y	Y	0.21	0.00
Pro	[2345]	184	1	0.20	0.20	0.20	0.20	Y	Y	Y	Y	0.20	0.00
Pro	[2345]	184	2	0.31	0.30	0.30	0.31	Y	Y	Y	Y	0.30	0.00
Pro	[2345]	184	3	0.16	0.16	0.16	0.16	Y	Y	Y	Y	0.16	0.00
Pro	[2345]	184	4	0.12	0.12	0.12	0.12	Y	Y	Y	Y	0.12	0.00
Pro	[2345]	258	0	0.22	0.22	0.22	0.22	Y	Y	Y	Y	0.22	0.00
Pro	[2345]	258	1	0.20	0.20	0.20	0.20	Y	Y	Y	Y	0.20	0.00
Pro	[2345]	258	2	0.31	0.31	0.31	0.31	Y	Y	Y	Y	0.31	0.00
Pro	[2345]	258	3	0.16	0.16	0.16	0.16	Y	Y	Y	Y	0.16	0.00
Pro	[2345]	258	4	0.11	0.11	0.12	0.12	Y	Y	Y	Y	0.12	0.00

Table A.6 Mass isotopomers from 50% U-<sup>13</sup>C Glc ILE.

AA	Fragment	m/z	Mass (n in m+n)	Biological Replicates				Consider Replicate				Overall	
				Rep 1	Rep 2	Rep 3	Rep 4	1	2	3	4	Avg	SD
Pro	[12345]	286	0	0.20	0.19	0.20	0.20	Y	Y	Y	Y	0.20	0.00
Pro	[12345]	286	1	0.13	0.14	0.13	0.12	Y	Y	Y	Y	0.13	0.00
Pro	[12345]	286	2	0.24	0.25	0.24	0.24	Y	Y	Y	Y	0.25	0.00
Pro	[12345]	286	3	0.21	0.21	0.21	0.21	Y	Y	Y	Y	0.21	0.00
Pro	[12345]	286	4	0.14	0.14	0.14	0.14	Y	Y	Y	Y	0.14	0.00
Pro	[12345]	286	5	0.08	0.08	0.08	0.08	Y	Y	Y	Y	0.08	0.00
Ser	[23]	288	0	0.44	0.44	0.42	0.44	Y	Y	Y	Y	0.44	0.01
Ser	[23]	288	1	0.21	0.21	0.26	0.20	Y	Y	Y	Y	0.22	0.03
Ser	[23]	288	2	0.35	0.35	0.32	0.36	Y	Y	Y	Y	0.34	0.02
Ser	[12]	302	0	0.49	0.49	0.49	0.49	Y	Y	Y	Y	0.49	0.00
Ser	[12]	302	1	0.10	0.10	0.11	0.10	Y	Y	Y	Y	0.10	0.00
Ser	[12]	302	2	0.41	0.41	0.40	0.42	Y	Y	Y	Y	0.41	0.01
Ser	[23]	362	0	0.44	0.44	0.42	0.44	Y	Y	Y	Y	0.43	0.01
Ser	[23]	362	1	0.21	0.21	0.27	0.20	Y	Y	Y	Y	0.22	0.03
Ser	[23]	362	2	0.35	0.36	0.32	0.35	Y	Y	Y	Y	0.34	0.02
Ser	[123]	390	0	0.41	0.41	0.39	0.42	Y	Y	Y	Y	0.41	0.01
Ser	[123]	390	1	0.14	0.14	0.17	0.13	Y	Y	Y	Y	0.15	0.02
Ser	[123]	390	2	0.12	0.12	0.15	0.12	Y	Y	Y	Y	0.12	0.01
Ser	[123]	390	3	0.33	0.33	0.29	0.34	Y	Y	Y	Y	0.32	0.02
Thr	[234]	376	0	0.31	0.30	0.31	0.30	Y	Y	Y	Y	0.30	0.00
Thr	[234]	376	1	0.28	0.28	0.28	0.28	Y	Y	Y	Y	0.28	0.00
Thr	[234]	376	2	0.29	0.29	0.29	0.29	Y	Y	Y	Y	0.29	0.00
Thr	[234]	376	3	0.13	0.13	0.12	0.13	Y	Y	Y	Y	0.13	0.00
Thr	[1234]	404	0	0.26	0.26	0.26	0.26	Y	Y	Y	Y	0.26	0.00
Thr	[1234]	404	1	0.21	0.21	0.21	0.20	Y	Y	Y	Y	0.21	0.00
Thr	[1234]	404	2	0.21	0.21	0.21	0.21	Y	Y	Y	Y	0.21	0.00
Thr	[1234]	404	3	0.22	0.22	0.21	0.22	Y	Y	Y	Y	0.22	0.00
Thr	[1234]	404	4	0.11	0.11	0.10	0.11	Y	Y	Y	Y	0.11	0.00
Tyr	[12]	302	0	0.51	0.51	0.51	0.51	Y	Y	Y	Y	0.51	0.00
Tyr	[12]	302	1	0.08	0.07	0.08	0.07	Y	Y	Y	Y	0.08	0.01
Tyr	[12]	302	2	0.41	0.42	0.40	0.42	Y	Y	Y	Y	0.41	0.01
Tyr	[23455667]	364	0	0.11	0.11	0.11	0.11	Y	Y	Y	Y	0.11	0.00
Tyr	[23455667]	364	1	0.08	0.08	0.08	0.07	Y	Y	Y	Y	0.08	0.00
Tyr	[23455667]	364	2	0.18	0.17	0.18	0.17	Y	Y	Y	Y	0.17	0.00
Tyr	[23455667]	364	3	0.13	0.13	0.13	0.13	Y	Y	Y	Y	0.13	0.00
Tyr	[23455667]	364	4	0.16	0.16	0.16	0.16	Y	Y	Y	Y	0.16	0.00
Tyr	[23455667]	364	5	0.11	0.11	0.11	0.11	Y	Y	Y	Y	0.11	0.00
Tyr	[23455667]	364	6	0.13	0.14	0.13	0.14	Y	Y	Y	Y	0.14	0.00
Tyr	[23455667]	364	7	0.04	0.04	0.04	0.04	Y	Y	Y	Y	0.04	0.00
Tyr	[23455667]	364	8	0.06	0.06	0.06	0.06	Y	Y	Y	Y	0.06	0.00
Tyr	[23455667]	438	0	0.10	0.10	0.10	0.10	Y	Y	Y	Y	0.10	0.00
Tyr	[23455667]	438	1	0.08	0.07	0.08	0.07	Y	Y	Y	Y	0.08	0.00
Tyr	[23455667]	438	2	0.17	0.17	0.17	0.17	Y	Y	Y	Y	0.17	0.00
Tyr	[23455667]	438	3	0.13	0.13	0.13	0.13	Y	Y	Y	Y	0.13	0.00
Tyr	[23455667]	438	4	0.16	0.16	0.16	0.17	Y	Y	Y	Y	0.16	0.00
Tyr	[23455667]	438	5	0.11	0.11	0.11	0.11	Y	Y	Y	Y	0.11	0.00
Tyr	[23455667]	438	6	0.14	0.14	0.14	0.14	Y	Y	Y	Y	0.14	0.00
Tyr	[23455667]	438	7	0.05	0.05	0.05	0.04	Y	Y	Y	Y	0.05	0.00
Tyr	[23455667]	438	8	0.07	0.06	0.06	0.07	Y	Y	Y	Y	0.06	0.00
Tyr	[123455667]	466	0	0.10	0.10	0.10	0.10	Y	Y	Y	Y	0.10	0.00
Tyr	[123455667]	466	1	0.07	0.07	0.08	0.07	Y	Y	Y	Y	0.07	0.00
Tyr	[123455667]	466	2	0.11	0.11	0.11	0.11	Y	Y	Y	Y	0.11	0.00
Tyr	[123455667]	466	3	0.16	0.15	0.15	0.15	Y	Y	Y	Y	0.16	0.00
Tyr	[123455667]	466	4	0.13	0.13	0.13	0.13	Y	Y	Y	Y	0.13	0.00
Tyr	[123455667]	466	5	0.12	0.13	0.12	0.13	Y	Y	Y	Y	0.13	0.00
Tyr	[123455667]	466	6	0.13	0.13	0.13	0.13	Y	Y	Y	Y	0.13	0.00
Tyr	[123455667]	466	7	0.08	0.08	0.08	0.08	Y	Y	Y	Y	0.08	0.00
Tyr	[123455667]	466	8	0.04	0.04	0.04	0.04	Y	Y	Y	Y	0.04	0.00
Tyr	[123455667]	466	9	0.05	0.05	0.05	0.05	Y	Y	Y	Y	0.05	0.00
Val	[2345]	186	0	0.22	0.22	0.22	0.22	Y	Y	Y	Y	0.22	0.00
Val	[2345]	186	1	0.15	0.14	0.14	0.14	Y	Y	Y	Y	0.14	0.00
Val	[2345]	186	2	0.34	0.34	0.34	0.35	Y	Y	Y	Y	0.34	0.00
Val	[2345]	186	3	0.15	0.15	0.14	0.15	Y	Y	Y	Y	0.15	0.00
Val	[2345]	186	4	0.14	0.14	0.15	0.15	Y	Y	Y	Y	0.15	0.00
Val	[2345]	260	0	0.22	0.22	0.23	0.22	Y	Y	Y	Y	0.23	0.00
Val	[2345]	260	1	0.16	0.15	0.15	0.15	Y	Y	Y	Y	0.15	0.00
Val	[2345]	260	2	0.35	0.35	0.35	0.35	Y	Y	Y	Y	0.35	0.00
Val	[2345]	260	3	0.12	0.12	0.12	0.12	Y	Y	Y	Y	0.12	0.00
Val	[2345]	260	4	0.15	0.15	0.15	0.15	Y	Y	Y	Y	0.15	0.00
Val	[12345]	288	0	0.22	0.22	0.22	0.22	Y	Y	Y	Y	0.22	0.00
Val	[12345]	288	1	0.13	0.13	0.13	0.12	Y	Y	Y	Y	0.13	0.00
Val	[12345]	288	2	0.22	0.22	0.22	0.22	Y	Y	Y	Y	0.22	0.00
Val	[12345]	288	3	0.21	0.21	0.21	0.21	Y	Y	Y	Y	0.21	0.00
Val	[12345]	288	4	0.09	0.09	0.08	0.09	Y	Y	Y	Y	0.09	0.00
Val	[12345]	288	5	0.14	0.14	0.14	0.14	Y	Y	Y	Y	0.14	0.00

### **A.7. Table A.7 Mass Isotopomers from 100% 1-<sup>13</sup>C Glc ILE.**

Mass isotopomer distributions from 100% 1-<sup>13</sup>C glucose ILE (**Table A.7**).

This table follows the scheme of **Table A.1**.

Table A.7 Mass isotopomers from 100% 1-<sup>13</sup>C Glc ILE.

AA	Fragment	m/z	Mass (n in m+n)	Biological Replicates			Consider Replicat			Overall	
				Rep 1	Rep 2	Rep 3	1	2	3	Avg	SD
Ala	[23]	232	0	0.87	0.88	0.87	Y	Y	Y	0.87	0.01
Ala	[23]	232	1	0.13	0.12	0.13	Y	Y	Y	0.12	0.00
Ala	[23]	232	2	0.01	0.00	0.01	Y	Y	Y	0.01	0.00
Ala	[123]	260	0	0.72	0.72	0.73	Y	Y	Y	0.73	0.00
Ala	[123]	260	1	0.26	0.26	0.26	Y	Y	Y	0.26	0.00
Ala	[123]	260	2	0.01	0.01	0.01	Y	Y	Y	0.01	0.00
Ala	[123]	260	3	0.00	0.00	0.00	Y	Y	Y	0.00	0.00
Arg	[2345]	340	0	0.71	0.73	0.70	Y	Y	Y	0.71	0.01
Arg	[2345]	340	1	0.23	0.22	0.23	Y	Y	Y	0.23	0.01
Arg	[2345]	340	2	0.04	0.04	0.04	Y	Y	Y	0.04	0.00
Arg	[2345]	340	3	0.02	0.01	0.01	Y	Y	Y	0.02	0.00
Arg	[2345]	340	4	0.01	0.01	0.01	Y	Y	Y	0.01	0.00
Arg	[12345]	442	0	0.38	0.39	0.32	Y	Y	Y	0.37	0.04
Arg	[12345]	442	1	0.15	0.14	0.13	Y	Y	Y	0.14	0.01
Arg	[12345]	442	2	0.34	0.34	0.39	Y	Y	Y	0.36	0.03
Arg	[12345]	442	3	0.11	0.11	0.13	Y	Y	Y	0.12	0.01
Arg	[12345]	442	4	0.02	0.02	0.02	Y	Y	Y	0.02	0.00
Arg	[12345]	442	5	0.00	0.00	0.00	Y	Y	Y	0.00	0.00
Asp	[12]	302	0	0.82	0.82	0.82	Y	Y	Y	0.82	0.00
Asp	[12]	302	1	0.18	0.17	0.17	Y	Y	Y	0.17	0.00
Asp	[12]	302	2	0.01	0.01	0.01	Y	Y	Y	0.01	0.00
Asp	[234]	316	0	0.80	0.81	0.80	Y	Y	Y	0.80	0.01
Asp	[234]	316	1	0.17	0.16	0.17	Y	Y	Y	0.17	0.01
Asp	[234]	316	2	0.02	0.02	0.02	Y	Y	Y	0.02	0.00
Asp	[234]	316	3	0.01	0.01	0.01	Y	Y	Y	0.01	0.00
Asp	[234]	390	0	0.82	0.82	0.82	Y	Y	Y	0.82	0.00
Asp	[234]	390	1	0.16	0.16	0.16	Y	Y	Y	0.16	0.00
Asp	[234]	390	2	0.02	0.02	0.02	Y	Y	Y	0.02	0.00
Asp	[234]	390	3	0.00	0.00	0.00	Y	Y	Y	0.00	0.00
Asp	[1234]	418	0	0.71	0.72	0.72	Y	Y	Y	0.72	0.01
Asp	[1234]	418	1	0.25	0.24	0.25	Y	Y	Y	0.25	0.01
Asp	[1234]	418	2	0.03	0.03	0.03	Y	Y	Y	0.03	0.00
Asp	[1234]	418	3	0.00	0.00	0.00	Y	Y	Y	0.00	0.00
Asp	[1234]	418	4	0.00	0.00	0.00	Y	Y	Y	0.00	0.00
Glu	[2345]	272	0	0.75	0.77	0.75	Y	Y	Y	0.75	0.01
Glu	[2345]	272	1	0.20	0.19	0.20	Y	Y	Y	0.20	0.01
Glu	[2345]	272	2	0.04	0.04	0.04	Y	Y	Y	0.04	0.00
Glu	[2345]	272	3	0.01	0.01	0.01	Y	Y	Y	0.01	0.00
Glu	[2345]	272	4	0.00	0.00	0.00	Y	Y	Y	0.00	0.00
Glu	[2345]	330	0	0.77	0.78	0.76	Y	Y	Y	0.77	0.01
Glu	[2345]	330	1	0.19	0.18	0.19	Y	Y	Y	0.19	0.01
Glu	[2345]	330	2	0.04	0.03	0.04	Y	Y	Y	0.03	0.00
Glu	[2345]	330	3	0.01	0.00	0.01	Y	Y	Y	0.00	0.00
Glu	[2345]	330	4	0.00	0.00	0.00	Y	Y	Y	0.00	0.00
Glu	[12345]	432	0	0.72	0.74	0.72	Y	Y	Y	0.73	0.01
Glu	[12345]	432	1	0.22	0.21	0.23	Y	Y	Y	0.22	0.01
Glu	[12345]	432	2	0.04	0.04	0.04	Y	Y	Y	0.04	0.00
Glu	[12345]	432	3	0.01	0.01	0.01	Y	Y	Y	0.01	0.00
Glu	[12345]	432	4	0.00	0.00	0.00	Y	Y	Y	0.00	0.00
Glu	[12345]	432	5	0.00	0.00	0.00	Y	Y	Y	0.00	0.00
Gly	[2]	218	0	0.92	0.92	0.91	Y	Y	Y	0.92	0.00
Gly	[2]	218	1	0.08	0.08	0.09	Y	Y	Y	0.08	0.00
Gly	[12]	246	0	0.87	0.87	0.86	Y	Y	Y	0.87	0.00
Gly	[12]	246	1	0.13	0.13	0.13	Y	Y	Y	0.13	0.00
Gly	[12]	246	2	0.00	0.00	0.00	Y	Y	Y	0.00	0.00
His	[2345]	196	0	0.41	0.42	0.41	Y	Y	Y	0.42	0.00
His	[2345]	196	1	0.48	0.48	0.47	Y	Y	Y	0.48	0.01
His	[2345]	196	2	0.09	0.09	0.09	Y	Y	Y	0.09	0.00
His	[2345]	196	3	0.01	0.01	0.02	Y	Y	Y	0.01	0.00
His	[2345]	196	4	0.00	0.00	0.01	Y	Y	Y	0.01	0.00
His	[23456]	338	0	0.40	0.40	0.40	Y	Y	Y	0.40	0.00
His	[23456]	338	1	0.48	0.49	0.47	Y	Y	Y	0.48	0.01
His	[23456]	338	2	0.09	0.09	0.10	Y	Y	Y	0.09	0.01
His	[23456]	338	3	0.01	0.01	0.01	Y	Y	Y	0.01	0.00
His	[23456]	338	4	0.01	0.01	0.01	Y	Y	Y	0.01	0.00
His	[23456]	338	5	0.00	0.00	0.01	Y	Y	Y	0.00	0.00
His	[123456]	440	0	0.38	0.38	0.37	Y	Y	Y	0.38	0.01
His	[123456]	440	1	0.48	0.47	0.47	Y	Y	Y	0.48	0.00
His	[123456]	440	2	0.12	0.12	0.13	Y	Y	Y	0.12	0.01
His	[123456]	440	3	0.02	0.02	0.02	Y	Y	Y	0.02	0.00
His	[123456]	440	4	0.00	0.00	0.00	Y	Y	Y	0.00	0.00
His	[123456]	440	5	0.00	0.00	0.00	Y	Y	Y	0.00	0.00
His	[123456]	440	6	0.00	0.00	0.00	Y	Y	Y	0.00	0.00
Ile	[23456]	200	0	0.68	0.70	0.68	Y	Y	Y	0.68	0.01
Ile	[23456]	200	1	0.25	0.24	0.25	Y	Y	Y	0.25	0.01
Ile	[23456]	200	2	0.06	0.05	0.06	Y	Y	Y	0.06	0.00
Ile	[23456]	200	3	0.01	0.01	0.01	Y	Y	Y	0.01	0.00

Ile	[23456]	200	4	0.00	0.00	0.00	Y	Y	Y	0.00	0.00
Ile	[23456]	200	5	0.00	0.00	0.00	Y	Y	Y	0.00	0.00
Ile	[23456]	274	0	0.68	0.70	0.67	Y	Y	Y	0.68	0.01
Ile	[23456]	274	1	0.25	0.24	0.25	Y	Y	Y	0.25	0.01
Ile	[23456]	274	2	0.06	0.06	0.06	Y	Y	Y	0.06	0.00
Ile	[23456]	274	3	0.01	0.01	0.01	Y	Y	Y	0.01	0.00
Ile	[23456]	274	4	0.00	0.00	0.00	Y	Y	Y	0.00	0.00
Ile	[23456]	274	5	0.00	0.00	0.00	Y	Y	Y	0.00	0.00
Leu	[23456]	200	0	0.69	0.70	0.68	Y	Y	Y	0.69	0.01
Leu	[23456]	200	1	0.24	0.23	0.25	Y	Y	Y	0.24	0.01
Leu	[23456]	200	2	0.06	0.05	0.06	Y	Y	Y	0.06	0.00
Leu	[23456]	200	3	0.01	0.01	0.01	Y	Y	Y	0.01	0.00
Leu	[23456]	200	4	0.00	0.00	0.00	Y	Y	Y	0.00	0.00
Leu	[23456]	200	5	0.00	0.00	0.00	Y	Y	Y	0.00	0.00
Leu	[23456]	274	0	0.69	0.70	0.69	Y	Y	Y	0.69	0.01
Leu	[23456]	274	1	0.25	0.24	0.24	Y	Y	Y	0.24	0.00
Leu	[23456]	274	2	0.06	0.05	0.06	Y	Y	Y	0.06	0.00
Leu	[23456]	274	3	0.01	0.01	0.01	Y	Y	Y	0.01	0.00
Leu	[23456]	274	4	0.00	0.00	0.00	Y	Y	Y	0.00	0.00
Leu	[23456]	274	5	0.00	0.00	0.00	Y	Y	Y	0.00	0.00
Lys	[23456]	329	0	0.68	0.70	0.67	Y	Y	Y	0.68	0.01
Lys	[23456]	329	1	0.25	0.24	0.26	Y	Y	Y	0.25	0.01
Lys	[23456]	329	2	0.06	0.05	0.06	Y	Y	Y	0.06	0.00
Lys	[23456]	329	3	0.01	0.01	0.01	Y	Y	Y	0.01	0.00
Lys	[23456]	329	4	0.00	0.00	0.00	Y	Y	Y	0.00	0.00
Lys	[23456]	329	5	0.00	0.00	0.00	Y	Y	Y	0.00	0.00
Lys	[123456]	431	0	0.59	0.60	0.59	Y	Y	Y	0.59	0.00
Lys	[123456]	431	1	0.32	0.32	0.32	Y	Y	Y	0.32	0.00
Lys	[123456]	431	2	0.08	0.08	0.07	Y	Y	Y	0.08	0.00
Lys	[123456]	431	3	0.01	0.01	0.01	Y	Y	Y	0.01	0.00
Lys	[123456]	431	4	0.00	0.00	0.00	Y	Y	Y	0.00	0.00
Lys	[123456]	431	5	0.00	0.00	0.00	Y	Y	Y	0.00	0.00
Lys	[123456]	431	6	0.00	0.00	0.00	Y	Y	Y	0.00	0.00
Lys	[123456]	488	0	0.59	0.60	0.59	Y	Y	Y	0.60	0.01
Lys	[123456]	488	1	0.33	0.32	0.32	Y	Y	Y	0.32	0.00
Lys	[123456]	488	2	0.07	0.07	0.07	Y	Y	Y	0.07	0.00
Lys	[123456]	488	3	0.01	0.01	0.01	Y	Y	Y	0.01	0.00
Lys	[123456]	488	4	0.01	0.00	0.00	Y	Y	Y	0.00	0.00
Lys	[123456]	488	5	0.00	0.00	0.00	Y	Y	Y	0.00	0.00
Lys	[123456]	488	6	0.00	0.00	0.00	Y	Y	Y	0.00	0.00
Met	[2345]	218	0	0.71	0.72	0.70	Y	Y	Y	0.71	0.01
Met	[2345]	218	1	0.25	0.24	0.25	Y	Y	Y	0.25	0.01
Met	[2345]	218	2	0.04	0.03	0.04	Y	Y	Y	0.04	0.00
Met	[2345]	218	3	0.00	0.00	0.00	Y	Y	Y	0.00	0.00
Met	[2345]	218	4	0.00	0.00	0.00	Y	Y	Y	0.00	0.00
Met	[2345]	292	0	0.71	0.72	0.71	Y	Y	Y	0.71	0.01
Met	[2345]	292	1	0.25	0.24	0.25	Y	Y	Y	0.25	0.01
Met	[2345]	292	2	0.04	0.04	0.04	Y	Y	Y	0.04	0.00
Met	[2345]	292	3	0.00	0.00	0.00	Y	Y	Y	0.00	0.00
Met	[2345]	292	4	0.00	0.00	0.00	Y	Y	Y	0.00	0.00
Met	[12345]	320	0	0.62	0.64	0.63	Y	Y	Y	0.63	0.01
Met	[12345]	320	1	0.31	0.30	0.31	Y	Y	Y	0.31	0.01
Met	[12345]	320	2	0.06	0.05	0.05	Y	Y	Y	0.05	0.00
Met	[12345]	320	3	0.00	0.01	0.01	Y	Y	Y	0.01	0.00
Met	[12345]	320	4	0.00	0.00	0.00	Y	Y	Y	0.00	0.00
Met	[12345]	320	5	0.00	0.00	0.00	Y	Y	Y	0.00	0.00
Phe	[23455667]	234	0	0.61	0.62	0.60	Y	Y	Y	0.61	0.01
Phe	[23455667]	234	1	0.28	0.28	0.29	Y	Y	Y	0.28	0.00
Phe	[23455667]	234	2	0.09	0.08	0.09	Y	Y	Y	0.08	0.00
Phe	[23455667]	234	3	0.02	0.02	0.02	Y	Y	Y	0.02	0.00
Phe	[23455667]	234	4	0.00	0.00	0.00	Y	Y	Y	0.00	0.00
Phe	[23455667]	234	5	0.00	0.00	0.00	Y	Y	Y	0.00	0.00
Phe	[23455667]	234	6	0.00	0.00	0.00	Y	Y	Y	0.00	0.00
Phe	[23455667]	234	7	0.00	0.00	0.00	Y	Y	Y	0.00	0.00
Phe	[23455667]	234	8	0.00	0.00	0.00	Y	Y	Y	0.00	0.00
Phe	[12]	302	0	0.89	0.89	0.89	Y	Y	Y	0.89	0.00
Phe	[12]	302	1	0.10	0.10	0.11	Y	Y	Y	0.10	0.00
Phe	[12]	302	2	0.01	0.01	0.01	Y	Y	Y	0.01	0.00
Phe	[123455667]	336	0	0.58	0.59	0.57	Y	Y	Y	0.58	0.01
Phe	[123455667]	336	1	0.29	0.29	0.30	Y	Y	Y	0.29	0.00
Phe	[123455667]	336	2	0.10	0.10	0.10	Y	Y	Y	0.10	0.00
Phe	[123455667]	336	3	0.02	0.02	0.02	Y	Y	Y	0.02	0.00
Phe	[123455667]	336	4	0.00	0.00	0.00	Y	Y	Y	0.00	0.00
Phe	[123455667]	336	5	0.00	0.00	0.00	Y	Y	Y	0.00	0.00
Phe	[123455667]	336	6	0.00	0.00	0.00	Y	Y	Y	0.00	0.00
Phe	[123455667]	336	7	0.00	0.00	0.00	Y	Y	Y	0.00	0.00
Phe	[123455667]	336	8	0.00	0.00	0.00	Y	Y	Y	0.00	0.00
Phe	[123455667]	336	9	0.00	0.00	0.00	Y	Y	Y	0.00	0.00
Pro	[2345]	184	0	0.77	0.78	0.77	Y	Y	Y	0.77	0.01
Pro	[2345]	184	1	0.20	0.19	0.20	Y	Y	Y	0.19	0.01

Pro	[2345]	184	2	0.03	0.03	0.03	Y	Y	Y	0.03	0.00
Pro	[2345]	184	3	0.00	0.00	0.00	Y	Y	Y	0.00	0.00
Pro	[2345]	184	4	0.00	0.00	0.00	Y	Y	Y	0.00	0.00
Pro	[2345]	258	0	0.77	0.78	0.76	Y	Y	Y	0.77	0.01
Pro	[2345]	258	1	0.20	0.19	0.20	Y	Y	Y	0.20	0.01
Pro	[2345]	258	2	0.03	0.03	0.03	Y	Y	Y	0.03	0.00
Pro	[2345]	258	3	0.00	0.00	0.00	Y	Y	Y	0.00	0.00
Pro	[2345]	258	4	0.00	0.00	0.00	Y	Y	Y	0.00	0.00
Ser	[23]	288	0	0.80	0.81	0.80	Y	Y	Y	0.80	0.00
Ser	[23]	288	1	0.18	0.18	0.19	Y	Y	Y	0.18	0.00
Ser	[23]	288	2	0.02	0.02	0.02	Y	Y	Y	0.02	0.00
Ser	[12]	302	0	0.87	0.87	0.86	Y	Y	Y	0.87	0.01
Ser	[12]	302	1	0.13	0.12	0.13	Y	Y	Y	0.13	0.01
Ser	[12]	302	2	0.00	0.00	0.00	Y	Y	Y	0.00	0.00
Ser	[23]	362	0	0.82	0.82	0.81	Y	Y	Y	0.81	0.00
Ser	[23]	362	1	0.17	0.17	0.18	Y	Y	Y	0.17	0.00
Ser	[23]	362	2	0.01	0.01	0.01	Y	Y	Y	0.01	0.00
Ser	[123]	390	0	0.77	0.77	0.76	Y	Y	Y	0.77	0.01
Ser	[123]	390	1	0.21	0.20	0.21	Y	Y	Y	0.21	0.00
Ser	[123]	390	2	0.02	0.02	0.02	Y	Y	Y	0.02	0.00
Ser	[123]	390	3	0.00	0.00	0.00	Y	Y	Y	0.00	0.00
Thr	[234]	376	0	0.83	0.84	0.82	Y	Y	Y	0.83	0.01
Thr	[234]	376	1	0.15	0.15	0.16	Y	Y	Y	0.15	0.01
Thr	[234]	376	2	0.01	0.02	0.02	Y	Y	Y	0.02	0.00
Thr	[234]	376	3	0.00	0.00	0.00	Y	Y	Y	0.00	0.00
Thr	[1234]	404	0	0.73	0.74	0.73	Y	Y	Y	0.73	0.01
Thr	[1234]	404	1	0.24	0.23	0.23	Y	Y	Y	0.23	0.01
Thr	[1234]	404	2	0.03	0.03	0.03	Y	Y	Y	0.03	0.00
Thr	[1234]	404	3	0.00	0.00	0.00	Y	Y	Y	0.00	0.00
Thr	[1234]	404	4	0.00	0.00	0.00	Y	Y	Y	0.00	0.00
Tyr	[12]	302	0	0.90	0.91	0.90	Y	Y	Y	0.90	0.00
Tyr	[12]	302	1	0.09	0.09	0.09	Y	Y	Y	0.09	0.00
Tyr	[12]	302	2	0.00	0.00	0.01	Y	Y	Y	0.00	0.00
Tyr	[23455667]	364	0	0.62	0.64	0.62	Y	Y	Y	0.63	0.01
Tyr	[23455667]	364	1	0.26	0.25	0.26	Y	Y	Y	0.26	0.01
Tyr	[23455667]	364	2	0.08	0.07	0.07	Y	Y	Y	0.08	0.00
Tyr	[23455667]	364	3	0.02	0.02	0.02	Y	Y	Y	0.02	0.00
Tyr	[23455667]	364	4	0.00	0.00	0.00	Y	Y	Y	0.00	0.00
Tyr	[23455667]	364	5	0.00	0.01	0.01	Y	Y	Y	0.00	0.00
Tyr	[23455667]	364	6	0.01	0.00	0.02	Y	Y	Y	0.01	0.01
Tyr	[23455667]	364	7	0.00	0.00	0.01	Y	Y	Y	0.00	0.00
Tyr	[23455667]	364	8	0.00	0.00	0.00	Y	Y	Y	0.00	0.00
Tyr	[23455667]	438	0	0.62	0.63	0.61	Y	Y	Y	0.62	0.01
Tyr	[23455667]	438	1	0.28	0.27	0.27	Y	Y	Y	0.27	0.00
Tyr	[23455667]	438	2	0.08	0.07	0.08	Y	Y	Y	0.07	0.01
Tyr	[23455667]	438	3	0.01	0.01	0.02	Y	Y	Y	0.01	0.00
Tyr	[23455667]	438	4	0.00	0.00	0.00	Y	Y	Y	0.00	0.00
Tyr	[23455667]	438	5	0.00	0.00	0.00	Y	Y	Y	0.00	0.00
Tyr	[23455667]	438	6	0.00	0.00	0.00	Y	Y	Y	0.00	0.00
Tyr	[23455667]	438	7	0.00	0.00	0.00	Y	Y	Y	0.00	0.00
Tyr	[23455667]	438	8	0.01	0.01	0.01	Y	Y	Y	0.01	0.00
Tyr	[123455667]	466	0	0.61	0.61	0.59	Y	Y	Y	0.60	0.01
Tyr	[123455667]	466	1	0.28	0.29	0.29	Y	Y	Y	0.29	0.00
Tyr	[123455667]	466	2	0.08	0.08	0.09	Y	Y	Y	0.09	0.01
Tyr	[123455667]	466	3	0.02	0.02	0.02	Y	Y	Y	0.02	0.00
Tyr	[123455667]	466	4	0.00	0.00	0.00	Y	Y	Y	0.00	0.00
Tyr	[123455667]	466	5	0.00	0.00	0.00	Y	Y	Y	0.00	0.00
Tyr	[123455667]	466	6	0.00	0.00	0.00	Y	Y	Y	0.00	0.00
Tyr	[123455667]	466	7	0.00	0.00	0.00	Y	Y	Y	0.00	0.00
Tyr	[123455667]	466	8	0.00	0.00	0.00	Y	Y	Y	0.00	0.00
Tyr	[123455667]	466	9	0.00	0.00	0.00	Y	Y	Y	0.00	0.00
Val	[2345]	186	0	0.74	0.75	0.74	Y	Y	Y	0.74	0.01
Val	[2345]	186	1	0.21	0.20	0.21	Y	Y	Y	0.20	0.01
Val	[2345]	186	2	0.04	0.03	0.04	Y	Y	Y	0.04	0.00
Val	[2345]	186	3	0.02	0.02	0.02	Y	Y	Y	0.02	0.00
Val	[2345]	186	4	0.00	0.00	0.00	Y	Y	Y	0.00	0.00
Val	[2345]	260	0	0.73	0.74	0.73	Y	Y	Y	0.73	0.01
Val	[2345]	260	1	0.22	0.22	0.23	Y	Y	Y	0.22	0.01
Val	[2345]	260	2	0.04	0.04	0.04	Y	Y	Y	0.04	0.00
Val	[2345]	260	3	0.01	0.00	0.00	Y	Y	Y	0.00	0.00
Val	[2345]	260	4	0.00	0.00	0.00	Y	Y	Y	0.00	0.00
Val	[12345]	288	0	0.61	0.61	0.61	Y	Y	Y	0.61	0.00
Val	[12345]	288	1	0.33	0.33	0.33	Y	Y	Y	0.33	0.00
Val	[12345]	288	2	0.06	0.05	0.06	Y	Y	Y	0.06	0.00
Val	[12345]	288	3	0.00	0.00	0.01	Y	Y	Y	0.01	0.00
Val	[12345]	288	4	0.00	0.00	0.00	Y	Y	Y	0.00	0.00
Val	[12345]	288	5	0.00	0.00	0.00	Y	Y	Y	0.00	0.00

**A.8. Table A.8 Parallel experiment: Mass Isotopomers from  $^{15}\text{N}$  urea instationary ILE.**

Mass isotopomer distributions from  $^{15}\text{N}$  urea ILE in parallel experiment (Table A.8). This table follows the scheme of Table A.1.

Metabolite		Fragment		m/z		Mass (n in m-n)		Table A.8 Parallel experiment: Mass isotopomers from <sup>15</sup> N urea instationary H.E.																			
								t = 0 min (control)																			
								Intracellular metabolites: biological and technical (MS) replicates																			
								Rep 1					Rep 2					Rep 3					Overall				
Tech 1	Tech 2	Tech 3	Avg	SE	Tech 1	Tech 2	Tech 3	Avg	SE	Tech 1	Tech 2	Tech 3	Avg	SE	Avg	SE											
Ala	[231]	158	1	0.99	0.99	0.99	0.99	0.00	0.00	0.99	0.99	0.99	0.99	0.00	0.00	0.99	0.99	0.99	0.99	0.00	0.00						
Ala	[231]	158	1	0.01	0.01	0.01	0.01	0.00	0.00	0.01	0.01	0.01	0.01	0.00	0.00	0.01	0.01	0.01	0.01	0.00	0.00						
Ala	[231]	232	0	1.00	1.00	1.00	1.00	0.00	0.00	1.00	1.01	1.01	1.00	0.00	0.00	1.00	1.00	1.01	1.00	0.00	0.00						
Ala	[231]	232	1	0.00	0.00	0.00	0.00	0.00	0.00	0.00	-0.01	-0.01	-0.01	0.00	0.00	0.00	0.00	-0.01	0.00	0.00	0.00						
Ala	[123]	260	0	1.01	1.01	1.02	1.01	0.00	0.00	1.01	1.01	1.01	1.01	0.00	0.00	1.00	1.01	1.01	1.01	0.00	0.00						
Ala	[123]	260	1	-0.01	-0.01	-0.02	-0.01	0.00	0.00	-0.01	-0.01	-0.01	-0.01	0.00	0.00	0.00	-0.01	-0.01	-0.01	0.00	-0.01						
Asp	[12]	302	0	1.00	0.99	1.01	1.00	0.00	0.00	1.00	1.00	1.00	1.00	0.00	0.00	1.00	1.01	1.00	1.01	0.00	0.00						
Asp	[12]	302	1	0.00	0.01	-0.01	0.00	0.00	0.00	-0.01	0.00	0.00	0.00	0.00	0.00	-0.01	-0.01	0.00	-0.01	0.00	0.00						
Asp	[234]	316	0	1.01	0.99	1.00	1.00	0.01	0.01	1.01	1.00	1.01	1.01	0.00	0.00	1.01	1.00	1.00	1.00	0.00	0.00						
Asp	[234]	316	1	-0.01	0.01	-0.01	0.00	0.01	0.01	-0.01	0.00	-0.01	-0.01	0.00	0.00	-0.01	0.00	0.00	0.00	0.00	0.01						
Asp	[12]	376	0	1.06	1.02	1.04	1.04	0.01	0.01	1.03	1.01	1.01	1.02	0.01	0.00	1.00	1.01	1.02	1.01	0.00	1.02						
Asp	[12]	376	1	-0.06	-0.02	-0.04	-0.04	0.01	0.01	-0.03	-0.01	-0.01	-0.02	0.01	0.00	0.00	-0.01	-0.02	-0.01	0.00	-0.02						
Asp	[234]	390	0	1.04	1.01	1.00	1.02	0.01	0.01	1.01	1.01	1.01	1.01	0.00	0.00	1.01	1.01	1.01	1.01	0.00	1.01						
Asp	[234]	390	1	-0.04	-0.01	0.00	-0.02	0.01	0.01	-0.01	-0.01	-0.01	-0.01	0.00	0.00	-0.01	-0.01	-0.01	-0.01	0.00	-0.01						
Asp	[1234]	418	0	1.00	1.02	1.02	1.02	0.01	0.01	1.01	1.02	1.02	1.02	0.00	0.00	1.02	1.01	1.01	1.01	0.00	1.02						
Asp	[1234]	418	1	0.00	-0.02	-0.02	-0.02	0.01	0.01	-0.01	-0.02	-0.02	-0.02	0.00	0.00	-0.02	-0.01	-0.01	-0.01	0.00	-0.02						
Glu	[2345]	272	0	1.01	1.00	1.00	1.01	0.00	0.00	1.01	1.01	1.01	1.01	0.00	0.00	1.00	1.00	1.00	1.00	0.00	1.00						
Glu	[2345]	272	1	-0.01	0.00	0.00	-0.01	0.00	0.00	-0.01	-0.01	-0.01	-0.01	0.00	0.00	0.00	0.00	0.00	0.00	0.00	-0.01						
Glu	[2345]	330	0	1.01	1.01	1.01	1.01	0.00	0.00	1.00	1.01	1.01	1.01	0.00	0.00	1.01	1.01	1.01	1.01	0.00	1.01						
Glu	[2345]	330	1	-0.01	-0.01	-0.01	-0.01	0.00	0.00	0.00	0.00	-0.01	-0.01	0.00	0.00	-0.01	-0.01	-0.01	-0.01	0.00	-0.01						
Glu	[2345]	404	0	1.03	1.01	1.01	1.02	0.00	0.00	1.02	1.02	1.02	1.02	0.00	0.00	1.02	1.02	1.02	1.02	0.00	1.02						
Glu	[2345]	404	1	-0.03	-0.01	-0.01	-0.02	0.00	0.00	-0.02	-0.02	-0.02	-0.02	0.00	0.00	-0.02	-0.02	-0.02	-0.02	0.00	-0.02						
Glu	[12345]	432	0	1.02	1.01	1.02	1.02	0.00	0.00	1.02	1.02	1.01	1.02	0.00	0.00	1.02	1.02	1.03	1.02	0.00	1.02						
Glu	[12345]	432	1	-0.02	-0.01	-0.02	-0.02	0.00	0.00	-0.02	-0.02	-0.01	-0.02	0.00	0.00	-0.02	-0.02	-0.03	-0.02	0.00	-0.02						
He	[23456]	200	0	1.01	1.01	1.00	1.01	0.00	0.00	1.01	1.01	1.01	1.01	0.00	0.00	1.01	1.01	1.01	1.01	0.00	1.01						
He	[23456]	200	1	-0.01	-0.01	-0.01	-0.01	0.00	0.00	-0.01	-0.01	-0.01	-0.01	0.00	0.00	-0.01	-0.01	-0.01	-0.01	0.00	-0.01						
He	[23456]	274	0	0.99	1.00	0.98	0.99	0.01	0.01	0.99	0.99	0.99	0.99	0.00	0.00	0.99	0.99	0.99	0.99	0.00	0.99						
He	[23456]	274	1	0.01	0.00	0.02	0.01	0.01	0.01	0.01	0.01	0.01	0.01	0.00	0.00	0.01	0.01	0.01	0.01	0.00	0.01						
He	[12]	302	0	0.99	1.01	1.01	1.00	0.00	0.00	1.01	1.00	1.00	1.00	0.00	0.00	1.00	1.00	1.00	1.00	0.00	1.00						
He	[12]	302	1	0.01	-0.01	-0.01	-0.01	0.00	0.00	-0.01	0.00	0.00	0.00	0.00	0.00	0.00	0.00	0.00	0.00	0.00	0.00						
Leu	[23456]	200	0	1.01	1.01	1.01	1.01	0.00	0.00	1.01	1.01	1.01	1.01	0.00	0.00	1.01	1.01	1.01	1.01	0.00	1.01						
Leu	[23456]	200	1	-0.01	-0.01	-0.01	-0.01	0.00	0.00	-0.01	-0.01	-0.01	-0.01	0.00	0.00	-0.01	-0.01	-0.01	-0.01	0.00	-0.01						
Leu	[23456]	274	0	1.01	1.00	1.00	1.00	0.00	0.00	1.00	1.00	1.00	1.00	0.00	0.00	1.00	1.00	1.00	1.00	0.00	1.00						
Leu	[23456]	274	1	-0.01	0.00	0.00	0.00	0.00	0.00	0.00	0.00	0.00	0.00	0.00	0.00	0.00	0.00	0.00	0.00	0.00	0.00						
Leu	[12]	302	0	1.00	1.00	1.00	1.00	0.00	0.00	1.00	1.00	1.00	1.00	0.00	0.00	1.00	1.00	1.00	1.00	0.00	1.00						
Leu	[12]	302	1	0.00	0.00	0.00	0.00	0.00	0.00	0.00	0.00	0.00	0.00	0.00	0.00	0.00	0.00	0.00	0.00	0.00	0.00						
Phe	[23455667]	234	0	1.01	1.00	1.01	1.01	0.00	0.00	1.01	1.00	1.01	1.01	0.00	0.00	1.02	1.01	1.01	1.01	0.00	1.01						
Phe	[23455667]	234	1	-0.01	0.00	-0.01	-0.01	0.00	0.00	-0.01	0.00	-0.01	-0.01	0.00	0.00	-0.02	-0.01	-0.01	-0.01	0.00	-0.01						
Phe	[12]	302	0	0.99	1.01	1.01	1.00	0.01	0.01	1.01	1.01	1.00	1.00	0.00	0.00	1.01	1.01	1.01	1.01	0.00	1.00						
Phe	[12]	302	1	0.01	-0.01	-0.01	0.00	0.01	0.01	-0.01	-0.01	0.00	0.00	0.00	0.00	-0.01	-0.01	-0.01	-0.01	0.00	0.01						
Phe	[23455667]	308	0	0.98	0.98	0.98	0.98	0.00	0.00	0.99	0.99	1.00	0.99	0.00	0.00	0.99	0.99	0.99	0.99	0.00	0.99						
Phe	[23455667]	308	1	0.02	0.02	0.02	0.02	0.00	0.01	0.01	0.01	0.00	0.01	0.00	0.01	0.01	0.01	0.01	0.01	0.00	0.01						
Phe	[123455667]	336	0	1.02	1.01	1.02	1.02	0.00	0.00	1.02	1.01	1.02	1.02	0.00	0.00	1.01	1.01	1.01	1.01	0.00	1.01						
Phe	[123455667]	336	1	-0.02	-0.01	-0.02	-0.02	0.00	0.00	-0.02	-0.01	-0.02	-0.02	0.00	0.00	-0.01	-0.01	-0.01	-0.01	0.00	-0.01						
Pro	[2345]	184	0	1.00	1.00	1.00	1.00	0.00	0.00	1.00	1.00	1.00	1.00	0.00	0.00	1.00	1.00	1.00	1.00	0.00	1.00						
Pro	[2345]	184	1	0.00	0.00	0.00	0.00	0.00	0.00	0.00	0.00	0.00	0.00	0.00	0.00	0.00	0.00	0.00	0.00	0.00	0.00						
Pro	[2345]	258	0	1.01	1.01	1.01	1.01	0.00	0.00	1.01	1.01	1.01	1.01	0.00	0.00	1.01	1.01	1.01	1.01	0.00	1.01						
Pro	[2345]	258	1	-0.01	-0.01	-0.01	-0.01	0.00	0.00	-0.01	-0.01	-0.01	-0.01	0.00	0.00	-0.01	-0.01	-0.01	-0.01	0.00	-0.01						
Pro	[12345]	286	0	1.01	1.01	1.01	1.01	0.00	0.00	1.01	1.01	1.01	1.01	0.00	0.00	1.01	1.01	1.01	1.01	0.00	1.01						
Pro	[12345]	286	1	-0.01	-0.01	-0.01	-0.01	0.00	0.00	-0.01	-0.01	-0.01	-0.01	0.00	0.00	-0.01	-0.01	-0.01	-0.01	0.00	-0.01						
Ser	[231]	288	0	0.99	1.01	1.01	1.00	0.01	0.01	1.00	1.00	1.00	1.00	0.00	0.00	1.00	0.99	1.00	1.00	0.00	1.00						
Ser	[231]	288	1	0.01	-0.01	-0.01	0.00	0.01	0.00	0.00	0.00	0.00	0.00	0.00	0.00	0.00	0.01	0.00	0.00	0.00	0.01						
Ser	[12]	302	0	1.01	1.01	1.01	1.01	0.00	0.00	1.01	1.00	0.99	1.00	0.01	0.01	1.01	1.01	1.00	1.01	0.00	1.01						
Ser	[12]	302	1	-0.01	-0.01	-0.01	-0.01	0.00	0.00	-0.01	0.00	0.01	0.00	0.01	0.01	-0.01	-0.01	0.00	-0.01	0.00	-0.01						
Ser	[23]	362	0	1.02	1.02	1.02	1.02	0.00	0.00	1.01	1.01	1.00	1.01	0.00	0.00	1.01	1.01	1.02	1.01	0.00	1.01						
Ser	[23]	362	1	-0.02	-0.02	-0.02	-0.02	0.00	0.00	-0.01	-0.01	0.00	-0.01	0.00	0.00	-0.01	-0.01	-0.02	-0.01	0.00	-0.01						
Ser	[123]	390	0	1.03	1.02	1.01	1.02	0.01	0.01	1.02	1.02	1.01	1.02	0.01	0.01	1.01	1.01	1.01	1.01	0.00	1.01						
Ser	[123]	390	1	-0.03	-0.02	-0.01	-0.02	0.01	0.01	-0.02	-0.02	-0.01	-0.02	0.01	0.01	-0.01	-0.01	-0.01	-0.01	0.00	-0.01						
Thr	[234]	376	0	0.99	1.07	1.01	1.02	0.02	0.02	1.01	1.02	1.02	1.02	0.00	0.00	1.02	1.01	1.01	1.01	0.00	1.02						
Thr	[234]	376	1	0.01	-0.07	-0.01	-0.02	0.02	0.02	-0.01	-0.02	-0.02	-0.02	0.00	0.00	-0.02	-0.01	-0.01	-0.01	0.00	-0.02						
Thr	[1234]	404	0	1.06	1.07	1.04	1.06	0.01	0.01	1.03	1.02	1.03	1.03	0.00	0.00	1.02	1.01	1.02	1.02	0.00	1.03						
Thr	[1234]	4																									







Table A.8 Parallel experiment: Mass isotopomers from <sup>15</sup> N urea stationary ILE (Cont).																			
t = 15 min																			
Metabolite	Fragment	m/z	Mass (n in m-n)	Intracellular metabolites: biological and technical (MS) replicates												Overall			
				Rep 1				Rep 2				Rep 3				Avg	SE		
				Tech 1	Tech 2	Tech 3	Avg	SE	Tech 1	Tech 2	Tech 3	Avg	SE	Tech 1	Tech 2			Tech 3	Avg
Ala	[231]	158	0	0.73	0.73	0.73	0.73	0.00	0.71	0.71	0.71	0.71	0.00	0.71	0.71	0.71	0.00	0.72	0.01
Ala	[231]	158	1	0.27	0.27	0.27	0.27	0.00	0.29	0.29	0.29	0.29	0.00	0.29	0.29	0.29	0.00	0.28	0.01
Ala	[231]	232	0	0.73	0.73	0.73	0.73	0.00	0.72	0.72	0.72	0.72	0.00	0.71	0.71	0.71	0.00	0.72	0.01
Ala	[231]	232	1	0.27	0.27	0.27	0.27	0.00	0.28	0.28	0.28	0.28	0.00	0.29	0.29	0.29	0.00	0.28	0.01
Ala	[123]	260	0	0.74	0.74	0.74	0.74	0.00	0.73	0.73	0.73	0.73	0.00	0.72	0.72	0.72	0.00	0.73	0.01
Ala	[123]	260	1	0.26	0.26	0.26	0.26	0.00	0.27	0.27	0.28	0.28	0.00	0.28	0.28	0.28	0.00	0.27	0.01
Asp	[121]	302	0	0.79	0.78	0.79	0.79	0.00	0.79	0.78	0.78	0.78	0.00	0.79	0.80	0.79	0.01	0.79	0.01
Asp	[121]	302	1	0.21	0.22	0.21	0.21	0.00	0.21	0.22	0.22	0.22	0.00	0.21	0.20	0.21	0.01	0.21	0.01
Asp	[234]	316	0	0.78	0.78	0.80	0.79	0.01	0.76	0.76	0.77	0.76	0.00	0.76	0.80	0.78	0.02	0.78	0.02
Asp	[234]	316	1	0.22	0.22	0.20	0.21	0.01	0.24	0.24	0.23	0.24	0.00	0.24	0.20	0.22	0.02	0.22	0.02
Asp	[121]	376	0	0.81	0.79	0.78	0.79	0.01	0.76	0.77	0.82	0.78	0.02	0.74	0.80	0.77	0.03	0.78	0.03
Asp	[121]	376	1	0.19	0.21	0.22	0.21	0.01	0.24	0.23	0.18	0.22	0.02	0.26	0.20	0.23	0.03	0.22	0.03
Asp	[234]	390	0	0.81	0.78	0.81	0.80	0.01	0.78	0.80	0.79	0.79	0.00	0.78	0.88	0.83	0.05	0.81	0.05
Asp	[234]	390	1	0.19	0.22	0.19	0.20	0.01	0.22	0.20	0.21	0.21	0.00	0.22	0.12	0.17	0.05	0.19	0.05
Asp	[1234]	418	0	0.79	0.79	0.79	0.79	0.00	0.79	0.78	0.79	0.79	0.00	0.78	0.77	0.78	0.00	0.78	0.00
Asp	[1234]	418	1	0.21	0.21	0.21	0.21	0.00	0.21	0.22	0.21	0.21	0.00	0.22	0.23	0.22	0.00	0.22	0.00
Glu	[2345]	272	0	0.65	0.65	0.65	0.65	0.00	0.66	0.66	0.66	0.66	0.00	0.65	0.67	0.66	0.01	0.66	0.01
Glu	[2345]	272	1	0.35	0.35	0.35	0.35	0.00	0.34	0.34	0.34	0.34	0.00	0.35	0.33	0.34	0.01	0.34	0.01
Glu	[2345]	330	0	0.66	0.66	0.66	0.66	0.00	0.66	0.66	0.66	0.66	0.00	0.66	0.66	0.66	0.00	0.66	0.00
Glu	[2345]	330	1	0.34	0.34	0.34	0.34	0.00	0.34	0.34	0.34	0.34	0.00	0.34	0.34	0.34	0.00	0.34	0.00
Glu	[2345]	404	0	0.66	0.67	0.66	0.66	0.00	0.67	0.68	0.66	0.67	0.00	0.66	0.69	0.67	0.01	0.67	0.01
Glu	[2345]	404	1	0.34	0.33	0.34	0.34	0.00	0.33	0.32	0.34	0.33	0.00	0.34	0.31	0.33	0.01	0.33	0.01
Glu	[12345]	432	0	0.66	0.66	0.67	0.66	0.00	0.66	0.67	0.66	0.66	0.00	0.66	0.66	0.66	0.00	0.66	0.00
Glu	[12345]	432	1	0.34	0.34	0.33	0.34	0.00	0.34	0.33	0.34	0.34	0.00	0.34	0.34	0.34	0.00	0.34	0.00
Ile	[23456]	200	0	0.95	0.95	0.95	0.95	0.00	0.96	0.96	0.96	0.96	0.00	0.95	0.95	0.95	0.00	0.95	0.00
Ile	[23456]	200	1	0.05	0.05	0.05	0.05	0.00	0.04	0.04	0.04	0.04	0.00	0.05	0.05	0.05	0.00	0.05	0.00
Ile	[23456]	274	0	0.92	0.94	0.93	0.93	0.00	0.94	0.94	0.94	0.94	0.00	0.93	0.94	0.93	0.00	0.94	0.00
Ile	[23456]	274	1	0.08	0.06	0.07	0.07	0.00	0.06	0.06	0.06	0.06	0.00	0.07	0.06	0.07	0.00	0.06	0.00
Ile	[121]	302	0	0.94	0.94	0.94	0.94	0.00	0.94	0.95	0.95	0.95	0.00	0.95	0.95	0.95	0.00	0.94	0.00
Ile	[121]	302	1	0.06	0.06	0.06	0.06	0.00	0.06	0.05	0.05	0.05	0.00	0.05	0.05	0.05	0.00	0.06	0.00
Leu	[23456]	200	0	0.95	0.95	0.96	0.95	0.00	0.97	0.97	0.97	0.97	0.00	0.96	0.97	0.96	0.00	0.96	0.00
Leu	[23456]	200	1	0.05	0.05	0.04	0.05	0.00	0.03	0.03	0.03	0.03	0.00	0.04	0.03	0.04	0.00	0.04	0.00
Leu	[23456]	274	0	0.95	0.95	0.95	0.94	0.01	0.95	0.95	0.95	0.95	0.00	0.94	0.95	0.95	0.01	0.94	0.01
Leu	[23456]	274	1	0.07	0.05	0.07	0.06	0.01	0.05	0.05	0.05	0.05	0.00	0.06	0.05	0.05	0.01	0.06	0.01
Leu	[121]	302	0	0.95	0.97	0.95	0.96	0.01	0.97	0.96	0.96	0.96	0.00	0.95	0.97	0.96	0.01	0.96	0.01
Leu	[121]	302	1	0.05	0.03	0.05	0.04	0.01	0.03	0.04	0.04	0.04	0.00	0.05	0.03	0.04	0.01	0.04	0.01
Phe	[23455667]	234	0	0.93	0.93	0.93	0.93	0.00	0.95	0.96	0.94	0.95	0.01	0.95	0.95	0.95	0.00	0.94	0.01
Phe	[23455667]	234	1	0.07	0.07	0.07	0.00	0.05	0.04	0.06	0.05	0.01	0.05	0.05	0.05	0.00	0.06	0.01	
Phe	[121]	302	0	0.95	0.95	0.95	0.95	0.00	0.96	0.95	0.95	0.96	0.00	0.94	0.94	0.94	0.00	0.95	0.00
Phe	[121]	302	1	0.05	0.05	0.05	0.00	0.04	0.05	0.05	0.04	0.00	0.06	0.06	0.06	0.00	0.05	0.00	
Phe	[23455667]	308	0	0.90	0.92	0.91	0.91	0.01	0.94	0.93	0.93	0.94	0.00	0.94	0.96	0.95	0.01	0.93	0.01
Phe	[23455667]	308	1	0.10	0.08	0.09	0.01	0.06	0.07	0.07	0.06	0.00	0.06	0.04	0.05	0.01	0.07	0.01	
Phe	[123455667]	336	0	0.94	0.94	0.94	0.94	0.00	0.95	0.96	0.96	0.96	0.00	0.97	0.95	0.96	0.01	0.95	0.01
Phe	[123455667]	336	1	0.06	0.06	0.06	0.00	0.05	0.04	0.04	0.04	0.04	0.00	0.03	0.05	0.04	0.01	0.05	0.01
Pro	[2345]	184	0	1.00	1.00	1.00	1.00	0.00	1.00	1.00	1.00	1.00	0.00	1.00	1.00	1.00	0.00	1.00	0.00
Pro	[2345]	184	1	0.00	0.00	0.00	0.00	0.00	0.00	0.00	0.00	0.00	0.00	0.00	0.00	0.00	0.00	0.00	0.00
Pro	[2345]	258	0	1.01	1.01	1.01	1.01	0.00	1.01	1.01	1.01	1.01	0.00	1.01	1.00	1.01	0.00	1.01	0.00
Pro	[2345]	258	1	-0.01	-0.01	-0.01	-0.01	0.00	-0.01	-0.01	-0.01	-0.01	0.00	-0.01	-0.00	-0.01	0.00	-0.01	0.00
Pro	[12345]	286	0	1.01	1.01	1.01	1.01	0.00	1.01	1.00	1.00	1.00	0.00	1.01	1.00	1.00	0.00	1.00	0.00
Pro	[12345]	286	1	-0.01	-0.01	-0.01	-0.01	0.00	-0.01	-0.00	-0.00	-0.00	0.00	-0.01	-0.00	-0.00	0.00	-0.00	0.00
Ser	[231]	288	0	0.99	0.99	0.99	0.98	0.00	0.99	0.99	1.00	0.99	0.00	1.00	0.98	0.99	0.01	0.99	0.01
Ser	[231]	288	1	0.01	0.01	0.03	0.02	0.00	0.01	0.01	0.00	0.01	0.00	0.00	0.02	0.01	0.01	0.01	0.01
Ser	[121]	302	0	1.00	1.00	0.99	1.00	0.00	0.99	1.00	0.98	0.99	0.01	0.98	0.99	0.99	0.00	0.99	0.01
Ser	[121]	302	1	0.00	0.00	0.01	0.00	0.00	0.01	0.00	0.02	0.01	0.01	0.02	0.01	0.01	0.00	0.01	0.01
Ser	[231]	362	0	0.99	1.00	1.00	1.00	0.00	0.99	1.00	1.00	1.00	0.00	1.00	1.01	1.00	0.01	1.00	0.01
Ser	[231]	362	1	0.01	0.00	0.00	0.00	0.00	0.01	0.00	0.00	0.00	0.00	-0.01	-0.00	0.00	0.01	0.00	0.01
Ser	[123]	390	0	1.00	0.99	0.99	0.99	0.00	1.02	1.02	1.01	1.02	0.00	0.99	1.02	1.00	0.01	1.00	0.01
Ser	[123]	390	1	0.00	0.01	0.01	0.01	0.00	-0.02	-0.02	-0.01	-0.02	0.00	0.01	-0.02	0.00	0.01	0.00	0.01
Thr	[234]	376	0	1.03	1.02	0.99	1.01	0.01	1.00	1.03	1.00	1.01	0.01	1.00	1.01	1.01	0.00	1.01	0.01
Thr	[234]	376	1	-0.03	-0.02	0.01	-0.01	0.01	0.00	-0.03	0.00	-0.01	0.01	0.00	-0.01	-0.01	0.00	-0.01	0.01
Thr	[1234]	404	0	1.01	0.99	1.02	1.01	0.01	0.98	1.01	1.03	1.01	0.01	1.02	1.04	1.03	0.01	1.01	0.01
Thr	[1234]	404	1	-0.01	0.01	-0.02	-0.01	0.01	0.02	-0.01	-0.03	-0.01	0.01	-0.02	-0.04	-0.03	0.01	-0.01	0.01
urea	[1]	231	0	0.01	0.01		0.01	0.00	0.01	0.01	0.01	0.01	0.00	0.01	0.01	0.01	0.00	0.01	0.00
urea	[1]	231	1	0.01	0.01		0.01	0.00	0.02	0.01	0.00	0.01	0.01	0.02	0.01	0.02	0.00	0.01	0.01
urea	[1]	231	2	0.98	0.98		0.98	0.00	0.97	0.98	0.99	0.98	0.01	0.97	0.98	0.98	0.00	0.98	0.01
urea	[1]	273	0																
urea	[1]	273	1																
urea	[1]	273	2																
Val	[2345]	186	0	0.94	0.94	0.94	0.94	0.00	0.96	0.96	0.96	0.96	0.00	0.95	0.95	0.95			

Table A.8 Parallel experiment: Mass isotopomers from <sup>15</sup> N urea stationary ILE (Cont).																					
t = 20 min																					
Metabolite	Fragment	m/z	Mass (n in m-n)	Intracellular metabolites: biological and technical (MS) replicates															Overall		
				Rep 1					Rep 2												
				Tech 1	Tech 2	Tech 3	Avg	SE	Tech 1	Tech 2	Tech 3	Avg	SE	Tech 1	Tech 2	Tech 3	Avg	SE	Avg	SE	
Ala	[231]	158	0	0.66	0.66	0.66	0.66	0.00	0.61	0.61	0.61	0.00	0.65	0.65	0.65	0.65	0.00	0.64	0.02		
Ala	[231]	158	1	0.34	0.34	0.34	0.34	0.00	0.39	0.39	0.39	0.00	0.35	0.35	0.35	0.35	0.00	0.36	0.02		
Ala	[231]	232	0	0.66	0.66	0.66	0.66	0.00	0.61	0.61	0.61	0.00	0.65	0.66	0.66	0.66	0.00	0.64	0.02		
Ala	[231]	232	1	0.34	0.34	0.34	0.34	0.00	0.39	0.39	0.39	0.00	0.35	0.34	0.34	0.34	0.00	0.36	0.02		
Ala	[123]	260	0	0.67	0.67	0.67	0.67	0.00	0.61	0.62	0.61	0.00	0.66	0.66	0.66	0.66	0.00	0.65	0.02		
Ala	[123]	260	1	0.33	0.33	0.33	0.33	0.00	0.39	0.38	0.39	0.00	0.34	0.34	0.34	0.34	0.00	0.35	0.02		
Asp	[12]	302	0	0.70	0.72	0.76	0.71	0.01	0.68	0.71	0.68	0.00	0.70	0.72	0.74	0.73	0.01	0.71	0.02		
Asp	[12]	302	1	0.30	0.28	0.24	0.29	0.01	0.32	0.29	0.32	0.00	0.30	0.28	0.26	0.27	0.01	0.29	0.02		
Asp	[234]	316	0	0.71	0.73	0.72	0.72	0.01	0.66	0.71	0.66	0.00	0.69	0.71	0.75	0.73	0.02	0.70	0.03		
Asp	[234]	316	1	0.29	0.27	0.28	0.28	0.01	0.34	0.29	0.34	0.00	0.31	0.29	0.25	0.27	0.02	0.30	0.03		
Asp	[12]	376	0	0.73	0.69	0.74	0.71	0.02	0.66	0.72	0.66	0.00	0.72	0.72	0.95	0.84	0.11	0.74	0.11		
Asp	[12]	376	1	0.27	0.31	0.26	0.29	0.02	0.34	0.28	0.34	0.00	0.28	0.28	0.05	0.16	0.11	0.26	0.11		
Asp	[234]	390	0	0.74	0.75	0.73	0.74	0.00	0.69	0.73	0.69	0.00	0.73	0.73	0.73	0.73	0.00	0.72	0.02		
Asp	[234]	390	1	0.26	0.25	0.27	0.26	0.00	0.31	0.27	0.31	0.00	0.27	0.27	0.27	0.27	0.00	0.28	0.02		
Asp	[1234]	418	0	0.71	0.70	0.72	0.71	0.01	0.69	0.71	0.69	0.00	0.71	0.72	0.72	0.72	0.00	0.70	0.01		
Asp	[1234]	418	1	0.29	0.30	0.28	0.29	0.01	0.31	0.29	0.31	0.00	0.29	0.28	0.28	0.28	0.00	0.30	0.01		
Glu	[2345]	272	0	0.61	0.61	0.61	0.61	0.00	0.56	0.60	0.56	0.00	0.60	0.60	0.59	0.60	0.01	0.59	0.02		
Glu	[2345]	272	1	0.39	0.39	0.39	0.39	0.00	0.44	0.40	0.44	0.00	0.40	0.40	0.41	0.40	0.01	0.41	0.02		
Glu	[2345]	330	0	0.61	0.61	0.61	0.61	0.00	0.57	0.61	0.57	0.00	0.61	0.61	0.61	0.61	0.00	0.60	0.02		
Glu	[2345]	330	1	0.39	0.39	0.39	0.39	0.00	0.43	0.43	0.43	0.00	0.39	0.39	0.39	0.39	0.00	0.40	0.02		
Glu	[2345]	404	0	0.61	0.61	0.61	0.61	0.00	0.57	0.61	0.57	0.00	0.61	0.62	0.61	0.61	0.01	0.60	0.02		
Glu	[2345]	404	1	0.39	0.39	0.39	0.39	0.00	0.43	0.43	0.43	0.00	0.39	0.38	0.39	0.39	0.01	0.40	0.02		
Glu	[12345]	432	0	0.61	0.62	0.61	0.61	0.00	0.57	0.60	0.57	0.00	0.60	0.62	0.62	0.62	0.00	0.60	0.02		
Glu	[12345]	432	1	0.39	0.38	0.39	0.39	0.00	0.43	0.43	0.43	0.00	0.40	0.38	0.38	0.38	0.00	0.40	0.02		
He	[23456]	200	0	0.95	0.96	0.98	0.95	0.01	0.91	0.90	0.90	0.00	0.94	0.95	0.95	0.95	0.00	0.94	0.02		
He	[23456]	200	1	0.05	0.04	0.05	0.05	0.01	0.09	0.10	0.10	0.00	0.06	0.05	0.05	0.05	0.00	0.06	0.02		
He	[23456]	274	0	0.93	0.93	0.93	0.93	0.00	0.88	0.89	0.89	0.00	0.93	0.93	0.94	0.93	0.01	0.92	0.01		
He	[23456]	274	1	0.07	0.07	0.07	0.07	0.00	0.12	0.11	0.11	0.00	0.07	0.07	0.06	0.07	0.01	0.08	0.01		
He	[12]	302	0	0.94	0.95	0.95	0.95	0.00	0.89	0.89	0.89	0.00	0.94	0.94	0.95	0.95	0.01	0.93	0.02		
He	[12]	302	1	0.06	0.05	0.05	0.05	0.00	0.11	0.11	0.11	0.00	0.06	0.06	0.05	0.05	0.01	0.07	0.02		
Leu	[23456]	200	0	0.96	0.95	0.96	0.96	0.00	0.91	0.91	0.91	0.00	0.96	0.96	0.95	0.95	0.00	0.94	0.02		
Leu	[23456]	200	1	0.04	0.05	0.04	0.04	0.00	0.09	0.09	0.09	0.00	0.04	0.04	0.05	0.05	0.00	0.06	0.02		
Leu	[23456]	274	0	0.94	0.93	0.93	0.93	0.00	0.86	0.88	0.87	0.01	0.94	0.94	0.94	0.94	0.00	0.91	0.02		
Leu	[23456]	274	1	0.06	0.07	0.07	0.07	0.00	0.14	0.12	0.13	0.01	0.06	0.06	0.06	0.06	0.00	0.09	0.02		
Leu	[12]	302	0	0.95	0.95	0.95	0.95	0.00	0.90	0.91	0.90	0.00	0.94	0.94	0.95	0.95	0.00	0.93	0.02		
Leu	[12]	302	1	0.05	0.05	0.05	0.05	0.00	0.10	0.09	0.10	0.00	0.06	0.06	0.05	0.05	0.00	0.07	0.02		
Phe	[23455667]	234	0	0.94	0.92	0.93	0.93	0.01	0.84	0.88	0.86	0.02	0.92	0.91	0.96	0.94	0.03	0.91	0.03		
Phe	[23455667]	234	1	0.06	0.08	0.07	0.07	0.01	0.16	0.12	0.14	0.02	0.08	0.09	0.04	0.06	0.03	0.09	0.03		
Phe	[12]	302	0	0.91	0.93	0.90	0.92	0.01	0.84	0.82	0.83	0.01	0.91	0.92	0.90	0.91	0.01	0.89	0.03		
Phe	[12]	302	1	0.09	0.07	0.10	0.08	0.01	0.16	0.18	0.17	0.01	0.09	0.08	0.10	0.09	0.01	0.11	0.03		
Phe	[23455667]	308	0	0.91	0.89	0.89	0.90	0.01	0.82	0.82	0.82	0.00	0.90	0.93	0.93	0.93	0.00	0.88	0.03		
Phe	[23455667]	308	1	0.09	0.11	0.11	0.10	0.01	0.18	0.18	0.18	0.00	0.10	0.07	0.07	0.07	0.00	0.12	0.03		
Phe	[123455667]	336	0	0.92	0.91	0.95	0.92	0.01	0.82	0.85	0.83	0.02	0.93	0.92	0.97	0.95	0.03	0.90	0.03		
Phe	[123455667]	336	1	0.08	0.09	0.05	0.08	0.01	0.18	0.15	0.17	0.02	0.07	0.08	0.03	0.05	0.03	0.10	0.03		
Pro	[2345]	184	0	1.00	1.00	1.00	1.00	0.00	1.00	1.00	1.00	0.00	1.00	1.00	1.00	1.00	0.00	1.00	0.00		
Pro	[2345]	184	1	0.00	0.00	0.00	0.00	0.00	0.00	0.00	0.00	0.00	0.00	0.00	0.00	0.00	0.00	0.00	0.00		
Pro	[2345]	258	0	1.01	1.01	1.01	1.01	0.00	1.01	1.01	1.01	0.00	1.01	1.01	1.00	1.01	0.00	1.01	0.00		
Pro	[2345]	258	1	-0.01	-0.01	-0.01	-0.01	0.00	-0.01	-0.01	-0.01	0.00	-0.01	-0.01	0.00	-0.01	0.00	-0.01	0.00		
Pro	[12345]	286	0	1.01	1.01	1.01	1.01	0.00	1.00	1.00	1.00	0.00	1.01	1.00	0.99	0.99	0.00	1.00	0.00		
Pro	[12345]	286	1	-0.01	-0.01	-0.01	-0.01	0.00	0.00	0.00	0.00	0.00	-0.01	0.00	0.01	0.01	0.00	0.00	0.00		
Ser	[23]	288	0	0.98	0.97	1.00	0.98	0.01	0.98	1.00	0.99	0.01	1.00	0.99	1.00	1.00	0.00	0.99	0.01		
Ser	[23]	288	1	0.02	0.03	0.00	0.02	0.01	0.02	0.00	0.01	0.01	0.00	0.01	0.00	0.00	0.00	0.01	0.01		
Ser	[12]	302	0	0.97	0.99	1.01	0.98	0.01	0.98	1.00	0.99	0.01	0.98	1.00	1.02	1.01	0.01	0.99	0.01		
Ser	[12]	302	1	0.03	0.01	-0.01	0.02	0.01	0.02	0.00	0.01	0.01	0.02	0.00	-0.02	-0.01	0.01	0.01	0.01		
Ser	[23]	362	0	0.99	1.00	1.00	0.99	0.01	1.01	1.00	1.00	0.01	0.99	0.99	0.99	0.99	0.00	0.99	0.01		
Ser	[23]	362	1	0.01	0.00	0.00	0.01	0.01	-0.01	0.00	0.00	0.01	0.01	0.01	0.01	0.01	0.00	0.01	0.01		
Ser	[123]	390	0	1.00	1.00	1.00	1.00	0.00	0.99	1.02	1.01	0.02	1.01	0.99	1.00	1.00	0.00	1.00	0.02		
Ser	[123]	390	1	0.00	0.00	0.00	0.00	0.00	0.01	-0.02	-0.01	0.02	-0.01	0.01	0.00	0.00	0.00	0.00	0.02		
Thr	[234]	376	0	1.05	1.09	1.05	1.06	0.03	1.04	1.05	1.04	0.00	1.00	1.00	1.03	1.02	0.02	1.04	0.03		
Thr	[234]	376	1	-0.05	-0.09	-0.05	-0.06	0.03	-0.04	-0.03	-0.04	0.00	0.00	0.00	-0.03	-0.02	0.02	-0.04	0.03		
Thr	[1234]	404	0	1.04	1.01	1.01	1.03	0.02	1.02	1.00	1.01	0.01	1.00	1.02	1.13	1.07	0.05	1.04	0.05		
Thr	[1234]	404	1	-0.04	-0.01	-0.01	-0.03	0.02	-0.02	0.00	-0.01	0.01	0.00	-0.02	-0.13	-0.07	0.05	-0.04	0.05		
urea	[1]	231	0						0.01	0.01	0.01	0.00	0.01	0.01	0.01	0.01	0.00	0.01	0.00		
urea	[1]	231	1						0.00	0.02	0.01	0.01	0.00	0.01	-0.03	-0.01	0.02	0.00	0.02		
urea	[1]	231	2						0.99	0.97	0.98	0.01	0.99	0.99	1.02	1.00	0.02	0.99	0.02		
urea	[1]	273	0	-0.02	-0.02	-0.01	-0.02	0.00											-0.02		
urea	[1]	273	1	0.14	0.14	0.14	0.14	0.00											0.14		
urea	[1]	273	2	0.88	0.88	0.86	0.88	0.00											0.88		
Val	[2345]	186	0	0.94	0.95	0.94	0.95	0.00	0.91	0.91	0.91	0.00	0.95								

**A.9. Table A.9 Parallel experiment: Mass Isotopomers from  $^{15}\text{N}$   
 $\text{NH}_4\text{Cl}$  instationary ILE.**

Mass isotopomer distributions from  $^{15}\text{N}$  ammonium chloride ILE in parallel experiment (**Table A.9**). This table follows the scheme of **Table A.1**.

		Table A.9 Parallel experiment: Mass isotopomers from <sup>15</sup> N NH <sub>4</sub> Cl instationary H.E.																										
		t = 5 min (control)															t = 10 min											
Metabolite	Fragment	m/z	Mass (n in m-n)	Intracellular metabolites: biological and technical (MS) replicates								Overall		Intracellular metabolites: biological and technical (MS) replicates										Overall				
				Rep 1			Rep 2			Avg	SE	Tech 1	Tech 2	Rep 1		Rep 2		Rep 3		Avg	SE							
				Tech 1	Tech 2	Avg	SE	Tech 1	Tech 2					Tech 3	Avg	SE	Tech 1	Tech 2	Avg			SE	Tech 1	Avg	SE			
Ala	[231]	158	0	0.92	0.91	0.92	0.00	0.89	0.89	0.90	0.30	0.86	0.86	0.85	0.86	0.00	0.83	0.83	0.83	0.00	0.80	0.80	0.00	0.80	0.80	0.83	0.02	
Ala	[231]	158	1	0.98	0.99	0.98	0.00	0.11	0.11	0.10	0.03	0.14	0.14	0.15	0.14	0.00	0.17	0.17	0.17	0.00	0.20	0.20	0.00	0.20	0.20	0.17	0.02	
Ala	[231]	232	0	0.93	0.93	0.93	0.00	0.91	0.91	0.92	0.31	0.87	0.87	0.89	0.88	0.01	0.84	0.84	0.84	0.00	0.80	0.80	0.00	0.80	0.80	0.84	0.02	
Ala	[231]	232	1	0.07	0.07	0.07	0.00	0.09	0.09	0.08	0.03	0.13	0.13	0.11	0.12	0.01	0.16	0.16	0.16	0.00	0.20	0.20	0.00	0.20	0.20	0.16	0.02	
Ala	[123]	260	0	0.94	0.94	0.94	0.00	0.92	0.92	0.93	0.31	0.88	0.88	0.91	0.89	0.01	0.84	0.85	0.84	0.01	0.82	0.82	0.00	0.82	0.82	0.85	0.02	
Ala	[123]	260	1	0.06	0.06	0.06	0.00	0.08	0.08	0.07	0.02	0.12	0.12	0.09	0.11	0.01	0.16	0.15	0.16	0.01	0.18	0.18	0.00	0.18	0.18	0.15	0.02	
Asp	[12]	302	0	0.94		0.94				0.94	0.47					0.93	0.93	0.93	0.00						0.93	0.00		
Asp	[12]	302	1	0.06		0.06				0.06	0.03					0.07	0.07	0.07	0.00						0.07	0.00		
Asp	[234]	316	0	1.02	0.88	0.95	0.07			0.95	0.47					1.00	1.23	1.11	0.12						1.00	1.11		1.11
Asp	[234]	316	1	-0.02	0.12	0.05	0.07			0.05	0.07					0.00	-0.23	-0.11	0.12						0.00	-0.23		-0.11
Asp	[12]	376	0	0.88	1.03	0.95	0.08			0.95	0.48					1.10	0.68	0.89	0.21						0.91	0.81	0.86	0.05
Asp	[12]	376	1	0.12	-0.03	0.05	0.08			0.05	0.08					-0.10	0.32	-0.11	0.21						-0.10	0.32		-0.11
Asp	[234]	390	0	1.02	1.04	1.03	0.01			1.03	0.51					0.90	0.86	0.88	0.02						0.90	0.86	0.88	0.02
Asp	[234]	390	1	-0.02	-0.04	-0.03	0.01			-0.03	0.01					0.10	0.14	0.12	0.02						0.10	0.14	0.12	0.02
Asp	[1234]	418	0	0.99	1.02	1.01	0.01			1.01	0.50					0.91	0.81	0.86	0.05						0.91	0.81	0.86	0.05
Asp	[1234]	418	1	0.01	-0.02	-0.01	0.01			-0.01	0.01					0.09	0.19	0.14	0.05						0.09	0.19	0.14	0.05
Glu	[2345]	272	0	0.90		0.90				0.90	0.45					0.79		0.79							0.79		0.79	0.45
Glu	[2345]	272	1	0.10		0.10				0.10	0.05					0.21		0.21							0.21		0.21	0.05
Glu	[2345]	330	0	0.95		0.95				0.95	0.48					0.79		0.79							0.79		0.79	0.48
Glu	[2345]	330	1	0.05		0.05				0.05	0.02					0.21		0.21							0.21		0.21	0.02
Glu	[2345]	404	0	0.99		0.99				0.99	0.50					0.82		0.82							0.82		0.82	0.50
Glu	[2345]	404	1	0.01		0.01				0.01	0.00					0.18		0.18							0.18		0.18	0.00
Glu	[12345]	432	0	0.90		0.90				0.90	0.45					0.82		0.82							0.82		0.82	0.45
Glu	[12345]	432	1	0.10		0.10				0.10	0.05					0.18		0.18							0.18		0.18	0.05
He	[23456]	200	0	0.99	0.97	0.98	0.01	0.99	0.99	0.98	0.33	0.98	0.98	0.97	0.98	0.00	0.96	0.96	0.96	0.00	0.96	0.96	0.00	0.96	0.96	0.96	0.96	0.33
He	[23456]	200	1	0.01	0.02	0.02	0.01	0.01	0.01	0.02	0.01	0.02	0.02	0.02	0.02	0.00	0.04	0.04	0.04	0.00	0.04	0.04	0.00	0.04	0.04	0.04	0.04	0.01
He	[23456]	274	0	0.95	0.95	0.95	0.00	0.96	0.96	0.95	0.32	0.96	0.96	0.94	0.95	0.01	0.94	0.92	0.93	0.01	0.95	0.95	0.00	0.95	0.95	0.94	0.01	
He	[23456]	274	1	0.05	0.05	0.05	0.00	0.04	0.04	0.05	0.02	0.04	0.04	0.06	0.05	0.01	0.06	0.08	0.07	0.01	0.05	0.05	0.00	0.05	0.05	0.06	0.01	
He	[12]	302	0	0.96	0.98	0.97	0.01	0.99	0.99	0.98	0.33	0.96	0.98	0.98	0.97	0.01	0.96	0.96	0.96	0.00	0.97	0.97	0.00	0.97	0.97	0.97	0.97	0.33
He	[12]	302	1	0.04	0.02	0.03	0.01	0.01	0.01	0.02	0.01	0.04	0.02	0.02	0.03	0.01	0.04	0.04	0.04	0.00	0.03	0.03	0.00	0.03	0.03	0.03	0.03	0.01
Leu	[23456]	200	0	0.98	0.98	0.98	0.00	0.98	0.98	0.98	0.33	0.99	0.99	0.97	0.98	0.01	0.97	0.97	0.97	0.00	0.99	0.99	0.00	0.99	0.99	0.98	0.01	
Leu	[23456]	200	1	0.02	0.02	0.02	0.00	0.02	0.02	0.02	0.01	0.01	0.01	0.01	0.01	0.03	0.03	0.03	0.03	0.00	0.01	0.01	0.00	0.01	0.01	0.01	0.01	0.03
Leu	[23456]	274	0	0.98	0.98	0.98	0.00	0.98	0.98	0.98	0.33	0.97	0.98	1.01	0.99	0.01	0.96	0.96	0.96	0.00	0.97	0.97	0.00	0.97	0.97	0.97	0.97	0.33
Leu	[23456]	274	1	0.02	0.02	0.02	0.00	0.02	0.02	0.02	0.01	0.03	0.02	-0.01	0.01	0.01	0.04	0.04	0.04	0.00	0.03	0.03	0.00	0.03	0.03	0.03	0.03	0.01
Leu	[12]	302	0	0.98	0.98	0.98	0.00	1.00	1.00	0.99	0.33	0.97	0.99	0.96	0.97	0.01	0.96	0.97	0.96	0.00	0.96	0.96	0.00	0.96	0.96	0.96	0.96	0.33
Leu	[12]	302	1	0.02	0.02	0.02	0.00	0.00	0.00	0.01	0.01	0.03	0.01	0.04	0.03	0.01	0.04	0.03	0.04	0.00	0.04	0.04	0.00	0.04	0.04	0.04	0.04	0.03
Phe	[23455667]	234	0	1.09	0.89	0.99	0.10			0.99	0.50					1.04	0.95	0.99	0.04						1.04	0.95	0.99	0.04
Phe	[23455667]	234	1	-0.09	0.11	0.01	0.10			0.01	0.10					-0.04	0.05	0.01	0.04						0.01	0.01	0.01	0.10
Phe	[12]	302	0	1.03	1.00	1.01	0.02			1.01	0.51					0.98	1.04	1.01	0.03						0.98	1.04	1.01	0.03
Phe	[12]	302	1	-0.03	0.00	-0.01	0.02			-0.01	0.02					0.02	-0.04	-0.01	0.03						-0.01	-0.01	-0.01	0.02
Phe	[23455667]	308	0	1.01		1.01				1.01	0.51					0.98	1.06	1.02	0.04						1.02		1.02	0.51
Phe	[23455667]	308	1	-0.01		-0.01				-0.01	0.01					0.02	-0.06	-0.02	0.04						-0.02		-0.02	0.01
Phe	[123455667]	336	0	1.04	1.00	1.02	0.02			1.02	0.51					0.94	1.03	0.98	0.04						0.98		0.98	0.51
Phe	[123455667]	336	1	-0.04	0.00	-0.02	0.02			-0.02	0.02					0.06	-0.03	0.02	0.04						0.02		0.02	0.02
Pro	[2345]	184	0	1.00	1.00	1.00	0.00	1.00	1.00	1.00	0.33	1.00	1.00	1.03	1.01	0.01	1.00	1.00	1.00	0.00	1.00	1.00	0.00	1.00	1.00	1.00	1.00	0.33
Pro	[2345]	184	1	0.00	0.00	0.00	0.00	0.00	0.00	0.00	0.00	0.00	0.00	-0.03	-0.01	0.01	0.00	0.00	0.00	0.00	0.00	0.00	0.00	0.00	0.00	0.00	0.00	0.00
Pro	[2345]	258	0	1.01	1.01	1.01	0.00	1.01	1.01	1.01	0.34	1.01	1.01	0.99	1.00	0.01	1.01	1.01	1.01	0.00	1.01	1.01	0.00	1.01	1.01	1.01	1.01	0.34

Table A.9 Parallel experiment: Mass isotopomers from <sup>15</sup> N NH <sub>4</sub> Cl instationary ILE (Cont).																	
Metabolite	Fragment	m/z	Mass (n in m-m)	t = 15 min						t = 20 min						Overall	
				Intracellular metabolites: biological and technical (MS)						Intracellular metabolites: biological and technical (MS) replicates							
				Rep 1			Rep 2			Rep 1			Rep 2				
				Tech 1	Tech 2	Tech 3	Avg	SE		Tech 1	Tech 2	Avg	SE	Tech 1	Avg	SE	
Ala	[23]	158	0	0.73	0.73	0.72	0.73	0.00	0.64	0.64	0.64	0.00	0.63	0.63	0.64	0.01	
Ala	[23]	158	1	0.27	0.27	0.28	0.27	0.00	0.36	0.36	0.36	0.00	0.37	0.37	0.36	0.01	
Ala	[23]	232	0	0.74	0.74	0.73	0.74	0.00	0.65	0.65	0.65	0.00	0.64	0.64	0.64	0.00	
Ala	[23]	232	1	0.26	0.26	0.27	0.26	0.00	0.35	0.35	0.35	0.00	0.36	0.36	0.36	0.00	
Ala	[123]	260	0	0.74	0.75	0.74	0.74	0.00	0.65	0.66	0.66	0.00	0.64	0.64	0.65	0.01	
Ala	[123]	260	1	0.26	0.25	0.26	0.26	0.00	0.35	0.34	0.34	0.00	0.36	0.36	0.35	0.01	
Asp	[12]	302	0	0.80	0.89		0.85	0.05									
Asp	[12]	302	1	0.20	0.11		0.15	0.05									
Asp	[234]	316	0	0.89			0.89										
Asp	[234]	316	1	0.11			0.11										
Asp	[12]	376	0	0.71	0.69		0.70	0.01									
Asp	[12]	376	1	0.29	0.31		0.30	0.01									
Asp	[234]	390	0	0.77	0.81		0.79	0.02									
Asp	[234]	390	1	0.23	0.19		0.21	0.02									
Asp	[1234]	418	0	0.76	0.87		0.81	0.06									
Asp	[1234]	418	1	0.24	0.13		0.19	0.06									
Glu	[2345]	272	0														
Glu	[2345]	272	1														
Glu	[2345]	330	0														
Glu	[2345]	330	1														
Glu	[2345]	404	0														
Glu	[2345]	404	1														
Glu	[12345]	432	0														
Glu	[12345]	432	1														
Ile	[23456]	200	0	0.96	0.94	0.98	0.96	0.01	0.94	0.95	0.95	0.00	0.93	0.93	0.94	0.01	
Ile	[23456]	200	1	0.04	0.06	0.02	0.04	0.01	0.06	0.05	0.05	0.00	0.07	0.07	0.06	0.01	
Ile	[23456]	274	0	0.96	0.94	0.91	0.94	0.01	0.93	0.93	0.93	0.00	0.93	0.93	0.93	0.00	
Ile	[23456]	274	1	0.04	0.06	0.09	0.06	0.01	0.07	0.07	0.07	0.00	0.07	0.07	0.07	0.00	
Ile	[12]	302	0	0.95	0.96	1.06	0.99	0.03	0.95	0.95	0.95	0.00	0.92	0.92	0.93	0.02	
Ile	[12]	302	1	0.05	0.04	-0.06	0.01	0.03	0.05	0.05	0.05	0.00	0.08	0.08	0.07	0.02	
Leu	[23456]	200	0	0.97	0.97	0.96	0.97	0.00	0.97	0.96	0.97	0.00	0.95	0.95	0.96	0.01	
Leu	[23456]	200	1	0.03	0.03	0.04	0.03	0.00	0.03	0.04	0.03	0.00	0.05	0.05	0.04	0.01	
Leu	[23456]	274	0	0.96	0.97	1.01	0.98	0.01	0.96	0.96	0.96	0.00	0.94	0.94	0.95	0.01	
Leu	[23456]	274	1	0.04	0.03	-0.01	0.02	0.01	0.04	0.04	0.04	0.00	0.06	0.06	0.05	0.01	
Leu	[12]	302	0	0.96	0.96	0.94	0.95	0.00	0.96	0.96	0.96	0.00	0.94	0.94	0.95	0.01	
Leu	[12]	302	1	0.04	0.04	0.06	0.05	0.00	0.04	0.04	0.04	0.00	0.06	0.06	0.05	0.01	
Phe	[2345667]	234	0	0.88	0.87		0.88	0.00									
Phe	[2345667]	234	1	0.12	0.13		0.12	0.00									
Phe	[12]	302	0	1.05	1.15		1.10	0.05									
Phe	[12]	302	1	-0.05	-0.15		-0.10	0.05									
Phe	[2345667]	308	0				0.90										
Phe	[2345667]	308	1				0.10										
Phe	[123455667]	336	0	1.09	1.10		1.10	0.00									
Phe	[123455667]	336	1	-0.09	-0.10		-0.10	0.00									
Pro	[2345]	184	0	1.00	1.00	1.07	1.02	0.02	1.00	1.01	1.00	0.00	1.01	1.01	1.01	0.01	
Pro	[2345]	184	1	0.00	0.00	-0.07	-0.02	0.02	0.00	-0.01	0.00	0.00	-0.01	-0.01	-0.01	0.01	
Pro	[2345]	258	0	1.01	1.01		1.01	0.00	1.00	1.00	1.00	0.00	1.03	1.03	1.01	0.01	
Pro	[2345]	258	1	-0.01	-0.01		-0.01	0.00	0.00	0.00	0.00	0.00	-0.03	-0.03	-0.01	0.01	
Pro	[12345]	286	0	1.00	1.00		1.00	0.00	0.99	1.02	1.01	0.02	0.98	0.98	0.99	0.02	
Pro	[12345]	286	1	0.00	0.00		0.00	0.00	0.01	-0.02	-0.01	0.02	0.02	0.02	0.01	0.02	
Ser	[23]	288	0	0.93	1.00		0.96	0.04	0.98	1.02	1.00	0.02			1.00		
Ser	[23]	288	1	0.07	0.00		0.04	0.04	0.02	-0.02	0.00	0.02			0.00		
Ser	[12]	302	0	0.95	0.95		0.95	0.00	0.96	1.22	1.09	0.13			1.09		
Ser	[12]	302	1	0.05	0.05		0.05	0.00	0.04	-0.22	-0.09	0.13			-0.09		
Ser	[23]	362	0	0.99	0.97		0.98	0.01	1.03	1.04	1.03	0.01			1.03		
Ser	[23]	362	1	0.01	0.03		0.02	0.01	-0.03	-0.04	-0.03	0.01			-0.03		
Ser	[123]	390	0	0.92	1.02		0.97	0.05	1.01	0.92	0.96	0.05			0.96		
Ser	[123]	390	1	0.08	-0.02		0.03	0.05	-0.01	0.08	0.04	0.05			0.04		
Thr	[234]	376	0	1.11	1.06		1.09	0.02	0.97	0.86	0.91	0.05	1.28	1.28	1.10	0.18	
Thr	[234]	376	1	-0.11	-0.06		-0.09	0.02	0.03	0.14	0.09	0.05	-0.28	-0.28	-0.10	0.18	
Thr	[1234]	404	0	1.24	1.01		1.12	0.11	0.79	1.18	0.98	0.19	0.85	0.85	0.92	0.19	
Thr	[1234]	404	1	-0.24	-0.01		-0.12	0.11	0.21	-0.18	0.02	0.19	0.15	0.15	0.08	0.19	
urea	[1]	231	0														
urea	[1]	231	1														
urea	[1]	231	2														
urea	[1]	273	0														
urea	[1]	273	1														
urea	[1]	273	2														
Val	[2345]	186	0	0.95	0.95	0.94	0.95	0.00	0.94	0.93	0.93	0.00	0.94	0.94	0.93	0.00	
Val	[2345]	186	1	0.05	0.05	0.06	0.05	0.00	0.06	0.07	0.07	0.00	0.06	0.06	0.07	0.00	
Val	[2345]	260	0	0.93	0.94	0.94	0.94	0.00	0.92	0.93	0.93	0.00	0.92	0.92	0.92	0.00	
Val	[2345]	260	1	0.07	0.06	0.06	0.06	0.00	0.08	0.07	0.07	0.00	0.08	0.08	0.08	0.00	
Val	[12345]	288	0	0.93	0.90	0.91	0.91	0.01	0.93	0.94	0.93	0.01	0.88	0.88	0.91	0.03	
Val	[12345]	288	1	0.07	0.10	0.10	0.09	0.01	0.07	0.06	0.07	0.01	0.12	0.12	0.09	0.03	
Val	[12]	302	0	0.96	0.97	0.97	0.97	0.00	0.92	0.95	0.94	0.02	0.96	0.96	0.95	0.02	
Val	[12]	302	1	0.04	0.03	0.03	0.03	0.00	0.08	0.05	0.06	0.02	0.04	0.04	0.05	0.02	

**A.10. Table A.10 Parallel experiment: Mass Isotopomers from  $^{15}\text{N}$   
 $\text{NaNO}_3$  instationary ILE.**

Mass isotopomer distributions from  $^{15}\text{N}$  sodium nitrate ILE in parallel experiment (**Table A.10**). This table follows the scheme of **Table A.1**.



Table A.10 Parallel experiment: Mass isotopomers from <sup>15</sup>N NaNO<sub>3</sub> stationary ILE.

Metabolite	Fragment	m/z	Mass (n in m+n)	t = 0 min (control)																t = 5 min															
				cellular metabolites: biological and technical (MS) replicates								Intracellular metabolites: biological and technical (MS) replicates								Overall															
				Rep 1				Rep 2				Rep 1				Rep 2				Rep 3		Overall													
				Tech 1	Tech 2	Tech 3	Avg	SE	Tech 1	Tech 2	Tech 3	Avg	SE	Tech 1	Tech 2	Tech 3	Avg	SE	Tech 1	Avg	Tech 1	Avg	Avg	SE											
Ala	[23]	158	0	0.98	0.98	0.98	0.98	0.00	0.00	0.98	0.99	0.99	0.99	0.00	0.00	0.99	0.99	0.98	0.98	0.99	0.00														
Ala	[23]	158	1	0.02	0.02	0.02	0.02	0.00	0.00	0.02	0.01	0.02	0.00	0.00	0.01	0.01	0.02	0.02	0.02	0.01	0.00														
Ala	[23]	232	0	1.00	1.00	1.00	1.00	0.00	0.00	1.00	1.00	1.00	1.00	0.00	0.00	1.00	1.00	1.00	1.00	1.00	0.00														
Ala	[23]	232	1	0.00	0.00	0.00	0.00	0.00	0.00	0.00	0.00	0.00	0.00	0.00	0.00	0.00	0.00	0.00	0.00	0.00	0.00														
Ala	[123]	260	0	1.01	1.01	1.01	1.01	0.00	0.00	1.00	1.01	1.00	0.00	0.00	1.01	1.01	1.01	1.01	1.01	1.01	0.00														
Ala	[123]	260	1	-0.01	-0.01	-0.01	-0.01	0.00	0.00	0.00	-0.01	0.00	0.00	0.00	-0.01	-0.01	-0.01	-0.01	-0.01	-0.01	0.00														
Asp	[12]	302	0	1.01	1.01	1.00	1.00	0.00	0.00	1.01	0.97	0.99	0.02	0.02	0.99	0.99	1.01	1.01	1.01	1.00	0.02														
Asp	[12]	302	1	-0.01	-0.01	0.00	0.00	0.00	0.00	-0.01	0.03	0.01	0.02	0.01	0.01	-0.01	-0.01	-0.01	-0.01	0.00	0.02														
Asp	[234]	316	0	1.01	1.01	1.01	1.01	0.00	0.00	0.98	0.98	0.98	0.00	0.00	0.93	0.93	1.01	1.01	0.97	0.02	0.02														
Asp	[234]	316	1	-0.01	-0.01	-0.01	-0.01	0.00	0.00	0.02	0.02	0.02	0.00	0.00	0.07	0.07	-0.01	-0.01	-0.01	0.03	0.02														
Asp	[12]	376	0	1.02	1.02	1.01	1.02	0.00	0.00	1.05	1.12	1.08	0.03	0.03	1.02	1.02	1.10	1.10	1.07	0.03	0.03														
Asp	[12]	376	1	-0.02	-0.02	-0.01	-0.02	0.00	0.00	-0.05	-0.12	-0.08	0.03	0.03	-0.02	-0.02	-0.10	-0.10	-0.07	0.03	0.03														
Asp	[234]	390	0	1.00	1.02	1.00	1.01	0.01	0.01	1.02	1.01	1.01	0.00	0.00	1.06	1.06	1.02	1.02	1.03	0.01	0.01														
Asp	[234]	390	1	0.00	-0.02	0.00	-0.01	0.01	0.01	-0.02	-0.01	-0.01	0.00	0.00	-0.06	-0.06	-0.02	-0.02	-0.03	0.01	0.01														
Asp	[1234]	418	0	1.02	1.02	0.99	1.01	0.01	0.01	1.01	1.00	1.00	0.00	0.00	1.14	1.14	0.99	0.99	1.05	0.05	0.05														
Asp	[1234]	418	1	-0.02	-0.02	0.01	-0.01	0.01	0.01	-0.01	0.00	0.00	0.00	0.00	-0.14	-0.14	0.01	0.01	-0.05	0.05	0.05														
Glu	[2345]	272	0	1.00	1.00	1.00	1.00	0.00	0.00	1.00	0.99	0.99	0.00	0.00	0.95	0.95	0.98	0.98	0.97	0.01	0.01														
Glu	[2345]	272	1	0.00	0.00	0.00	0.00	0.00	0.00	0.00	0.01	0.01	0.00	0.00	0.05	0.05	0.02	0.02	0.03	0.01	0.01														
Glu	[2345]	330	0	1.00	1.01	1.01	1.01	0.00	0.00	0.99	0.99	0.99	0.00	0.00	1.02	1.02	0.99	0.99	1.00	0.01	0.01														
Glu	[2345]	330	1	0.00	-0.01	-0.01	-0.01	0.00	0.00	0.01	0.01	0.01	0.00	0.00	-0.02	-0.02	0.01	0.01	0.00	0.01	0.01														
Glu	[2345]	404	0	1.02	1.01	1.01	1.01	0.00	0.00	1.02	1.00	1.01	0.01	0.01	1.18	1.18	1.01	1.01	1.07	0.06	0.06														
Glu	[2345]	404	1	-0.02	-0.01	-0.01	-0.01	0.00	0.00	-0.02	0.00	-0.01	0.01	0.01	-0.18	-0.18	-0.01	-0.01	-0.07	0.06	0.06														
Glu	[12345]	432	0	1.03	1.02	1.02	1.02	0.00	0.00	1.01	1.01	1.01	0.00	0.00	1.02	1.02	1.00	1.00	1.01	0.00	0.00														
Glu	[12345]	432	1	-0.03	-0.02	-0.02	-0.02	0.00	0.00	-0.01	-0.01	-0.01	0.00	0.00	-0.02	-0.02	0.00	0.00	-0.01	0.00	0.00														
Ile	[23456]	200	0	1.01	1.01	1.00	1.01	0.00	0.00	1.00	1.00	1.00	0.00	0.00	1.00	1.00	1.00	1.00	1.00	0.00	0.00														
Ile	[23456]	200	1	-0.01	-0.01	0.00	-0.01	0.00	0.00	0.00	0.00	0.00	0.00	0.00	0.00	0.00	0.00	0.00	0.00	0.00	0.00														
Ile	[23456]	274	0	0.98	0.99	0.99	0.98	0.00	0.00	0.99	0.98	0.98	0.00	0.00	0.97	0.97	1.00	1.00	0.98	0.01	0.01														
Ile	[23456]	274	1	0.02	0.01	0.01	0.02	0.00	0.01	0.02	0.02	0.02	0.00	0.03	0.03	0.00	0.00	0.02	0.01	0.01	0.01														
Ile	[12]	302	0	0.99	1.01	1.00	1.00	0.00	0.00	0.99	1.00	1.00	0.00	0.01	1.01	0.99	0.99	0.99	1.00	0.00	0.00														
Ile	[12]	302	1	0.01	-0.01	0.00	0.00	0.00	0.00	0.01	0.00	0.00	0.00	0.00	-0.01	-0.01	0.01	0.01	0.00	0.00	0.00														
Leu	[23456]	200	0	1.00	1.01	1.01	1.01	0.00	0.00	1.01	1.00	1.01	0.00	0.00	1.00	1.00	1.00	1.00	1.00	0.00	0.00														
Leu	[23456]	200	1	0.00	-0.01	-0.01	-0.01	0.00	0.00	-0.01	0.00	-0.01	0.00	0.00	0.00	0.00	0.00	0.00	0.00	0.00	0.00														
Leu	[23456]	274	0	1.00	1.00	0.99	1.00	0.00	0.00	1.00	0.99	1.00	0.00	0.00	0.98	0.98	1.00	1.00	0.99	0.01	0.01														
Leu	[23456]	274	1	0.00	0.00	0.01	0.00	0.00	0.00	0.00	0.01	0.00	0.00	0.00	0.02	0.02	0.00	0.00	0.01	0.01	0.01														
Leu	[12]	302	0	1.00	0.99	1.01	1.00	0.00	0.00	1.00	1.00	1.00	0.00	0.00	0.98	0.98	0.99	0.99	0.99	0.01	0.01														
Leu	[12]	302	1	0.00	0.01	-0.01	0.00	0.00	0.00	0.00	0.00	0.00	0.00	0.00	0.02	0.02	0.01	0.01	0.01	0.01	0.01														
Phe	[23455667]	234	0	1.00	1.01	1.00	1.01	0.00	0.00	1.00	1.02	1.01	0.01	0.01	0.95	0.95	1.01	1.01	0.99	0.02	0.02														
Phe	[23455667]	234	1	0.00	-0.01	0.00	-0.01	0.00	0.00	0.00	-0.02	-0.01	0.01	0.05	0.05	-0.01	-0.01	-0.01	-0.01	0.01	0.02														
Phe	[12]	302	0	1.01	1.01	1.00	1.01	0.00	0.00	1.01	1.05	1.03	0.02	0.02	1.05	1.05	1.01	1.01	1.03	0.02	0.02														
Phe	[12]	302	1	-0.01	-0.01	0.00	-0.01	0.00	0.00	-0.01	-0.05	-0.03	0.02	0.02	-0.05	-0.05	-0.01	-0.01	-0.03	0.02	0.02														
Phe	[23455667]	308	0	0.99	0.98	1.00	0.99	0.00	0.00	1.00	0.97	0.98	0.02	0.01	1.01	0.99	0.99	0.99	1.00	0.02	0.02														
Phe	[23455667]	308	1	0.01	0.02	0.00	0.01	0.00	0.00	0.00	0.03	0.02	0.02	0.02	-0.01	-0.01	0.01	0.01	0.00	0.02	0.02														
Phe	[123455667]	336	0	1.01	1.02	1.01	1.01	0.00	0.00	1.00	1.08	1.04	0.04	0.04	1.12	1.12	1.02	1.02	1.06	0.04	0.04														
Phe	[123455667]	336	1	-0.01	-0.02	-0.01	-0.01	0.00	0.00	0.00	-0.08	-0.04	0.04	-0.12	-0.12	-0.02	-0.02	-0.06	-0.06	0.04	0.04														
Pro	[2345]	184	0	1.00	1.00	1.00	1.00	0.00	0.00	1.00	1.00	1.00	0.00	0.00	1.00	1.00	1.00	1.00	1.00	0.00	0.00														
Pro	[2345]	184	1	0.00	0.00	0.00	0.00	0.00	0.00	0.00	0.00	0.00	0.00	0.00	0.00	0.00	0.00	0.00	0.00	0.00	0.00														
Pro	[2345]	258	0	1.01	1.01	1.01	1.01	0.00	0.00	1.01	1.01	1.01	0.00	0.00	1.00	1.00	1.01	1.01	1.01	0.00	0.00														
Pro	[2345]	258	1	-0.01	-0.01	-0.01	-0.01	0.00	0.00	-0.01	-0.01	-0.01	0.00	0.00	0.00	0.00	-0.01	-0.01	-0.01	0.00	0.00														
Pro	[12345]	286	0	1.01	1.01	1.00	1.01	0.00	0.00	1.01	1.00	1.01	0.00	0.00	1.00	1.00	1.00	1.00	1.00	0.00	0.00														
Pro	[12345]	286	1	-0.01	-0.01	0.00	-0.01	0.00	0.00	-0.01	0.00	-0.01	0.00	0.00	0.00	0.00	0.00	0.00	0.00	0.00	0.00														
Ser	[23]	288	0	1.00	0.99	0.97	0.99	0.01	0.01	0.98	0.91	0.94	0.03	0.03	0.91	0.91	0.97	0.97	0.94	0.03	0.03														
Ser	[23]	288	1	0.00	0.01	0.03	0.01	0.01	0.01	0.02	0.09	0.06	0.03	0.03	0.09	0.09	0.03	0.03	0.06	0.03	0.03														
Ser	[12]	302	0	1.00	1.00	1.01	1.00	0.00	0.00	1.01	1.02	1.01	0.01	0.01	0.99	0.99	0.99	0.99	1.00	0.01	0.01														
Ser	[12]	302	1	0.00	0.00	-0.01	0.00	0.00	0.00	-0.01	-0.02	-0.01	0.01	0.01	0.01	0.01	0.01	0.01	0.00	0.01	0.01														
Ser	[23]	362	0	1.01	1.01	1.00	1.01	0.00	0.00	1.02	0.99	1.00	0.01	0.01	1.01	1.01	1.01	1.01	1.01	0.01	0.01														
Ser	[23]	362	1	-0.01	-0.01	0.00	-0.01	0.00	0.00	-0.02	0.01	0.00	0.01	-0.01	-0.01	-0.01	-0.01	-0.01	-0.01	0.01	0.01														
Ser	[123]	390	0	1.00	1.01	1.02	1.01	0.00	0.00	1.01	1.01	1.01	0.00	0.00	0.99	0.99	1.02	1.02	1.01	0.01	0.01														
Ser	[123]	390	1	0.00	-0.01	-0.02	-0.01	0.00	0.00	-0.01	-0.01	-0.01	0.00	0.01	0.01	-0.02	-0.02	-0.02	-0.01	0.01	0.01														
Thr	[234]	376	0	1.00	1.03	1.01	1.01	0.01	0.01	1.05	1.02	1.04	0.01	0.01	1.02	1.02	1.02	1.02	1.02	0.01	0.01														
Thr	[234]	376	1	0.00	-0.03	-0.01	-0.01	0.01	0.01	-0.05	-0.02	-0.04	0.01	0.01	-0.02	-0.02	-0.02	-0.02	-0.02	0.01	0.01														
Thr	[1234]	404	0	1.01	1.01	1.01	1.01	0.00	0.00	1.02	1.01	1.02	0.00																						

Metabolite	Fragment	m/z	Mass (n in m+n)	t = 10 min						t = 15 min		t = 20 min	
				ar metabolites: biological and technical (MS)				Overall		tes: biological and tec		tes: biological and tec	
				Rep 1		Rep 2		Avg	SE	Rep 1		Rep 1	
Tech 1	Avg	Tech 1	Avg	Avg	SE	Tech 1	Avg	Tech 1	Avg				
Ala	[23]	158	0	0.97	0.97	0.98	0.98	0.98	0.00	0.98	0.98	0.98	0.98
Ala	[23]	158	1	0.03	0.03	0.02	0.02	0.02	0.00	0.02	0.02	0.02	0.02
Ala	[23]	232	0	0.99	0.99	1.00	1.00	0.99	0.00	0.99	0.99	0.99	0.99
Ala	[23]	232	1	0.01	0.01	0.00	0.00	0.01	0.00	0.01	0.01	0.01	0.01
Ala	[123]	260	0	0.99	0.99	1.01	1.01	1.00	0.01	1.00	1.00	1.01	1.01
Ala	[123]	260	1	0.01	0.01	-0.01	-0.01	0.00	0.01	0.00	0.00	-0.01	-0.01
Asp	[12]	302	0	1.00	1.00	0.98	0.98	0.99	0.01	0.99	0.99	0.98	0.98
Asp	[12]	302	1	0.00	0.00	0.02	0.02	0.01	0.01	0.01	0.01	0.02	0.02
Asp	[234]	316	0	0.99	0.99	1.07	1.07	1.03	0.04	1.02	1.02	0.98	0.98
Asp	[234]	316	1	0.01	0.01	-0.07	-0.07	-0.03	0.04	-0.02	-0.02	0.02	0.02
Asp	[12]	376	0	1.00	1.00	0.92	0.92	0.96	0.04	1.12	1.12	1.05	1.05
Asp	[12]	376	1	0.00	0.00	0.08	0.08	0.04	0.04	-0.12	-0.12	-0.05	-0.05
Asp	[234]	390	0	1.03	1.03	1.02	1.02	1.02	0.01	1.05	1.05	1.02	1.02
Asp	[234]	390	1	-0.03	-0.03	-0.02	-0.02	-0.02	0.01	-0.05	-0.05	-0.02	-0.02
Asp	[1234]	418	0	0.99	0.99	1.03	1.03	1.01	0.02	1.02	1.02	0.98	0.98
Asp	[1234]	418	1	0.01	0.01	-0.03	-0.03	-0.01	0.02	-0.02	-0.02	0.02	0.02
Glu	[2345]	272	0	0.88	0.88	0.99	0.99	0.93	0.06	0.98	0.98	0.97	0.97
Glu	[2345]	272	1	0.12	0.12	0.01	0.01	0.07	0.06	0.02	0.02	0.03	0.03
Glu	[2345]	330	0	0.98	0.98	1.00	1.00	0.99	0.01	0.98	0.98	0.99	0.99
Glu	[2345]	330	1	0.02	0.02	0.00	0.00	0.01	0.01	0.02	0.02	0.01	0.01
Glu	[2345]	404	0	1.01	1.01	1.01	1.01	1.01	0.00	0.98	0.98	1.00	1.00
Glu	[2345]	404	1	-0.01	-0.01	-0.01	-0.01	-0.01	0.00	0.02	0.02	0.00	0.00
Glu	[12345]	432	0	0.99	0.99	1.01	1.01	1.00	0.01	1.00	1.00	0.99	0.99
Glu	[12345]	432	1	0.01	0.01	-0.01	-0.01	0.00	0.01	0.00	0.00	0.01	0.01
Ile	[23456]	200	0	0.99	0.99	1.00	1.00	0.99	0.01	1.01	1.01	1.00	1.00
Ile	[23456]	200	1	0.01	0.01	0.00	0.00	0.01	0.01	-0.01	-0.01	0.00	0.00
Ile	[23456]	274	0	0.97	0.97	0.98	0.98	0.98	0.00	0.99	0.99	0.98	0.98
Ile	[23456]	274	1	0.03	0.03	0.02	0.02	0.02	0.00	0.01	0.01	0.02	0.02
Ile	[12]	302	0	0.98	0.98	1.00	1.00	0.99	0.01	1.00	1.00	0.98	0.98
Ile	[12]	302	1	0.02	0.02	0.00	0.00	0.01	0.01	0.00	0.00	0.02	0.02
Leu	[23456]	200	0	0.99	0.99	1.00	1.00	0.99	0.01	1.00	1.00	1.00	1.00
Leu	[23456]	200	1	0.01	0.01	0.00	0.00	0.01	0.01	0.00	0.00	0.00	0.00
Leu	[23456]	274	0	0.97	0.97	1.00	1.00	0.99	0.01	0.99	0.99	0.99	0.99
Leu	[23456]	274	1	0.03	0.03	0.00	0.00	0.01	0.01	0.01	0.01	0.01	0.01
Leu	[12]	302	0	0.97	0.97	0.99	0.99	0.98	0.01	0.97	0.97	0.99	0.99
Leu	[12]	302	1	0.03	0.03	0.01	0.01	0.02	0.01	0.03	0.03	0.01	0.01
Phe	[23455667]	234	0	0.99	0.99	1.01	1.01	1.00	0.01	0.99	0.99	0.98	0.98
Phe	[23455667]	234	1	0.01	0.01	-0.01	-0.01	0.00	0.01	0.01	0.01	0.02	0.02
Phe	[12]	302	0	0.99	0.99	1.00	1.00	1.00	0.00	1.02	1.02	0.98	0.98
Phe	[12]	302	1	0.01	0.01	0.00	0.00	0.00	0.00	-0.02	-0.02	0.02	0.02
Phe	[23455667]	308	0	0.98	0.98	0.99	0.99	0.99	0.01	1.03	1.03	1.04	1.04
Phe	[23455667]	308	1	0.02	0.02	0.01	0.01	0.01	0.01	-0.03	-0.03	-0.04	-0.04
Phe	[123455667]	336	0	1.02	1.02	0.99	0.99	1.01	0.01	1.00	1.00	1.02	1.02
Phe	[123455667]	336	1	-0.02	-0.02	0.01	0.01	-0.01	0.01	0.00	0.00	-0.02	-0.02
Pro	[2345]	184	0	1.00	1.00	1.00	1.00	1.00	0.00	1.00	1.00	1.00	1.00
Pro	[2345]	184	1	0.00	0.00	0.00	0.00	0.00	0.00	0.00	0.00	0.00	0.00
Pro	[2345]	258	0	1.00	1.00	1.00	1.00	1.00	0.00	1.00	1.00	1.01	1.01
Pro	[2345]	258	1	0.00	0.00	0.00	0.00	0.00	0.00	0.00	0.00	-0.01	-0.01
Pro	[12345]	286	0	0.99	0.99	1.01	1.01	1.00	0.01	1.00	1.00	1.01	1.01
Pro	[12345]	286	1	0.01	0.01	-0.01	-0.01	0.00	0.01	0.00	0.00	-0.01	-0.01
Ser	[23]	288	0	0.91	0.91	0.98	0.98	0.94	0.03	0.90	0.90	0.89	0.89
Ser	[23]	288	1	0.09	0.09	0.02	0.02	0.06	0.03	0.10	0.10	0.11	0.11
Ser	[12]	302	0	0.99	0.99	1.02	1.02	1.00	0.02	1.03	1.03	1.01	1.01
Ser	[12]	302	1	0.01	0.01	-0.02	-0.02	0.00	0.02	-0.03	-0.03	-0.01	-0.01
Ser	[23]	362	0	0.99	0.99	1.00	1.00	0.99	0.01	0.98	0.98	1.01	1.01
Ser	[23]	362	1	0.01	0.01	0.00	0.00	0.01	0.01	0.02	0.02	-0.01	-0.01
Ser	[123]	390	0	1.00	1.00	1.02	1.02	1.01	0.01	1.02	1.02	1.01	1.01
Ser	[123]	390	1	0.00	0.00	-0.02	-0.02	-0.01	0.01	-0.02	-0.02	-0.01	-0.01
Thr	[234]	376	0	1.04	1.04	1.01	1.01	1.02	0.02	1.04	1.04	0.99	0.99
Thr	[234]	376	1	-0.04	-0.04	-0.01	-0.01	-0.02	0.02	-0.04	-0.04	0.01	0.01
Thr	[1234]	404	0	0.99	0.99	1.01	1.01	1.00	0.01	1.06	1.06	1.02	1.02
Thr	[1234]	404	1	0.01	0.01	-0.01	-0.01	0.00	0.01	-0.06	-0.06	-0.02	-0.02
urea	[1]	231	0										
urea	[1]	231	1										
urea	[1]	231	2										
urea	[1]	273	0										
urea	[1]	273	1										
urea	[1]	273	2										
Val	[2345]	186	0	0.99	0.99	1.00	1.00	0.99	0.00	1.00	1.00	1.00	1.00
Val	[2345]	186	1	0.01	0.01	0.00	0.00	0.01	0.00	0.00	0.00	0.00	0.00
Val	[2345]	260	0	0.97	0.97	0.98	0.98	0.97	0.01	0.98	0.98	0.97	0.97
Val	[2345]	260	1	0.03	0.03	0.02	0.02	0.03	0.01	0.02	0.02	0.03	0.03
Val	[12345]	288	0	0.97	0.97	0.99	0.99	0.98	0.01	0.95	0.95	0.97	0.97
Val	[12345]	288	1	0.03	0.03	0.01	0.01	0.02	0.01	0.05	0.05	0.03	0.03
Val	[12]	302	0	1.02	1.02	1.00	1.00	1.01	0.01	1.03	1.03	1.02	1.02
Val	[12]	302	1	-0.02	-0.02	0.00	0.00	-0.01	0.01	-0.03	-0.03	-0.02	-0.02

## References

- Abdullahi, A.S., Underwood, G.J.C., Gretz, M.R., 2006. Extracellular matrix assembly in diatoms (Bacillariophyceae). V. Environmental effects on polysaccharide synthesis in the model diatom, *Phaeodactylum tricornutum*. *Journal of Phycology* 42, 363–378.
- AbuOun, M., Suthers, P.F., Jones, G.I., Carter, B.R., Saunders, M.P., Maranas, C.D., Woodward, M.J., Anjum, M.F., 2009. Genome scale reconstruction of a Salmonella metabolic model: comparison of similarity and differences with a commensal Escherichia coli strain. *Journal of Biological Chemistry* 284, 29480–29488.
- Ahn, W.S., Antoniewicz, M.R., 2013. Parallel labeling experiments with [1,2-<sup>13</sup>C]glucose and [U-<sup>13</sup>C]glutamine provide new insights into CHO cell metabolism. *Metab. Eng.* 15, 34–47.
- Akhani, H., Barroca, J., Koteeva, N., Voznesenskaya, E., Franceschi, V., Edwards, G., Ghaffari, S.M., Ziegler, H., Lammers, T.G., 2005. *Bienertia sinuspersici* (Chenopodiaceae): A new species from southwest Asia and discovery of a third terrestrial C<sub>4</sub> plant without Kranz anatomy. *Systematic Botany* 30, 290–301.
- Allen, Andrew E., Dupont, C.L., Oborník, M., Horák, A., Nunes-Nesi, A., McCrow, J.P., Zheng, H., Johnson, D.A., Hu, H., Fernie, A.R., Bowler, C., 2011. Evolution and metabolic significance of the urea cycle in photosynthetic diatoms. *Nature* 473, 203–207.
- Allen, Andrew E., Moustafa, A., Montsant, A., Eckert, A., Kroth, P.G., Bowler, C., 2011. Evolution and functional diversification of fructose bisphosphate aldolase genes in photosynthetic marine diatoms. *Mol Biol Evol* 29, 367–379.
- Allen, M.B., Arnon, D.I., 1955. Studies on Nitrogen-Fixing Blue-Green Algae. I. Growth and Nitrogen Fixation by *Anabaena cylindrica* Lemm1. *Plant Physiol* 30, 366–372.
- Alonso, A.P., Val, D.L., Shachar-Hill, Y., 2011. Central metabolic fluxes in the endosperm of developing maize seeds and their implications for metabolic engineering. *Metabolic Engineering* 13, 96–107.
- Alonso, D.L., Segura del Castillo, C.I., Grima, E.M., Cohen, Z., 1996. First insights into improvement of eicosapentaenoic acid content in *Phaeodactylum tricornutum* (Bacillariophyceae) by induced mutagenesis. *Journal of Phycology* 32, 339–345.
- Antoniewicz, M.R., Kelleher, J.K., Stephanopoulos, G., 2007. Elementary metabolite units (EMU): A novel framework for modeling isotopic distributions. *Metabolic Engineering* 9, 68–86.
- Ball, C.A., Sherlock, G., Parkinson, H., Rocca-Sera, P., Brooksbank, C., Causton, H.C., Cavalieri, D., Gaasterland, T., Hingamp, P., Holstege, F., Ringwald, M., Spellman, P., Stoekert, C.J., Jr, Stewart, J.E., Taylor, R., Brazma, A., Quackenbush, J., Microarray Gene Expression Data (MGED) Society, 2002. Standards for microarray data. *Science* 298, 539.
- Bowes, G., 1991. Growth at elevated CO<sub>2</sub>: photosynthetic responses mediated through Rubisco. *Plant, Cell & Environment* 14, 795–806.
- Bowler, C., Allen, A.E., Badger, J.H., Grimwood, J., Jabbari, K., et al., 2008. The *Phaeodactylum* genome reveals the evolutionary history of diatom genomes. *Nature* 456, 239–244.
- Boyle, N.R., Morgan, J.A., 2011. Computation of metabolic fluxes and efficiencies for biological carbon dioxide fixation. *Metabolic Engineering* 13, 150–158.

- Brazma, A., Hingamp, P., Quackenbush, J., Sherlock, G., Spellman, P., Stoeckert, C., Aach, J., Ansorge, W., Ball, C.A., Causton, H.C., Gaasterland, T., Glenisson, P., Holstege, F.C.P., Kim, I.F., Markowitz, V., Matese, J.C., Parkinson, H., Robinson, A., Sarkans, U., Schulze-Kremer, S., Stewart, J., Taylor, R., Vilo, J., Vingron, M., 2001. Minimum information about a microarray experiment (MIAME)—toward standards for microarray data. *Nat Genet* 29, 365–371.
- Brown, R.H., 1978. A Difference in N Use Efficiency in C3 and C4 Plants and its Implications in Adaptation and Evolution. *Crop Science* 18, 93.
- Burkhardt, S., Amoroso, G., Riebesell, U., Sultemeyer, D., 2001. CO<sub>2</sub> and HCO<sub>3</sub><sup>-</sup> uptake in marine diatoms acclimated to different CO<sub>2</sub> concentrations. *Limnol. Oceanogr.* 46, 1378–1391.
- Burns, R.C., Hardy, R.W.F., 1975. Nitrogen fixation in bacteria and higher plants. 21, 189pp.
- Caemmerer, S. von, Farquhar, G.D., 1981. Some relationships between the biochemistry of photosynthesis and the gas exchange of leaves. *Planta* 153, 376–387.
- Caemmerer, S. von, Quick, W.P., Furbank, R.T., 2012. The Development of C4 Rice: Current Progress and Future Challenges. *Science* 336, 1671–1672.
- Ceron Garcia, M., Camacho, F.G., Miron, A.S., Sevilla, J.M.F., Chisti, Y., Grima, E.M., 2006. Mixotrophic production of marine microalga *Phaeodactylum tricorutum* on various carbon sources. *Journal of microbiology and biotechnology* 16, 689.
- Chauton, M.S., Winge, P., Brembu, T., Vadstein, O., Bones, A.M., 2013. Gene regulation of carbon fixation, storage, and utilization in the diatom *Phaeodactylum tricorutum* acclimated to light/dark cycles. *Plant Physiol.* 161, 1034–1048.
- Choi, J., Grossbach, M.T., Antoniewicz, M.R., 2012. Measuring complete isotopomer distribution of aspartate using gas chromatography/tandem mass spectrometry. *Anal. Chem.* 84, 4628–4632.
- Crown, S.B., Antoniewicz, M.R., 2012. Selection of tracers for 13C-metabolic flux analysis using elementary metabolite units (EMU) basis vector methodology. *Metabolic Engineering* 14, 150–161.
- Crown, S.B., Indurthi, D.C., Ahn, W.S., Choi, J., Papoutsakis, E.T., Antoniewicz, M.R., 2011. Resolving the TCA cycle and pentose-phosphate pathway of *Clostridium acetobutylicum* ATCC 824: Isotopomer analysis, in vitro activities and expression analysis. *Biotechnol J* 6, 300–305.
- Dai, Z., Ku, M., Edwards, G.E., 1993. C4 Photosynthesis (The CO<sub>2</sub>-Concentrating Mechanism and Photorespiration). *Plant Physiology* 103, 83–90.
- De Riso, V., Raniello, R., Maumus, F., Rogato, A., Bowler, C., Falciatore, A., 2009. Gene silencing in the marine diatom *Phaeodactylum tricorutum*. *Nucleic Acids Res.* 37, e96–e96.
- Duanmu, D., Miller, A.R., Horken, K.M., Weeks, D.P., Spalding, M.H., 2009. Knockdown of limiting-CO<sub>2</sub>-induced gene *HLA3* decreases HCO<sub>3</sub><sup>-</sup> transport and photosynthetic Ci affinity in *Chlamydomonas reinhardtii*. *Proc. Natl. Acad. Sci. U.S.A* 106, 5990–5995.
- Dunstan, G.A., Volkman, J.K., Barrett, S.M., Leroi, J.-M., Jeffrey, S.W., 1993. Essential polyunsaturated fatty acids from 14 species of diatom (Bacillariophyceae). *Phytochemistry* 35, 155–161.

- Edwards, G.E., Franceschi, V.R., Voznesenskaya, E.V., 2004. Single-cell C<sub>4</sub> photosynthesis versus the dual-cell (Kranz) paradigm. *Annual Review of Plant Biology* 55, 173–196.
- Edwards, J.S., Palsson, B.O., 2000. Metabolic flux balance analysis and the in silico analysis of *Escherichia coli* K-12 gene deletions. *BMC Bioinformatics* 1, 1.
- Ellis, R.J., 2010. Biochemistry: Tackling unintelligent design. *Nature* 463, 164–165.
- Eppley, R.W., Renger, E.H., 1974. Nitrogen Assimilation of an Oceanic Diatom in Nitrogen-Limited Continuous Culture1. *Journal of Phycology* 10, 15–23.
- Evans, J.R., Loreto, F., 2004. Acquisition and diffusion of CO<sub>2</sub> in higher plant leaves, in: *Photosynthesis, Advances in Photosynthesis and Respiration*. Springer Netherlands, pp. 321–351.
- Fabris, M., Matthijs, M., Rombauts, S., Vyverman, W., Goossens, A., Baart, G.J.E., 2012. The metabolic blueprint of *Phaeodactylum tricornutum* reveals a eukaryotic Entner-Doudoroff glycolytic pathway. *Plant J.* 70, 1004–1014.
- Falkowski, P.G., Barber, R.T., Smetacek, V., 1998. Biogeochemical controls and feedbacks on ocean primary production. *Science* 281, 200–206.
- Feist, A.M., Henry, C.S., Reed, J.L., Krummenacker, M., Joyce, A.R., Karp, P.D., Broadbelt, L.J., Hatzimanikatis, V., Palsson, B.Ø., 2007. A genome-scale metabolic reconstruction for *Escherichia coli* K-12 MG1655 that accounts for 1260 ORFs and thermodynamic information. *Mol Syst Biol* 3.
- Feng, X., Bandyopadhyay, A., Berla, B., Page, L., Wu, B., Pakrasi, H.B., Tang, Y.J., 2010a. Mixotrophic and photoheterotrophic metabolism in *Cyanotheca* sp. ATCC 51142 under continuous light. *Microbiology (Reading, Engl.)* 156, 2566–2574.
- Feng, X., Tang, K.-H., Blankenship, R.E., Tang, Y.J., 2010b. Metabolic flux analysis of the mixotrophic metabolisms in the green sulfur bacterium *Chlorobaculum tepidum*. *J. Biol. Chem.* 285, 39544–39550.
- Fujimori, K., Ohta, D., 1998. Isolation and characterization of a histidine biosynthetic gene in *Arabidopsis* encoding a polypeptide with two separate domains for phosphoribosyl-ATP pyrophosphohydrolase and phosphoribosyl-AMP cyclohydrolase. *Plant Physiology* 118, 275–283.
- Furbank, R.T., von Caemmerer, S., Sheehy, J., Edwards, G., 2009. C<sub>4</sub> rice: a challenge for plant phenomics. *Funct. Plant Biol.* 36, 845–856.
- Govindjee, U., 2012. *Photosynthesis V2: Development, Carbon Metabolism, and Plant Productivity*. Elsevier.
- Haimovich-Dayana, M., Garfinkel, N., Ewe, D., Marcus, Y., Gruber, A., Wagner, H., Kroth, P.G., Kaplan, A., 2013. The role of C<sub>4</sub> metabolism in the marine diatom *Phaeodactylum tricornutum*. *New Phytologist* 197, 177–185.
- Hammond, S.M., Bernstein, E., Beach, D., Hannon, G.J., 2000. An RNA-directed nuclease mediates post-transcriptional gene silencing in *Drosophila* cells. *Nature* 404, 293–296.
- Hayward, J., 1968. Studies on the growth of *Phaeodactylum tricornutum*. II. The effect of organic substances on growth. *Physiologia Plantarum* 21, 100–108.
- Heldt, H.-W., Piechulla, B., 2010. *Plant Biochemistry*, 4th ed. Academic Press.
- Hempel, F., Bozarth, A.S., Lindenkamp, N., Klingl, A., Zauner, S., Linne, U., Steinbuchel, A., Maier, U.G., 2011. Microalgae as bioreactors for bioplastic production. *Microbial Cell Factories* 10, 81.
- Hong, S.H., Park, S.J., Moon, S.Y., Park, J.P., Lee, S.Y., 2003. In silico prediction and validation of the importance of the Entner-Doudoroff pathway in poly(3-hydroxybutyrate) production by metabolically engineered *Escherichia coli*. *Biotechnol. Bioeng.* 83, 854–863.

- Hopkinson, B.M., Dupont, C.L., Allen, A.E., Morel, F.M.M., 2011. Efficiency of the CO<sub>2</sub>-concentrating mechanism of diatoms. *Proc Natl Acad Sci U S A* 108, 3830–3837.
- Isermann, N., Wiechert, W., 2003. Metabolic isotopomer labeling systems. Part II: structural flux identifiability analysis. *Mathematical Biosciences* 183, 175–214.
- Iyer, V., Sriram, G., Shanks, J.V., 2007. Metabolic flux maps of central carbon metabolism in plant systems, in: Wurtele, E.S., Nikolau, B.J. (Eds.), *Concepts in Plant Metabolomics*. Springer, Dordrecht, the Netherlands, pp. 125–144.
- Jamai, A., Salomé, P.A., Schilling, S.H., Weber, A.P.M., McClung, C.R., 2009. *Arabidopsis* photorespiratory serine hydroxymethyltransferase activity requires the mitochondrial accumulation of ferredoxin-dependent glutamate synthase. *Plant Cell* 21, 595–606.
- Kajala, K., Covshoff, S., Karki, S., Woodfield, H., Tolley, B.J., Dionora, M.J.A., Mogul, R.T., Mabilangan, A.E., Danila, F.R., Hibberd, J.M., Quick, W.P., 2011. Strategies for engineering a two-celled C<sub>4</sub> photosynthetic pathway into rice. *J. Exp. Bot.* 62, 3001–3010.
- Kauffman, K.J., Prakash, P., Edwards, J.S., 2003. Advances in flux balance analysis. *Current Opinion in Biotechnology* 14, 491–496.
- Khamis, S., Lamaze, T., Lemoine, Y., Foyer, C., 1990. Adaptation of the Photosynthetic Apparatus in Maize Leaves as a Result of Nitrogen Limitation Relationships between Electron Transport and Carbon Assimilation. *Plant Physiol.* 94, 1436–1443.
- Kirk, J.T.O., 1994. *Light and Photosynthesis in Aquatic Ecosystems*. Cambridge University Press.
- Kocharin, K., Siewers, V., Nielsen, J., 2013. Improved polyhydroxybutyrate production by *Saccharomyces cerevisiae* through the use of the phosphoketolase pathway. *Biotechnol. Bioeng.* 110, 2216–2224.
- Kramer, P.J., 1981. Carbon Dioxide Concentration, Photosynthesis, and Dry Matter Production. *BioScience* 31, 29–33.
- Krebs, H.A., Henseleit, K., 1932. Untersuchungen über die Harnstoffbildung im Tierkörper. *Hoppe-Seyler's Zeitschrift für physiologische Chemie* 210, 33–66.
- Kroth, P.G., Chiovitti, A., Gruber, A., Martin-Jezequel, V., Mock, T., Parker, M.S., Stanley, M.S., Kaplan, A., Caron, L., Weber, T., Maheswari, U., Armbrust, E.V., Bowler, C., 2008. A model for carbohydrate metabolism in the diatom *Phaeodactylum tricornutum* deduced from comparative whole genome analysis. *PLoS ONE* 3, e1426.
- Lawlor, D.W., 2002. Carbon and nitrogen assimilation in relation to yield: mechanisms are the key to understanding production systems. *J. Exp. Bot.* 53, 773–787.
- Lawlor, D.W., Cornic, G., 2002. Photosynthetic carbon assimilation and associated metabolism in relation to water deficits in higher plants. *Plant, Cell & Environment* 25, 275–294.
- Lee, J.M., Gianchandani, E.P., Papin, J.A., 2006. Flux balance analysis in the era of metabolomics. *Brief Bioinform* 7, 140–150.
- Lewin, J.C., 1958. The taxonomic position of *Phaeodactylum tricornutum*. *J Gen Microbiol* 18, 427–432.
- Libourel, I.G.L., Gehan, J.P., Shachar-Hill, Y., 2007. Design of substrate label for steady state flux measurements in plant systems using the metabolic network of *Brassica napus* embryos. *Phytochemistry* 68, 2211–2221.

- Liu, X., Duan, S., Li, A., Xu, N., Cai, Z., Hu, Z., 2009. Effects of organic carbon sources on growth, photosynthesis, and respiration of *Phaeodactylum tricornutum*. *J Appl Phycol* 21, 239–246.
- Livak, K.J., Schmittgen, T.D., 2001. Analysis of relative gene expression data using real-time quantitative PCR and the  $2^{-\Delta\Delta CT}$  method. *Methods* 25, 402–408.
- Long, S.P., 1999. Environmental responses, in *C<sub>4</sub> Plant Biology*. Academic Press, San Diego, Calif. 215–249.
- Lopez, P.J., Desclés, J., Allen, A.E., Bowler, C., 2005. Prospects in diatom research. *Current Opinion in Biotechnology* 16, 180–186.
- Maheswari, U., Jabbari, K., Petit, J.-L., Porcel, B.M., Allen, A.E., Cadoret, J.-P., De Martino, A., Heijde, M., Kaas, R., La Roche, J., Lopez, P.J., Martin-Jézéquel, V., Meichenin, A., Mock, T., Schnitzler Parker, M., Vardi, A., Armbrust, E.V., Weissenbach, J., Katinka, M., Bowler, C., 2010. Digital expression profiling of novel diatom transcripts provides insight into their biological functions. *Genome Biol* 11, R85.
- Masakapalli, S.K., Lay, P.L., Huddleston, J.E., Pollock, N.L., Kruger, N.J., Ratcliffe, R.G., 2010. Subcellular flux analysis of central metabolism in a heterotrophic *Arabidopsis thaliana* cell suspension using steady-state stable isotope labeling. *Plant Physiology* 152, 602–609.
- Masoudi-Nejad, A., Goto, S., Endo, T.R., Kanehisa, M., 2008. KEGG bioinformatics resource for plant genomics research, in: Edwards, D. (Ed.), *Plant Bioinformatics, Methods in Molecular Biology*. Humana Press, pp. 437–458.
- Möllney, M., Wiechert, W., Kownatzki, D., de Graaf, A.A., 1999. Bidirectional reaction steps in metabolic networks: IV. Optimal design of isotopomer labeling experiments. *Biotechnol. Bioeng.* 66, 86–103.
- Morales-Sánchez, D., Tinoco-Valencia, R., Kyndt, J., Martinez, A., 2013. Heterotrophic growth of *Neochloris oleoabundans* using glucose as a carbon source. *Biotechnology for Biofuels* 6, 100.
- Nargund, S., Sriram, G., 2013. Designer labels for plant metabolism: Statistical design of isotope labeling experiments for improved quantification of flux in complex plant metabolic networks. *Mol. BioSyst.* 9, 99–112.
- Nikolau, B.J., Perera, M.A.D.N., Brachova, L., Shanks, B., 2008. Platform biochemicals for a biorenewable chemical industry. *Plant J* 54, 536–545.
- Nöh, K., Wiechert, W., 2006. Experimental design principles for isotopically instationary <sup>13</sup>C labeling experiments. *Biotechnology and Bioengineering* 94, 234–251.
- Nymark, M., Valle, K.C., Brembu, T., Hancke, K., Winge, P., Andresen, K., Johnsen, G., Bones, A.M., 2009. An integrated analysis of molecular acclimation to high light in the marine diatom *Phaeodactylum tricornutum*. *PLoS ONE* 4, e7743.
- O’Leary, M.H., 1988. Carbon Isotopes in Photosynthesis. *BioScience* 38, 328–336.
- Onbaşıoğlu, Özdamar, 2001. Parallel simulated annealing algorithms in global optimization. *Journal of Global Optimization* 19, 27–50.
- Park, J., Okita, T.W., Edwards, G.E., 2010. Expression profiling and proteomic analysis of isolated photosynthetic cells of the non-Kranz *C<sub>4</sub>* species *Bienertia sinuspersici*. *Funct. Plant Biol.* 37, 1–13.
- Press, W.H., Teukolsky, S.A., Vetterling, W.T., Flannery, B.P., 2007. *Numerical Recipes 3rd Edition: The Art of Scientific Computing*, 3rd ed. Cambridge University Press.

- Quek, L.-E., Wittmann, C., Nielsen, L.K., Krömer, J.O., 2009. OpenFLUX: efficient modelling software for  $^{13}\text{C}$ -based metabolic flux analysis. *Microbial Cell Factories* 8, 25.
- Reinfelder, J.R., 2011. Carbon concentrating mechanisms in eukaryotic marine phytoplankton. *Annu. Rev. Marine. Sci.* 3, 291–315.
- Reinfelder, J.R., Kraepiel, A.M.L., Morel, F.M.M., 2000. Unicellular  $\text{C}_4$  photosynthesis in a marine diatom. *Nature* 407, 996–999.
- Reinfelder, J.R., Milligan, A.J., Morel, F.M.M., 2004. The role of the  $\text{C}_4$  pathway in carbon accumulation and fixation in a marine diatom. *Plant Physiol.* 135, 2106–2111.
- Ren, Q., Chen, K., Paulsen, I.T., 2007. TransportDB: a comprehensive database resource for cytoplasmic membrane transport systems and outer membrane channels. *Nucleic Acids Research* 35, D274–D279.
- Resendis-Antonio, O., Reed, J.L., Encarnación, S., Collado-Vides, J., Palsson, B.Ø., 2007. Metabolic reconstruction and modeling of nitrogen fixation in *Rhizobium etli*. *PLoS Comput Biol* 3, e192.
- Sage, R.F., 2002. Are crassulacean acid metabolism and  $\text{C}_4$  photosynthesis incompatible? *Functional Plant Biol.* 29, 775–785.
- Schena, M., Shalon, D., Davis, R.W., Brown, P.O., 1995. Quantitative Monitoring of Gene Expression Patterns with a Complementary DNA Microarray. *Science* 270, 467–470.
- Schwender, J., Goffman, F., Ohlrogge, J.B., Shachar-Hill, Y., 2004. Rubisco without the Calvin cycle improves the carbon efficiency of developing green seeds. *Nature* 432, 779–782.
- Shanks, J.V., 2005. Phytochemical engineering: Combining chemical reaction engineering with plant science. *AIChE J.* 51, 2–7.
- Sheehy, J.E., Mitchell, P.L., Hardy, B., 2007. Charting new pathways to  $\text{C}_4$  rice. *Int. Rice Res. Inst.*
- Siaut, M., Heijde, M., Mangogna, M., Montsant, A., Coesel, S., Allen, A., Manfredonia, A., Falciatore, A., Bowler, C., 2007. Molecular toolbox for studying diatom biology in *Phaeodactylum tricorutum*. *Gene* 406, 23–35.
- Simionato, D., Basso, S., Giacometti, G.M., Morosinotto, T., n.d. Optimization of light use efficiency for biofuel production in algae. *Biophysical Chemistry.*
- Singh, B.K., 1998. *Plant Amino Acids (Books in Soils, Plants, & the Environment)*, 1st ed. CRC.
- Slack, C.R., Hatch, M.D., 1967. Comparative studies on the activity of carboxylases and other enzymes in relation to the new pathway of photosynthetic carbon dioxide fixation in tropical grasses. *Biochem J* 103, 660–665.
- Slosson, E.E., 1920. *Creative chemistry: descriptive of recent achievements in the chemical industries.* Century Co.
- Smetacek, V., 1999. Diatoms and the ocean carbon cycle. *Protist* 150, 25–32.
- Smith, N.A., Singh, S.P., Wang, M.-B., Stoutjesdijk, P.A., Green, A.G., Waterhouse, P.M., 2000. Gene expression: Total silencing by intron-spliced hairpin RNAs. *Nature* 407, 319–320.
- Spreitzer, R.J., Salvucci, M.E., 2002. Rubisco: Structure, regulatory interactions, and possibilities for a better enzyme. *Annual review of plant biology* 53, 449–475.
- Sriram, G., Fulton, D.B., Iyer, V.V., Peterson, J.M., Zhou, R., Westgate, M.E., Spalding, M.H., Shanks, J.V., 2004. Quantification of compartmented metabolic fluxes in developing soybean embryos by employing biosynthetically directed fractional  $^{13}\text{C}$  labeling, two-dimensional [ $^{13}\text{C}$ ,  $^1\text{H}$ ]



- nuclear magnetic resonance, and comprehensive isotopomer balancing. *Plant Physiol.* 136, 3043–3057.
- Sriram, G., Fulton, D.B., Shanks, J.V., 2007. Flux quantification in central carbon metabolism of *Catharanthus roseus* hairy roots by <sup>13</sup>C labeling and comprehensive bondomer balancing. *Phytochemistry* 68, 2243–2257.
- Sriram, G., Rahib, L., He, J.-S., Campos, A.E., Parr, L.S., Liao, J.C., Dipple, K.M., 2008. Global metabolic effects of glycerol kinase overexpression in rat hepatoma cells. *Molecular Genetics and Metabolism* 93, 145–159.
- Sriram, G., Shanks, J.V., 2004. Improvements in metabolic flux analysis using carbon bond labeling experiments: bondomer balancing and Boolean function mapping. *Metabolic Engineering* 6, 116–132.
- Stephanopoulos, G., 1999. Metabolic fluxes and metabolic engineering. *Metab. Eng.* 1, 1–11.
- Szyperski, T., 1998a. <sup>13</sup>C-NMR, MS and metabolic flux balancing in biotechnology research. *Quarterly Reviews of Biophysics* 31, 41–106.
- Szyperski, T., 1998b. <sup>13</sup>C-NMR, MS and metabolic flux balancing in biotechnology research. *Quarterly Reviews of Biophysics* 31, 41–106.
- Taiz, L., Zeiger, E., 2006. *Plant physiology*. Sinauer Associates, Sunderland, Mass.
- Tesson, B., Genet, M.J., Fernandez, V., Degand, S., Rouxhet, P.G., Martin-Jézéquel, V., 2009. Surface chemical composition of diatoms. *ChemBioChem* 10, 2011–2024.
- Tran, L.M., Rizk, M.L., Liao, J.C., 2008. Ensemble modeling of metabolic networks. *Biophysical Journal* 95, 5606–5617.
- Ukeles, R., Rose, W., 1976. Observations on organic carbon utilization by photosynthetic marine microalgae. *Marine Biology* 37, 11–28.
- Valenzuela, J., Mazurie, A., Carlson, R.P., Gerlach, R., Cooksey, K.E., Peyton, B.M., Fields, M.W., 2012. Potential role of multiple carbon fixation pathways during lipid accumulation in *Phaeodactylum tricornutum*. *Biotechnol Biofuels* 5, 40.
- Vega-Sánchez, M.E., Ronald, P.C., 2010. Genetic and biotechnological approaches for biofuel crop improvement. *Curr. Opin. Biotech.* 21, 218–224.
- Vitousek, P.M., Aber, J.D., Howarth, R.W., Likens, G.E., Matson, P.A., Schindler, D.W., Schlesinger, W.H., Tilman, D.G., 1997. HUMAN ALTERATION OF THE GLOBAL NITROGEN CYCLE: SOURCES AND CONSEQUENCES. *Ecological Applications* 7, 737–750.
- Voznesenskaya, E.V., Franceschi, V.R., Kiirats, O., Artyusheva, E.G., Freitag, H., Edwards, G.E., 2002. Proof of C<sub>4</sub> photosynthesis without Kranz anatomy in *Bienertia cycloptera* (Chenopodiaceae). *The Plant Journal* 31, 649–662.
- Voznesenskaya, E.V., Franceschi, V.R., Kiirats, O., Freitag, H., Edwards, G.E., 2001. Kranz anatomy is not essential for terrestrial C<sub>4</sub> plant photosynthesis. *Nature* 414, 543–546.
- Ward, J.K., Tissue, D.T., Thomas, R.B., And, ., Strain, B.R., 1999. Comparative responses of model C<sub>3</sub> and C<sub>4</sub> plants to drought in low and elevated CO<sub>2</sub>. *Global Change Biology* 5, 857–867.
- Weitzel, M., Nöh, K., Dalman, T., Niedenführ, S., Stute, B., Wiechert, W., 2012. <sup>13</sup>CFLUX2 – High-performance software suite for <sup>13</sup>C-metabolic flux analysis. *Bioinformatics*.
- Wen, Z.-Y., Chen, F., 2003. Heterotrophic production of eicosapentaenoic acid by microalgae. *Biotechnology Advances* 21, 273–294.
- Wiechert, W., 2001. <sup>13</sup>C metabolic flux analysis. *Metabolic Engineering* 3, 195–206.
- Wiechert, W., Möllney, M., Isermann, N., Wurzel, M., de Graaf, A.A., 1999a. Bidirectional reaction steps in metabolic networks: III. Explicit solution and

- analysis of isotopomer labeling systems. *Biotechnology and Bioengineering* 66, 69–85.
- Wiechert, W., Möllney, M., Isermann, N., Wurzel, M., Graaf, A.A. de, 1999b. Bidirectional reaction steps in metabolic networks: III. Explicit solution and analysis of isotopomer labeling systems. *Biotechnology and Bioengineering* 66, 69–85.
- Wiechert, W., Möllney, M., Petersen, S., de Graaf, A.A., 2001. A universal framework for  $^{13}\text{C}$  metabolic flux analysis. *Metabolic Engineering* 3, 265–283.
- Wiechert, W., Nöh, K., in press. Isotopically non-stationary metabolic flux analysis: complex yet highly informative. *Current Opinion in Biotechnology* 0, 0.
- Wiechert, W., Siefke, C., Graaf, A.A. de, Marx, A., 1997. Bidirectional reaction steps in metabolic networks: II. Flux estimation and statistical analysis. *Biotechnology and Bioengineering* 55, 118–135.
- Wiechert, W., Wurzel, M., 2001. Metabolic isotopomer labeling systems. Part I: global dynamic behavior. *Math Biosci* 169, 173–205.
- Winden, W.A. van, Heijnen, J.J., Verheijen, P.J.T., 2002. Cumulative bondomers: A new concept in flux analysis from 2D [ $^{13}\text{C}$ ,  $^1\text{H}$ ] COSY NMR data. *Biotechnology and Bioengineering* 80, 731–745.
- Winden, W.A.V., Wittmann, C., Heinzle, E., Heijnen, J.J., 2002. Correcting mass isotopomer distributions for naturally occurring isotopes. *Biotechnology and Bioengineering* 80, 477–479.
- Wittmann, C., Heinzle, E., 2001. Modeling and Experimental Design for Metabolic Flux Analysis of Lysine-Producing *Corynebacteria* by Mass Spectrometry. *Metabolic Engineering* 3, 173–191.
- Yang, T.H., Heinzle, E., Wittmann, C., 2005. Theoretical aspects of  $^{13}\text{C}$  metabolic flux analysis with sole quantification of carbon dioxide labeling. *Comput. Biol. Chem.* 29, 121–133.
- Yokota, A., Shigeoka, S., 2008. Engineering photosynthetic pathways, in: *Advances in Plant Biochemistry and Molecular Biology*. Pergamon, pp. 81–105.
- Yongmanitchai, W., Ward, O.P., 1991. Growth of and omega-3 fatty acid production by *Phaeodactylum tricornutum* under different culture conditions. *Appl Environ Microbiol* 57, 419–425.
- Yoon, J.M., Zhao, L., Shanks, J.V., 2013. Metabolic engineering with plants for a sustainable biobased economy. *Annual Review of Chemical and Biomolecular Engineering* 4, 211–237.
- Young, J.D., Shastri, A.A., Stephanopoulos, G., Morgan, J.A., 2011a. Mapping photoautotrophic metabolism with isotopically nonstationary  $^{13}\text{C}$  flux analysis. *Metabolic Engineering* 13, 656–665.
- Young, J.D., Shastri, A.A., Stephanopoulos, G., Morgan, J.A., 2011b. Mapping photoautotrophic metabolism with isotopically nonstationary  $^{13}\text{C}$  flux analysis. *Metabolic Engineering* 13, 656–665.
- Young, J.D., Walther, J.L., Antoniewicz, M.R., Yoo, H., Stephanopoulos, G., 2008. An elementary metabolite unit (EMU) based method of isotopically nonstationary flux analysis. *Biotechnology and Bioengineering* 99, 686–699.
- Yuan, J.S., Tiller, K.H., Al-Ahmad, H., Stewart, N.R., Stewart Jr., C.N., 2008. Plants to power: bioenergy to fuel the future. *Trends in Plant Science* 13, 421–429.
- Zamboni, N., Fischer, E., Sauer, U., 2005. FiatFlux - a software for metabolic flux analysis from  $^{13}\text{C}$ -glucose experiments. *BMC Bioinformatics* 6, 209.
- Zaslavskaja, L.A., Lippmeier, J.C., Shih, C., Ehrhardt, D., Grossman, A.R., Apt, K.E., 2001. Trophic conversion of an obligate photoautotrophic organism through metabolic engineering. *Science* 292, 2073–2075.

- Zhang, P., Foerster, H., Tissier, C.P., Mueller, L., Paley, S., Karp, P.D., Rhee, S.Y., 2005. MetaCyc and AraCyc. Metabolic pathway databases for plant research. *Plant Physiology* 138, 27–37.
- Zhu, X.-G., Long, S.P., Ort, D.R., 2010a. Improving photosynthetic efficiency for greater yield. *Annu. Rev. Plant Biol.* 61, 235–261.
- Zhu, X.-G., Shan, L., Wang, Y., Quick, W.P., 2010b. C4 Rice – an Ideal Arena for Systems Biology Research. *Journal of Integrative Plant Biology* 52, 762–770.